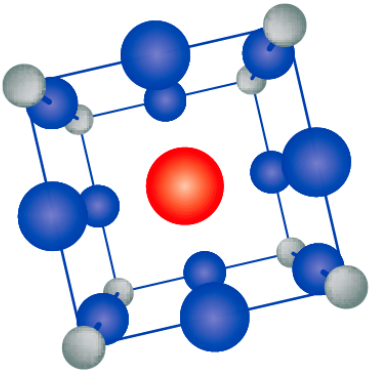

MaNEP
SWITZERLAND

Materials with Novel Electronic Properties

National Centre of Competence in Research

PROGRESS REPORT

Year 8

April 1st 2008 – March 31st 2009

Part I. *Scientific and other activities*

FNSNF
Fonds national suisse
Schweizerischer Nationalfonds
Fondo nazionale svizzero
Swiss National Science Foundation

Die Nationalen Forschungsschwekpunkte (NFS) sind ein Förderinstrument des Schweizerischen Nationalfonds.
Les Pôles de recherche nationaux (PRN) sont un instrument d'encouragement du Fonds national suisse.
The National Centres of Competence in Research (NCCR) are a research instrument of the Swiss National Science Foundation.

FNSNF
SWISS NATIONAL SCIENCE FOUNDATION

www.snf.ch
Wildhainweg 3, P.O. Box 8232, CH-3001 Berne

Division for Targeted Research
National Centres of Competence in Research

NCCR: 8th Progress Report - Cover Sheet

Title of the NCCR	Materials with Novel Electronic Properties (MaNEP)
NCCR Director Name, first name Institution address Office phone number E-mail	Prof. Øystein Fischer UNIVERSITE DE GENEVE, Faculté des Sciences Département de Physique de la Matière Condensée 24 quai Ernest-Ansermet, CH-1211 Genève 4 022 379 62 70 Oystein.Fischer@unige.ch

Contents

We have indicated in grey the parts which are not included in this report, and will be sent to the Swiss National Science Foundation at a later time.

1 Executive summary

This report is the last one of MaNEP Phase II and covers the period April 1, 2008 until March 31, 2009. We have largely completed the research program of the six collaborative projects and the most recent results are given in this report. This corresponds to the work of 32 main investigators with their groups. This year a lot of effort was also spent to prepare Phase III described in the Proposal submitted at the same time as this report.

Research

Project 1. This project deals with a wide range of topics in the general field of strongly correlated electron and low-dimensional systems. Among the recent results obtained this year, we can mention novel results in quantum spin systems, involving Luttinger liquid systems, Bose-Einstein condensation of magnons, the study of the possible appearance of an exciton insulator in 1T-$TiSe_2$, a new and unusual first order phase transition between a Na-"solid" and a Na-"liquid" in $Na_{0.82}CoO_2$ and tuneable spin-orbit coupling observed by angle resolved photoemission spectroscopy at the surface of $Bi_xPb_{1-x}Ag_2$.

Project 2. MaNEP focuses here on the extraordinary challenge to understand superconductivity observed in several classes of novel materials, in particular high temperature superconductivity. Major progress was achieved in understanding the interplay between spin correlations and superconductivity in the cuprates, based on neutron scattering, scanning tunneling spectroscopy and optical investigations. We furthermore report on field effect modulation of superconductivity in the $LaAlO_3/SrTiO_3$ interface and first observations concerning superconductivity in the Fe pnictides. Using neutron scattering we explored the unusual ground state of $CeCoIn_5$.

Projects 3 and 4. These projects focus on the preparation of single crystals of high quality and the search for new materials with novel electronic properties. The participation of six different laboratories has strongly enhanced MaNEP efforts and supply of high quality materials. An important highlight this year was the fast action by MaNEP members to fabricate single crystals of the new Fe pnictides, first the 1111 compound $SmFeAsO_{1-x}F_y$ with a T_c of 54 K followed by materials like $Ba_{1-x}Rb_xFe_2As_2$. A number of other crystals and compounds have also been investigated.

Project 5. This project aims at producing and understanding the behavior of thin and ultrathin oxide films, the behavior of interfaces as well as multilayers. The Neuchâtel/Geneva collaboration on photoemission studies of ultrathin ferroelectric films continues to give striking results. A new type of improper ferroelectricity has been observed in $PbTiO_3/SrTiO_3$ multilayers, new results have been obtained in domain wall behavior in $BiFeO_3$ films and magneto-electric effects have been observed in ferroelectric/manganite bilayers. Progress towards superconducting single photon detectors is also reported.

Project 6. An important result in the domain of applied superconductivity is the improvement of critical currents at moderately high fields confirming that MgB2 is a serious candidate for moderately high field applications. The new surface technology, introduced last year, has led to several new industrial contacts and a first new project has been launched with the watchmaker Vacheron Constantin. In the domain of hydrogen as an energy vector a collaboration with ASULAB (Swatch Group) has also been launched. A further key result this year was to master the epitaxial deposition of perovskites on Silicon. This technology, which has been realized by a few other groups before, is, however, essential for a number of applications of perovskite devices and opens therefore new possibilities for MaNEP.

Knowledge and technology transfer

Our activities in this field concentrated largely on the preparation of the third phase and our

aim to attract a few new industrial partners. Two new partners for larger collaborations resulted. On the one hand, we have entered into detailed discussions with ASULAB (Swatch Group) on research in the field of use of hydrogen as an energy vector and on the other hand we have elaborated the conditions for collaboration with Vacheron Constantin. Both these companies will be partners in Phase III of MaNEP. Furthermore, several shorter term mandates have been concluded. The bonds to the Geneva Economic Promotion generated positive results such as meetings, publications and invitation to events.

Education, training and advancement of women

Education. The MaNEP doctoral school is now established and teaching activities are well under way. The MaNEP Winter School took place in the week of January 11 – 16, 2009 and was one highlight of the year with seventy students and seven teachers interacting in a very stimulating atmosphere.

Outreach. Physiscope, presented last year, has continued to operate this year with great success and the visitor count passed already the 1000 mark. A key event was the inauguration of Physiscope on October 3, 2008 with the participation of the minister in charge of the Geneva department of public education, Charles Beer. This year, the Physiscope joined forces with Europhysics Fun and a stimulating meeting of the European Network took place in Geneva in the week of March 31 to April 4, 2009.

Advancement of women. Eleven female students, distributed on four institutions, participated to the 2008 internships. We have also, involving the Equality Office of the University of Geneva, started preparing new actions which we plan for the third phase. Two new women members will join the MaNEP Forum in Phase III.

Public relations

In order to broaden our approach towards public relations we have initiated a collaboration with a Swiss artist Etienne Krähenbühl to stimulate a new science inspired piece of art. The aim is that an inauguration event will take place in December 2009 to conclude the Geneva University's 450^{th} anniversary. This year we also had a partnership with CERN to collaborate on public events, at CERN, at two occasions.

2 Research

2.1 Structure of the NCCR and status of integration

2.1.1 Structure of the NCCR

This section provides an up-to-date summary of the organization of MaNEP, the Swiss National Centre of Competence in Research (NCCR) on Materials with Novel Electronic Properties.

Academic institutions members of MaNEP

- University of Geneva (UniGE), home institution
- University of Neuchâtel (UniNE) – until March 31, 2009
- University of Fribourg (UniFR)
- University of Berne (UniBE)
- University of Zurich (UniZH)
- Federal Institute of Technology, Lausanne (EPFL)
- Federal Institute of Technology, Zurich (ETHZ)
- Paul Scherrer Institute (PSI)
- Materials Science and Technology Research Institute (Empa)

Industrial Partners

- ABB, Baden
- Bruker BioSpin, Fällanden
- MecSens, Geneva
- Metrolab, Lausanne
- Phasis, Geneva
- Swiss Neutronics, Villigen

Scientific Committee

- Øystein Fischer, UniGE, director
- László Forró, EPFL
- Jürg Hulliger, UniBE
- Manfred Sigrist, ETHZ
- Jean-Marc Triscone, UniGE
- Dirk van der Marel, UniGE, deputy director

Research groups (MaNEP Forum)

From academic institutions:

- Philipp Aebi, UniNE and UniFR
- Dionys Baeriswyl, UniFR
- Christian Bernhard, UniFR
- Gianni Blatter, ETHZ
- Markus Büttiker, UniGE
- Leonardo Degiorgi, ETHZ
- Øystein Fischer, UniGE
- René Flükiger, UniGE
- László Forró, EPFL
- Thierry Giamarchi, UniGE
- Marco Grioni, EPFL
- Martin Hasler, EPFL
- Jürg Hulliger, UniBE
- Janusz Karpinski, ETHZ
- Hugo Keller, PSI and UniZH
- Giorgio Margaritondo, EPFL
- Dirk van der Marel, UniGE
- Joël Mesot, PSI – ETHZ
- Frédéric Mila, EPFL
- Elvezio Morenzoni, PSI
- Alberto Morpurgo, UniGE
- Reinhard Nesper, ETHZ
- Hans-Rudolf Ott, ETHZ
- Patrycja Paruch, UniGE
- Christoph Renner, UniGE
- T. Maurice Rice, ETHZ
- Andreas Schilling, UniZH
- Louis Schlapbach, Empa
- Manfred Sigrist, ETHZ
- Jean-Marc Triscone, UniGE
- Matthias Troyer, ETHZ
- Klaus Yvon, UniGE

From industrial partners:

- Markus Abplanalp, ABB
- Daniel Eckert, Bruker BioSpin
- Willy Hofer, MecSens
- Pascal Sommer, Metrolab
- Jorge Cors, Phasis
- Peter Böni, Swiss Neutronics

Advisory Board

- Piero Martinoli, chair, Università della Svizzera Italiana
- Dave Blank, University of Twente, Netherlands
- Robert J. Cava, Princeton University, USA
- Antoine Georges, Ecole Normale Supérieure, France
- Denis Jérôme, University Paris Sud, Orsay, France
- Andrew Millis, Columbia University, USA
- George Sawatzky, University of British Columbia, Canada

Internal Evaluation Board

- Øystein Fischer, UniGE, director
- René Flükiger, UniGE
- László Forró, EPFL
- Jürg Hulliger, UniBE
- Dirk van der Marel, UniGE, deputy director
- Hans-Rudolf Ott, ETHZ
- Christoph Renner, UniGE, deputy director
- T. Maurice Rice, ETHZ
- Manfred Sigrist, ETHZ
- Jean-Marc Triscone, UniGE

Management (UniGE)

- Øystein Fischer, director
- Dirk van der Marel, deputy director
- Christoph Renner, deputy director
- Marie Bagnoud, administrative manager
- Christophe Berthod, education
- Renald Cartoni, technical organization
- Pascal Cugny, accountant
- Michel Decroux, scientific manager, education and training, advancement of women
- Lidia Favre-Quattropani, scientific manager
- Sophie Griessen, management secretary
- Matthias Kuhn, knowledge and technology transfer
- Ivan Maggio-Aprile, computer and internet resources
- Anne Rougemont, communication

Collaborative projects

1 Strongly interacting electrons, low dimensional and quantum fluctuation dominated systems

Project leader:

- M. Sigrist (ETHZ)

Members:

- G. Blatter (ETHZ)
- M. Büttiker (UniGE)
- L. Degiorgi (ETHZ)
- L. Forró (EPFL)
- T. Giamarchi (UniGE)
- M. Grioni (EPFL)
- D. van der Marel (UniGE)
- J. Mesot (PSI – ETHZ)
- F. Mila (EPF)
- H.-R. Ott (ETHZ)
- P. Paruch (UniGE)
- T. M. Rice (ETHZ)
- L. Schlapbach (Empa)
- M. Sigrist (ETHZ)
- M. Troyer (ETHZ)

Contributions from:

- Ph. Aebi (UniNE and UniFR)
- D. Baeriswyl (UniFR)
- Ø. Fischer (UniGE)
- C. Renner (UniGE)

2 Superconductivity, unconventional mechanisms and novel materials

Project leader:

- D. van der Marel (UniGE)

Members:

- D. Baeriswyl (UniFR)
- C. Bernhard (UniFR)
- G. Blatter (ETHZ)
- Ø. Fischer (UniGE)
- T. Giamarchi (UniGE)
- M. Grioni (EPFL)
- H. Keller (PSI)
- D. van der Marel (UniGE)

- J. Mesot (PSI – ETHZ)
- E. Morenzoni (PSI)
- T. M. Rice (ETHZ)
- M. Sigrist (ETHZ)

Contribution from:

- J.-M. Triscone (UniGE)

3 Crystal growth

Project leader:

- L. Forró (EPFL)

Members:

- J. Karpinski (ETHZ)
- D. van der Marel (UniGE)
- J. Mesot (PSI – ETHZ)
- G. Margaritondo (EPFL)

4 Novel materials

Project leader:

- J. Hulliger (UniBE)

Members:

- L. Forró (EPFL)
- J. Hulliger (UniBE)
- J. Karpinski (ETHZ)
- R. Nesper (ETHZ)
- L. Schlapbach (Empa)

5 Thin films, artificial materials and novel devices

Project leader:

- J.-M. Triscone (UniGE)

Members:

- P. Aebi (UniNE and UniFR)
- Ø. Fischer (UniGE)
- D. van der Marel (UniGE)
- A. Morpurgo (UniGE)
- P. Paruch (UniGE),
- A. Schilling (UniZH)
- J.-M. Triscone (UniGE)

6 Industrial applications and preapplication development

Project leader:

- Ø. Fischer (UniGE)

Members:

- M. Abplanalp (ABB)
- D. Eckert (Bruker BioSpin)
- Ø. Fischer (UniGE)
- R. Flükiger (UniGE)
- L. Forró (EPFL)
- M. Hasler (EPFL)
- J. Mesot (PSI – ETHZ)
- R. Nesper (ETHZ)
- C. Renner (UniGE)
- J.-M. Triscone (UniGE)
- K. Yvon (UniGE)

2.1.2 Status of integration

The change in structure of MaNEP after the first phase was intended to stimulate relations, synergies and collaborations between the different groups. In the six collaborative projects, MaNEP members collaborate towards common goals. Thus this organization by itself stimulates contacts between the groups and it fosters collaborations. This is illustrated by the fact that several smaller meetings have been organized during phase II. For instance the crystal growth group in Geneva, the STM and the optics group in Geneva as well as the ARPES groups at PSI, at EPFL and in Neuchâtel have been meeting regularly. The goal of this collaboration is to compare and to analyze the different results obtained on the electronic properties of the HTS superconductor $Bi_2Sr_2Ca_2Cu_3O_{10}$. Numerous other collaborations have developed as summarized at the end of each project report.

As planned, we have launched during phase II new calls for collaborative projects. We have also appointed mobile post-docs. These positions are extremely useful for fostering collaborations since the mobile post-doc is appointed to work on projects which include several groups at different institutions. A mobile post-doc worked at the interface of the spectroscopy groups at UniGE, PSI and EPFL and another between theory groups at ETHZ (Troyer) and EPFL (Mila)

The MaNEP Winter School 2009 was another event stimulating integration between the groups. Students from ETHZ, EPFL, UniGE, UniFR, PSI and Empa gathered for one week in a stimulating environment. We also organized six internal workshops in January 2009 where the Forum Members of MaNEP contributing to the six different projects gathered and discussed in detail the results obtained.

Four years after the reorganization we observe a significant progress of the synergies within the MaNEP community. In the third phase we shall continue with collaborative projects, slightly reorganized to further stimulate collaboration between theorists, experimentalists and materials scientists.

The milestones (see appendix) prove to be a valuable instrument of integration. Our milestones are revised and discussed among the members of the projects during the Internal Workshops. This discussion gives to the members of each Project an instrument to assess the progression of research and provides the group leaders with a global vision of the status of each project.

During the second phase we experience that MaNEP is increasingly recognized within the scientific community as well as by the authorities and the general public. MaNEP is also more and more considered as a partner in Swiss science (invitations to co-organize the Swiss Physical Society meeting, invitations to give our opinions on new projects, etc).

The MaNEP groups in the leading house are well integrated with new collaborations between them coming up. Integration with other parts of the home institution (UniGE) is already considerable and this aspect was reinforced by launching our project "PhysiScope" in collaboration with the Physics Department at the University. This new tool is now operational and scientists from different groups, also outside MaNEP, collaborate to improve and run this novel approach towards outreach. This project, a new instrument dedicated to knowledge transfer, has the full support of the University and its communication office as well as the Faculty of Sciences. It will also help MaNEP to integrate into the Canton of Geneva with the endorsement of the secondary schools as well as the financial support from private foundations in Geneva.

2.2 Results since the last progress report

This section reports on the research performed in the six MaNEP projects for the period from April 1st 2008 to March 31st 2009.

Project 1 — Strongly interacting electrons, low-dimensional and quantum fluctuation dominated systems

Project leader: M. Sigrist (ETHZ)

Participating members: G. Blatter (ETHZ), M. Büttiker (UniGE), L. Degiorgi (ETHZ), L. Forró (EPFL), T. Giamarchi (UniGE), M. Grioni (EPFL), D. van der Marel (UniGE), J. Mesot (PSI), F. Mila (EPFL), H.-R. Ott (ETHZ), P. Paruch (UniGE), T. M. Rice (ETHZ), L. Schlapbach (Empa), M. Sigrist (ETHZ), M. Troyer (ETHZ). Contributions from Ph. Aebi (UniNE and UniFR), D. Baeriswyl (UniFR), Ø. Fischer (UniGE), C. Renner (UniGE).

Introduction: The progress report of this project covers a wide range of topics within the field of strongly correlated electron and low-dimensional systems encompassing areas such as quantum spin systems, heavy fermion materials, charge density wave compounds and carbon-based systems. It also reaches out to topics beyond the original framework of this project which are, however, considered relevant to our efforts, e.g. the physics of cold-atoms and mesoscopic systems. Our interest lies on the experimental and theoretical exploration of novel phases and phenomena in materials which is to a large extend motivated by the challenging problems encountered in the search for fundamental concepts in modern condensed matter physics.

Summary and highlights

We report on the study of novel phases induced by magnetic fields in spin dimer systems, such as the spin ladder $(Hpip)_2CuBr_4$ which displays Luttinger liquid behavior, $SrCu_2(BO_3)_2$ with its peculiar magnetization plateaus and $BaCuSi_2O_6$ undergoing a Bose-Einstein condensation of magnons. The research efforts on cold atoms include studies on dynamical properties used to identify a Mott-insulating phase of fermionic atoms in an optical lattice, on new phases possible in systems of bosonic atoms with long range interaction or "disordered" (bichromatic) lattices and on the issue of temperature calibration in experiments.

Systems with charge density wave (CDW) order represent a further important subject, which comprises the Raman study of the influence of electron-phonon interaction on the CDW state in rare-earth tritellurides and the exploration of the possible realization of an excitonic insulator and of the nature of the pressure induced superconductivity in 1T-$TiSe_2$. The pressure-induced magnetic order of the $4f$-compound $PrCu_2$ was studied by means of nuclear quadrupole resonance (NQR). Among to the transition metal oxides two systems were in our focus: sodium cobaltates and the colossal magneto-resistance manganites. An unusual first order transition between a Na-"liquid" and Na-"solid" phase in $Na_{0.82}CoO_2$ was observed in nuclear magnetic resonance (NMR) measurements. A scanning tunneling microscopy (STM) study elucidates the role of polarons in the metal-insulator transition of manganite films.

Tunable spin-orbit coupling was observed by angle-resolved photoemission spectroscopy (ARPES) detecting the the spin splitting of electronic bands at surfaces of $Bi_xPb_{1-x}Ag_2$. Moreover the reconstruction of electronic states and their transport properties were studied theoretically for basic models of interfaces between band- and Mott-insulators. New developments in the theoretical treatment of doped Mott-insulators and quantum phase transitions based on the concept of fidelity are reported. The development of a new impurity solver represents an important breakthrough for the application of dynamical mean field theory. By means extensive computational simulations the issue of supersolidity in ^{4}He has been further clarified.

The study of carbon related materials comprises infrared spectroscopy measurements of

the electric-field-induced gap in graphene bilayer systems, the theoretical analysis of transport properties in graphene nano-ribbons and electronic properties of carbon nanotubes combined with ferroelectrica and with artificially introduced defects. Our research in mesoscopic physics addresses issues of quantum measurements based on "quantum state tomography" using shot noise and the extension of fluctuation relation beyond the standard linear response regime. Finally, we report on new developments on the side computational algorithms and on the installation of a new high-vacuum STM facility with the aim to perform spin polarized STM studies.

1 Magnetism in quantum spin systems

In recent years the study of quantum dimer systems tunable by magnetic fields through quantum phase transitions has been one of the important areas of our research. In this period we report on the progress in the study of three specific systems, the spin ladders $(Hpip)_2CuBr_4$ and the frustrated dimer systems $SrCu_2(BO_3)_2$ and $BaCuSi_2O_6$ (Han purple). In a magnetic field the ladder system enters a regime described by a Luttinger liquid and is investigated by the PSI group of Joël Mesot by means of neutron scattering supported by the group of Thierry Giamarchi (UniGE) for the theoretical discussion. The other two compounds show unusual magnetization plateaus ($SrCu_2(BO_3)_2$) and a magnon Bose-Einstein condensation (BEC) in a magnetic field, as analyzed theoretically by the EPFL group of Frédéric Mila.

1.1 Phase diagram and controllable Luttinger liquid properties in spin ladder compounds

For one dimensional systems, Luttinger liquid (LL) theory [1] plays the same paradigmatic role as Fermi liquid theory plays for interacting fermions. Several characteristic features of the LL model have been observed in various experimental realizations, such as the power law behavior of some correlation or spectral functions. However, since the details of the interaction are rarely known, only a crude estimate of the power law exponents is usually possible. A precise quantitative check of the LL model was thus still missing. It is usually also not possible to check the universality of the LL theory, namely that several different correlations are totally fixed by a set of LL parameters (the velocity of excitations u and the LL exponent K).

Remarkably, spin ladder system opens the door to such a quantitative test. Its ground state consists of singlets made by the spins on the rungs. Applying a magnetic field transforms some of these singlets into triplets (triplons), that behave in one dimension essentially as interacting spinless fermions. This provides a system in which the band of triplons can go from totally empty to filled (one triplon per rung) by changing the magnetic field. In addition, since the microscopic Hamiltonian is perfectly characterized (all the exchange constant can be directly measured by neutrons or extracted from the magnetization measurements), there is no adjustable parameters for the LL theory. A spin ladder system in an experimentally accessible field range is $(C_5H_12N)_2CuBr_4$ [$(Hpip)_2CuBr_4$].

Over the last few years $(Hpip)_2CuBr_4$ has been investigated by Mesot and collaborators at PSI. With previous direct observation of magnon fractionalization this group clarified the nature of the spin excitation spectrum and demonstrated its tunability by an applied magnetic field [2]. Complementary to this study, they additionally investigated the phase diagram in temperature and magnetic field of this material by measurements of the specific heat and the magneto-caloric effect [3]. Their findings demonstrate the presence of an extended spin LL phase between the two field-induced quantum critical points and over a broad range of temperature (Fig. 1).

The recent extension of this study to lowest temperatures led also to the discovery of a field-induced, antiferromagnetically ordered phase [4]. Moreover, neutron diffraction and the magneto-caloric effect (MCE) was used to investigate this "classical" phase (Fig. 2) – a consequence of weak interladder coupling.

Aiming at a quantitative test of universal LL properties, Giamarchi and collaborators used a combination of techniques (Bethe Ansatz, exact diagonalization, time dependent density matrix renormalization group (DMRG) allowing a calculation at finite temperature) and computed the specific heat and magneto-caloric effects, to show a remarkable agreement between the predicted and measured quantities across the entire phase diagram [3]. Their study confirms that this system is remarkably well described by weakly coupled ladders. In addition, the peaks in the specific heat allow to map out the region in which the LL theory is applicable to this system. The LL parameters

could be determined directly using DMRG (*no* adjustable parameters) and the analytical formulas of the LL theory to compare with various quantities such as the NMR relaxation time $1/T_1$, the critical temperature to the ordered three-dimensional phase (directly related to the intraladder spin-spin correlation), and the ordered transverse moment. These predictions have been compared to the experimental results measured either by NMR [5] or neutrons [4]. The agreement is remarkable as shown in Fig. 3 providing the first quantitative test of the LL theory.

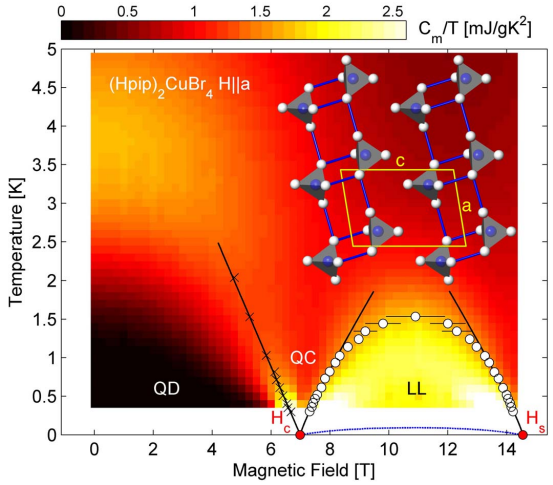

Figure 1: *Magnetic field – temperature phase diagram of $(Hpip)_2CuBr_4$ showing quantum disordered (QD), quantum critical (QC), and spin LL phases. The contour plot shows the magnetic specific heat as $C_m(T,B)/T$.*

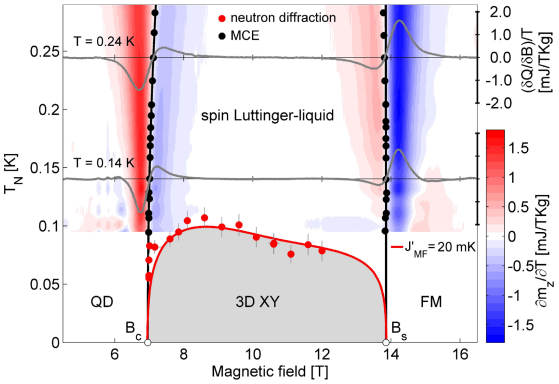

Figure 2: *Summary of the results on the field-induced ordered phase of $(Hpip)_2CuBr_4$. The crossover temperature to the spin Luttinger liquid phase is derived from MCE measurements (black dots) and the phase transition to the BEC (3D – XY magnetic order) from neutron diffraction (red dots). The contour plot is based on 18 individual field scans of the MCE (two shown as gray lines). The red line is based on a theoretical fit and accounts for the spin Luttinger-liquid state in the ladder subunits.*

The properties of the ordered phase turn out to be highly unconventional, influenced strongly by the spin LL state of the ladder subunits. Mesot and collaborators determined directly the order parameter (transverse magnetization), the ordering temperature, the spin structure, and the critical exponents around the transition. Using a minimal, microscopic model for the interladder coupling the quantum fluctuation corrections to the mean-field interaction were calculated by Giamarchi's group. In view of the rich phenomenology of spin ladders, this collaborative program is continued to address the quantum statistics of interacting triplons in one dimension and the spectrum emerging from the upper triplet modes in the spin LL phase. While the data analysis is ongoing, the latter results

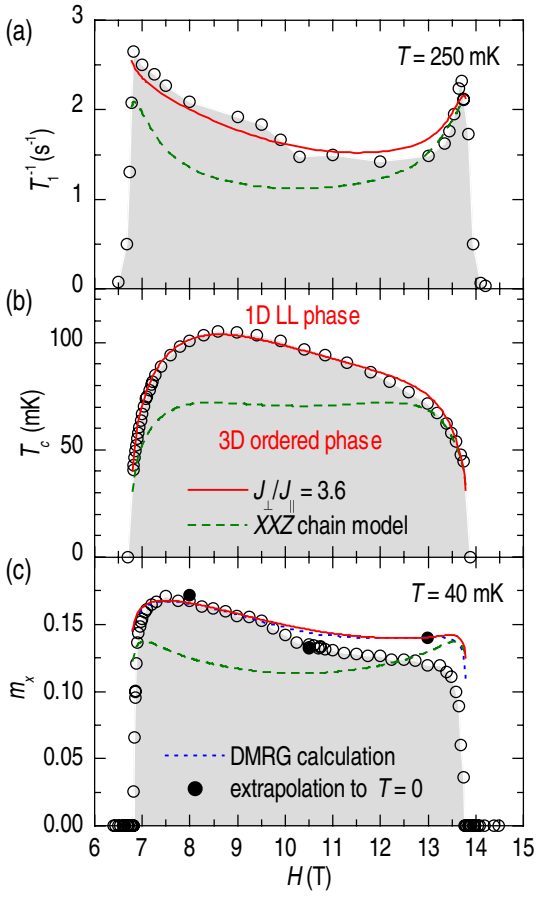

Figure 3: *Comparison of the predictions (red curve) of the LL theory with NMR data. The only adjustable parameter in the top curve is a single number, the hyperfine coupling constant. For the middle curve, the interladder coupling constant J' and for the bottom one an overall number relating the NMR splitting and the magnetization. The remarkable agreement of the whole magnetic field dependence provides a quantitative test of the LL theory.*

represent a major experimental breakthrough in spin ladder physics that considerably extends and possibly completes the understanding of the field-induced spin LL in a quantum spin ladder.

1.2 Magnetization plateaus of $SrCu_2(BO_3)_2$

Since the detection of magnetization plateaus in the two-dimensional frustrated quantum magnet $SrCu_2(BO_3)_2$ ten years ago, a lot of activity has been devoted to this system.

a) *Plateau sequence* Motivated by recent and conflicting reinvestigations of the magnetization curve, Mila and collaborators have developed an essentially unbiased method to predict quantitatively the plateau sequence. This method is based on a high-order expansion of the effective Hamiltonian by means of a perturbative continuous unitary transformation, combined with a mean-field investigation of the spin version of the effective Hamiltonian. This study has revealed an unexpected sequence of plateaus at 2/9, 1/6, 1/9 and 2/15 upon increasing the interdimer coupling [6]. The magnetization curve as a function of the interdimer coupling is plotted in Fig. 4, and the structure of the plateaus is depicted in Fig. 5. Recent, still unpublished, data seem to confirm the presence of two new plateaus at 2/15 and 1/6.

b) *Torque anomalies at magnetization plateaus* The group of Mila has also investigated the effect of Dzyaloshinskii-Moriya (DM) interactions on torque measurements of quantum magnets with magnetization plateaus in the context of a frustrated spin-$\frac{1}{2}$ ladder [7]. Using extensive DMRG simulations, they showed that the DM contribution to the torque is peaked at the critical fields, and that the total torque is non-monotonous if the DM interaction is large enough compared to the g-tensor anisotropy. More remarkably, if the DM vectors point in a principal direction of the g-tensor, torque measurements close to this direction will show well defined peaks even for small DM interaction, leading to a very sensitive way to detect the critical fields. Mila and collaborators propose to test this effect in the two-dimensional plateau system $SrCu_2(BO_3)_2$ [7].

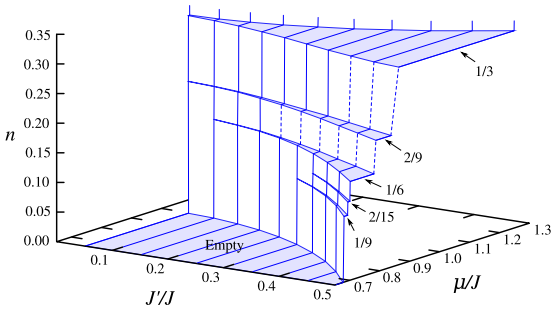

Figure 4: *Magnetization plateaus as a function of μ and J'/J. The boson density n is equal to the magnetization in units of the saturation value, and the chemical potential μ is equal to the magnetic field B.*

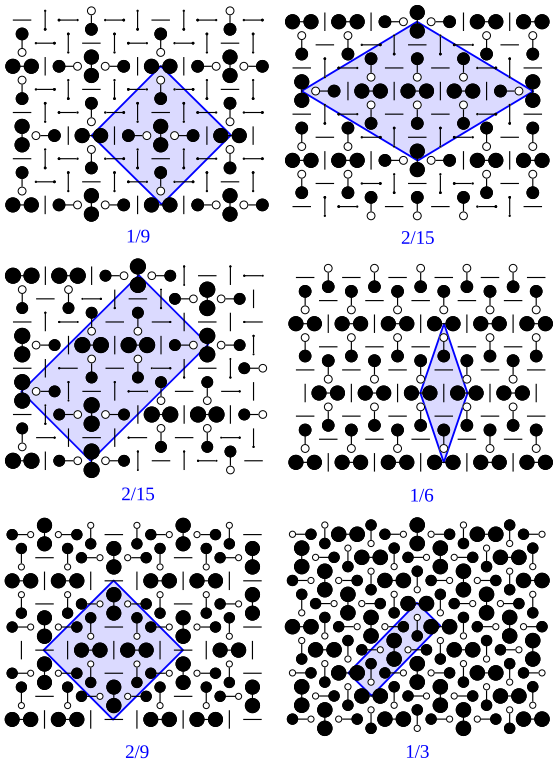

Figure 5: *Spin density (S^z) profile of the main plateaus at $J'/J = 0.5$. Full (empty) circles correspond to magnetization along (opposite to) the magnetic field. The radius of the circles is proportional to the magnetization amplitude.*

1.3 Theory of field-induced BEC in $BaCuSi_2O_6$

The closing of the gap of quantum magnets subjected to an external magnetic field is most conveniently interpreted as a Bose-Einstein condensation (BEC) of magnons, with a critical temperature T_c that scales with the field as $(H - H_c)^{2/D}$, where D is the effective dimensionality. The observation of a linear law ($T_c \propto (H - H_c)$) in the layered spin-$\frac{1}{2}$ dimer compound with frustrated interlayer coupling, known as Han purple $BaCuSi_2O_6$, came as a surprise in view of the three-dimensional structure of the system. Building on recent inelastic neutron scattering and NMR data, Laflorencie and Mila have investigated this issue in the context of a frustrated model with

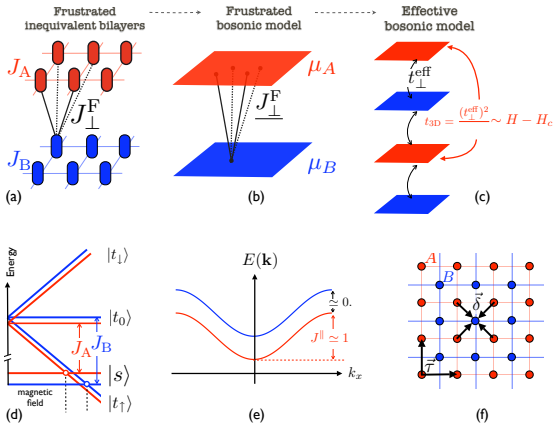

Figure 6: *Schematic models for $BaCuSi_2O_6$: (a) frustrated bilayer array with two types of dimers; (b) and (c) effective bosonic models in the field-induced critical regime: (b) frustrated hard-core bosons model with different chemical potential; (c) non-frustrated hard-core boson model with a field-dependent effective transverse hopping (see text); (d) the four energy states of isolated dimers A and B versus the external magnetic field; (e) triplet dispersions in isolated bilayers induced by the inter-dimer couplings $J^{\parallel}$; (f) view of the frustrated lattice (a) from above with the unit vectors τ and δ.*

two types of bilayers. A semiclassical treatment of the effective hard-core boson model shows that perfect interlayer frustration leads to a 2D-like critical exponent without logarithmic corrections and to a 3D low-temperature phase with different but non-vanishing triplet populations in both types of bilayers. These results suggest a simple phenomenology in terms of a field-dependent transverse coupling in the context of which the entire field-temperature phase diagram can be reproduced by means of Quantum Monte Carlo simulations [8]. The hierarchy of effective models that lead to this simple picture is summarized in Fig. 6.

1.4 Anomalous magnetic excitations in $Cu_2Te_2O_5X_2$

In a recently submitted paper [9], Prša *et al.* in Mesot's group present a neutron scattering study of the complex spin excitations in the coupled $S = 1/2$ tetrahedra systems $Cu_2Te_2O_5X_2$ (X = Cl, Br). Two anomalous features of the data cannot be adequately explained by their mean-field/RPA analysis: (1) the magnitude of the observed energy gaps and (2) the weakness of the Goldstone-like mode. This behavior on the way from isolated cluster states to the spin-waves of conventional ordered magnets may represent a new general type of behavior, strongly influenced by intercluster quantum fluctuations which has not been addressed in theory so far.

2 Cold atoms in optical lattices

The recent progress in cooling and manipulating cold fermionic gases in optical lattices allows to investigate phenomena at ever lower temperatures, where many-body effects generate new (quantum) phases of much interest in condensed matter physics. The high degree of isolation poses great challenges to their experimental investigation, while, at the same time, it allows to study features of many-body systems far from equilibrium. In a recent work, both aspects have been addressed, the problem of probing an equilibrium system as well as its evolution away from the equilibrium state. Discussing experiments on fermionic atoms in an optical lattice the ETHZ group of Gianni Blatter developed a theoretical scheme to analyze the so-called dynamical generation of double occupancy in order to establish a criterion for a Mott-insulating phase in such a system. The group of Thierry Giamarchi (UniGE) discussed two aspects of bosonic atoms: (1) the realization of a Haldane phase for bosonic atoms with long ranged interactions in an optical lattice and (2) the effect of disorder introduced by a bichromatic optical lattice. The group of Matthias Troyer (ETHZ) has performed *ab initio* simulations of ultracold gases in optical lattices in order to provide a scheme for experimental temperature calibration.

2.1 Dynamical generation of double occupancy

In a recent experiment the group of Tilman Esslinger at ETHZ has probed their strongly correlated system of fermionic ^{40}K atoms via excitations by modulating the lattice potential (hopping matrix element t) and subsequently measuring the number of doubly occupied lattice sites [80], a technique called "dynamical generation of double occupancy" (DGDO). By characterizing the (non)-linear response corresponding to such an experiment, Huber and collaborators in Blatter's group provide a theoretical interpretation of this experiment [10, 11]. Developing an extension of a slave-boson-type of mean field theory, they find criterions to conclude via the DGDO techniques that a Mott phase can be inferred from these measurements, provided that sufficiently low temperatures $k_BT \ll t$ can be reached.
For short times of modulation, this procedure can be used to obtain information about

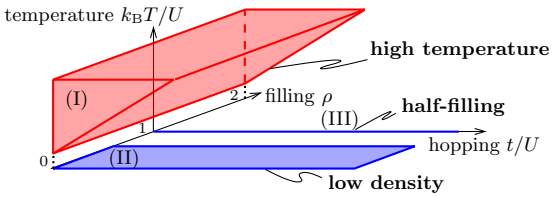

Figure 7: *Regimes where the dynamically generated double occupancy probe is analyzed: high temperatures (I) are discussed in the atomic limit; the regime at zero temperature and low densities (II) involves the solution of a two-particle problem; the situation at half filling and $T = 0$ (III) is done within a slave-spin mean-field analysis.*

the equilibrium state [10]. For long modulation times, the system is driven away from its ground state and the experiments show a saturation in the double-occupancy. For values $t/U \ll 1$ (U: onsite particle-particle repulsion), the evolution of the system and its non-equilibrium steady state were analyzed via mapping the problem to an effective two-level system coupled to an external bath and undergoing (in)coherent Rabi oscillations [11].

The theoretical analysis of the DGDO technique involves exactly solvable limiting cases of the Hubbard-like Hamiltonian of this system, namely the atomic limit ($t = 0$) and the two-particle problem, with results relevant in the regimes $U, T \gg t$ and for band filling $\rho \ll 1$ (set $k_B = 1$), see regimes (I) and (II) in Fig. 7. In order to discuss the Mott physics within the DGDO technique at low temperatures, regime (III) in Fig. 7, use is made of a slave-spin mean-field approximation which captures the most relevant physics on both the t and U scale.

A further interesting aspect is the evolution of the system into a non-equilibrium steady state. In the experiment, a saturation of doubly occupied sites is reached on a time-scale of the order of one hopping time $\propto \hbar/t$ which suggests that a local description should capture the essential physics. Focusing on one bond with a singlet state and a doublon-hole state (Fig. 8), Huber and coworkers show that the lattice modulation drives Rabi oscillations with frequency $\Omega_R = 2\delta t/\hbar$. The coupling to the rest of the system is taken into account by an effective bath. In this treatment the generated doublons diffusing into the bath do not decay and eventually lead to the observed saturation in a driven non-equilibrium steady-state. In order to cope with some short-comings of this local approach a systematic improvement via inclusion of larger clusters and a self-consistent treatment of the system-bath interactions is currently under way.

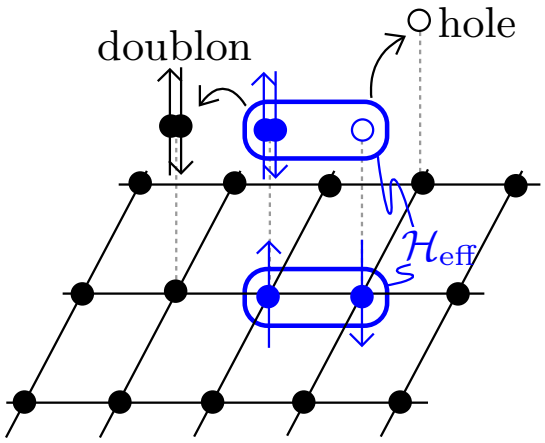

Figure 8: *Illustration of the effective Hilbert space $\mathcal{H}_{eff}$ consisting of one bond embedded in an array of sites. The bath degrees of freedom consist of all doublon-hole configurations where the pair resides on a different bond than where it was created.*

2.2 Haldane phase in cold atomic systems

Recently ultracold polar molecules or atoms with large magnetic dipole moments have allowed to have long range interactions present in cold atomic gases. Giamarchi and collaborators studied the consequences of such interactions on the properties of bosons in a lattice. With nearest neighbor repulsion, two phases are naively possible: (i) a Mott-insulator with one boson per site, occurring when the nearest neighbor repulsion V is weak compared to the on-site U; (ii) a charge density wave of bosons, with a regular arrangement of two and zero bosons per site, when $V \gg U$. Remarkably a third phase was found [81] at the boundary between these two phases. Giamarchi and collaborators analyzed in details the properties of such a phase [12], using both numerical (DMRG) and analytical techniques (bosonization). This phase is the analogous of the Haldane phase for spin 1 systems and possesses a hidden topological order (string order). They showed that the string order parameter can be directly experimentally probed. Moreover they investigated the consequences of such a phase for systems made of coupled bosonic chains.

2.3 Bosons in bichromatic lattices

Cold atomic gases have provided also a remarkable system to study the competition between interactions and disorder in quantum systems. For bosons such a competition can lead to the appearance of a Bose glass phase. One very efficient way to study this issue is to introduce the "disorder" by adding a second periodic potential incommensurate with

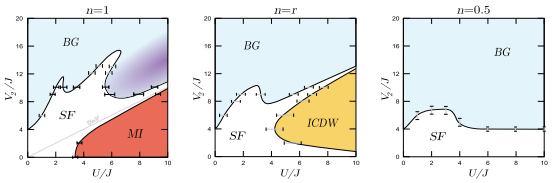

Figure 9: *Phase diagram of bosons in a bichromatic lattice for several densities n. r is the ratio of the potential wavelength. J is the kinetic energy, U the onsite repulsion and V_2 the strength of the second periodic potential. MI, SF and ICDW denotes a Mott-insulator, a superfluid and an incommensurate charge density wave. Due to the bichromatic lattice there is a Bose glass (BG) phase, analogous to the one existing for disordered bosons.*

the first lattice potential [82]. Such systems represent in fact quasi-crystals and it is, thus, important to understand how much they resemble a disordered system. For this purpose Giamarchi's group performed such a study using DMRG and analytical (bosonization etc.) techniques. They computed the phase diagram (Fig. 9), and showed that it contains features similar to the ones of the disordered case [13]. They determined the position of the various phases (among them a gapless localized phase corresponding to the Bose glass) and studied the expansion properties of such a system. This analysis should allow for a better comparison with the existing and coming experiments on such systems.

2.4 Computational approach to the Hubbard model in optical lattices

In view of the property that ultra-cold atomic gases constitute physical realizations of idealized models of strongly interacting many-body systems, such as the Hubbard model for bosons, the group of Troyer focused on quantitative validations of experiments and testing their use as analog quantum simulators. In Ref. [14] they have investigated the question of heating as the optical lattice is ramped up and a Bose gas enters the Mott-insulator regime. Their results state that the gas stays cold enough to remain degenerate deep into the Mott regime. Furthermore, they could show that the standard time-of-flight images used to measure momentum distributions differ significantly from the true momentum distribution, since the expansion times are too short and near-field Fresnel effects significantly broaden peaks in the distribution [15]. Finally, Scarola *et al.* propose a probe to measure the "core compressibility" to check the existence of incompressible phases in trapped fermionic atoms in optical lattices [16].

3 Charge density wave system

Rare-earth tri-tellurides (RTe$_3$, with R = La – Sm, Gd – Tm) were recently revisited and recognized as an intriguing example of easily tunable 2D materials undergoing a charge density wave (CDW) phase transition. The formation of the CDW condensate, within Te-layers, is to a large extent driven by Fermi surface (FS) nesting. Consequently, the FS is gapped over a sizeable portion. In continuation of their previous studies, the ETHZ group of Leo Degiorgi has investigated the influence of the electron-phonon coupling using Raman scattering and X-ray diffraction measurements.
The manner in which superconductivity and other types of electronic order combine continues to remain an ongoing puzzle. A recent addition to this story has come from the discovery of superconductivity in copper-intercalated 1T-TiSe$_2$, in the vicinity of the CDW state that was also proposed as a possible realization of the excitonic condensate. In this project the groups of Philipp Aebi (UniNE and UniFR) and of László Forró (EPFL) explore the possible realization of an excitonic insulting phase and pressure-induced superconductivity in this system. In addition the EPFL group of Marco Grioni has used angle-resolved photoemission spectroscopy (ARPES) to investigate the evolution of electronic properties in the related compound 1T-TiS$_2$ upon doping Nb for Ti.

3.1 RTe$_3$: evidence for CDW lattice coupling

The electron-phonon coupling is of fundamental relevance for the development of several types of charge ordering in solids, of which the charge density wave (CDW) state. One class of quasi-2D compounds well suited to address this issue are the rare-earth (R) tri-tellurides, RTe$_3$, which host a CDW state already at 300 K. In their first optical investigations, Degiorgi and collaborators have observed the excitation across the CDW-gap and discovered that this gap is progressively reduced upon compressing the lattice either with chemical substitution (i.e. by changing R) or with externally applied pressure.
The coupling between vibrational modes and CDW condensate in these prototype 2D systems has been investigated in Degiorgi's group by means of Raman scattering response [17]. These studies were performed for quasi-two-dimensional rare-earth tri-tellurides RTe$_3$

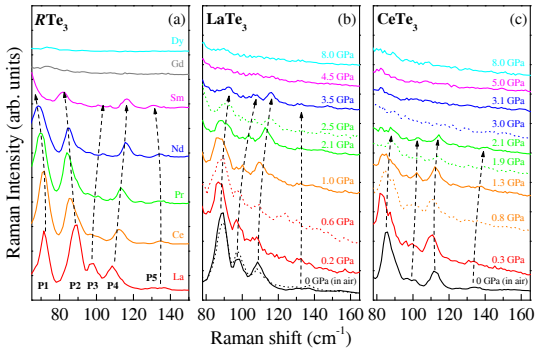

Figure 10: *Raman scattering spectra at 300 K for the RTe_3 series at ambient pressure (a), and for $LaTe_3$ (b) and $CeTe_3$ (c) for increasing (continuous lines) and decreasing (dashed lines) pressure. All spectra have been shifted for clarity.*

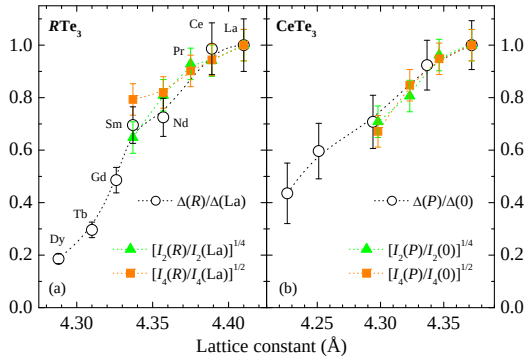

Figure 11: *Comparison between the amplitude of the CDW-gap (open circles) and the integrated intensities (I) of the P2 (full triangles) and P4 (full squares) peaks, raised to 1/4 and 1/2, respectively (see text) as a function of the lattice constant for the RTe_3 series (a) and for $CeTe_3$ under pressure (b). All quantities are normalized to their starting values.*

(R = La, Ce, Pr, Nd, Sm, Gd and Dy) at ambient pressure, and for $LaTe_3$ and $CeTe_3$ under externally applied pressure. Fig. 10a summarizes the Raman scattering spectra for the whole RTe_3 series (i.e. chemical pressure). Four distinct modes at 72, 88, 98 and 109 cm^{-1} and a weak bump at 136 cm^{-1} (labelled P1-P5, respectively) can be identified in the La compound. The P1 mode slightly softens from La to Nd and slowly moves outside the measurable spectral range at ambient pressure. The remaining modes weakly disperse and progressively disappear when going from the La to the Dy compound along the rare-earth series.

Panels b and c in Fig. 10 display the Raman scattering spectra of $LaTe_3$ and $CeTe_3$ under increasing and decreasing externally applied pressure. For the applied pressure the behavior of the different modes is very similar to the case of chemical pressure, supporting the conclusion that both types of pressure change the system equivalently. The pressure dependence is fully reversible since upon decreasing pressure the modes reappear again. The observed phonon peaks can be ascribed to the Raman active modes for both the undistorted as well as the distorted lattice in the CDW state by means of a first principle calculation.

A further important result is the observation of a systematic decrease of the integrated intensity (I) of the most prominent peaks P2 and P4 in the Raman spectra of Fig. 10 with pressure, which bears a striking similarity with the behavior of the amplitude of the CDW-gap Δ (i.e. the order parameter) upon compressing the lattice, as obtained from the optical conductivity. Fig. 11 shows that the intensities of the P2 and P4 peaks scale fairly well with Δ^4 and Δ^2, respectively, suggestive of a coupling between the lattice vibrational modes and the CDW condensate. This is not surprising, as calculations predict the existence of these peaks only for the distorted lattice structure. Furthermore, the specific behavior ($I \sim \Delta^q$, q=2 or 4) is consistent with theoretical predictions for the intensity in the distorted phase of originally silent modes, obtained from a group theoretical analysis in the framework of Landau's theory of second order phase transitions.

Degiorgi and collaborators performed additionally an X-ray diffraction study on the $LaTe_3$ and $CeTe_3$ compounds as a function of pressure from which they can extract the lattice constants and the CDW modulation wavevector. The data show that the intensity of the CDW satellite peaks tend to zero with increasing pressure, thus providing direct evidence for a pressure-induced quenching of the CDW phase. These findings further support the equivalence between chemical and applied pressure in RTe_3 , put forward by the previous report on optical investigations [18].

3.2 1T-$TiSe_2$: excitonic insulator

In the early 1960s, a new insulating phase was predicted to possibly exist at low temperature in solids having small energy gaps: the excitonic insulator. Jérome *et al.* [83] published an extended study of this phase developing a BCS-like theory of its ground state. However, at that time an experimental realization of this phase was missing.

The excitonic insulator phase may occur in a semi-metallic or semiconducting system exhibiting a small (negative, respectively positive) gap. Indeed, for a low carrier density, the Coulomb interaction is weakly screened,

allowing therefore bound states of holes and electrons, called excitons, to build up in the system. If the binding energy E_B of such pairs is larger than the gap E_G, the energy to create an exciton becomes negative, so that the ground state of the normal phase becomes unstable with respect to the spontaneous formation of excitons. According to Jérome *et al.* [83], at low temperature, these excitons may condense into a macroscopic coherent state in a manner similar to Cooper pairs in conventional BCS superconductors. Kohn [84] argued that exciton condensation may lead to the formation of charge density waves (CDW) of purely electronic origin (neglecting any lattice distortion), characterized by an order parameter.

1T-$TiSe_2$ is a layered transition-metal dichalcogenide exhibiting a commensurate $(2 \times 2 \times 2)$ CDW [85] accompanied by a periodic lattice distortion below the transition temperature of $T_c \cong 200$ K. The origin of its CDW phase was controversial for a long time. Different scenarios have been proposed, the best candidates being a band Jahn-Teller effect [86] and the excitonic insulator phase. An angle-resolved photoemission spectroscopy (ARPES) study by the group of Aebi, evidencing directly the CDW, gave recently much support to the latter by comparison between experiment and theory [19]. Photoemission intensity maps were generated with the spectral function calculated in the framework of the exciton condensate model which was previously adapted to $TiSe_2$.

Recently a detailed model calculation has been presented by Aebi's group [20]. In particular, the renormalized band dispersions arising in the CDW phase, as a consequence of a non-zero order parameter Δ, and their spectral weight are analyzed to show the effect of the exciton condensation on the band structure. The discrepancy with density functional theory (DFT) is also discussed. Indeed, DFT predicts for $TiSe_2$ a semi-metallic configuration, with a large overlap of the order of 500 meV between the valence and conduction bands. A possible reconciliation of DFT prediction with the room temperature band structure derived from ARPES is obtained in two steps (Fig. 12). First, in the normal phase ($\Delta = 0$ meV) as a consequence of a slight uncontrolled Ti doping of the sample, the valence band of Se $4p$ character is partially shifted into the occupied states, while the conduction bands remain mainly unchanged (Fig. 12a to Fig. 12b). Secondly, strong excitonic fluctuations (above T_c) are mimicked in the system by considering a non-zero order parameter (Fig. 12b to Fig. 12c). This last band structure (Fig. 12c) shows a very good agreement with experiment. In other words, by the combined effects of Ti doping and excitonic fluctuations, the DFT band structure is shown to be similar to what is measured at room temperature.

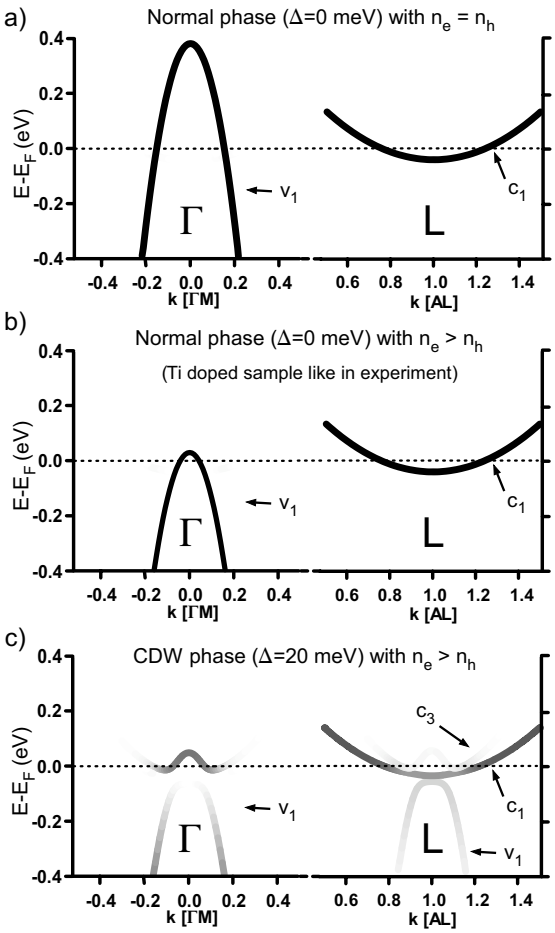

Figure 12: *Calculated band structure of $TiSe_2$ in the framework of the exciton condensate model. a) To ensure charge neutrality, given by an equal number of holes and electrons for this semimetal, the valence band, having a small effective mass, is high in the unoccupied states for the normal phase ($\Delta = 0$ meV). This configuration is similar to what density functional theory predicts near the Fermi level. b) As a consequence of the slight Ti doping present in the $TiSe_2$ samples, the valence band is partially shifted into the occupied states. c) At room temperature already, strong excitonic fluctuations, modelized by a non-zero order parameter ($\Delta = 20$ meV), renormalize strongly the dispersions and the spectral weights. This last band structure turns out to be very similar to what is observed, reconciliating in this way density functional theory with the experiment. The normal state ($\Delta = 0$ meV) dispersions, which correspond to the case b), have been fitted from the experiment.*

3.3 1T-$TiSe_2$: pressure-induced superconductivity

Recent findings of superconductivity in copper-intercalated 1T-$TiSe_2$ triggered a great deal of activity [19][87, 88, 89, 90, 91, 92, 93] due to the possible connection between the superconductivity and the CDW or, possibly, excitonic insulating state. The superconductivity in Cu_xTiSe_2 was found to appear as the CDW state fades away with doping, in a certain region around a critical doping [87]. The dependence of the superconducting transition temperature on the copper content shows a dome-like structure, characteristically found in phase diagrams of cuprate high temperature superconductors, some heavy fermion compounds and layered organics [94, 95, 96]. The superconductivity in those compounds is thought to be tightly related to neighboring antiferromagnetic ordering, with superconductivity located around a (purely electronic) quantum critical point (QCP) [97, 95]. On the other hand, the case of 1T-$TiSe_2$ signals the possibility of a novel state, where superconductivity appears around a new type of quantum critical point, unrelated to magnetic degrees of freedom [90, 93], although more conventional scenarios have also been proposed [89].

In order to examine the role of the quantum critical point in connection with superconductivity the route via pressure was chosen by Forró's group. The single crystal 1T-$TiSe_2$ samples used for this study were grown by a conventional vapor transport method and the sample stoichiometry was verified by X-ray and resistivity measurements. Pressure measurements in the low-pressure range of 0 – 2 GPa were carried out using a standard piston cylinder pressure cell, while those in the pressure range of 2 – 10 GPa were performed in an opposed anvil Bridgeman-type pressure cell with tungsten carbide anvils and steatite medium. A dilution refrigeration cryostat was used to achieve base temperatures of 70 mK.

Fig. 13 shows the evolution of the resistivity with temperature and pressure. In the low-pressure range up to 1.1 GPa the resistivity curves resemble closely in shape to the one at the ambient pressure [85], although the strong upturn in resistivity that signals the CDW transition becomes gradually less pronounced as pressure increases. Also, the CDW transition temperature, T_{CDW}, identified as the point of maximal upturn in $\rho(T)$ [85], gradually shifts to lower temperatures. In this pressure range the resistivity above the transition shows a weak non-metallic temperature dependence.

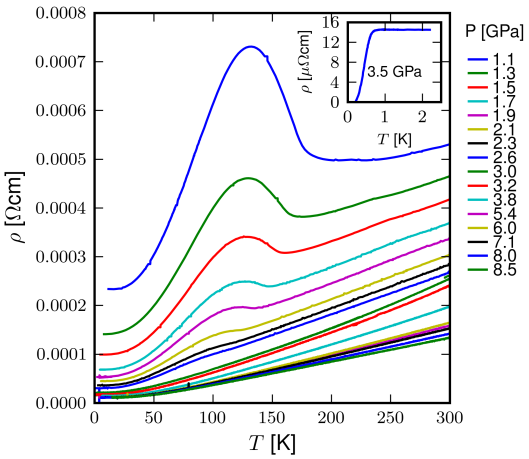

Figure 13: *Pressure dependent resistivity measurements of 1T-$TiSe_2$. The ambient pressure run was omitted to emphasize the high pressure data. The inset shows the emergent superconducting transition at pressures above 3 GPa.*

At temperatures well below the transition the electrons uncondensed into the CDW state give the metallic character to the resistivity. Further application of pressure uncovers a high-temperature region where the resistivity behaves linearly with temperature, as expected from a well-behaved metallic system dominated by electron- phonon scattering. Simultaneously the temperature of the CDW transition decreases monotonously and becomes difficult to identify above 2.5 GPa, whereas above 3 GPa any identifiable sign of CDW transition disappears in the resistivity measurements. In the pressure range of 2 – 4 GPa superconductivity appears at low temperature (Fig. 13, inset).

The new phase diagram of pristine 1T-$TiSe_2$ under pressure complements and puts recently

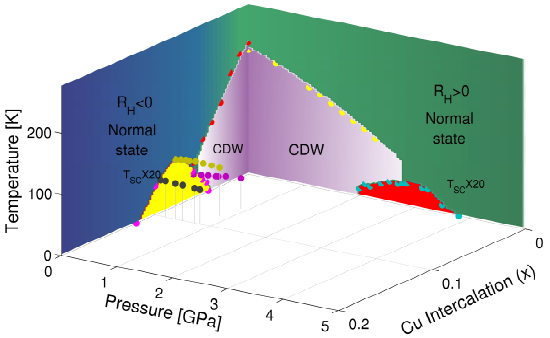

Figure 14: *The present knowledge of the phase diagram of 1T-Cu_xTiSe_2, where the horizontal axes stand for pressure and the content x of the intercalated copper. The empty space between two superconducting domes on the axes suggests future investigations in this compound.*

reported superconductivity in Cu-intercalated 1T-$TiSe_2$ in a new light. Fig. 14 summarizes our present knowledge of the phase diagram of 1T-$TiSe_2$ in the temperature, pressure and copper doping content parameter space. It is based on the present study in Forró's group and recent work by Morosan *et al.* [87] and by Budko *et al.* [88]. The absence of dopants in the present case implies that closure of the superconducting dome in 1T-$TiSe_2$ is unrelated to impurity-induced pair-breaking. Forró and collaborators have also shown that qualitatively different electronic states appear along the P and x axes, marked by different signs of the Hall coefficient in the normal state, dissimilar maximum superconducting transition temperatures T_c^{Max} (1.8 K versus 4.15 K for pressure and intercalation, respectively) and diverse magnetic properties of the superconducting state. These differences leave open the question, whether two separate superconducting domes emerge in this phase diagram, corresponding to two distinct critical points. The alternative perspective of a critical line in the $T = 0$ plane of Fig. 14, covered by a "superconducting tunnel", is a challenging topic for future studies.

3.4 1T-$Nb_xTi_{1-x}S_2$; doping of a 2D semiconductor

Grioni's group has studied by ARPES 1T-TiS_2, another member of this family, and the effect of Nb substitution for Ti on the electronic structure. Pure 1T-TiS_2 is predicted to be a semiconductor, but previous optics and transport measurements have given inconsistent energy gap values ranging from to more than 1 eV down to nearly zero. The sample exhibits metallic conductivity down to 4.2 K. This is illustrated by the ARPES data of Fig. 15. The energy-momentum intensity map clearly shows an indirect gap of 0.7 eV between the top of the Se $4p$ valence band at the Γ point, and the bottom of the Ti $3d$ conduction band at the M point. It corresponds to a degenerate semiconductor, with shallow and elongated electron pockets centered at the M points. The metallic character is clearly due to additional carriers – most probably the result of a slight off-stoichiometry – which populate the bottom of the conduction band. These pockets get progressively deeper when Ti (d^2) is substituted by Nb (d^3), as shown in Fig. 15a, but the electrical conductivity actually decreases, and an insulating state develops below ∼100 K.

This unexpected behavior is clarified by the evolution of the spectral function at the Fermi surface. Fig. 16 shows spectra measured at

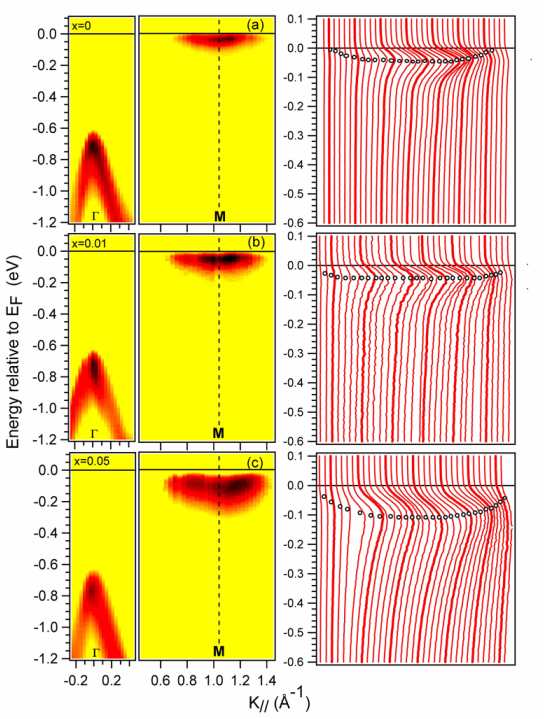

Figure 15: *Left: ARPES intensity maps of 1T-$Nb_xTi_{(1-x)}S_2$ for $x = 0$ (a); $x = 0.01$ (b) and $x = 0.05$ (c) around the Γ and M points of the Brillouin zone. The right panel shows the ARPES spectra around M.*

the edge of the M-point pocket for $x = 0$ and $x = 0.05$, symmetrized around the Fermi energy (E_F) to remove the metallic cutoff. At $x = 0$ a coherent quasiparticle peak develops at low temperature, with weak incoherent sidebands reflecting moderate correlations. By contrast, the spectral function is mostly incoherent in the $x = 0.05$ sample, and a narrow pseudogap opens at low temperature around E_F. The presence of a pseudogap suggests that the added carriers experience stronger interac-

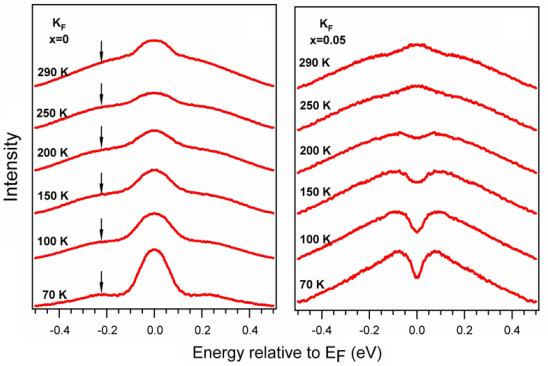

Figure 16: *Symmetrized ARPES spectra of 1T-$Nb_xTi_{(1-x)}S_2$ ($x = 0$, left; $x = 0.05$, right) measured at the Fermi surface. The coherent QP peak is suppressed by doping, and replaced by a narrow dip.*

tions, possibly suggesting an approaching electronic instability (e.g. a CDW) which cannot fully develop due to disorder and the increasing "fuzziness" of the Fermi surface.

4 $PrCu_2$: tuning magnetism with pressure in a $4f$-electron system

The group of Hans-Ruedi Ott (ETHZ) investigated the magnetic properties of $PrCu_2$ by means of nuclear quadrupole resonance (NQR) under varying pressure and temperature. This intermetallic compound is a Van Vleck paramagnet but, due to a spontaneous ordering among the Pr^{3+} quadrupole moments, exhibits an induced cooperative Jahn-Teller (JT) distortion at $T_{JT} = 7.6$ K. Neutron-diffraction experiments reveal the existence of an incommensurate antiferromagnetic (AF) order of the $4f$ Pr^{3+} magnetic moments below 54 mK [21]. Moreover the application of pressures exceeding 12 kbar establishes an AF order among the local Pr^{3+} moments below $T_{AF} \approx 9$ K [98, 99].

The mean-field calculations considering the crystal electric field (CEF) effect on the $4f$ electron orbitals of the Pr^{3+} ions indicate that the growth of the exchange interaction between the $4f$ Pr^{3+} magnetic moments can lead to the onset of a magnetically ordered phase of $PrCu_2$ at high pressures [22]. The comparison between the calculated and the experimental phase diagram is shown in Fig. 17a. The results of the calculations clearly show that the $P-T$ phase diagram of $PrCu_2$ can be explained by simply introducing a pressure-dependent exchange coupling between nearest-neighbor Pr-ions.

In order to gain more information on the transition itself, Ott and collaborators carried out NQR experiments at 7.8 and 15.5 kbar and various different temperatures between 0.65 and 300 K. The NQR spectra recorded at 15.5 kbar for $T \leq 10$ K are shown in Fig. 17b. On approaching $T_{AF} \simeq T_{JT}$ from above, the spin-echo intensity is progressively reduced and eventually reaches the detection limit below 6.25 K. A tiny spin-echo is then recovered only at the much lower temperature of 0.65 K. Upon cooling a blurring of the main peak is noted. The spectral weight is transferred to lower frequencies, and the signal extends over a broader spectral range.

In these data there is no evidence for the line splitting expected for a commensurate order. In the present case the broadening is apparently so severe that the spin-echo falls below the detection limit below 6.25 K. Upon further cooling, the ordered magnetic moment satu-

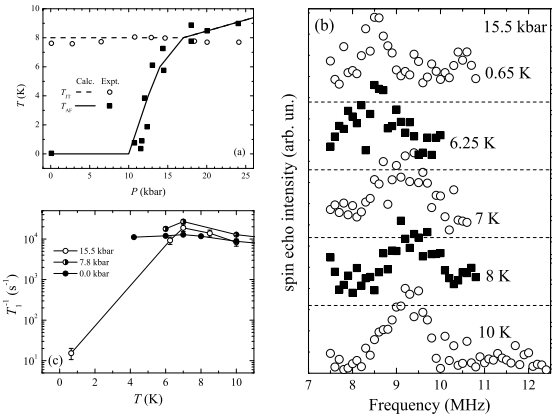

Figure 17: *(a) Pressure-temperature phase diagram of $PrCu_2$ for $P < 26$ kbar and $T < 10$ K. Open and full symbols reproduce the experimentally determined values of T_{JT} and T_{AF}, respectively (data from [98, 99]). Dashed and solid lines represent T_{JT} and T_{AF}, respectively, calculated within the molecular-field CEF model, as described in the text. (b) ^{63,65}Cu-NQR spectra of $PrCu_2$ at 15.5 kbar and as a function of temperature. Dashed lines indicate the zero-intensity line for each spectrum. (c) ^{63,65}Cu-NQR spin-lattice relaxation rates of $PrCu_2$ as a function of temperature and for different pressures: 0.0 (full symbols), 7.8 (half-filled symbols), and 15.5 kbar (open symbols).*

rates and the spectral weight transfer stops. Eventually, at much lower temperatures, the large difference between the thermal populations of the nuclear levels provokes an enhancement of the spectral intensity until it exceeds the noise level again at 0.65 K. The presence of a diffuse background in the spectrum at this temperature is an indication for an incommensurate order, as is the AF magnetic phase at ambient pressure below 54 mK which suggests that $PrCu_2$ tends to adopt an incommensurate magnetic order.

The temperature dependencies of the spin-lattice relaxation rate T_1^{-1} and the spin-spin relaxation rate T_2^{-1} have been measured under pressure. Down to 7 K the relaxation rates measured at 15.5 kbar are of similar magnitude as those measured at lower pressure. Upon further cooling to 0.65 K, T_2^{-1} decreases by a factor of approximately 4 and T_1^{-1} exhibits a dramatic drop of more than three orders of magnitude (Fig. 17c). On approaching T_{JT} from above, increasing fluctuations of the electric-field gradient lead to a slight enhancement of the relaxation rates. As the system enters the quadrupole-ordered JT phase, these fluctuations are reduced. At low pressure ($P <$ 12 kbar) the magnetic moments are disordered in the JT phase and sizable magnetic fluctua-

tions below T_{JT} lead to rather high relaxation rates at low temperature. At 15.5 kbar, however, the JT transition is accompanied by AF ordering and the magnetic degrees of freedom are reduced, as well. Consequently a much larger decrease in the relaxation rates is expected and observed.

5 Transition metal oxides

Transition metal oxides represent another important class of materials where strong electron correlation leads to spectacular properties. One important group, the cuprates, are part of Project 2 as they give rise to high-temperature superconductivity. Here we report on new NMR results for Na_xCoO_2 by the group of Hans-Ruedi Ott (ETHZ) showing evidence for a transition between a Na-"liquid" and a Na-"frozen" phase. Øystein Fischer's group studies the role of polarons in the metal-insulator transition in manganite thin films by means of STM.

5.1 Na_xCoO_2: two-dimensional Na-liquid

The recent activities in probing the physical behavior of the compound series Na_xCoO_2 ($0.3 < x < 1$) revealed a number of exciting features with respect to structural, electronic, magnetic and superconducting properties upon varying x. Quite generally these compounds may be regarded as composed of stacks of alternating Na and Co-O layers. The role of the Na layers and the x dependence of the Na-ion arrangements have been discussed in the recent years. The itinerant electronic and the magnetic degrees of freedom are concentrated in the Co-O layers. Depending on the value of the Na concentration x, different ground states were identified. The work reported here is a detailed ^{23}Na NMR investigation of the compound $Na_{0.8}CoO_2$ done by Ott's group at ETHZ. The data are to some extent in conflict with previously published details of structural features of the Na sublattice. Results of diffraction experiments were discussed in relation with models describing selected static vacancy arrangements, while aspects of the motion of Na-ions have been addressed to a much lesser extent. The new results give clear evidence that the dynamics of the Na ions is a dominating factor for the understanding of these compounds at temperatures exceeding 200 K, where a growing diffusion of the Na-ions sets in. Upon increasing temperature, this motion leads to a first order phase transition, most likely indicating the melting of the 2D layers of the Na sublattice at 291 K [23].

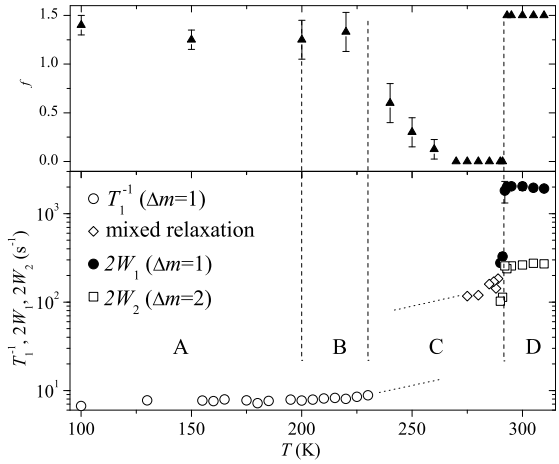

Figure 18: *The upper panel contains the relative intensity f of the satellites with respect to the central line. In the lower panel, ^{23}Na NMR spin-lattice relaxation rates of $Na_{0.8}CoO_2$ between 100 and 310 K are shown. Hereby, different relaxation mechanisms were considered.*

This melting is reflected in the ^{23}Na NMR spectra and in the spin-lattice relaxation rate (Fig. 18). A drastic change occurs, i.e. an abrupt quenching of the quadrupolar satellite component of the spectrum between 295 and 290 K, but no significant variation of the rather narrow and Lorentzian shaped central line in the same temperature interval is observed. Upon further reduction of the temperature, the quadrupolar satellites reappear below 270 K. The most obvious result is the drastic change in the relaxation behavior between 292 and 291 K. It indicates the first order transition that was previously reported, based on results from diffraction and resistivity experiments.

Considering the details in the NMR data across the transition, i.e. no significant change in the narrow signal of the central line, the abrupt reappearance of narrowed satellites and the discontinuous change in relaxation features, it seems difficult to identify the transition to be of common structural type. In particular, these data are not compatible with any structural change from one static arrangement of inequivalent Na sites to another, a possible scenario if it is kept in mind that $x = 0.8$. Instead these observations could suggest that for $T \geq 292$ K the Na layers adopt a 2D-liquid state, in the sense that the motion of the Na ions prevents the formation of a static structure with a well defined allocation of sites. Indeed the ^{23}Na NMR response here resembles that previously observed in superionic conductors with planar Na layers.

5.2 Local electronic properties of manganite thin films

The colossal magneto-resistance (CMR) effect, and the associated insulator-to-metal transition at $T = T_{MI}$, are a manifestation of the subtle balance of competing interactions coupling spin, orbital, charge and lattice degrees of freedom in manganites. While the double exchange mechanism [100] was proposed to explain the ferromagnetic metallic ground state, transport properties of the high-temperature insulating phase have been attributed to the presence of polarons [101]. However there is no consensus on the fate of these polarons at the transition. Moreover, the competition between different interactions is thought to give rise to the coexistence of different phases at the nano- or microscopic scale [102].

Scanning tunneling spectroscopy (STS) was used in Fischer's group to study two kinds of $La_{0.67}Ca_{0.33}MnO_3$ (LCMO) samples [24]: ultrathin highly-strained films grown on $SrTiO_3$ (STO) ($T_{MI} = 153.8$ K) and weakly-strained films grown on $NdGaO_3$ (NGO) ($T_{MI} = 235$ K). For both types of films, the topography exhibits plateaus separated with steps of multiple unit cell height. At all temperatures, tunneling conductance maps do not reveal any static phase separation over the typical length scales of topographic features [25].

Normalized conductance spectra are presented in Fig. 19a and b. In the paramagnetic insulating phase, the curves exhibit for both types of films a depletion close to zero bias, flanked by kinks or conductance peaks. This depletion becomes increasingly marked on cooling towards T_{MI} and survives in the metallic phase.

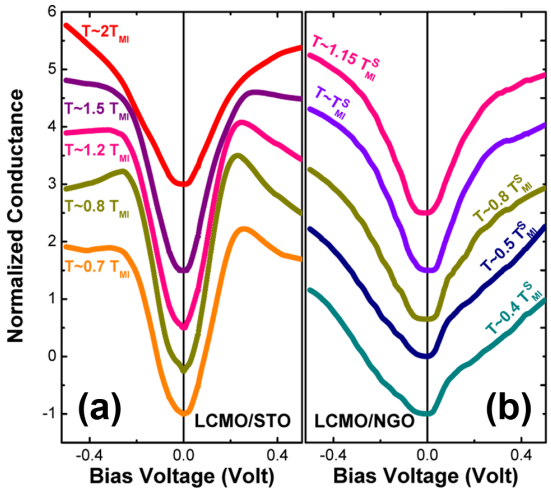

Figure 19: *(a) and (b) Normalized conductance at different temperatures for the high- and the low-strained samples.*

In the case of the highly-strained film (Fig. 19a), peak-like features identified as the spectral signature of polarons [26] develop at the flanks of the depletion and become increasingly sharp as temperature decreases. Above T_{MI}, the peaks broaden and are no longer observed at 310 K, probably because of a shortening of quasiparticle lifetime. For the weakly strained films (Fig. 19b), only a kink is detected, which becomes more pronounced and shifts towards lower energies on cooling below T_{MI}. Both films exhibit a polaronic gap/pseudogap in the insulating phase, and more strikingly also in the metallic phase. The gap magnitude globally decreases upon cooling (Fig. 20a).

Two scenarii have been invoked as possible explanations for the observed spectroscopic properties. The first involves the appearance below T_{MI} of a low-energy quasiparticle corresponding to coherent polarons [103]. The second model implies the presence of charge-order antiferromagnetic correlations [104]. These correlations are more stable in the insulating phase, giving rise to a "pseudogap" in the density of states (DOS) and thermally activated resistivity. They survive below T_{MI} but are disfavored by the onset of long-range ferromagnetic order. The site-averaged DOS calculated as a function of temperature in Ref. [104] exhibits a pseudogap above and below T_{MI}, in agreement with the tunneling data. Moreover, the gap magnitude is predicted to decrease when the temperature is lowered, as the STS data reveal (Fig. 20a and b).

The zero-bias conductance (ZBC) in the tunneling spectra has been analyzed at different temperatures. In the high-temperature phase the ZBC decreases on cooling for both the highly and the weakly-strained films. As temperature decreases, the ZBC reaches a minimum close to $T = T_{MI}$ and then increases upon further cooling. This evolution mimics the tem-

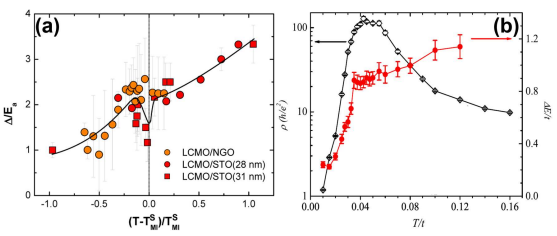

Figure 20: *(a) (Pseudo)gap estimated from normalized conductance curves for LCMO films. (b) Calculated resistivity (black) and half distance between the peaks in the DOS (red) as a function of temperature from Ref. [104] ($T_{MI} \sim 0.04t$, t: nearest-neighbor hopping amplitude).*

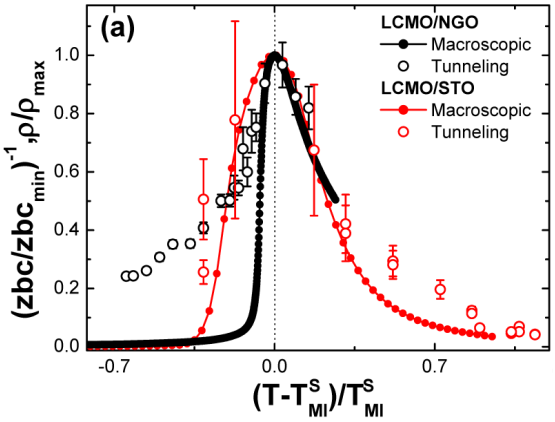

Figure 21: *Macroscopic resistivity (full circles) and inverse zero-bias conductance (open circles) as a function of the reduced temperature* $(T - T_{MI})/T_{MI}$ *for both high (red) and low (black) strain samples.*

perature dependence of the macroscopic conductivity (Fig. 21). While the behavior of the ZBC in the insulating phase could be explained in terms of thermal smearing, the same argument cannot be invoked for the ZBC evolution in the metallic phase. However, the measurements are in good quantitative agreement with the theoretical predictions of the temperature dependence of the DOS at the Fermi level in [104].

The measurements of Fischer and collaborators indicate that the low temperature phase of the studied materials is an unconventional metal. Although it is not possible to discern to what extent the two evoked scenarii provide a correct description of manganite physics, their data are in good agreement with the model which considers a competition between antiferromagnetic and ferromagnetic interactions [104]. This opens up interesting directions for future work. Further insight into the problem may be brought from high-energy-resolution STS measurements in the energy range of the quasiparticle peak predicted in the coherent polarion scenario [103], or by studying the effect of disorder.

6 Electronic properties at surfaces and interfaces

The enormous progress in the fabrication of high-quality heterostructures based on complex oxide materials and their control by external parameters, for example by the electric field effect [27], has been a driving force for the search of new interface phenomena with potential for novel devices. Moreover, superstructures based on materials with strong electronic correlations pose fundamental new questions about the nature of the electronic phases with the possibility for superconductivity and other unusual orders or correlations in charge, orbital and spin channel, as well as extraordinary transport properties. The activities of the ETHZ group of Manfred Sigrist is devoted to developing theoretical tools and, in particular, to investigate transport properties in this type of inhomogeneous correlated electron systems. The reduced symmetry at interfaces as well as surfaces can have a strong impact on the electronic structure, for instance through the lack of inversion symmetry. The spin-orbit coupling appearing under such conditions can lead to a sizable spin-orbit coupling as demonstrated by the EPFL group of Marco Grioni for $Bi_xPb_{(1-x)}Ag_2$ alloys which allow for a tuning of the coupling strength.

6.1 Spin-orbit-split states in surface alloys

Following on the recent discovery of a giant spin-orbit splitting (Rashba effect) in the $BiAg_2$ and $PbAg_2$ surface alloys, Grioni and collaborators have studied how the electronic structure – namely the splitting of the spin-polarized bands – evolves between the two extreme compositions in the structurally ordered mixed $Bi_xPb_{(1-x)}Ag_2$ alloy [28]. The ARPES maps of Fig. 22 reveals an energy shift of the Fermi level in a rigid band fashion across the spin-orbit-split manifold, when Bi (p^5) replaces Pb (p^4). The momentum and energy splitting are progressively enhanced on the Bi-rich side. These data show that it is possible to chemically tune the Fermi level either

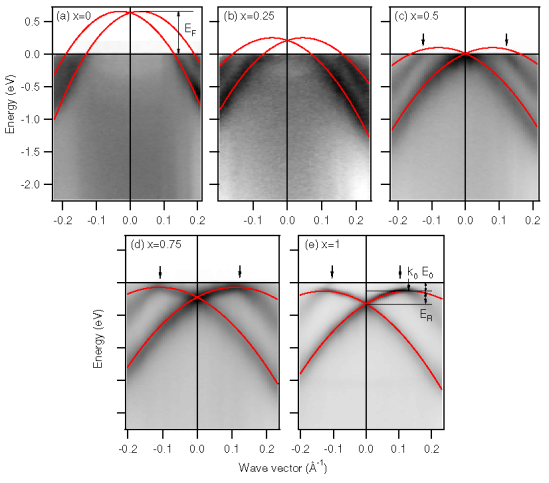

Figure 22: *ARPES intensity maps for a mixed* $Bi_xPb_{(1-x)}Ag_2$ *alloy grown on an Ag(111) substrate, showing the progressive shift in energy – and increased momentum separation – of the spin-orbit split bands.*

above or below the crossing point of the bands at Γ. Injecting current across the alloy layer would then result in different values of the spin-polarization, with potentially interesting applications in spintronics. This work is performed in collaboration with groups at MPI Stuttgart, and at MPI Halle (theory).

6.2 Thermoelectrical effects in correlated heterostructures

Rüegg, Pilgram and Sigrist [29] have shown that the paramagnetic metallic state realized in a model of a Mott-insulator/band insulator heterostructure shows unusual electronic properties which emerge because of the spatially non-uniform structure in combination with strong electronic correlations. The theoretical method applied is based on an extension of the slave-boson theory by Kotliar and Ruckenstein [29]. It was suggested that features of the electronic structure reminiscent of heavy fermion physics (the hybridization of itinerant and localized degrees of freedom in the interface region) provide favorable conditions to enhance the low-temperature thermoelectrical properties [30]. Rüegg *et al.* extended the study of the thermoelectrical quantities for various superlattice geometries and model parameters. They showed that the largest contributions to the Seebeck coefficient originate from the interface region. It can be enhanced by correlation effects as well as through sharpening of the charge profile at the interface [30, 31]. Thermopower is also connected to entropy contributions which can be increased through the presence of localized (orbital and spin) degrees of freedom. This aspect can be addressed using a generalization of Heikes formula to strongly correlated superlattices which offers a route to access the thermopower in the high-temperature limit. The analysis shows, however, that the loss of spatial coherence of the electronic states due to thermal fluctuations suppresses the favorable conditions obtained as a consequence of the interface in the low-temperature limit. The interpolation between the two limits is in progress and will, hopefully, allow to design a strategy for the optimization of the thermoelectric effect in structured correlated electron systems.

7 Theoretical and computational studies of strongly correlated electron systems, quantum phase transitions and exotic phases

The theoretical discussion of strongly correlated electron systems represents one of the great challenges in this condensed matter physics. Here we report on new approaches which are tested in order to tackle problems such as the doped Mott-insulators or quantum phase transitions. Recently also the study of time evolution has become important in the context of experimental probes for cold-atoms in optical traps. These approaches are studied in the group of Dionys Baeriswyl and Vladimir Gritsev (UniFR). The ETHZ group of Matthias Troyer reports an important breakthrough in the development of a new impurity solver for dynamical mean field theory. Moreover, this group has important results clarifying the situation of supersolidity in ^{4}He and discussing new topological phases such as strongly correlated anyonic models. As a specific example of electronic properties at a quantum phase transition, the group of Manfred Sigrist (ETHZ) discussed the magneto-striction effect at the metamagnetic transition of a single-layer Ca-Sr-ruthenate system and compared it with recent experimental results.

7.1 Crossover phenomena and fidelity

In an ongoing study in the group of Baeriswyl, the theoretical description of the crossover from "itinerant" to "localized" many-body ground states is investigated. A first attempt using the comparison of two variational wave functions for the Hubbard model, one continuously linked to the $U = 0$ limit, the other to the infinite U limit, did not produce satisfactory results, except maybe at or close to half filling. Therefore, Baeriswyl and collaborators started to examine a criterion, which is sometimes applied to quantum phase transitions, the so-called ground state fidelity or fidelity susceptibility. The idea is to calculate the overlap between the ground states of systems with infinitesimally close parameters, say J_μ and $J_\mu + \Delta J_\mu$ in the case of the anisotropic Heisenberg model. The fidelity susceptibility is the second derivative of the overlap with respect to ΔJ_μ. This quantity diverges in the thermodynamic limit at a second order phase transition. Calculations in Baeriswyl's group for the XXZ-Heisenberg chain confirm this picture for the transition from a paramagnetic to a ferromagnetic state at $J_z = -J_{xy}$, where already for a chain with 24 sites the fidelity susceptibility exhibits a very pronounced peak.

Recently Baeriswyl and collaborators applied this concept to the problem of the BCS-BEC crossover for the soluble Richardson model (the reduced BCS Hamiltonian in the context of superconductivity). Their preliminary results

indicate that the fidelity susceptibility is well suited for characterizing this crossover.

7.2 Band-insulator to Mott-insulator transition

Electrons in solids are subject to both a single-particle potential and the Coulomb interaction. A wealth of interesting phenomena can be produced when the form of the single-particle potential deviates from that of the ideal crystal due to, for example, structural transitions, lattice vibrations, defects or impurities. A simple Hamiltonian that incorporates the combined effects of interactions and reduced translational symmetry in a particularly transparent manner is the ionic Hubbard model, in which the single-particle energy alternates between neighboring sites. Baeriswyl and collaborators have investigated this model in the neighborhood of the band-insulator to Mott-insulator transition in the strong coupling limit [32], where the Hamiltonian can be mapped onto an effective spin-1 model. Using large-scale DMRG calculations for the effective model together with an extensive finite-size scaling analysis, they have confirmed that the two insulating phases are separated by an intermediate spontaneously dimerized phase. Moreover, they found that the transition from the ionic band-insulating phase to the dimerized phase is Ising, and the transition from the dimerized phase to the Mott-insulating phase is Kosterlitz-Thouless, in agreement with field-theory-based predictions.

7.3 Time evolution in quantum many-body systems

The study of quench dynamics in quantum spin chains was motivated by recent experiments with ultra-cold atoms in optical lattices [105]. By applying both numerical and analytical methods, Gritsev and collaborators were able to address a number of interesting open questions in this context. The basis of their work was an implementation of a matrix product algorithm for infinite chains (TEBD method [106]).
In a first work [107] a method for the controllable generation of non-local entangled pairs was proposed using spinor atoms loaded in an optical superlattice. Gritsev and collaborators studied also the non-equilibrium dynamics of the one-dimensional ferromagnetic Heisenberg Hamiltonian and showed that the time evolution of a state of decoupled triplets on each double well leads to the formation of a highly entangled state where short-distance antiferromagnetic correlations coexist with longer-distance ferromagnetic correlations.
A second project [108] studies the unitary time evolution of antiferromagnetic order in anisotropic Heisenberg chains, initially prepared in a pure quantum state far from equilibrium. Their analysis indicates that the antiferromagnetic order imprinted in the initial state vanishes exponentially. Depending on the anisotropy parameter, oscillatory or non-oscillatory relaxation dynamics is observed.

7.4 General fermionic models

a) *Dynamical mean field theory (DMFT)* In the group of Troyer the new weak coupling quantum Monte Carlo (QMC) solver [33] has been applied to the Hubbard model in a plaquette-DMFT simulation [34]. The strong coupling solver has been applied to a 3-orbital model with full Coulomb interaction [35], where a spin-freezing transition and non-Fermi liquid behavior have been found.

b) *Universal behavior of resonant fermions* In the BEC-BCS crossover there is no phase transition, but still universal behavior at the resonance point at which the energy of a bound pair of two fermions is in resonance with the bottom of the band of unbound fermions. In the dilute limit all properties at this point are universal in units of the reduced temperature T/E_F where E_F is the Fermi energy. Using quantum Monte Carlo simulations the value of the universal properties could be determined including the universal critical temperature around this point [36].

7.5 Supersolids

The supersolid state of matter, a phase that is at the same time solid and superfluid, is one of the most intriguing phases of matter, since it combines two properties that are seemingly contradictory and mutually exclusive: liquid and solid, and is hence a strange and exotic quantum mechanical state if it is found.

a) *Supersolid Helium* Following experimental evidence for the possible existence of a supersolid in ^{4}He [109, 110], Troyer and collaborators have performed more *ab initio* quantum Monte Carlo simulations of solid Helium. In the past year they have found that the previously observed phase separation of vacancies [37] is a classical effect also present in classical solids [38]. The previously reported superflow along crystal defects [39, 40] is due to local strains in the crystal that close the gap for vacancy formation [41]. Another related project

concerns the effect of ^{3}He and how it binds to dislocations [42]. In two-dimensional ^{4}He films on substrates a supersolid phase has also been conjectured and has been the subject of simulations. They found, however, that no supersolid appears in Helium films on graphite and that a commensurate 4/7-phase is also absent in Helium films on graphite, counter to wide belief [43].

b) *Spin supersolids* Supersolid behavior can occur not only for bosons but also in spin models, where a "spin supersolid" refers to a spin model with long-range order in both the XY-plane (the "superfluid") and the Z axis (the "solid"). In publication [44] Troyer's group investigated the mapping of such a spin model to well-understood bosonic models and identified correlated magnon hopping terms as the mechanism for supersolidity in these spin models.

7.6 Topological phases and anyonic models

A topological quantum liquid phase, if realized in an experiment, could pave the way towards stable, robust and decoherence-free quantum bits: it can encode information in a non-local topological property and no local source of noise can disturb this quantum bit. In this context Troyer and collaborators have performed the following investigations.

a) *Engineering topological phases.* Their simulations [45] of a topological quantum bit based on Josephson junctions [46] show that while such a device will indeed exhibit topological order, however the operating temperatures are far too low for current technology.

b) *Nonabelian topological phases* Even more interesting is a non-abelian topological phase with deconfined non-abelian anyonic excitations, since their braiding would allow universal quantum computation. They have shown, however, that one seemingly promising approach to such phases based on "loop gas" models will unfortunately not exhibit any topological phase in models with local interactions [47].

c) *Interacting anyons* To investigate the interactions between non-abelian anyons, Troyer and coworkers have continued simulations on anyonic generalizations of quantum spin models. They have shown that the critical gapless ground states of these models are due to an unusual symmetry [48], and have calculated the phase diagrams of models with longer-range interactions [49] and spin-1 models [48]. A pedagogically written article on how to derive such models has been written [50]. It turns out that many of these anyonic chains exactly map to many exactly solvable statistical mechanics models. These models that so far were just toy models now have microscopic realizations. Similar phases have been found in related anyonic models on high-genus surfaces [51].

7.7 Simulation of exotic quantum phases and quantum phase transitions

Recently a theory of deconfined quantum criticality [111] has been proposed for an unconventional quantum phase transition between two phases with different broken symmetries, which is forbidden by Landau theory. However, by simulating the effective action of the proposed deconfined critical point, Troyer and collaborators could show that also in the SU(2) case the transition is weakly first order [52], just as they had previously shown for the U(1) $\times$ U(1) case, and is in contrast to the proposed theory [53] but consistent with Landau theory. In further projects they have investigated unusual thermal spin canting in an orbital compass model [54], a ladder-model showing Bose-metal phases [55] and a CORE-investigation of the quantum phase transition between a spin gap phase and Néel order when coupling plaquettes in a Heisenberg antiferromagnet [56].

7.8 Magneto-striction effects in $Ca_{2-x}Sr_xRuO_4$

The complex phase diagram of $Ca_{2-x}Sr_xRuO_4$ shows in the doping range $0.2 \leq x \leq 0.5$ antiferromagnetic correlations and a metamagnetic transition at low temperatures [112]. Structural effects accompanying this metamagnetic transition have been studied by Kriener *et al.* [113] measuring thermal expansion and magneto-striction coefficients for different temperatures and magnetic fields. These data suggest a close relation between the crystal structure and spin and possibly orbital correlations. Based on previous theoretical work [57] describing this system within a generalized Kugel-Khomskii model of localized spin and orbital degrees of freedom, Roldan, Rüegg and Sigrist [58] have investigated the extension of this model to include the coupling to the elastic lattice. A theoretical phase diagram has been determined using a mean-field approximation and it could be shown that the metamagnetic transition is combined with a structural transition. The comparison with the experimental $T - x$ phase diagram [112] suggests that the elastic constant of the lattice is affected by Sr doping (difference

of ionic radius of Ca and Sr) giving rise to a lattice distortion as a function of x at low enough temperatures. The calculated temperature and magnetic-field dependences of the magnetization and of the lattice distortion are consistent with the experimental findings [113].

8 Spectroscopy and transport properties in bismuth- and carbon-based materials

Graphite and bismuth belong to the most prominent examples of elemental semi-metals which display exceptional electronic properties. Despite of many years of research still a large number of important open questions remain to be answered. Moreover, the recent discovery of fabricating single-layer graphene has revived the interest in this class of materials tremendously raising a lot of new questions. Actual research efforts also extend to nano-size carbon systems, such as carbon nanotubes (CNT) or nanographene ribbons which represent well-defined one-dimensional electronic systems. Such systems are of great interest for fundamental studies as well as for their potential applications. Within this project the group of Dirk van der Marel (UniGE) has devoted their interest to optical spectroscopy of bilayer graphene and bismuth ($Bi_{1-x}Sb_x$). Transport properties through quantum point contacts within graphene nano-ribbons were investigated theoretically in the group of Manfred Sigrist (ETHZ). The electronic properties of CNT were explored in Patrycja Paruch's group (UniGE) in combination with ferroelectric films and by the group of L. Schlapbach/O. Gröning (Empa) for the effect of defects in the CNT.

8.1 Infrared spectroscopy of bilayer graphene

Based on a simple band model of π-electrons and electrostatics arguments one expects that in bilayer graphene (Fig. 23a) the effect of gate-induced doping is, apart from a mere shift of the chemical potential, to open a gap Δ_g between the valence and the conduction bands [114] as shown in panel (b). Van der Marel's group obtained infrared spectra (0.1-1 eV) (panel c) of electrostatically gated bilayer graphene as a function of the gate voltage V_g and compared it with the tight binding Slonczewski-Weiss-McClure calculations (panel d) [59]. All major spectral features corresponding to the expected interband transitions are identified in the spectra: strong peaks (B and C) due to transitions between parallel split-off bands and onset-like features (A, D, E) due to transitions between valence

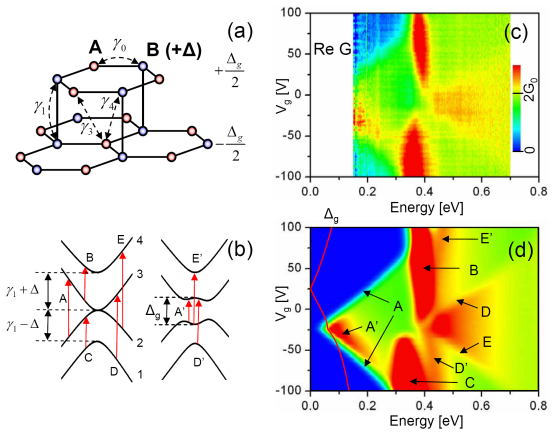

Figure 23: *(a) The stacking structure of bilayer graphene the hopping terms of the tight binding SWMcC model. (b) The band structure near the K points with the interband optical transitions shown by arrows. The measured (c) and calculated (d) optical conductance as a function of the photon energy and the gate voltage.*

and conduction bands. This indicates that the band structure is satisfactorily captured by the tight binding model. A strong gate voltage dependence of these structures and a significant electron-hole asymmetry is observed that can be used to extract several band parameters. However, the structures related to the gate-induced bandgap (A′, D′, E′) are much less pronounced in the experiment than predicted by the tight binding model. The work to establish the origin of this discrepancy is in progress.

8.2 Transport properties in graphene nano-ribbons

Wakabayashi and Sigrist have extended their study of transport properties in graphene nano-ribbons to the situation of point contact like constrictions in a ribbon with random impurity scattering. In the last project period this group reported on the localization effect in disorder zigzag nano-ribbons of graphene demonstrating that for a spatially slowly modulated potential one conducting channel remains unaffected [60]. The constriction induces zero-conductance Fano resonances in the low-energy single channel transport region near the Dirac points. This means that perfect back scattering occurs at energies specific to the constriction shape and dimension. The random potential then introduces statistical fluctuations in the resonance energy, such that conductance fluctuations close to the resonance become comparable to the ensemble averaged dimensionless conductance [61]. This represents a further unusual effect of potential scattering

in the transport of graphene ribbons.

8.3 Combining carbon nanotubes and epitaxial ferroelectric thin films

The exceptional electrical properties and small diameter of carbon nanotubes (CNT) have made them an intensely researched material for device applications and fundamental studies of low-dimensional physics [115]. Conventional field-effect device architecture has been widely used to control CNT charge carrier density, generally using SiO_2 as a dielectric material. An interesting alternative system, potentially allowing both ferroelectric gating of the CNT and local control of domain structures in the ferroelectric film, would be a ferroelectric field effect device, using an epitaxial ferroelectric thin film in place of the usual dielectric.

a) *Polarization switching* Paruch's group (UniGE) fabricated prototype devices by chemical vapor decomposition growth of single-walled CNT directly on the $BaTiO_3$ thin films. The high temperatures and reductive atmosphere of this process led to surface deterioration of the perovskite oxide ferroelectric, although both macroscopic and local measurements confirmed the retention of ferroelectric properties. In these devices, Paruch and coworkers demonstrated polarization control using the CNT as a local field source, creating linear domains precisely following the position of the CNT (determined from previous non-contact atomic force microscopy) as shown in Fig. 24a and b. The written domain structures remained stable over the 1-2 day experiment duration, even once the CNT had been completely removed from the surface by repeated piezoforce microscopy measurements.

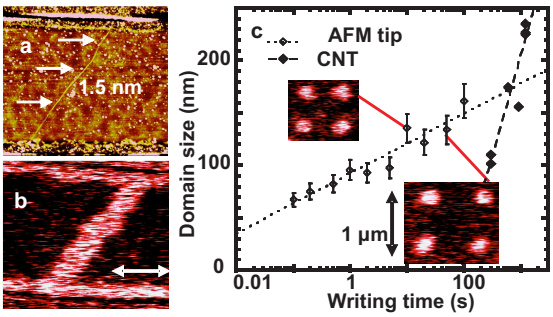

Figure 24: *(a) AFM topography showing CNT position and diameter (indicated). (b) P_{DOWN} domain formed by negative voltage pulse (-10 V, 20 min) applied to the conducting substrate in the same device. (c) The half-width of the CNT-written domains and the radius of circular nanoscale domains (insets))written with 12 V pulses applied to the AFM tip show different domain growth rates as a function of writing time.*

The size of the resulting domains was compared with that of nanoscale AFM-written domains (Fig. 24c) which appear to grow faster close to the tip, but slower for larger-size domains. This behavior is qualitatively in agreement with the numerical simulation of the electric field produced in each case [62].

b) *Effect of ferroelectric polarization on the electronic properties* In Paruch's group transconductance measurements of the CNT-$BaTiO_3$ devices were performed. They find a "memory effect" as shown in Fig. 25 with the conduction through the CNT changing as a result of previous application of voltage pulses of a defined polarity to the conducting substrate under the epitaxial ferroelectric thin film. However, the direction of this effect (*p-type* CNT showing increased zero-field conduction after the application of a positive voltage pulse, V_P and decreased conduction after the application of a negative voltage pulse), and of the counter-clockwise hysteretic response under continuous gate voltage sweeps V_G, as well as its finite persistence (∼500 s in vacuum at 200 K) suggested that this was an effect of charge injection into surface trap states [62]. A similar effect had been observed in standard field-effect devices using CNT on SiO_2 [116].

These transport data suggest that *ferroelectric* field effect is not the dominant mechanism controlling the electronic properties of the carbon nanotubes in the devices. Partial measurements carried out with multi-tube devices based on CNT spin-coated onto polycrystalline ferroelectrics [117] suggest that ferroelectric field effect modulation of charge carrier density could be possible in such systems, where the ferroelectric surface remains undeteriorated. To fabricate single-tube de-

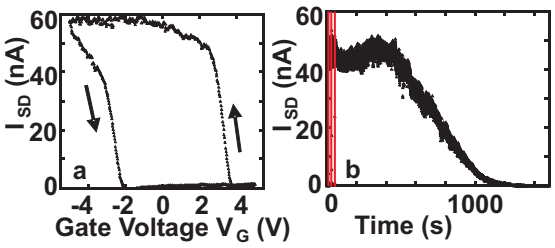

Figure 25: *(a) Large counter-clockwise hysteresis observed in CNT conduction (V_{SD} = 10 mV) as a function of a continuously swept V_G at ambient conditions. (b) Positive V_P (applied at times indicated by red lines) results in CNT conduction which persists for over 500 s at 200 K.*

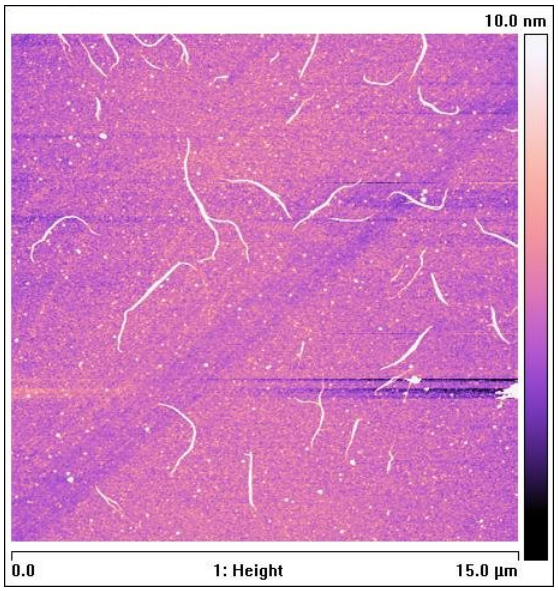

Figure 26: *Dispersed single walled carbon nanotubes onto Si/SiO_2 from suspension in isopropyl alcohol and PVP.*

vices, Paruch and coworkers will use separate growth substrates during CNT growth, then transfer and controllably place individual CNT onto an undeteriorated ferroelectric surface, a technique successfully demonstrated for transfers between different SiO_2 substrates [118].
Before embarking on this more challenging fabrication step, they will test whether pristine ferroelectric surfaces do indeed improve device transport properties using multi-tube devices based on CNTs dispersed onto epitaxial monocrystalline $Pb(Zr_{0.2}Ti_{0.8})O_3$ ferroelectric films. Currently, they are in the process of optimizing this procedure to obtain a uniform deposition of individual single-walled CNT, as shown in Fig. 26 on a test Si/SiO_2 substrate.

8.4 Defects on carbon nanostructures

Defects on CNT are investigated by Schlapbach/Gröning and collaborators at Empa in view of novel electronic properties and devices for potential applications.

a) *Negative differential resistance at hydrogen induced defect levels* The operation of different important electronic components such as Esaki or resonant tunneling diodes relies on negative differential resistance (NDR). With the urge for device miniaturization, NDR has been searched for in different nanoscale systems. Here the group of Schlapbach/Gröning could realize a NDR system with atomic dimensions. Hydrogen chemisorption sites on semiconducting single walled carbon nanotubes

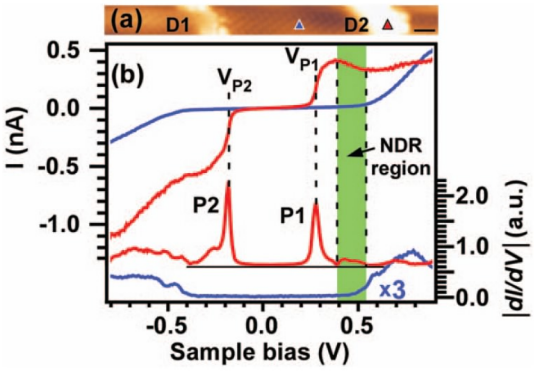

Figure 27: *a) STM topography image of a SWNT with two H-plasma induced defects (D1, D2). b) $I-V$ curve and dI/dV spectrum recorded at the red and blue triangle in a), respectively, with the NDR region shaded in green.*

(SWNT) are characterized by the appearance of energetically and spatially strongly localized states. These states are often observed in pairs symmetric to the mid gap level. The Empa group could show that such paired states are produced by chemisorbed hydrogen dimers [63]. In scanning tunneling spectroscopy (STS) these states show small energetic FWHM of 50 meV and less.
In the range of positive sample bias addressing the unoccupied density of states (DOS) we find an NDR region associated with defect energy states in the $I-V$ characteristics. This situation is shown in Fig. 27, where the NDR region is displayed as the green shaded area.
The NDR shows a pronounced dependence on

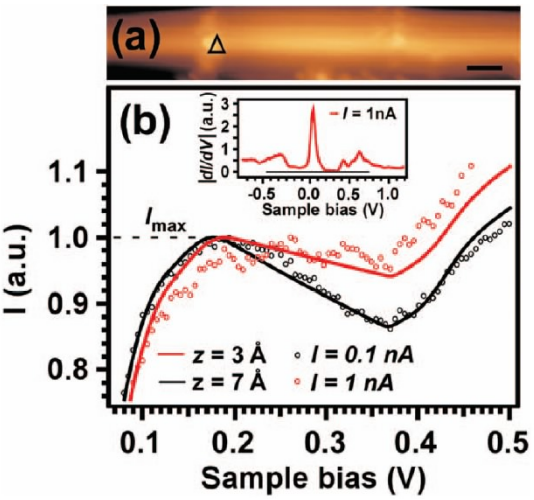

Figure 28: *a) STM topography image of a SWNT with N-plasma induced defects. b) Experimental $I-V$ characteristics in the NDR region at two different tunneling resistances (markers) and corresponding fits using the bias dependent barrier height tunneling model.*

the tunneling resistance and in turn on the tip-sample separation in the STS measurements. This defect-induced NDR behavior could be quantitatively explained and described using a bias depending tunneling barrier height tunneling model [64]. The result of the measurement and the numerical modelling are shown in Fig. 28 for an N-plasma induced defect.

b) *Ar^+ ion induced local modification of semiconducting SWNT* Local, controllable modification of the electronic structure of carbon nanomaterials is important for the development of carbon-based nanoelectronics. By combining density functional theory with low-temperature STM/STS experiments of Ar^+ ion irradiated SWNT, Schlapbach/Gröning and coworkers studied the changes of the electronic structure. They showed that individual irradiation induced defects can give rise to single and multiple peaks in the band gap of semiconducting SWNT (Fig. 29) [65].
These results not only shed light on the abundance of irradiation-induced defects in carbon nanotubes and their signatures in STS spectra (and LDOS), but also suggest a way how the STM can be used to engineer such defects, based on their stability under the elevated tunneling currents. Here it was observed that chemisorption related defects can be desorbed without leaving any trace on the SWNT [65].

c) *Scattering dynamics at defects in metallic SWNT* The group of Schlapbach/Gröning has realized intratube quantum dots (QD) on metallic SWNT by means of medium energy Ar^+ ion irradiation, with QD length ranging

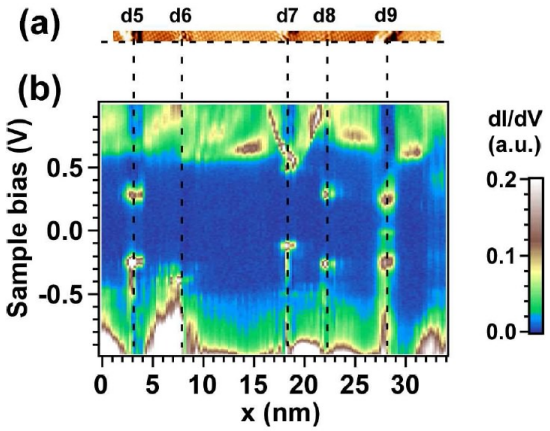

Figure 29: *STM/STS images of a segment of a semiconducting SWNT exposed to 200 eV Ar ions. (a) STM topography image with five defect sites $d5-d9$. (b) dI/dV - scan recorded along the horizontal dashed line. $U_s = 1$ V, $I_s = 0.1$ nA, $T = 5.22$ K, $U_{mod} = 15$ mV, $x_{res} = 0.22$ nm.*

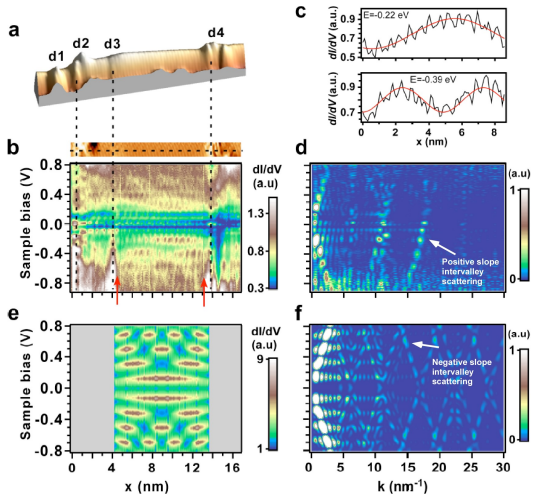

Figure 30: *a) 3D STM topography image of a metallic SWNT with Ar ion induced defects. b) The STS dI/dV map over the region between d3 and d4. c) dI/dV line profiles of the first two quasi-bound state modes with a corresponding sinusoidal fit (red). d) Fourier transformed STS map of b) showing scattering branches of intravalley (close to the origin) and intervalley type. e) and f) Corresponding theoretical simulations in the Fabry-Pérot resonator model.*

between 9 nm and 20 nm. The corresponding energy splitting of the quasi-bound states amounts to 200 meV and is significantly larger than the thermal broadening at room temperature. By means of experimental Fourier transformed STS in conjunction with a theoretical Fabry-Pérot electron resonator model, a complete description of the scattering processes of electrons confined between consecutive defects is given, with clear signatures for inter and intravalley scattering. Further, scattering effects were identified, arising from the lift of degeneracy of the Dirac cones (Fig. 30).
The experimental observation that for the intervalley scattering the positively sloped branch is always significantly stronger than the negatively sloped one still awaits theoretical understanding [66].

8.5 Metal-insulator transition in $Bi_{0.935}Sb_{0.065}$.

Recently interest in bismuth and $Bi_{1-x}Sb_x$ alloys has been raised due to the presence of a massless 3D Dirac cone [119], and the associated physics of "relativistic" particles near the metal-insulator transition. This transition can be observed as a function of pressure or Sb concentration. A topological Dirac insulating state has been predicted [120] and confirmed for $Bi_{1-x}Sb_x$ alloys using ARPES [121]. This state corresponds to an insulating bulk, with metallic Dirac-cone states at the surface. In addition,

a mysterious phase diagram has been found under high magnetic field, for which charge fractionalization in three space dimensions has been suggested [122, 123]. Due to the low density of electrons and holes in these materials, the plasmons (collective excitations of the free carriers) have a very low excitation energy: less than 0.04 eV in $Bi_{1-x}Sb_x$, which should be compared to 15 eV in pure aluminum. An important role of interactions within the electron-hole plasma is suggested by the observation of coupled states of a conduction electron and a plasmon in pure bismuth [67].

The group of van der Marel has performed a detailed optical study of $Bi_{1-x}Sb_x$ with $x = 6.5\%$ by means of infrared reflectometry. A linear decrease of the plasma frequency with the temperature was observed. The optical conductivity revealed an unusual feature in the far-infrared range which tracks the evolution of the plasma frequency and – rather surprisingly – broadens as the temperature decreases. Fig. 31 presents the absolute reflectivity measured perpendicular to the trigonal axis in the far infrared range. The drastic drop of the reflectivity corresponds to the plasmon energy, which is proportional to the square root of the free carrier density. As the extrapolation of this frequency to zero temperature is almost equal to zero, $Bi_{0.935}Sb_{0.065}$ is situated close to the

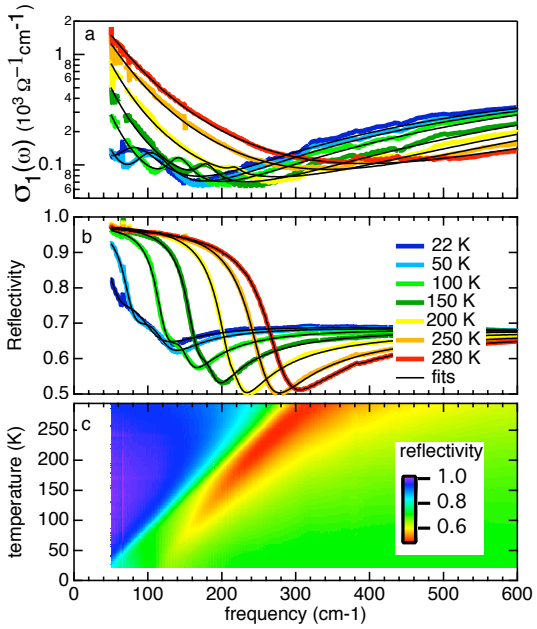

Figure 31: *Absolute reflectivity and optical conductivity of $Bi_{0.935}Sb_{0.065}$.*
As a function of frequency (a) optical conductivity and (b) absolute reflectivity at different temperatures; (c) temperature-frequency color plot of the absolute reflectivity.

metal-insulator transition, with a correspondingly low free carrier density ($\sim 10^{17}$ cm^{-3}). Close inspection reveals a secondary minimum for temperatures below 200 K. This additional feature, which also shows up as the small but clear peak in $\sigma_1(\omega)$ (Fig. 31a), is remarkable for two reasons. First, its energy varies with temperature and tracks exactly the temperature evolution of the plasmon energy. While this "mystery excitation" energy is close to the plasma energy, it can not be the plasmon itself since plasmons have longitudinal polarization, whereas excitations seen in $\sigma_1(\omega)$ can only have a polarization transverse to their propagation direction. Second, the peak becomes broader as the temperature decreases, i.e. as the density of thermally excited free carriers is reduced. According to the standard many-body treatment of the single component electron gas the ratio E_{Corr}/E_{kin} (Coulomb correlation energy/kinetic energy) depends on the free carrier density n as $E_{Corr}/E_{kin} \propto n^{-1/3}$. Hence, by reducing n, a transition from a metal to an insulating Wigner-crystal should occur at some critical value n_c. It is tempting to associate the observed broadening of the "mystery-mode" in $\sigma_1(\omega)$, when the free carrier density is reduced, with the approach to a Wigner crystalline state. However, by substituting experimental values for the mass and screening in bismuth, van der Marel and collaborators find that E_{Corr}/E_{kin} is far too small to fulfill the conditions for Wigner crystallization. On the other hand, this theory is based on a plasma of free electrons with an isotropic mass, whereas $Bi_{1-x}Sb_x$ is a plasma containing two components of opposite charge: electrons and holes, each having different and strongly anisotropic effective masses. Theoretical analysis is presently in progress to identify the various possible states of matter in such a two-component plasma, and the possible relation of these phases to the experimental observations with and without external magnetic field.

9 Mesoscopics: quantum coherent electron transport

A number of systems discussed in this report can display mesoscopic electronic properties. In this context various questions have been addressed by the group of Markus Büttiker (UniGE). This discussion is also extended to areas which are concerned with quantum measurements that are also relevant for the analysis and characterization of quantum phase transitions as well as for the fundamental aspects connected with quantum computation devices.

9.1 Quantum state tomography with shot noise

Generally, the density matrix determines the possible probabilities for the outcomes of measurements on the quantum state. It is therefore of fundamental interest to determine the density matrix. This requires measurements on an ensemble of many identically prepared states and the measurement of a complete set of observables of the state. The reconstruction of the quantum state wave function via such a series of measurements is known as quantum state tomography. Once the density matrix is known the entanglement content of the state can be determined for instance by calculating the concurrence.

A particular goal is the detection of quasiparticle entanglement with the help of quantum state tomography in mesoscopic conductors. For this purpose Büttiker and collaborators concentrate on orbital entanglement (not spin) which has the adavantage that all steps, the generation, manipulation and detection of entangled states can be carried out in a single normal conductor. A quantum tomography of orbitally entangled states has been discussed in Ref. [69]. Quantum tomography requires the same number of measurements as an entanglement test based on a Bell inequality. However with quantum state tomography certain entangled states are detected which do not lead to a violation of a Bell inequality.

The structure of interest is shown in Fig. 32. A mesoscopic conductor is connected to M reservoirs which are biased to inject current and N-M reservoirs which are grounded. In addition the conductor is via beam splitters connected to detector reservoirs $A_\pm$ and $B_\pm$. In addition there are gates which permit to vary the phases ϕ_A and ϕ_B. A number of different settings of the transmission probabilities of the beam splitters and the phases permit to extract the reduced two particle density matrix from current and shot noise measurements [69].

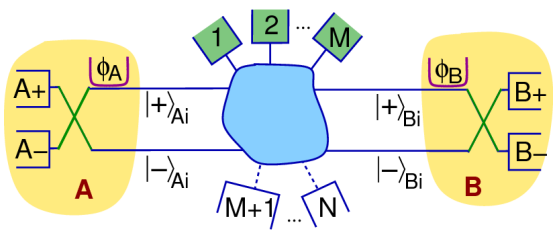

Figure 32: *Quantum state tomography of a mesoscopic conductor with M biased and $N-M$ grounded contacts and two pairs of leads which send particles to phase gates ϕ_A and ϕ_B and beam splitters at A and B [68].*

A particular example is a conductor which exhibits a two-particle Aharonov-Bohm effect [70] in the shot noise in a geometry in which all conductance matrix elements are independent of the Aharonov-Bohm flux. The predicted two-particle Aharonov-Bohm effect has recently been experimentally observed by Neder *et al.* [124]. To assess the degree of entanglement in the experiment a quantum state tomography at finite temperature and in the presence of dephasing is needed.

Quantum information theory assumes that projective measurements exist in which the two-particle density matrix at a given energy is projected out of the many body state. The resulting entanglement is called the *projected entanglement* [68]. Importantly current measurements and measurements of current-current correlations of shot noise of a conductor are not of this nature. At zero temperature the detector contacts can themselves emit particles and contribute to correlations. Current correlation measurements provide information only on the energy integrated current. In experiment only a *reduced* density matrix can be obtained from current and shot noise correlation experiments and only a *reduced* entanglement can be determined.

For a conductor which exhibits the two particle Aharonov-Bohm effect, Büttiker and collaborators present an analysis which determines the concurrence and the Bell parameters of projective and reduced measurements [68]. The results are summarized in Fig. 33 which shows the areas of non-zero entanglement in the plane

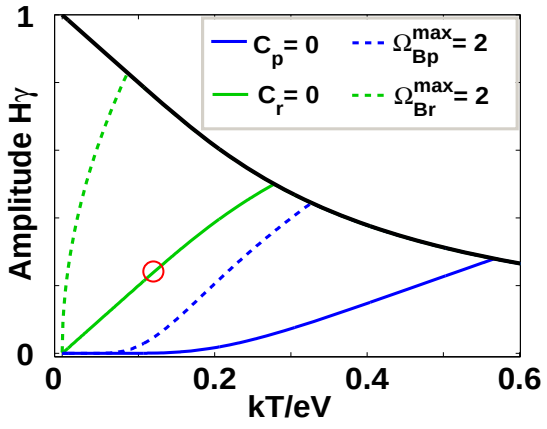

Figure 33: *Amplitude of the two-particle Aharonov-Bohm oscillations in the shot noise versus kT/eV: above to the left of the different lines the reduced (projected) entanglement is finite. Quantum state tomography yields finite entanglement above the solid lines, a Bell test above the broken lines. The red circle corresponds to the parameters of the experiment [68].*

of the amplitude of the two-particle Aharonov-Bohm oscillations versus temperature. Projective measurement gives the largest area in this plot, a Bell inequality violation with a current correlations determined from a realistic shot measurement gives the smallest area. The detectable entanglement in the experiment of Neder *et al.* [124] is close to zero, it is situated right at the boundary of the entanglement detectable with the reduced density matrix determined from quantum state tomography.

9.2 Fluctuation relations

The fluctuation dissipation theorem is a cornerstone of linear response theory. It connects a transport coefficient like conductance to noise properties of the system like the spectral density of equilibrium current fluctuations. There has long been an interest in the extension of this theorem to transport beyond the linear regime. Recently such theorems have appeared in mesoscopic physics where they are formulated for the charge transferred through a conductor in a certain time. The statistics of this transferred charged Q is described by a distribution $P(Q,\tau)$ where τ is the measurement time. The first moment of this distribution is proportional to the current through the conductor, the second moment to the noise, etc. A generalized fluctuation relation takes the form

$$P(Q,\tau)/P(-Q,\tau) = \exp(VQ/kT) \qquad (2.1)$$

where V is the applied voltage. This is a fluctuation relation [125] since the argument of the exponential contains only theormodynamically conjugate variables. In the presence of a magnetic field it was argued that the relation should be

$$P(Q,\tau,B)/P(-Q,\tau,-B) = \exp(VQ/kT)\,. \qquad (2.2)$$

However this relation is in contradiction with both theory [71, 72] and experiments [126, 127] which have demonstrated that, to second order in voltage, the current of a two terminal structure can have contributions which are asymmetric in magnetic field. To second order in voltage, there is a contribution to the current which is proportional to the magnetic field and the voltage squared. This is an interaction effect predicted and verified for chaotic cavities and subsequently for a variety of different conductors, like rings pierced by a magnetic flux. Therefore, such terms asymmetric in magnetic field seem to be universal.
Büttiker and collaborators have derived a fluctuation relation which is valid even for samples with a magnetic field asymmetry [73]. Instead of the detailed balance conditions of Eqs. 2.1 and 2.2, the fluctuation relation uses only a global detailed balance condition, namely [73]

$$\sum_Q P(Q,\tau) = \sum_Q P(-Q,\tau)\,\exp(VQ/kT) = 1\,. \qquad (2.3)$$

The asmmetry in the second order conductance is related to a noise contribution which to lowest order is proportional to temperature, magnetic field and voltage [73], [128]. Such a linear in voltage term in the noise spectral density implies that the equilibrium Johnson-Nyquist noise is not the minimal current noise of such a conductor but that there exists a range of voltages for one magnetic field polarity for which the noise is smaller [73]. There are no known noise measurements which exhibit such a behavior.

9.3 Two particle physics with mesoscopic capacitors

A quantum coherent mesoscopic capacitor formed with a cavity connected to a single channel lead exhibits a charge relaxation resistance which is quantized at half a von Klitzing resistance quantum [129, 130][74]. The group of Büttiker has examined the effect of dephasing on charge relaxation resistance [75].
A mesoscopic capacitor subjected to large amplitude pulses of the right magnitude can be made to emit or absorb single electrons [131][76]. The transfer of an electron from one mesoscopic capacitor to another [77] has here been studied. The efficiency of this transfer can be investigated by considering the mean squared current: this current is nullified if the transfer is perfect. Alternatively if the potentials applied to the two capacitors are nearly synchronous both capacitors emit nearly simultaneously an electron and the arrangement works as a two particle emitter. Possibly such an arrangement can be used to generate entangled states on demand.

10 New algorithms and new instruments

10.1 Algorithmic developments

Algorithmic developments are at the core of progress in computer simulations of quantum systems, and the project of Troyer's group has also a strong algorithmic component. They have continued the development of new quantum Monte Carlo solver for dynamical mean field theory (DMFT) and the fermionic impurity problem [132]. Their new weak-coupling solver [33] complements

a strong-coupling solver developed previously [78]. In another project they have generalized the contractor-renormalization group (CORE) method to model with constraints that could not be treated with the standard CORE method [79]

10.2 Spin polarized STM

In the group of Christoph Renner (UniGE) a new variable temperature ultrahigh-vacuum scanning tunneling microscope (STM) was installed in 2008.
The goal is to develop a spin polarized STM to map the magnetic texture of correlated electron materials such as colossal magneto-resistance (CMR) manganites with atomic scale spatial resolution. Renner's group is working towards implementing a scheme based on Mott scattering [133] using a commercial scanning tunneling microscope (STM) platform. A new laboratory was built during the first half of 2008. The STM was assembled in its dedicated Faraday cage and successfully commissioned in October 2008. It is an ultrahigh-vacuum (5×10^{-11} mbar at 300 K) variable temperature (4.8 – 320 K) setup. In addition to the STM capabilities, it features a range of surface analysis and preparation techniques including hot and cold sample stages, RHEED, hydrogen cracker, fusion cells and e-beam evaporators.
The STM performance and atomic scale fabrication techniques have been successfully tested by growing and imaging self-assembled Bi-nanolines on Si(001) (Fig. 34). The aim of this work on Bi is to build a solid state model system to explore fundamental properties of one dimensional physics. The idea is to grow very long single atom wires of selected species using the Bi-nanolines as a template [134].
The implementation of the spin-polarised STM is steadily progressing. The Bruno scheme [133] puts very demanding constraints on the tunneling current preamplifier. Two prototypes have been built and are about to be tested. The spin polarized STM further relies on custom designed microfabricated tips (Fig. 35). A process flow has been elaborated and the necessary masks have been completed. The first tips are expected to be ready within a couple of months.

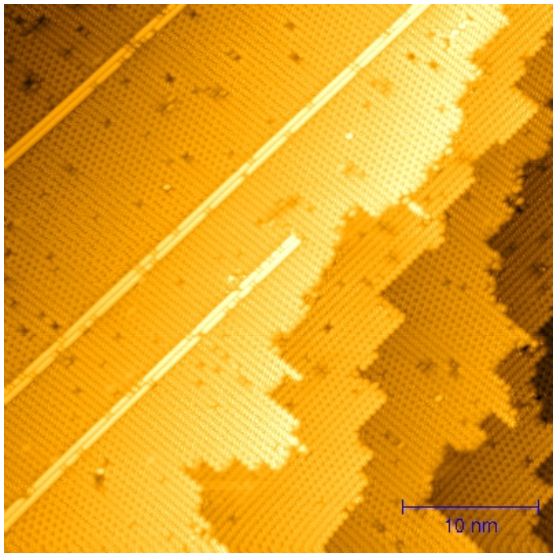

Figure 34: *Bi-nanolines grown in situ on a bare Si(001) surface.*

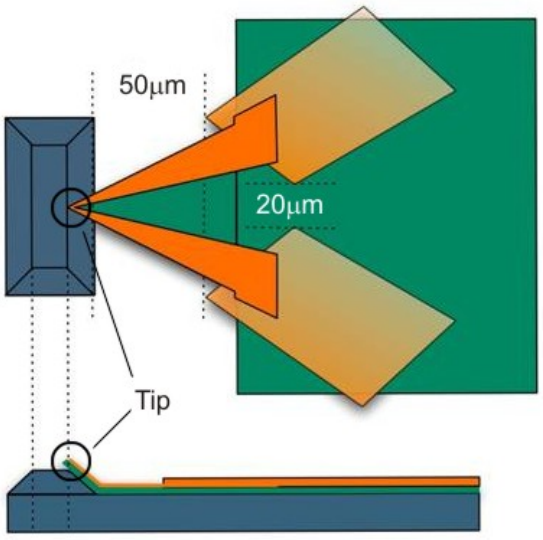

Figure 35: *Schematic top and side views of the Mott STM tip.*

11 Collaborative efforts

The collaborative efforts are numerous and first of all driven through the formation of specific communities working on similar subjects with common problems and themes. This is especially obvious for topics such as quantum spin systems, charge density wave systems, ultra-cold atoms and carbon-related materials which form larger entities within Project 1. The fact that MaNEP provides a common forum to discuss different subjects has indeed stimulated a number of common endeavors. Highly successful examples of this for the reported period in Project 1 are the extensive collaboration between the experimental group of Joël Mesot and the theory group of Thierry Giamarchi on the spin ladder systems and the joined activity on the 1T-$TiSe_2$ between the groups of László Forró and Philipp Aebi. All theoretical and computational physics groups entertain a common scene to discuss various aspects

of the theoretical treatment of strongly correlated many-body systems and features of complex quantum entanglement under a large variety of conditions. The availability of the ALPS code library and tutorials provided by Troyer's group are a very beneficial support for both theory and experimental groups. Several research efforts within Project 1 are also closely connected with other projects in MaNEP. A considerable part of the sample synthesis and crystal growth for experiments in Project 1 happens with MaNEP through Projects 3 and 4. Moreover, many of the theoretical studies reported in Project 1 are of direct relevance for Project 2 on unconventional superconductivity, most prominently for cuprates, and for Project 5 on thin films and novel devices, in the context of electronic reconstruction at interfaces and surfaces.

MaNEP-related publications

[1] T. Giamarchi, *Quantum Physics in One Dimension* (Oxford University Press, Oxford, 2004).

► [2] B. Thielemann, C. Rüegg, H. M. Rønnow, A. M. Läuchli, J.-S. Caux, B. Normand, D. Biner, K. W. Krämer, H.-U. Güdel, J. Stahn, K. Habicht, K. Kiefer, M. Boehm, D. F. McMorrow, and J. Mesot, Physical Review Letters **102**, 107204 (2008).

► [3] C. Rüegg, K. Kiefer, B. Thielemann, D. F. McMorrow, V. Zapf, B. Normand, M. B. Zvonarev, P. Bouillot, C. Kollath, T. Giamarchi, S. Capponi, D. Poilblanc, D. Biner, and K. W. Krämer, Physical Review Letters **101**, 247202 (2008).

► [4] B. Thielemann, C. Rüegg, K. Kiefer, H. M. Rønnow, B. Normand, P. Bouillot, C. Kollath, E. Orignac, R. Citro, T. Giamarchi, A. M. Läuchli, D. Biner, K. Krämer, F. Wolff-Fabris, V. S. Zapf, M. Jaime, J. Stahn, N. B. Christensen, B. Grenier, D. F. McMorrow, and J. Mesot, Physical Review B **79**, 020408(R) (2009).

► [5] M. Klanjšek, H. Mayaffre, C. Berthier, M. Horvatić, B. Chiari, O. Piovesana, P. Bouillot, C. Kollath, E. Orignac, R. Citro, and T. Giamarchi, Physical Review Letters **101**, 137207 (2008).

► [6] J. Dorier, K. P. Schmidt, and F. Mila, Physical Review Letters **101**, 250402 (2008).

► [7] S. R. Manmana and F. Mila, Europhysics Letters **85**, 27010 (2009).

► [8] N. Laflorencie and F. Mila, Physical Review Letters **102**, 060602 (2009).

[9] K. Prša, H. M. Rønnow, O. Zaharko, N. B. Christensen, J. Jensen, J. Chang, S. Streule, M. Jiménez-Ruiz, H. Berger, M. Prester, and J. Mesot, *submitted to* Physical Review Letters (2009).

► [10] S. D. Huber and A. Rüegg, Physical Review Letters **102**, 065301 (2009).

► [11] F. Hassler and S. D. Huber, Physical Review A **79**, 021607 (2009).

► [12] E. Berg, E. G. Dalla Torre, T. Giamarchi, and E. Altman, Physical Review B **77**, 245119 (2008).

► [13] G. Roux, T. Barthel, I. P. McCulloch, C. Kollath, U. Schollwöck, and T. Giamarchi, Physical Review A **78**, 023628 (2008).

[14] L. Pollet, C. Kollath, K. Van Houcke, and M. Troyer, New Journal of Physics **10**, 065001 (2008).

► [15] F. Gerbier, S. Trotzky, S. Fölling, U. Schnorrberger, J. D. Thompson, A. Widera, I. Bloch, L. Pollet, M. Troyer, B. Capogrosso-Sansone, N. Prokof'ev, and B. Svistunov, Physical Review Letters **101**, 155303 (2008).

[16] V. W. Scarola, L. Pollet, J. Oitmaa, and M. Troyer, arXiv:0809.3239 (2008).

► [17] M. Lavagnini, M. Baldini, A. Sacchetti, D. Di Castro, B. Delley, R. Monnier, J. H. Chu, N. Ru, I. R. Fisher, P. Postorino, and L. Degiorgi, Physical Review B **78**, 201101(R) (2008).

[18] A. Sacchetti, C. L. Condron, S. N. Gvasaliya, F. Pfuner, M. Lavagnini, M. Baldini, M. F. Toney, M. Merlini, M. Hanfland, J. Mesot, J.-H. Chu, I. R. Fisher, P. Postorino, and L. Degiorgi, arXiv:0811.0338 (2008).

[19] H. Cercellier, C. Monney, F. Clerc, C. Battaglia, L. Despont, M. G. Garnier, H. Beck, P. Aebi, L. Patthey, H. Berger, and L. Forró, Physical Review Letters **99**, 146403 (2007).

► [20] C. Monney, H. Cercellier, F. Clerc, C. Battaglia, E. F. Schwier, C. Didiot, M. G. Garnier, H. Beck, P. Aebi, H. Berger, L. Forró, and L. Patthey, Physical Review B **79**, 045116 (2009).

[21] A. Sacchetti, M. Weller, J. L. Gavilano, R. Mudliar, B. Pedrini, K. Magishi, H.-R. Ott, R. Monnier, B. Delley, and Y. Ōnuki, Physical Review B **77**, 144404 (2008).

[22] A. Sacchetti, M. Weller, H.-R. Ott, and Y. Ōnuki, The European Physical Journal B **66**, 307 (2008).

► [23] M. Weller, A. Sacchetti, H.-R. Ott, K. Mattenberger, and B. Batlogg, Physical Review Letters **102**, 056401 (2009).

► [24] S. Seiro, E. Koller, Y. Fasano, and Ø. Fischer, Applied Physics Letters **91**, 091913 (2007).

[25] S. Seiro, Y. Fasano, I. Maggio-Aprile, O. Kuffer, and Ø. Fischer, Journal of Magnetism and Magnetic Materials **310**, e243 (2007).

► [26] S. Seiro, Y. Fasano, I. Maggio-Aprile, E. Koller, O. Kuffer, and Ø. Fischer, Physical Review B **77**, 020407(R) (2008).

► [27] A. D. Caviglia, S. Gariglio, N. Reyren, D. Jaccard, T. Schneider, M. Gabay, S. Thiel, G. Hammerl, J. Mannhart, and J.-M. Triscone, Nature **456**, 624 (2008).

► [28] C. R. Ast, D. Pacilé, L. Moreschini, M. C. Falub, M. Papagno, K. Kern, M. Grioni, J. Henk, A. Ernst, S. Ostanin, and P. Bruno, Physical Review B **77**, 014007(R) (2008).

[29] A. Rüegg, S. Pilgram, and M. Sigrist, Physical Review B **75**, 195117 (2007).

► [30] A. Rüegg, S. Pilgram, and M. Sigrist, Physical Review B **77**, 245118 (2008).

[31] A. Rüegg and M. Sigrist, arXiv:0812.0442 (2008).

[32] L. Tincani, R. M. Noack, and D. Baeriswyl, arXiv:0902.1057 (2009).

► [33] E. Gull, P. Werner, O. Parcollet, and M. Troyer, Europhysics Letters **82**, 57003 (2008).

► [34] E. Gull, P. Werner, X. Wang, M. Troyer, and A. J. Millis, Europhysics Letters **84**, 37009 (2008).

► [35] P. Werner, E. Gull, M. Troyer, and A. J. Millis, Physical Review Letters **101**, 166405 (2008).

► [36] E. Burovski, E. Kozik, N. V. Prokof'ev, B. V. Svistunov, and M. Troyer, Physical Review Letters **101**, 090402 (2008).

[37] M. Boninsegni, A. B. Kuklov, L. Pollet, N. Prokof'ev, B. V. Svistunov, and M. Troyer, Physical Review Letters **97**, 080401 (2006).

[38] P. N. Ma, L. Pollet, M. Troyer, and F.-C. Zhang, Journal of Low Temperature Physics **152**, 156 (2008).

[39] L. Pollet, M. Boninsegni, A. B. Kuklov, N. V. Prokof'ev, B. V. Svistunov, and M. Troyer, Physical Review Letters **98**, 135301 (2007).

[40] M. Boninsegni, A. Kuklov, L. Pollet, N. Prokof'ev, B. V. Svistunov, and M. Troyer, Physical Review Letters **99**, 035301 (2007).

► [41] L. Pollet, M. Boninsegni, A. Kuklov, N. Prokof'ev, B. Svistunov, and M. Troyer, Physical Review Letters **101**, 097202 (2008).

► [42] P. Corboz, L. Pollet, N. Prokof'ev, and M. Troyer, Physical Review Letters **101**, 155302 (2008).

[43] P. Corboz, M. Boninsegni, L. Pollet, and M. Troyer, Physical Review B **78**, 245414 (2008).

[44] J.-D. Picon, A. F. Albuquerque, K. P. Schmidt, N. Laflorencie, M. Troyer, and F. Mila, Physical Review B **78**, 184418 (2008).

[45] A. F. Albuquerque, H. G. Katzgraber, M. Troyer, and J. Blatter, Physical Review B **78**, 014503 (2008).

[46] L. B. Ioffe, M. V. Feigel'man, A. Ioselevich, D. Ivanov, M. Troyer, and G. Blatter, Nature **415**, 503 (2002).

► [47] M. Troyer, S. Trebst, K. Shtengel, and C. Nayak, Physical Review Letters **101**, 230401 (2008).

[48] C. Gils, E. Ardonne, S. Trebst, A. W. W. Ludwig, M. Troyer, and Z. Wang, arXiv:0810.2277 (2008).

► [49] S. Trebst, E. Ardonne, A. Feiguin, D. A. Huse, A. W. W. Ludwig, and M. Troyer, Physical Review Letters **101**, 050401 (2008).

[50] S. Trebst, M. Troyer, Z. Wang, and A. W. W. Ludwig, Progress of Theoretical Physics Supplement **176** (2008).

[51] C. Gils, arXiv:0902.0168 (2009).

► [52] A. B. Kuklov, M. Matsumoto, N. V. Prokof'ev, B. V. Svistunov, and M. Troyer, Physical Review Letters **101**, 050405 (2008).

[53] A. B. Kuklov, N. V. Prokof'ev, B. V. Svistunov, and M. Troyer, Annalen der Physik **321**, 1602 (2006).

[54] V. W. Scarola, K. B. Whaley, and M. Troyer, Physical Review B **79** (2009).

[55] D. N. Sheng, O. I. Motrunich, S. Trebst, E. Gull, and M. P. A. Fisher, Physical Review B **78**, 54520 (2008).

[56] A. F. Albuquerque, M. Troyer, and J. Oitmaa, Physical Review B **78**, 132402 (2008).

[57] M. Sigrist and M. Troyer, EPJB **39**, 207 (2004).

► [58] R. Roldán, A. Rüegg, and M. Sigrist, The European Physical Journal B **64**, 185 (2008).

[59] A. B. Kuzmenko, E. van Heumen, D. van der Marel, P. Lerch, P. Blake, K. S. Novoselov, and A. K. Geim, arXiv:0810.2400 (2008).

[60] K. Wakabayashi, Y. Takane, and M. Sigrist, Physical Review Letters **99**, 036601 (2007).

[61] K. Wakabayashi and M. Sigrist, Journal of the Physical Society of Japan **77**, 113708 (2008).

► [62] P. Paruch, A.-B. Posadas, M. Dawber, C. H. Ahn, and P. L. McEuen, Applied Physics Letters **93**, 132901 (2008).

[63] G. Buchs, Local Modification and Characterization of the Electronic Structure of Carbon Nanotubes, Ph.D. thesis, University of Basel (2008).

► [64] G. Buchs, P. Ruffieux, P. Gröning, and O. Gröning, Applied Physics Letters **93**, 073115 (2008).

[65] A. Tolvanen, G. Buchs, P. Ruffieux, P. Gröning, O. Gröning, and A. Krasheninnikov, *to be published in* Physical Review B (2009).

[66] G. Buchs, D. Bercioux, H. Grabert, and O. Gröning, *submitted to* Physical Review Letters (2009).

[67] R. Tediosi, N. P. Armitage, E. Giannini, and D. van der Marel, Physical Review Letters **99**, 016406 (2007).

[68] P. Samuelsson, I. Neder, and M. Büttiker, arXiv:0808.4090 (2008).

[69] P. Samuelsson and M. Büttiker, Physical Review B **73**, 041305 (2006).

[70] P. Samuelsson, E. V. Sukhorukov, and M. Büttiker, Physical Review Letters **92**, 026805 (2004).

[71] D. Sánchez and M. Büttiker, Physical Review Letters **93**, 106802 (2004).

[72] M. L. Polianksi and M. Büttiker, Physical Review Letters **96**, 156804 (2006).

► [73] H. Förster and M. Büttiker, Physical Review Letters **101**, 136805 (2008).

[74] S. E. Nigg, R. López, and M. Büttiker, Physical Review Letters **97**, 206804 (2006).

[75] S. E. Nigg and M. Büttiker, Physical Review B **77**, 085312 (2008).

► [76] M. Moskalets, P. Samuelsson, and M. Büttiker, Physical Review Letters **100**, 086601 (2008).

► [77] J. Splettstoesser, S. Ol'khovskaya, M. Moskalets, and M. Büttiker, Physical Review B **78**, 205110 (2008).

[78] P. Werner, A. Comanac, L. de' Medici, M. Troyer, and A. J. Millis, Physical Review Letters **97**, 076405 (2006).

[79] A. F. Albuquerque, H. G. Katzgraber, and M. Troyer, arXiv:0805.2290 (2008).

Other references

[80] R. Jördens, N. Strohmaier, K. Günter, H. Moritz, and T. Esslinger, Nature **455**, 204 (2008).

[81] E. G. Dalla Torre, E. Berg, and E. Altman, Physical Review Letters **97**, 260401 (2006).

[82] L. Fallani, J. E. Lye, V. Guarrera, C. Fort, and M. Inguscio, Physical Review Letters **98**, 130404 (2007).

[83] D. Jérome, T. M. Rice, and W. Kohn, Physical Review **158**, 462 (1967).

[84] W. Kohn, Physical Review Letters **19**, 439 (1967).

[85] F. J. Di Salvo, D. E. Moncton, and J. V. Waszczak, Physical Review B **14**, 4321 (1976).

[86] H. P. Hughes, Journal of Physics C **10**, L319 (1977).

[87] E. Morosan, H. W. Zandbergen, B. S. Dennis, J. W. G. Bos, Y. Onose, T. Klimczuk, A. P. Ramirez, N. P. Ong, and R. J. Cava, Nature Physics **2**, 544 (2006).

[88] S. L. Bud'ko, P. C. Canfield, E. Morosan, R. J. Cava, and G. M. Schmiedeshoff, Journal of Physics: Condensed Matter **19**, 176230 (2007).

[89] J. F. Zhao, H. W. Ou, G. Wu, B. P. Xie, Y. Zhang, D. W. Shen, J. Wei, L. X. Yang, J. K. Dong, M. Arita, H. Namatame, M. Taniguchi, X. H. Chen, and D. L. Feng, Physical Review Letters **99**, 146401 (2007).

[90] S. Y. Li, G. Wu, X. H. Chen, and L. Taillefer, Physical Review Letters **99**, 107001 (2007).

[91] G. Wu, H. X. Yang, L. Zhao, X. G. Luo, T. Wu, G. Y. Wang, and X. H. Chen, Physical Review B **76**, 024513 (2007).

[92] D. Qian, D. Hsieh, L. Wray, E. Morosan, N. L. Wang, Y. Xia, R. J. Cava, and M. Z. Hasan, Physical Review Letters **98**, 117007 (2007).

[93] H. Barath, M. Kim, J. F. Karpus, S. L. Cooper, P. Abbamonte, E. Fradkin, E. Morosan, and R. J. Cava, Physical Review Letters **100**, 106402 (2008).

[94] P. A. Lee, N. Nagaosa, and X.-G. Wen, Reviews of Modern Physics **78**, 17 (2006).

[95] V. A. Sidorov, M. Nicklas, P. G. Pagliuso, J. L. Sarrao, Y. Bang, A. V. Balatsky, and J. D. Thompson, Physical Review Letters **89**, 157004 (2002).

[96] J. Wosnitza, Journal of Low Temperature Physics **146**, 641 (2007).

[97] J. L. Tallon, J. W. Loram, G. V. M. Williams, J. R. Cooper, I. R. Fisher, J. D. Johnson, M. P. Staines, and C. Bernhard, Physica Status Solidi (b) **215**, 531 (1999).

[98] T. Naka, J. Tang, J. Ye, A. Matsushita, T. Matsumoto, R. Settai, and Y. Ōnuki, Journal of the Physical Society of Japan **72**, 1758 (2003).

[99] T. Naka, L. A. Ponomarenko, A. de Visser, A. Matsushita, R. Settai, and Y. Ōnuki, Physical Review B **71**, 024408 (2005).

[100] C. Zener, Physical Review **82**, 403 (1951).

[101] A. J. Millis, P. B. Littlewood, and B. I. Shraiman, Physical Review Letters **74**, 5144 (1995).

[102] E. Dagotto, *Nanoscale Phase Separation and Colossal Magnetoresistance* (Springer-Verlag, Berlin, 2003).

[103] N. Mannella, W. L. Yang, K. Tanaka, X. J. Zhou, H. Zheng, J. F. Mitchell, J. Zaanen, T. P. Devereaux, N. Nagaosa, Z. Hussain, and Z.-X. Shen, Physical Review B **76**, 233102 (2007).

[104] R. Yu, S. Dong, C. Şen, G. Alvarez, and E. Dagotto, Physical Review B **77**, 214434 (2008).

[105] S. Trotzky, P. Cheinet, S. Fölling, M. Feld, U. Schnorrberger, A. Rey, A. Polkovnikov, E. Demler, M. Lukin, and I. Bloch, Science **319**, 295 (2008).

[106] G. Vidal, Physical Review Letters **98**, 070201 (2007).

[107] P. Barmettler, A. Rey, E. Demler, M. Lukin, I. Bloch, and V. Gritsev, Physical Review A **78**, 012330 (2008).

[108] P. Barmettler, M. Punk, V. Gritsev, E. Demler, and E. Altman, arXiv:0810.4845 (2008).

[109] E. Kim and M. H. W. Chan, Science **305**, 1941 (2004).

[110] E. Kim and M. H. W. Chan, Nature **427**, 225 (2004).

[111] T. Senthil, A. Vishwanath, L. Balents, S. Sachdev, and M. P. A. Fisher, Science **303**, 1490 (2004).

[112] S. Nakatsuji and Y. Maeno, Physical Review B **62**, 6458 (2000).

[113] M. Kriener, P. Steffens, J. Baier, O. Schumann, T. Zabel, T. Lorenz, O. Firedt, R. Muller, A. Gukasov, P. G. Radaelli, P. Reutler, A. Revcolevschi, S. Nakatsuji, Y. Maeno, and M. Braden, Physical Review Letters **95**, 267403 (2005).

[114] E. McCann, Physical Review B **74**, 161403(R) (2006).

[115] M. S. Dresselhaus, G. Dresselhaus, and P. Avouris, *Carbon Nanotubes* (Springer, Berlin, 2001).

[116] M. S. Fuhrer, B. M. Kim, T. D. Dürkop, and T. Brintlinger, Nano Letters **2**, 755 (2002).

[117] T. Sakurai, T. Yoshimura, S. Akita, N. Fujimura, and Y. Nakayama, Japanese Journal of Applied Physics **45**, 1036 (2006).

[118] X. M. H. Huang, R. Caldwell, L. Huang, S. C. Jun, M. Huang, M. Y. Sfeir, S. P. O'Brien, and J. Hone, Nano Letters **5**, 1515 (2005).

[119] J. C. Y. Teo, L. Fu, and C. L. Kane, Physical Review B **78**, 045426 (2008).

[120] L. Fu and C. L. Kane, Physical Review B **76**, 045302 (2007).

[121] D. Hsieh, D. Qian, L. Wray, Y. Xia, Y. S. Hor, R. J. Cava, and M. Z. Hasan, Nature **452**, 970 (2008).

[122] K. Behnia, L. Balicas, and Y. Kopelevich, Science **317**, 1729 (2007).

[123] L. Li, J. G. Checkelsky, Y. S. Hor, C. Uher, A. F. Hebard, R. J. Cava, and N. P. Ong, Science **321**, 547 (2008).

[124] I. Neder, N. Ofek, Y. Chung, M. Heiblum, D. Mahalu, and V. Umansky, Nature **448**, 333 (2007).

[125] J. Tobiska and Y. V. Nazarov, Physical Review B **72**, 235328 (2005).

[126] D. M. Zumbühl, C. M. Marcus, M. P. Hanson, and A. C. Gossard, Physical Review Letters **96**, 206802 (2006).

[127] R. Leturcq, D. Sánchez, G. Götz, T. Ihn, K. Ensslin, D. C. Driscoll, and A. C. Gossard, Physical Review Letters **96**, 126801 (2006).

[128] D. Sánchez, Physical Review B **79**, 045305 (2008).

[129] M. Büttiker, H. Thomas, and A. Prêtre, Physics Letters A **180**, 364 (1993).

[130] J. Gabelli, G. Fève, J.-M. Berroir, B. Plaçais, A. Cavanna, B. Etienne, Y. Jin, and D. C. Glattli, Science **313**, 499 (2006).

[131] G. Fève, A. Mahé, J. M. Berroir, T. Kontos, B. Plaçais, D. C. Glattli, A. Cavanna, B. Etienne, and Y. Jin, Science **316**, 1169 (2007).

[132] A. Georges, G. Kotliar, W. Krauth, and M. J. Rozenberg, Reviews of Modern Physics **68**, 13 (1996).

[133] P. Bruno, Physical Review Letters **79**, 4593 (1997).

[134] J. H. G. Owen, K. Miki, and D. R. Bowler, Journal of Materials Science **41**, 4568 (2006).

Project 2 Superconductivity, unconventional mechanisms and novel materials

Project leader: D. van der Marel (UniGE)

Participating members: D. Baeriswyl (UniFR), C. Bernhard (UniFR), G. Blatter (ETHZ), Ø. Fischer (UniGE), T. Giamarchi (UniGE), M. Grioni (EPFL), H. Keller (PSI), D. van der Marel (UniGE), J. Mesot (PSI), E. Morenzoni (PSI), T. M. Rice (ETHZ), M. Sigrist (ETHZ). Contribution from J.-M. Triscone (UniGE).

Introduction: Current-flow with zero loss of energy is the most spectacular consequence of the phenomenon of superconductivity. Project 2 unites the research activities of one of the world highest concentrations of experts on superconductivity. The project pushes the limits of (i) the quantitative understanding how superconductivity arises in specific compounds, (ii) the search for new superconducting materials, and (iii) the search for new phenomena associated with superconductivity. The importance and high impact of these results is testified by the large number of scientific publications in highly reputed scientific journals, and the disproportionately strong presence of Swiss representatives to international conferences in the field of superconductivity.

Summary and highlights

Major progress was achieved in understanding the interplay between spin-correlations and superconductivity in the high-T_c cuprates, and how high-T_c superconductivity results from this interplay. Neutron scattering results imply a competition between superconductivity and static antiferromagnetism. Isotope substitution has revealed sign reserved effects on the spin-glass phase as compared to the superconducting phase. The scanning tunneling spectra reveal coupling of the conduction electrons to the sharp spin-resonance mode at momentum (π, π) . Optical spectra of a broad range of different high-T_c cuprates reveals coupling to both phonons and spin-fluctuations. The spin-fluctuation part of the inelastic scattering was found to correlate with the doping dependence of T_c. Theoretical study of the Hubbard model showed that superconductivity with d-wave symmetry requires that the Fermi surface exhibits antiferromagnetic "hot spots".

The exploration of novel superconducting phases is of crucial importance, first of all because it leads to the discovery of novel superconducting states of matter, and secondly because it helps to complete our understanding of various superconducting phenomena. Several discoveries were made in the field of unconventional superconductivity. Using neutron diffraction, $CeCoIn_5$ was found to adopt a multicomponent ground state close to the upper critical field, which simultaneously carries cooperating magnetic and superconducting orders. In the 3 Kelvin phase of Sr_2RuO_4 a filamentary form of superconductivity has been identified, having spontaneous currents running as a consequence of time reversal symmetry breaking. Optical studies of the ferromagnetic heavy fermion superconductor UGe_2 have revealed that the magnetic order triggers the transition into a state characterized by heavy and weakly scattered charge carriers, which are strongly coupled to the magnetic modes. Scanning tunneling microscopy studies revealed two-gap superconductivity in the Chevrel phase compounds. Field effect modulation of superconductivity at the $LaAlO_3/SrTiO_3$ interface show the existence of a quantum phase transition between a superconducting and an insulating phase at the $LaAlO_3/SrTiO_3$ interface. In the insulating region of the phase diagram a large (40% at 8 T) negative magnetoresistance has been observed, possibly due to weak localization.

Using scanning tunneling spectroscopy it was shown that the vortex phase diagram of single layer Bi-2201 is governed by a temperature dependence of the anisotropy, and that vortex pinning is moderate. Superlayers of ferromagnetic $La_{2/3}Ca_{1/3}MnO_3$ (LCMO) and superconducting $YBa_2Cu_3O_7$ (YBCO) were found to display strong modulation of the ferromagnetic moment in the LCMO layers when the YBCO becomes superconducting. The magnetic properties of the $La_{2/3}Ca_{1/3}MnO_3$ were observed to strongly respond to lattice strain effects due to a lattice mismatch at the substrate-film interface, as well as pressure. Unexpected large dissipation free supercurrents were observed with μSR to flow through and in 50 nm thick antiferromagnetic $PrBa_2Cu_3O_7$ barriers sandwiched

between two superconducting $YBa_2Cu_3O_7$ layers, reflecting the presence of induced superfluid density in the antiferromagnetic barrier.

1 Microscopic properties of the cuprates

1.1 Resonant X-ray scattering experiments on cuprates (*M. Grioni*)

For many years angle-resolved photoemission (ARPES) and optics have been the spectroscopic techniques of choice to study the electronic structure of the cuprates. Neutron scattering experiments on the other hand have been very successful in probing the magnetic structure and properties. Although quite powerful, each of these techniques has weaknesses: ARPES is very surface sensitive; optics is limited to $Q = 0$ excitations, and neutrons require large samples. Emerging spectroscopies like resonant inelastic X-ray scattering (RIXS) are therefore welcome as possible sources of complementary, and sometimes unique, information. RIXS is the X-ray analog of traditional Raman spectroscopy. Energy losses are measured in a photon scattering process where the energy of the incident beam is tuned to a characteristic absorption edge of the material. This yields chemically selective, Q-dependent, information on electronic and collective excitations. Moreover, optically-forbidden transitions, e.g. *dd* excitations in TM compounds, are accessible to RIXS.

The SAXES collaboration which includes Politecnico di Milano, the SLS and the EPFL group (Grioni) has developed a spectrometer which enables RIXS experiments with soft X-rays and a world record resolving power $E/\Delta E = 10'000$ [1]. In collaboration with D. van der Marel (UniGE) and H. Rønnow (EPFL) we have exploited these performances to study the paradigmatic insulating cuprate $Sr_2CuCl_2O_2$ (SCOC) at the Cu L_3 ($2p \rightarrow 3d$, $h\nu = 930$ eV) edge. The RIXS spectrum of Fig. 1 shows, with unprecedented clarity, strong losses in the 1.5 – 2.5 eV energy range. They correspond to final states where the single hole of the Cu^{2+} ion has been scattered from the $(x^2 - y^2)$ orbital to one of the higher lying crystal field states of the D_{4h} tetragonal field. The energies of these optically-forbidden *dd* transitions can be quite accurately reproduced by a single-ion calculation, which then yields the crystal field parameters.

The superior resolution of the SAXES spectrometer provides a first view of the fine structure in the quasielastic response (Fig. 2). In the particular conditions of scattering angle and photon polarization of the experiment, the elastic peak (at $E = 0$) is strongly suppressed. This sharply contrasts with hard X-ray RIXS data at the Cu K-edge, which are dominated by the elastic scattering. Two loss features are identified at 300 meV and 100 meV. Further preliminary measurements have shown that these features clearly disperse as a function of the transferred momentum Q, and therefore correspond to collective excitations. The

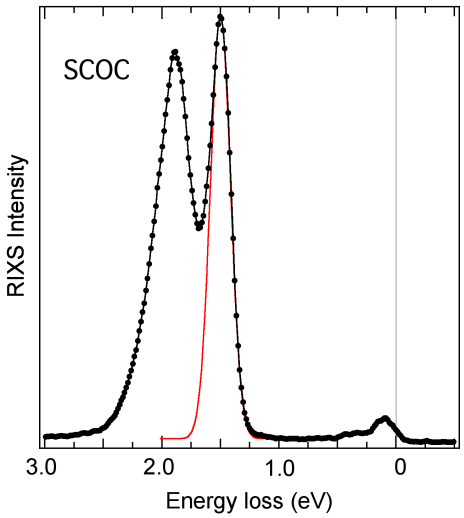

Figure 1: *Cu L_3 RIXS spectrum of $Sr_2CuCl_2O_2$ measured with the SAXES spectrometer of the SLS.*

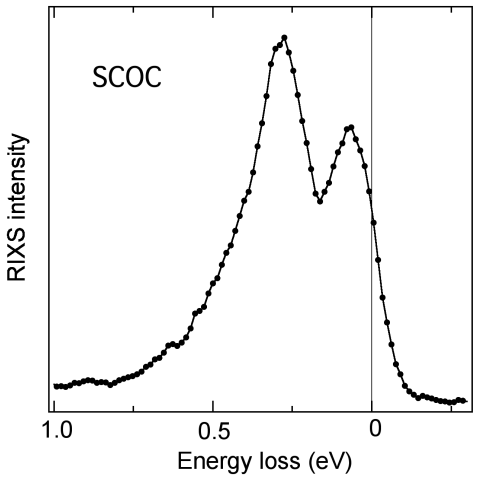

Figure 2: *Quasielastic RIXS response of $Sr_2CuCl_2O_2$. Two distinct low-energy losses are identified. The elastic peak at zero energy is strongly suppressed.*

more energetic mode is assigned to a bimagnon excitation, i.e. the coherent excitation of two magnons in the 2D AFM background. Similar RIXS collective losses have been reported at the Cu L- and K-edges of other cuprates [39, 40] but are considerably better defined here thanks to the improved resolution. Their energy exceeds for all Q values the energy of a single magnon, and approaches a value of $4J \sim 500$ meV at the zone boundary. The lower energy loss could be due to the superposition of intensities from a single magnon – which is expected to be weaker than the bimagnon – and of a phonon mode. This will be clarified by more detailed Q-dependent experiments that are in progress. It is of course interesting to see how these low-energy losses are modified in metallic, namely superconducting cuprates. We have performed preliminary experiments on samples of the BSCCO family. Data for the two-layer optimally-doped ($T_c = 92$ K) Bi-2212 are shown in Fig. 3 for two polarization states of the incident beam: within (H) and perpendicular (V) to the horizontal scattering plane, and a 90° scattering angle. Losses are observed in both cases with energies as large as 700 meV, but with a different intensity distribution. Clearly the situation is more complex than for insulating SCOC because a continuum of intraband electron-hole excitations is now available within the hybrid Cu-O conduction band. Optical measurements can probe this continuum, but only at the zone center ($Q = 0$). In future experiments we will measure the Q-dependence of these spectral features, which will reflect the band dispersion – including above E_F – and provide information on spin correlations in the normal and the superconducting phase.

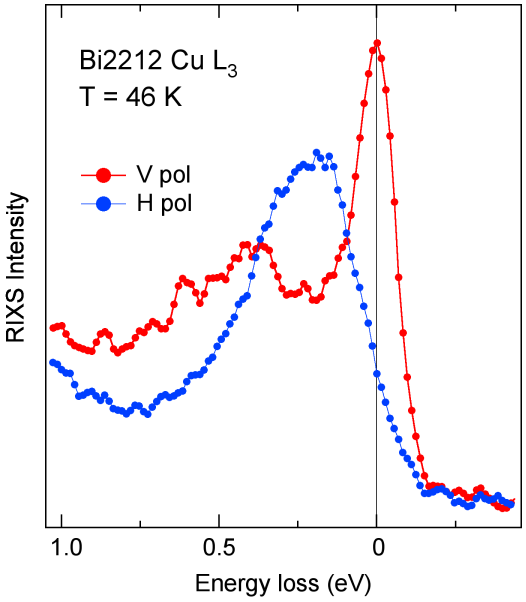

Figure 3: *RIXS spectra of optimally doped Bi-2212 for two polarization states of the X-ray beam.*

1.2 Tuning competing orders in $La_{2-x}Sr_xCuO_4$ by a magnetic field (*J. Mesot*)

We have performed a systematic study of the competition between antiferromagnetism and superconductivity in the vicinity of 1/8 doping. By combining μSR and neutron diffraction results obtained on the same single crystals we were able to derive a $H - x$ phase diagram for the ordered Cu moment (Fig. 4).
Our results clearly support the notion of competing superconducting (SC) and static antiferromagnetic (AF) order parameters. The systematics of our data shows that the existence of AF is intrinsic and not due to defects or chemical inhomogeneities. Any suppression of superconductivity either by a change in chemistry or by an external perturbation goes along with a concurrent and systematic enhancement of static magnetism [2].

a) *Possible spin density wave induced Fermi surface reconstruction* We used the suppression of superconductivity near the 1/8-anomaly to study the low-temperature electronic structure in the pseudogap phase of La-based cuprates. For $La_{1.48}Nd_{0.4}Sr_xCuO_4$ and $La_{2-x}Sr_xCuO_4$ (LSCO) with x $\approx$ 1/8 we found two opposite dispersing Fermi arcs as shown in Fig. 5. The secondary Fermi arc appears only for x $\approx$ 1/8 and not in LSCO with $x = 0.105$ and $x = 0.145$. It is thus tempting to interpret these results in terms of a spin density wave induced Fermi surface reconstruction. However the weak temperature dependence of this

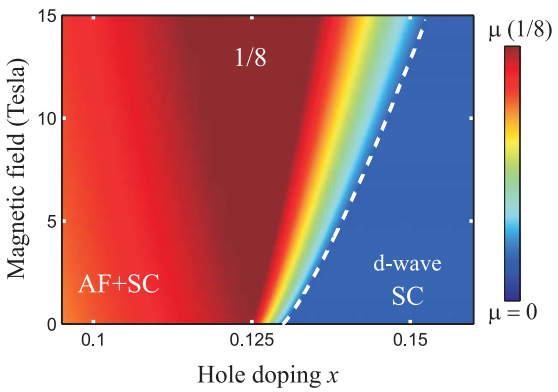

Figure 4: *Schematic doping-field phase diagram for $La_{2-x}Sr_xCuO_4$. The ordered moment is given in false colors with red (blue) as the maximum (minimum).*

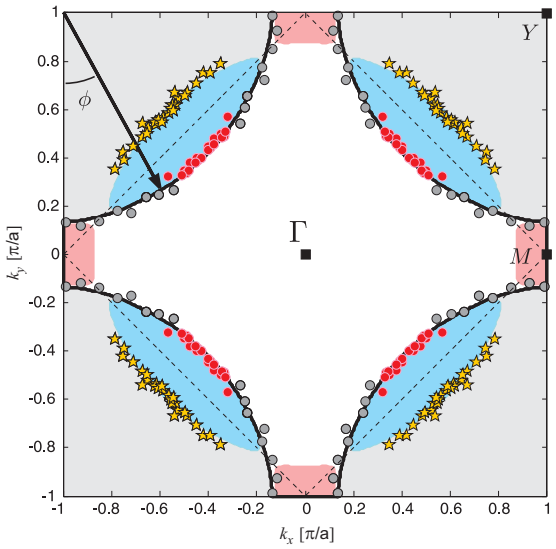

Figure 5: *Fermi surface of Nd-LSCO $x = 1/8$. The gray points indicate the Fermi momenta underlying the pseudogap while the red points define the Fermi arc of gapless quasiparticles. The yellow stars are the discovered secondary branch.*

secondary branch extending well above both spin and charge ordering temperatures by contrast suggests that the secondary branch is an effect of the lattice structure like the so-called shadow band observed in Bi-2212. Our results can therefore only be understood in terms to a non-trivial interplay between spin and lattice degrees of freedom [3].

1.3 Coexisting antiphase superconductivity and antiferromagnetism in the stripe phase at doping 1/8 (*T.M. Rice*)

The discovery that stripes have antiphase superconductivity coexisting with spin density wave order was a big surprise [41, 42]. Yang *et al.* performed renormalized mean field theory calculations which give evidence for a strong synergy between these orders, but within the present scheme are not enough to give absolute stability [4]. The results confirm the subtle interplay between these normally competing orders in cuprates.

1.4 Coherent *d*-wave superconducting gap in underdoped $La_{2-x}Sr_xCuO_4$ (*J. Mesot*)

We present an ARPES study on moderately underdoped $La_{1.855}Sr_{0.145}CuO_4$ at temperatures below and above the superconducting transition temperature. Unlike previous studies of this material, we observe sharp spectral peaks along the entire underlying Fermi surface in the superconducting state. These peaks trace out an energy gap that follows a simple *d*-wave form, with a maximum superconducting gap of 14 meV. Our results are consistent with a single gap picture for the cuprates. Furthermore our data on the even more underdoped sample $La_{1.895}Sr_{0.105}CuO_4$ also show sharp spectral peaks, even at the antinode, with a maximum superconducting gap of 26 meV [5].

1.5 Modelling and imaging the essential role of spin-fluctuations in high-T_c superconductivity (Ø. Fischer)

The signature of bosonic collective modes in the tunneling spectra of high-T_c superconductors are actively investigated in our group [6]. These modes appear as conductance dips in the spectra. Using a strong coupling model which takes into account the realistic band structure of the material, and the coupling of quasiparticles with a $(\pi - \pi)$ collective excitation, we can fit our spectra and reproduce most of the characteristic spectral features with a remarkably high accuracy. Following the initial studies in Bi-based compounds [7], low-noise measurements and refinements in the fitting procedure allow to reveal systematic trends. It appears that the role played by the Van Hove singularity (vHs) is preeminent in layered cuprates, accounting for the particle-hole asymmetry and the abnormally intense coherence peaks in materials like $Bi_2Sr_2Ca_2Cu_3O_{10+\delta}$ (Bi-2223) [8]. All evidences suggest that the collective excitation responsible for the dip-hump feature seen in tunneling is the $(\pi - \pi)$ spin resonance revealed by inelastic neutron scattering experiments [43]. Both the magnitude and the

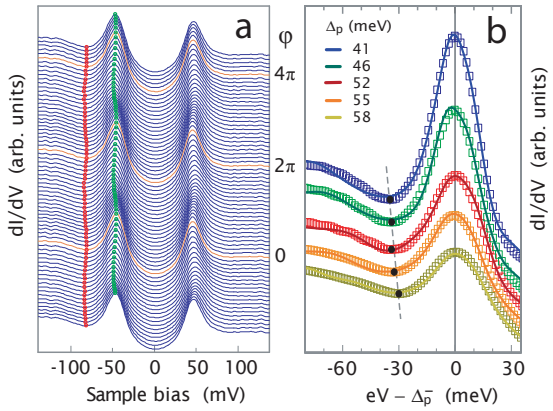

Figure 6: *Spatial modulation of the gap and dip energy. (a) Evolution of the dI/dV spectra with the phase φ (orange: spectra measured at the minima of the corrugation; green dots: coherence peaks; red dots: dip). (b) Negative-bias part of the Δ_p-averaged spectra (open symbols: experimental data); lines are fits with a strong-coupling model.*

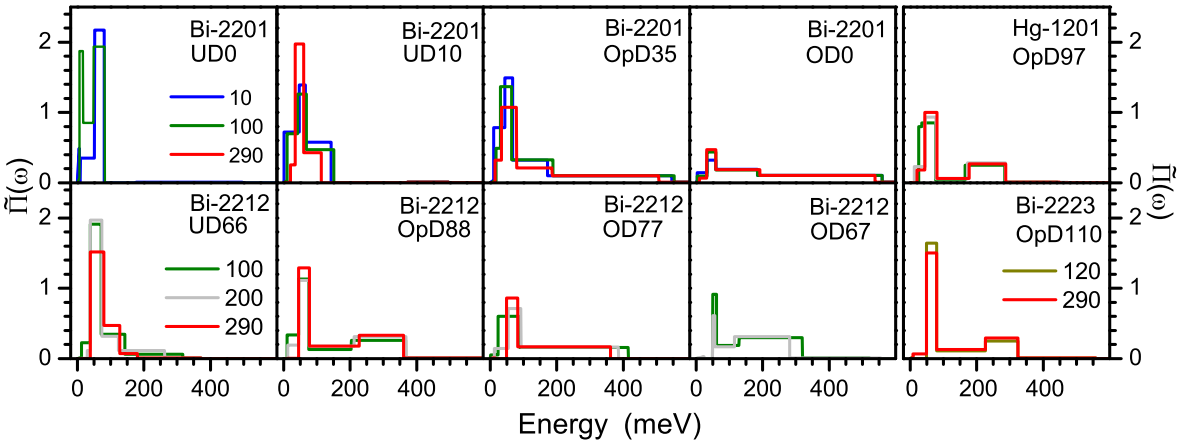

Figure 7: *Electron-boson coupling function $\tilde{\Pi}(\omega)$ for Bi-2201 at four different charge carrier concentrations (10 K, 100 K, 290 K), Bi-2212 at four charge carrier concentrations, and optimally doped Bi-2223 and Hg-1201 (100 K, 200 K, 290 K).*

doping dependence of the mode energy are in agreement with the neutron data. Analysis of strongly underdoped $Bi_2Sr_2CaCu_2O_{8+\delta}$ (Bi-2212) and of the single-layer Bi-2201 are in progress. The same model has been used to fit tunneling spectra of $YBa_2Cu_3O_{7-\delta}$ considering bilayer splitting. In this material, similarly to Bi-2212 and Bi-2223, the collective mode energy (10 – 30 meV) decreases when the gap magnitude increases.

A new systematics has been revealed by imaging the distribution of the spectroscopic features in real space in Bi-2223 with scanning tunneling microscopy (STM). We observe that the gap magnitude, a direct measure of the pairing strength, is periodically modulated on a length scale of about 5 crystal unit-cells, following the structural supermodulation present in Bi-based cuprates (Fig. 6a).

Fitting the STM data (Fig. 6b) with a strong-coupling model [44][7] allowed us to image the collective mode energy (CME) at the atomic scale and reveal a modulation that also follows the superstructure. The CME and the gap are locally anticorrelated. These findings support that the collective mode probed in our study is related to superconductivity, and is most likely the antiferromagnetic spin resonance. Our results, in particular the CME value of 30 – 40 meV, are in agreement with the spin-fluctuation-mediated pairing scenario [45], in which the spin resonance in high-T_c's is a consequence of pairing.

1.6 Optical determination of the pairing mechanism in the cuprates (*D. van der Marel*)

According to the standard model of superconductivity, electrons form pairs due to a retarded attractive interaction mediated by virtual bosonic excitations in the solid. The bosonic excitations constitute the glue which binds the electrons together, similar to the way in which forces are transmitted between elementary particles. In a solid the bosons transmitting the interaction are fluctuations of the nuclear coordinates, spin-polarization, electric charge or current. Aforementioned effective electron-electron interaction can be expressed with the help of the density of states of these bosons multiplied by the electron-boson coupling, or "glue-function" $\tilde{\Pi}(\omega)$.

In the absence of a glue and of scattering off impurities the effect of applying an ac electric field to the electron gas is to induce a purely reactive current response, characterized by the imaginary optical conductivity $4\pi\sigma(\omega) = i\omega_p^2/\omega$. The effect of coupling the electrons to bosonic excitations is revealed by a finite, frequency dependent dissipation. We have calculated the glue-function from the optical spectra of a large number of four Bi-2201 crystals with different hole concentrations, optimally doped Hg-1201 [9] and Bi-2223 [10], as well as four Bi-2212 crystals [11] with different hole concentrations. The results are displayed on Fig. 7. We observe two main features in $\tilde{\Pi}(\omega)$: a robust peak at 50 – 60 meV and a broad continuum. The upper limit of $\tilde{\Pi}(\omega)$ is situated around approximately 300 meV for optimally doped single-layer Hg-1201, and for the bilayer and trilayer samples. Interestingly the continuum extends to the highest energies for the weakly overdoped samples (550 meV for the single-layer samples and 400 meV for the bilayers). There is also a clear trend of a contraction of the continuum to lower energies when the carrier concentration is reduced. The most prominent feature, present in all spectra reproduced

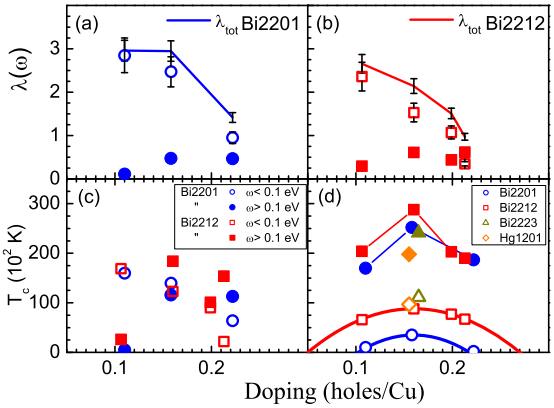

Figure 8: *Experimental critical temperatures (open symbols) and upper limit on T_c calculated from Eliashberg theory using the room temperature glue functions as input (closed symbols).*

in Fig. 7, is a peak corresponding to an average frequency of 55 meV. This peak is practically independent of temperature (up to room temperature) and sample composition, within our error bars. Moreover, the amplitude and width are essentially temperature independent.

With the help of the Eliashberg equations we calculated an upper limit on the critical temperature from these experimentally measured glue functions. Obviously, the actual critical temperatures will be lower as a result of the pair-breaking contributions in $\tilde{\Pi}(\omega)$. The critical temperature can be calculated straightforwardly from the Eliashberg equations [46] when $\tilde{\Pi}(\omega)$ is known. As shown in Fig. 8, the T_c's are in the 150 – 300 K range, and they correlate with the experimentally observed doping trends of T_c. The dome-shaped trend in the calculation is a consequence of the increasing energy scale of $\tilde{\Pi}(\omega)$ and the decreasing overall coupling constant as a function of doping. We took this analysis a step further by calculating T_c from the glue spectra below 100 meV ($\tilde{\Pi}_{pk}$) and above 100 meV ($\tilde{\Pi}_{cnt}$). In the case of overdoped Bi-2212 with $T_c = 66$ K we obtain only $T_c = 22$ K from $\tilde{\Pi}_{pk}$, whereas $\tilde{\Pi}_{cnt}$ gives 154 K, implying that the glue-function above 100 meV is of crucial importance for the pairing-mechanism. Since only electronic excitations have such high energies, an important contribution to the high-T_c mechanism comes apparently from coupling to spin fluctuations [47, 48, 49, 50].

1.7 Oxygen isotope effects within the phase diagram of cuprates (*H. Keller*)

In 1990 the UniZH group started a project on isotope effects in cuprate high-temperature superconductors (HTS's) which was initiated by

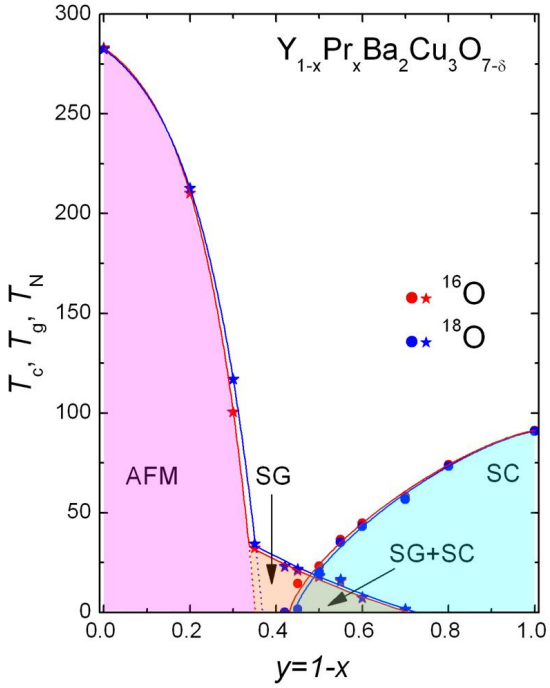

Figure 9: *Dependence of the superconducting transition (T_c), the spin-glass ordering (T_g), and the antiferromagnetic ordering (T_N) temperatures for $^{16}O/^{18}O$ substituted $Y_xPr_{1-x}Ba_2Cu_3O_{7-\delta}$ on the Pr content x. The solid lines are guides to the eye. The areas denoted by "AFM", "SG", and "SC" represent the antiferromagnetic, the spin-glass and the superconducting regions, respectively. "SG+SC" corresponds to the region where spin-glass magnetism coexist with superconductivity.*

K. Alex Müller. Several novel oxygen isotope ($^{16}O/^{18}O$) effects (OIE's) on different quantities in cuprates were observed, such as on the transition temperature T_c (including site-selective OIE), the in-plane magnetic penetration depth $\lambda_{ab}(0)$ (including site-selective OIE), the anisotropy parameter γ, the pseudogap temperature T^*, the charge-ordering temperature T_{co}, the superconducting energy gap Δ_0, the Néel temperature T_N, the spin-glass freezing temperature T_g, and the EPR line width Γ [51, 52, 53][12, 13, 14]. These unconventional OIE's were detected in different cuprate HTS families by using various types of samples (powders, single crystals, films) and experimental techniques (SQUID, magnetic torque, μSR, EPR, XANES, neutron scattering).

Cuprate HTS's exhibit a rich phase diagram (Fig. 9). The undoped parent compounds are characterized by a long range 3D antiferromagnetic (AFM) order, which is rapidly destroyed when holes are doped into the CuO_2 planes. Short-range AFM correlations survive, however, well in the superconducting (SC) region of the phase diagram by forming a spin-

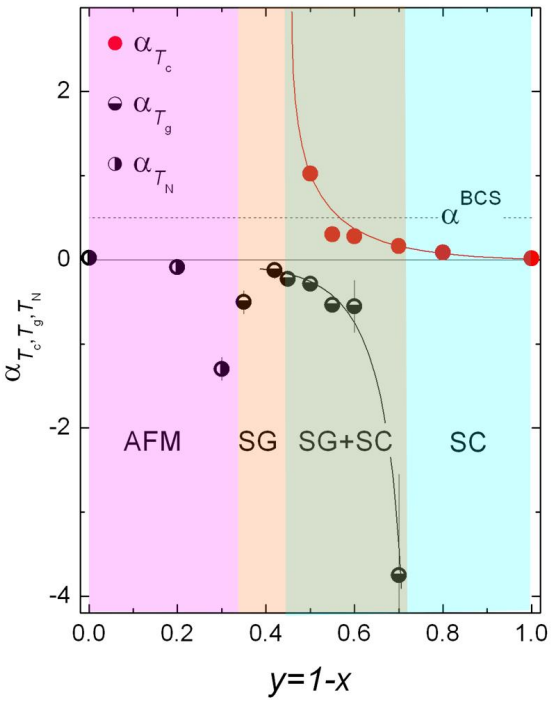

Figure 10: *OIE exponents α_{T_c}, α_{T_g}, and α_{T_N} for $^{16}O/^{18}O$ substituted $Y_xPr_{1-x}Ba_2Cu_3O_{7-\delta}$ as a function of the Pr content x. The dashed line corresponds to $\alpha_{T_c}^{BCS} = 0.5$. The solid lines are guides to the eye. The meaning of the areas denoted by "AFM", "SG", "SG+SC", and "SC" are the same as in Fig. 9.*

glass (SG) state. Upon the onset of superconductivity this phase persists for a limited doping range, suggesting that SC and SG phases coexist within a certain doping range. With increasing doping, the superconducting transition temperature T_c increases. Correspondingly, four phases can be differentiated: the AFM phase, the SG phase, the SG+SC phase, and the SC phase. How these phases are related to each other is an open and controversial issue, and until now experiments are missing which could provide a fundamental link between them. In particular, it is very interesting to investigate the OIE's on the corresponding transition temperatures between the various phases. Several years ago we observed a huge OIE on the spin-glass freezing temperature T_g in $La_{2-x}Sr_xCu_{1-z}Mn_zO_4$ ($x = 0.03$ and 0.05; $z = 0.02$) by means of μSR [54]. This is a clear signature that the spin dynamics in cuprates are ultimately correlated with lattice vibrations.

Recently, we performed a detailed OIE study of the various phases (SC, SG+SC, SG, AFM) in the prototype cuprate system $Y_{1-x}Pr_xBa_2Cu_3O_{7-\delta}$ by means of μSR and magnetization experiments. These techniques have the advantage of being direct, bulk sensitive, unambiguous and able to measure T_c as well as T_g in the region where both coexist [15]. The results are sumarized in Figs. 9 and 10. All phases exhibit an OIE which is strongest, where the respective phase terminates. Note that the OIE on the magnetic phases (SG and AFM) are sign reversed as compared to the one on the superconducting phase. Another interesting anticorrelation is observed in the region where spin-glass magnetism coexist with superconductivity (SG+SC). Here a small OIE on T_c corresponds to a large OIE on T_g in sequence and vice versa. This behavior suggests that in this regime phase separation sets in where the superfluid density coexists with a SG related one. Since the isotope effect on T_c can be accounted for through polaron formation [16], the one on T_g is expected to originate from the same physics. By relating the AFM transition temperature to the metal insulator transition, a reduction in kinetic energy caused by polaron formation is proposed to explain this OIE as well. The various OIE's reported here, clearly evidence that lattice effects are effective in all phases of cuprate superconductors and impose serious constraints on theories for cuprate superconductivity.

1.8 Superconductivity in the 2D repulsive Hubbard model (*D. Baeriswyl*)

One of the central issues in the field of high-temperature superconductors has been – and for some researchers still is – the question whether pairing in the cuprates arises from purely repulsive interactions, as proposed by Anderson more than two decades ago [55]. This question has been studied extensively in the framework of the two-dimensional (repulsive) Hubbard model (and the related $t - J$ model). Recent progresses, both in dynamical mean-field theory and in variational calculations, has strengthened the case for the existence of a superconducting phase in the Hubbard model, with a (d-wave) gap parameter reasonably close to experimental values for intermediate interaction strengths (U of the order of the bandwidth).

Most previous studies of the Hubbard model have been restricted to nearest-neighbor hopping, where electron doping does not differ from hole doping. In our recent studies we have discovered that the addition of second-neighbor hopping (which breaks the electron-hole symmetry) changes this behavior substantially [17]. While the hole-doped side is "localized" and shows kinetic-energy driven superconductivity with a large condensation en-

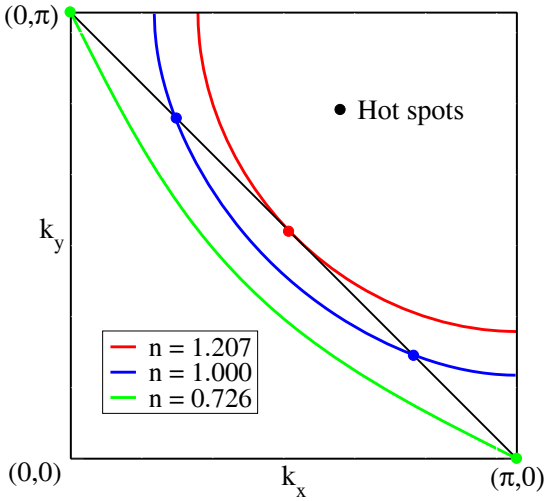

Figure 11: *Fermi surfaces for three different electron densities.*

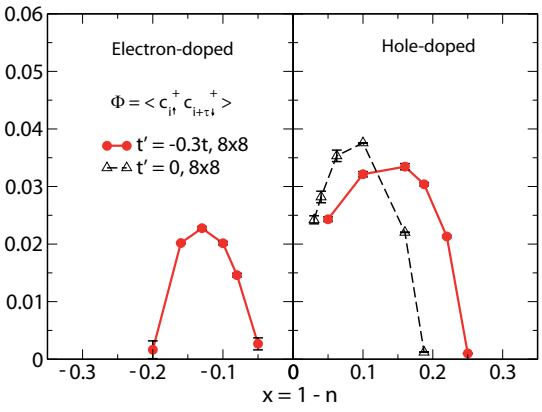

Figure 12: *Superconducting order parameter as a function of doping for an 8×8 lattice. For comparison, the result for $t' = 0$ is also shown.*

ergy, the electron-doped side is itinerant, with a potential-energy driven superconductivity and a small condensation energy.

The Hubbard Hamiltonian $\hat{H} = \hat{H}_0 + U\hat{D}$ consists of a hopping term ("kinetic energy")

$$\hat{H}_0 = -\sum_{i,j,\sigma} t_{ij} c^\dagger_{i\sigma} c_{j\sigma}$$

and an on-site repulsion $U\hat{D}$, where $\hat{D} = \sum_i n_{i\uparrow} n_{i\downarrow}$ is the number of doubly occupied sites, $n_{i\sigma} = c^\dagger_{i\sigma} c_{i\sigma}$, and the operator $c^\dagger_{i\sigma}$ ($c_{i\sigma}$) creates (annihilates) an electron at site i with spin σ.

We have used the trial ground state

$$|\Psi\rangle = e^{-h\hat{H}_0/t} e^{-g\hat{D}} |\Psi_0\rangle\,, \qquad (2.1)$$

where g and h are (real) variational parameters and $|\Psi_0\rangle$ is a BCS state with d-wave symmetry. In our previous study of the simple Hubbard model – $t_{ij} = t$ for nearest-neighbor sites, 0 otherwise – [18] we have found that the wave function (2.1) exhibits d-wave pairing below a (hole or electron) doping concentration of 0.18. The restriction to nearest-neighbor hopping leads to a (bare) Fermi surface which disagrees qualitatively with photoemission experiments on layered cuprates. Therefore we have applied our approach to the more realistic case of both nearest (t) and next-nearest neighbor hopping (t') with canonical parameters $U = 8t$, $t' = -0.3t$. The bare single-particle spectrum

$$\epsilon_{\boldsymbol{k}} = -2t(\cos k_x + \cos k_y) - 4t' \cos k_x \cos k_y$$

leads to the Fermi surfaces of Fig. 11. The innermost line (green) corresponds to the van Hove filling where the Fermi surface passes through the saddle points at $(\pi, 0)$ and $(0, \pi)$. These crossings between the Fermi surface and the magnetic zone boundary (the "hot spots") move inwards as the density n is increased and finally merge (outermost line, red). Hot spots are restricted to electron densities $0.726 < n < 1.206$. Our results, to be discussed below, indicate that superconductivity occurs only in this range.

The minimization of the energy expectation value with respect to the trial state (2.1) requires extensive Monte Carlo simulations. Fig. 12 shows the result for the superconducting order parameter $\Phi = |\langle c^\dagger_{i\uparrow} c^\dagger_{j_i\downarrow}\rangle|$ as a function of doping concentration $x = 1 - n$. The corresponding result for $t' = 0$ [18] is completely electron-hole symmetric and reproduced only in the right panel. On the hole-doped side superconductivity exists for $0 < x < 0.25$ (the gap parameter Δ remains finite, but the order parameter Φ vanishes for $x \to 0$), i.e. in a larger region than for $t' = 0$. In contrast, on the electron-doped side the superconducting region is reduced to $-0.2 < x < -0.05$. Thus we find indeed that superconductivity is restricted to densities where the (bare) Fermi surface passes through hot spots (see Fig. 11). Remarkably, for electron doping, the gap is suppressed very close to half filling, even in the absence of competing antiferromagnetic long-range order. The marked difference between electron and hole doping is confirmed by the condensation energy $E_{cond} = E(0) - E(\Delta)$, which is one order of magnitude smaller for electron doping than for hole doping. Moreover, the energy gain due to superconductivity is mostly associated with a gain in kinetic energy for hole doping, while it is due to the more conventional gain in potential energy for electron doping.

1.9 Flux phases in three band systems (*T. Giamarchi*)

Recently the question of whether orbital currents could exist in the pseudogap regime of cuprate materials has received much attention, with the proposal by C. M. Varma that for a three band model of the copper-oxygen planes orbital currents with $q = 0$ period could exist while absent for the single band one, and recent neutron experiments which observe moments that would be compatible with such a pattern. Of course the situation in the high-T_c context is still quite open and reliable calculations on this issue are quite challenging. To investigate this issues we followed two different routes

a) *Doped Cu–O ladders* As described in the previous report we have investigated a Cu–O ladder. The one dimensional nature of the system allows to take the effects of the extra orbitals and of the interaction into account using a controlled analytical technique. In the three band model (see previous report) a new massless phase, carrying orbital currents, exists. Such a phase is absent for simple interactions in the single band model. We have pursued the analysis of such a phase, and in particular looked at the consequences for the NMR relaxation [19].

b) *Variational study of flux phases in the cuprates* In order to study the question of flux phases for the cuprates we performed [20] a variational Monte Carlo (VMC) investigation of the three band Hubbard model based on a Gutzwiller projected wave function that allows for the possibility of orbital currents. This provides a method free from numerical limitations even for large system sizes, for which current instabilities are treated on an equal footing with other instabilities. We left the pattern of current free to be determined by the minimization of energy in our variational study. We thus allow both for phases with $q = \pi$ current pattern, such as the D-density wave, and $q = 0$ such as the ones that were proposed by C. M. Varma, to be treated on an equal footing.
If we only consider the Cu-O plane we find that the only phase that is potentially stabilized is a phase with a $q = 0$ current pattern and with a staggered symmetry (θ_2). Other symmetries or phases that break the translational symmetry are much higher in energy. However, as the system size gets larger, the energy gain decreases strongly, making it unclear whether such a phase would survive in the thermodynamic limit.

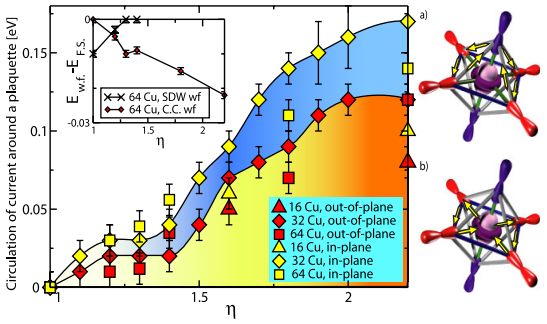

Figure 13: *Circulation of current around a $p_x - p_z - p_y$ plaquette (triangles) and around a $p_x - d_{3z2-r2} - p_y$ plaquette (squares) measured in our best variational Ansatz for the eight band Hubbard model. The phenomenological parameter η renormalizes the amplitudes of the out-of-plane transfer integrals. The symmetry of the orbital current pattern is Θ_2 like: there are two out-of-plane current loops in the upper pyramid (a) and two current loops in the Cu plane (b). Finally, the current pattern in the lower pyramid (not shown) is obtained by a horizontal mirror reflection of the upper pyramid. The calculations were done at $x = 0.125$ hole doping, and with periodic boundary conditions. Inset: energies for both the SDW wave function and the circulating currents (CC) ones showing the stabilization of the CC phase for $\eta > 1.2$.*

We thus propose modifications of the Hamiltonian that take into account apical oxygens or three-body terms and strongly stabilize such current patterns. In particular, taking into account the apical oxygens allows for the a stabilization of the current patterns with a similar symmetry (Fig. 13)
This is in good agreement with the neutron data on the $YBa_2Cu_3O_7$ compound that observe moments which are not perpendicular to the Cu-O planes but tilted, and with recent data on the mercury compounds.

1.10 Breakdown of Landau Fermi liquid behavior in overdoped cuprates (*T. M. Rice*)

Recent experiments have shed new light on the evolution of the electronic properties of the cuprate superconductors. They stimulated Rice and collaborators to examine their implications for the underlying microscopic theory. Hussey and his collaborators, by applying large magnetic fields, could follow the normal state in overdoped single-layer Tl-cuprates down to low temperatures and found an anistropic T-linear (not T^2) inelastic scattering rate whose magnitude increased with decreasing hole doping [56]. Earlier functional renormalization group (fRG) calculations on a 2-dimensional Hubbard model had found a

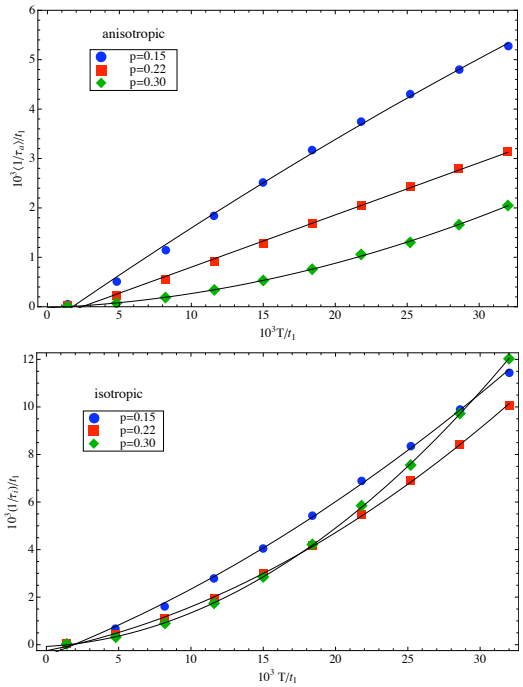

Figure 14: *Temperature dependence of the anisotropic and the isotropic components of the quasiparticle scattering rate at the Fermi energy for different hole dopings p where the lines are fits using a quadratic polynomial.*

strongly anisotropic scattering vertex in this doping range which leads to d-wave pairing but also subdominant instabilities in other channels. Ossadnik *et al.* [21] extended these fRG calculations to obtain the inelastic scattering rate in the normal state after suppressing d-wave pairing through elastic scattering. The calculations, shown in Fig. 14, agree well with experiment and confirm the key role of anisotropic scattering connecting antinodal regions predicted by the fRG calculations.

1.11 Anisotropic quasiparticle scattering rates in $La_{2-x}Sr_xCuO_4$ (*J. Mesot*)

A comprehensive ARPES study of the momentum and energy dependence of the quasiparticle scattering rate was carried out in nearly optimally doped LSCO. The dominant inelastic scattering channel scales linearly with binding energy up to the high-energy waterfall structure E1 (Fig. 15). Remarkably both the elastic and inelastic channels are highly anisotropic in momentum with a minimum along the zone diagonal. These results, well described in terms of an anisotropic marginal Fermi liquid phenomenology, pose new information about the so-called strange metal phase of the normal state of high-temperature superconductors [22].

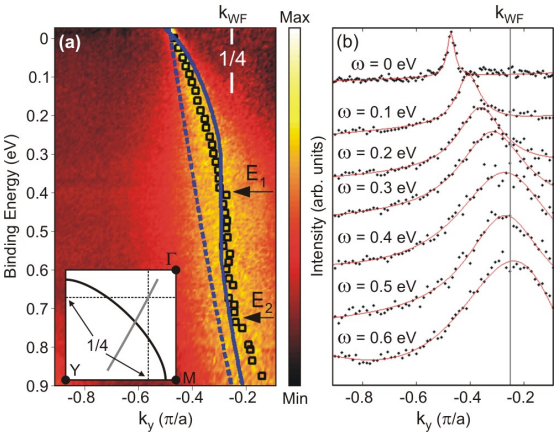

Figure 15: *(a) Normalized ARPES spectra, recorded on $x = 0.145$, for the nodal cut shown in the inset. Black squares represent the peak positions of the momentum dispersion curves (MDCs). Dashed blue line represents the bare-band dispersion k. Solid blue line represents the renormalized dispersion obtained from discussions below. (b) MDCs for energies up to 0.6 eV. The red lines represent fits to the data with a Lorentzian line shape on a sloping background.*

1.12 Particle-hole anisotropy on the Fermi arcs in underdoped cuprates (*T. M. Rice*)

Recent ARPES experiments (see previous subsection) found pronounced anisotropy on the Fermi arcs away from the nodal direction in the normal pseudogap phase [57]. Such behavior supports the opening of a gap along the Umklapp surface, which is the key ingredient in a phenomenological propagator proposed by Rice and collaborators earlier. Key features of the quasiparticle dispersion in the normal phase are nicely reproduced by this propagator as well as the coherent dispersion measured by scanning tunneling microscopy in the superconducting state at low temperatures [23].

2 Novel superconductors

2.1 STS on oxypnictides (*Ø. Fischer*)

Possible multiband superconductivity in oxypnictides focus the interest of a number of recent investigations [58]. Scanning tunneling spectroscopy (STS) is a key technique to answer the question of whether the different Fermi surface sheets are associated with different gaps, which is of crucial importance in order to identify the mechanisms of superconductivity in these compounds. We performed our STS measurements on as-grown surfaces of a $SmFeAsO_{0.86-x}F_x$ single crystal with $T_c = 45$ K [24] at 4.2K (Fig. 16).
At low bias voltage the spectra present a con-

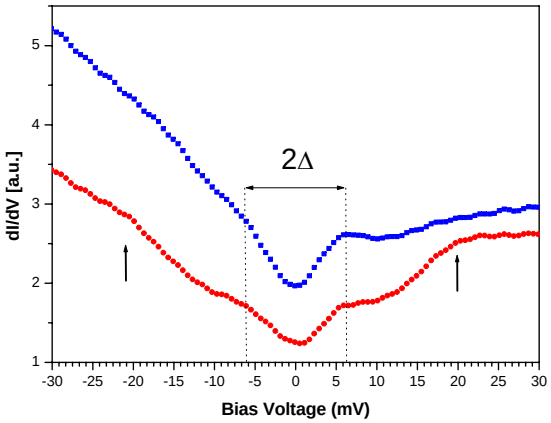

Figure 16: *Tunneling spectra measured on a $SmFeAsO_{0.8}F_{0.2}$ single crystal at 4.2 K; dotted lines: low energy gap; arrows: high bias gap-like features.*

ductance depletion, flanked by kinks or faint peaks (dotted lines). The mean gap value amounts to 7 ± 1 meV. A second gap-like feature is detected at voltages around 20 meV (arrows). In contrast to the low energy ones, these peaks vary in height, are much wider, and are located over a broader energy scale. Moreover, their energy locations are often not symmetric with respect to the Fermi level. The high bias conductance is voltage dependent with a strong particle-hole asymmetry, strikingly similar to the one measured in a number of high-T_c cuprates [6], possibly indicating strong electronic correlations. The 7 meV value found for the low energy gap is in agreement with the values measured in point contact spectroscopy [25], and the $2\Delta/kT_c = 3.6$ ratio suggests that this spectroscopic feature is the signature of a s-wave superconducting gap. However, caution imposes on the interpretation of the high-energy feature observed in $SmFeAsO_{0.86-x}F_x$ as a second superconducting gap, since it is not systematically detected for empty and occupied states and it is particle-hole asymmetric. Detailed studies of the temperature dependence of the spectral features, vortex core spectroscopy or tunneling along different crystallographic directions are needed to clarify this point.

2.2 Spin triplet superconductivity in ruthenates (*M. Sigrist*)

The chiral p-wave superconductivity in Sr_2RuO_4 remains one of the research activities in the group of Sigrist. During the last year two features were mainly studied, one concerning the implications of chirality on the surface states and the observation of the second phase transition with in the inhomogeneous 3 Kelvin phase in eutectic Sr_2RuO_4–Ru samples.

a) *Chirality sensitive effect on surface states* A large number of experiments give evidence of the realization of a chiral p-wave pairing state in Sr_2RuO_4 with the structure $\boldsymbol{d}(\boldsymbol{k}) = \hat{z}(k_x \pm ik_y)$. The chirality is of orbital nature due to the angular momentum of the Cooper pair along the z-axis. In a recent study Sigrist and coworkers explored new features which can result from this pairing symmetry [26]. It is known that this superconducting phase supports chiral edge states (Andreev bound states) at the boundary with low-energy spectrum $E_{k_\parallel,\pm} \propto \pm k_\parallel$ where the sign $\pm$ corresponds to the sign of chirality. These states can actually be observed in quasiparticle tunneling experiments as zero-bias anomalies in the tunneling spectrum. These states are modified by an external magnetic field pointing along the z-axis through a "Doppler shift" of the form $E_{k_\parallel,\pm} \rightarrow E_{k_\parallel,\pm} \pm (e/c)\boldsymbol{v}_F \cdot \boldsymbol{A}$. This gives rise to an increase or decrease of the Fermi velocity depending on the orientation of the magnetic field. Consequently the density of states will be enhanced (suppressed) when the field is parallel (antiparallel) to the direction chirality. This asymmetric behavior of the density of states as a function of the magnetic field could be observed in a tunneling experiment. An important further result of this behavior is that vortices close to the surface would increase or decrease the local density of states at the surface (Fig. 17) which corresponds to lowering or raising, respectively, the potential energy of the vortex yielding a modification of the Bean-Livingston barrier of vortices. Thus, a flux line with its vorticity parallel (antiparallel) to the chirality of the superconducting condensate would be repelled (attracted) by the surface.

2.3 Phase transition in the 3 Kelvin phase of Sr_2RuO_4 (*M. Sigrist*)

There is considerable evidence that the onset inhomogeneous superconducting phase observed at roughly $T_{cf} = 3K$ above the bulk superconducting transition at $T_{cb} = 1.5K$ is of filamentary nature. It is due to the nucleation of superconductivity on interface between Sr_2RuO_4 and small Ru-metal inclusions. This state does not break time reversal symmetry unlike the bulk phase. Consequently there would be an additional transition temperature $T_{cb} < T^* < T_{cf}$ where time reversal symmetry is violated. In order to reach a phase compatible with the bulk superconducting phase this transition is of weak first

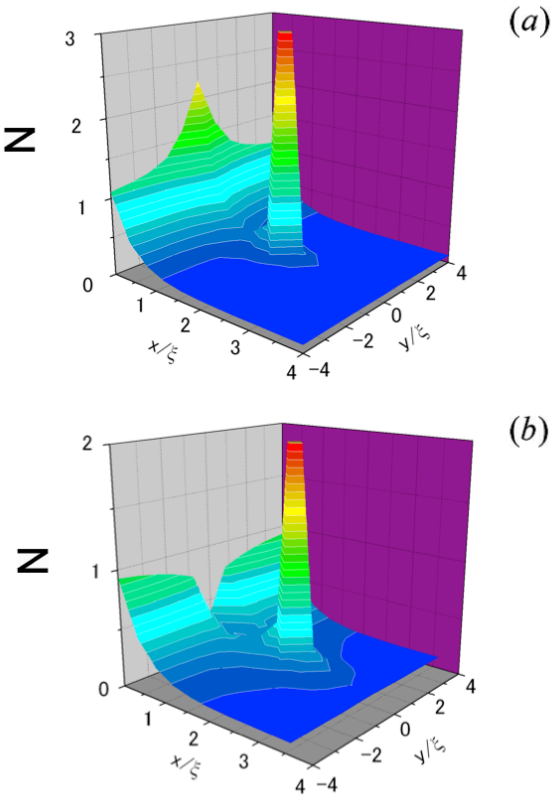

Figure 17: *Local density of states plot for a flux line at a distance $x = 2\xi$ from the surface at $x = 0$ in the chiral p-wave state (ξ: coherence length). (a) Vorticity parallel to the chirality yields an enhanced density of state shadow at the surface with a repulsive effect. (b) Vorticity antiparallel to the chirality yields a reduced density of state shadow at the surface with an attractive effect.*

order [27]. The phase below T^* forms a superconducting network with spontaneous currents running as a consequence of time reversal symmetry breaking. Kanayasu and coworkers [27] show that this phase has two characteristic features which distinguish it from the phase above T^* and agree well with recent experiments. First, the critical current is different for positive and negative flow direction [59]. Second the quasiparticle tunneling spectrum between Ru and Sr_2RuO_4 has a zero-bias anomaly [60]. In this way the theoretical transition at T^* can be identified with the experimentally observed onset of the two features which occurs consistently for both around 2.3 K.

2.4 Coupled superconducting and magnetic order in $CeCoIn_5$ (*J. Mesot*)

Strong magnetic fluctuations can provide a coupling mechanism for electrons that leads to unconventional superconductivity. Magnetic order and superconductivity have been found to coexist in a number of magnetically mediated superconductors, but these order parameters generally compete.

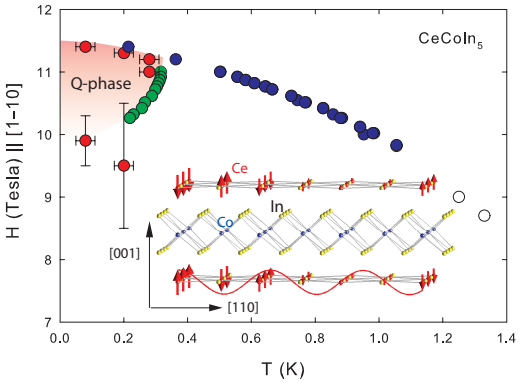

Figure 18: *H-T phase diagram of $CeCoIn_5$ with the magnetically ordered phase indicated by the red shaded area. The blue and open circles indicate a first- and second-order transition measured by specific heat, separating the superconducting from the normal phase. The green circles indicate a second order phase transition inside the superconducting phase, and the red circles indicate the onset of magnetic order, showing that the magnetic order only exists in the Q phase. Inset: magnetic structure of $CeCoIn_5$ at $T = 60$ mK and $H = 11$ T. The red arrows show the direction of the static magnetic moments located on Ce^{3+}, and the yellow and blue circles indicate the position of the In and Co ions. The solid red line indicates the amplitude of the Ce^{3+} magnetic moment along the c-axis, projected on the (h, h, l) plane.*

We report that close to the upper critical field, $CeCoIn_5$ adopts a multicomponent ground state that simultaneously carries cooperating magnetic and superconducting orders. Suppressing superconductivity in a first-order transition at the upper critical field leads to the simultaneous collapse of the magnetic order, showing that superconductivity is necessary for the magnetic order (Fig. 18). A symmetry analysis of the coupling between the magnetic order and the superconducting gap function suggests a form of superconductivity that is associated with a nonvanishing momentum [28].

2.5 Optical spectra of the ferromagnetic heavy fermion superconductor UGe_2. (*D. van der Marel*)

The possibility of unconventional superconductivity mediated by ferromagnetic fluctuations has long been a subject of theoretical speculation [61, 62]. Interest in this subject has been recently piqued with the discovery of superconductivity coexisting with the ferromagnetic state of UGe_2 under pressure [63]. UGe_2

is a strongly anisotropic uniaxial ferromagnet with filled $5f$ electron states. Due to correlations and conduction band-$5f$ hybridization, carrier masses are found to be strongly enhanced $(10 - 25m_0)$ [64] although specific heat coefficients still fall an order of magnitude short of the largest values found in antiferromagnetic uranium-based heavy fermion (HF) compounds. UGe_2 exhibits a Curie temperature that strongly decreases with increasing pressure from about 53 K at ambient pressure to full suppression around 16 kbar. Superconductivity exists in a pressure region from 10 to 16 kbar, just below the complete suppression of ferromagnetism [63]. Although superconductivity and ferromagnetism are usually found to be antagonistic phenomena, the observation fits within the now common scenario of finding superconductivity near the zero temperature termination of a magnetic phase. In this sense it seemed quite natural to associate the superconductivity with being mediated by the magnetic fluctuations that diverge at a quantum critical point (QCP) perhaps as in the case of pressure driven superconductivity in the antiferromagnetic HF superconductors. However, the para- to ferromagnetic transition is strongly first-order and is not associated with a peak in the effective electronic mass or superconducting transition temperature. It therefore appears that superconductivity is not directly related to the quantum phase transition connecting the ferromagnetic and paramagnetic states [65, 66]. In addition to the main ferromagnetic transition, there appears to be an additional weak first-order transition of more enigmatic origin at lower temperatures (for $p = 0$; $T_x = 30$ K and for $T = 0$; $p_x \approx 12.5$ kbar), which has been identified via resistivity [65, 67, 68], magnetization [66] and heat capacity [67, 68].

We have conducted a detailed optical study of UGe_2 single crystal using infrared reflectivity and spectroscopic ellipsometry. We have found a renormalized zero frequency mode with a large frequency dependent effective mass and scattering rate below the upper ferromagnetic transition T_C. They recover their unrenormalized values above T_C and for $\omega > 40$ meV. In contrast no sign of an anomaly is seen at $T_x \sim 30$ K. In the ferromagnetic state, we find signatures of a strong coupling to the longitudinal magnetic fluctuations which have been proposed to mediate unconventional superconductivity in this compound. In the optical spectra shown in Fig. 19 we observe a rather strong, but incomplete, suppression of $1/\tau(\omega)$ for frequencies smaller than about 50 cm^{-1}. The suppression of the scattering rate is reminiscent of fully spin-polarized ferromagnets like CrO_2 [69]. UGe_2 has indeed a small minority spin population at E_F [70, 71]. Longitudinal fluctuations, which can possibly mediate exotic superconductivity, have been found by neutron scattering [72]. It is interesting that our spectra give a strong indication of a coupling of charge to these longitudinal fluctuations, which were originally proposed as a possibility to mediate superconductivity in ferromagnetic compounds.

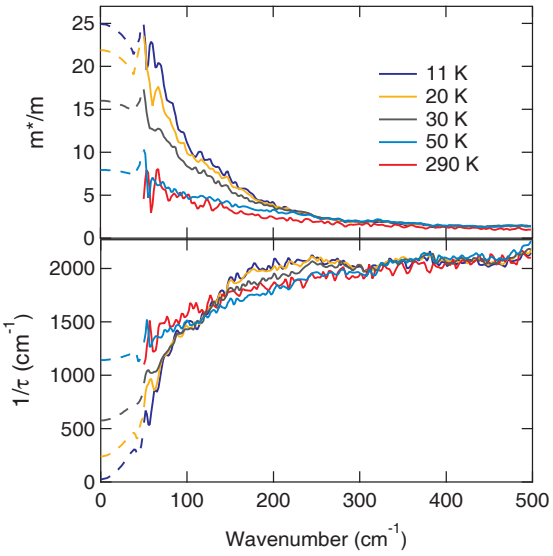

Figure 19: *The effective mass and the scattering rate as a function of photon energy derived from the extended Drude model with $\hbar\omega_p = 3.5$ eV. The dashed lines below 50 cm^{-1} show the extrapolation toward zero frequency obtained using the dc transport in the fitting process.*

The observed suppression in the scattering rate is additional to that expected generically for HF compounds below their coherence temperatures. The usual expectation is that the effective mass m^* and the quasiparticle lifetime τ^* are renormalized by approximately the same factor [73]. In contrast, comparing the low temperature scattering rates and masses with their high temperature unrenormalized values we find the ratios $\frac{m^*}{m} \approx 6$ and $\frac{\tau^*}{\tau} \approx 50$, which disagree by a factor of 8 (Fig. 20). The additional scattering suppression which onsets at T_C implies a strong coupling between HF effects and magnetic ones with important implications for superconductivity. The relatively large mass enhancement suggests the evolution of renormalized itinerant charge carriers out of a Fermi gas coupled to a lattice of $5f$ local orbitals. Our observations suggest an interplay between spin-polarization and the HF coherent state. The optical data indicate that the magnetic order triggers the transition into a

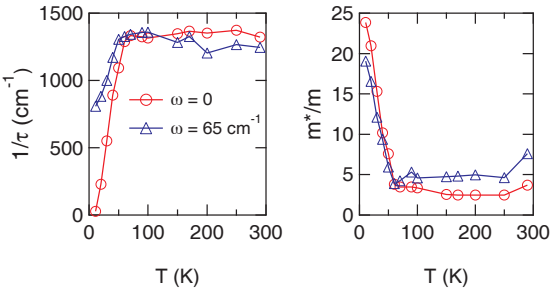

Figure 20: *Temperature dependence of the effective mass and the scattering rate of UGe_2 for two frequencies.*

state characterized by heavy and weakly scattered charge carriers. Our data are consistent with a strong coupling to the longitudinal magnetic modes which have been suggested to mediate superconductivity in this compound.

2.6 Phonon signatures in the tunneling spectra of $RbOs_2O_6$ (*Ø. Fischer*)

Tunneling conductance spectra on $RbOs_2O_6$ single crystals (T_c of 5.5 K) reveal a clear signature of a superconducting gap of the order of 1 meV, which yields a $2\Delta/kT_c$ of 3, close to the *s*-wave BCS ratio. Strikingly, temperature dependent spectroscopy reveals that the gap remains open up to 7.4 K, 2 K above the bulk T_c. The detailed analysis of the tunneling spectra indicate the presence of conductance dips at energies slightly higher than the coherence peak energies. Since the conductance dips are characteristic signatures of the coupling of quasiparticle with collective mode excitations [6], we analyzed our data with an inversion procedure based on the strong coupling Eliashberg model that allows to extract from the spectra the phonon density of states α^2F. Fig. 21 (top) shows that the experimental points (blue) are better fitted when phonon modes are considered in the quasiparticle DOS (green solid line) than using a simple BCS model (pink dotted line). The bottom panel shows the extracted α^2F spectrum with a peak at $\sim$ 2.4 mV interpreted as the strong phonon mode related to a rattling motion of the alkali atom [74, 75].

The discrepancy between the phonon energy reported in bulk measurements [29][75] and the one extracted from the STS data suggests that the frequency associated to the Rb rattling mode is somehow altered at the surface. Calculations confirm that the lower phonon frequency we detect is consistent with the 2 K T_c increase observed in our tunneling spectroscopy measurements.

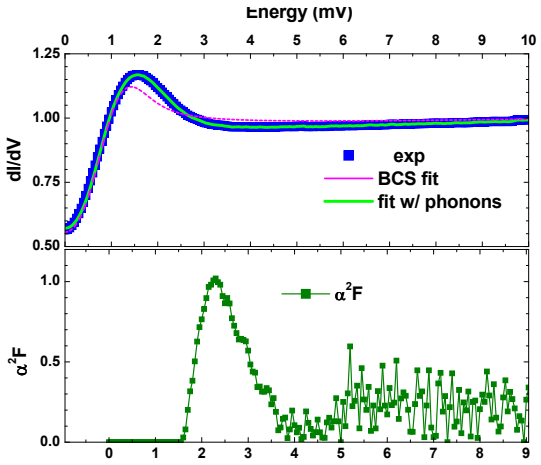

Figure 21: *Top: raw spectrum of $RbOs_2O_6$ (blue) fitted with a s-wave BCS model (pink) and including the phonon density of states (green). Bottom: extracted α^2F phonon DOS.*

2.7 Strongly-coupled multi-gap superconductivity in Chevrel phases (*Ø. Fischer*)

Chevrel phases MMo_6X_8 (M = metallic ion, X = S, Se) occupy a key position since their very small coherence lengths and high upper critical fields (H_{c2}) approach values seen in high-T_c cuprates and oxypnictides. We performed local spectroscopic studies of these materials in order to conclusively determine the nature of the order parameter in these compounds and to eventually explain their anomalously high H_{c2} values.

Scanning tunneling spectroscopy (STS) has been performed on room-temperature-cleaved samples of $SnMo_6S_8$ (T_c = 14.2 K, H_{c2} $\sim$ 38 T) and $PbMo_6S_8$ (T_c = 14.9 K, H_{c2} $\sim$ 60 T) at 400 mK in $< 10^{-7}$ mbar environment. $SnMo_6S_8$ reveals atomically flat terraces separated by steps of twice the unit cell parameter (5.5 Å). Spectra taken on the terraces are homogeneous with a gap of 3 meV, as seen in the Fig. 22(i) and (iv). However, spectra taken on the steps between terraces (positions 1 and 3 on the topographic profile of Fig. 22(ii) display additional peaks at $\sim \pm 1$ meV which are suggestive of a second superconducting gap (Fig. 22(iii) and (v)).

On $PbMo_6S_8$ although the surfaces are of rather lower quality, the average spectra display a kink at $\sim \pm 1$ meV, clearly demonstrating the presence of states within the 3 meV gap. The results indicate that interband scattering effects are present, and that in some cases, the two bands gradually merge into a single "intermediate" band, revealing only one gap in the spectra, in agreement with previous measurements [30].

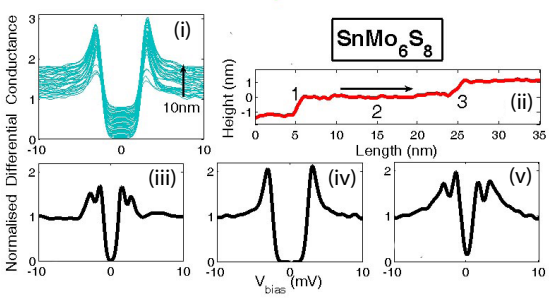

Figure 22: *(i) Homogeneous spectra over 10 nm on an atomically flat terrace. (ii) Topographic profile along a 35 nm path. (iii), (iv) and (v) Individual spectra taken at points 1, 2, 3, respectively, along (ii).*

STS measurements were complemented by the heat capacity of $SnMo_6S_8$, $PbMo_6S_8$ and $LaMo_6S_8$ in fields up to 28 T. For $SnMo_6S_8$ our data are well-fitted by a two-band model dominated by a strongly-coupled ($2\Delta/kT_c = 5$) gap together with a small weak-coupling contribution. This compares favorably with our STS data in which the gaps have coupling ratios 4.9 and 1.6. In $PbMo_6S_8$ and $LaMo_6S_8$ ($T_c = 6.9$ K) our data are again well-fitted using a combination of a dominant strongly-coupled band with a small weak-coupling component. We conclude that our specific heat data validate the double-gap scenario seen by STS, suggesting it is common to other Chevrel phases.

2.8 Superconductivity at the $LaAlO_3/SrTiO_3$ interface (*J.-M. Triscone*)

Previous studies of $LaAlO_3/SrTiO_3$ heterostructures have revealed the presence of a superconducting electron gas confined at the $LaAlO_3/SrTiO_3$ interface. Finding superconductivity at the interface between two good band insulators has generated a lot of interest and numerous studies of this system have been started worldwide.

It is today accepted that the growth conditions determine the electronic properties of this type of heterostructures. In our studies, conducting interfaces were prepared depositing more than 3 unit cells of $LaAlO_3$ on top of TiO_2-terminated (001) $SrTiO_3$ single crystal substrates. The films were grown by pulsed laser deposition at 800°C in 10^{-4} mbar of O_2 with a repetition rate of 1 Hz and energy fluence of 0.6 J/cm^2. The growth and the thickness were monitored *in situ* using reflection high energy electron diffraction (RHEED). After the deposition, the films were annealed in 200 mbar of O_2 at about 600°C for 1 hour and then cooled down to room temperature in the same atmosphere. A full description of the thin film growth, structural characterisation and measurements on transport properties in the normal state can be found in [31].

a) *Anisotropy of the superconducting transport properties at the $LaAlO_3/SrTiO_3$ interface* The extent of the electron gas at the interface became an important issue as one was trying to understand the doping mechanism leading to the conducting interface. Analyses of the superconducting properties lead us to conclude that the electron gas at the $LaAlO_3/SrTiO_3$ interface condenses in a two dimensional (2D) superconducting (SC) state [32]. In this case, a large anisotropy should be observed depending on whether the magnetic field is applied parallel or perpendicular to the interface. We thus measured the superconducting properties in magnetic fields applied either perpendicular or parallel to the plane of the film. Analyses of these transport properties allow us to estimate the thickness of the SC layer. Fig. 23 shows resistive SC transitions in magnetic fields applied perpendicular (top) and parallel (bottom) to the interface. In these experiments we are able to align the sample in the magnetic field with a precision of about 0.15° thanks to the use of a piezoelectric goniometer in the dilution cryostat. To determine the superconducting thickness, we define the temperature T^* as the temperature at which the sheet resistance is 50% of $R_s(T = 400\text{ mK})$. The characteristic $H_{\parallel}(T)$ for the parallel and $H_{\perp}(T)$ for the perpendicular field directions are shown on Fig. 24a.

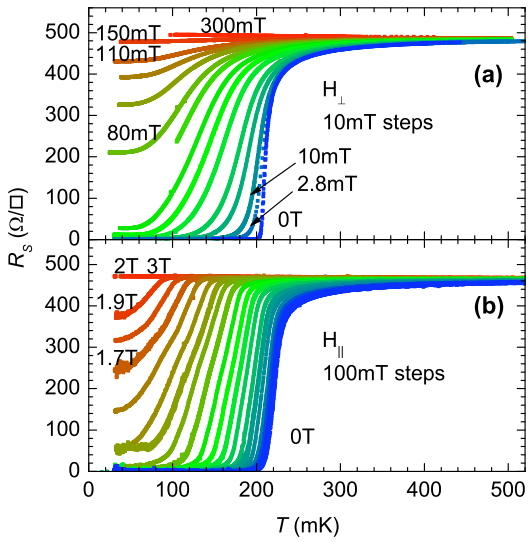

Figure 23: *Sheet resistance versus temperature curves of a single sample for different magnetic fields, either applied perpendicular (a) or parallel (b) to the interface. The zero temperature critical field is about 20 times larger in the latter case.*

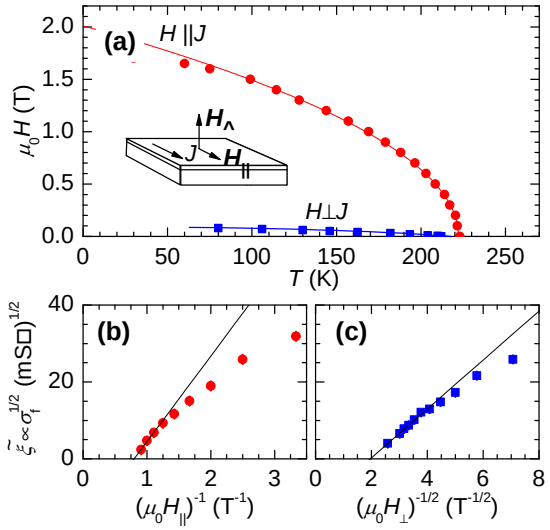

Figure 24: *(a) Characteristic magnetic field – temperature extracted from Fig. 23 using the 50% criterion. The line for parallel magnetic fields is a fit to the data using the formula for a 2D SC system. (b) Square root of the fluctuation sheet conductance as a function of the inverse of the parallel magnetic field at $T = T_{BKT}$. (c) Square root of the fluctuation sheet conductance as a function of the square root inverse of the perpendicular magnetic field at $T = T_{BKT}$. Lines are fitted to the data in the high field limit.*

The temperature dependence for the parallel field direction is following the expected mean field behavior for a 2D film: $H_\parallel(T) \propto (1 - T/T^*(H = 0))^{1/2}$. Analyses of the data using a mean field approach lead to an in-plane coherence length $\xi_\parallel(T) = (\Phi_0/(2\pi\mu_0 H_\perp))^{1/2}$ of about 70 nm at $T = 0$. Using this information, one can extract the thickness d of the SC gas using the Tinkham formula: $d = \sqrt{3}\Phi_0/(\pi\xi_\parallel\mu_0 H_\parallel)$. We find $d \approx 10$ nm. We have previously shown that the resistivity data observed are consistent with a Kosterlitz-Thouless transition. In this case the mean field approach is questionable and the determination of the mean field T_c is an issue. We thus performed scaling analyses which do not rely on a mean field scenario. Such an approach is pointing to a very similar superconducting thickness. Finally, we also analyzed the divergence of the correlation length at the critical temperature. The correlation length which is related to the square root of the sheet conductance diverges at T_c in zero magnetic field. In field the divergence is bounded by the magnetic length which goes as $(\Phi_0/H_\perp)^{1/2}$ for the perpendicular case and $\Phi_0/(dH_\parallel)$ for the parallel one in the high field limit. Fig. 24b and c shows the square root of the fluctuation sheet conductance as a function of the inverse of the parallel magnetic field at $T = T_{BKT}$ (the Kosterlitz-Thouless transition temperature) and as a function of the square root inverse of the perpendicular magnetic field at $T = T_{BKT}$. Lines are fit to the data in the high field limit. One obtains from the ratio of the slopes in the high field limit again a value for d close to 10 nm.

b) *Modulation of superconductivity at the $LaAlO_3/SrTiO_3$ interface by field effect* The two-dimensional electron gas present at the $LaAlO_3/SrTiO_3$ interface is thought to be the result of an electronic reconstruction related to a polar discontinuity at the interface. How the response of the system is modified under an electric field effect? To answer this question, several field effect devices have been fabricated with the purpose to study the response of the system, especially in the superconducting phase, to an external electric field. The $SrTiO_3$ single crystal itself has been used as a gate dielectric since it is characterized by a large dielectric constant at low temperatures. The variation of carrier concentration induced by the application of an electric field has been measured by means of Hall effect and differential capacitance measurements. The sheet resistance as a function of temperature for different applied gate voltages has been measured down to 20 mK. Fig. 25 shows sheet resistance versus temperature for one device. For large negative voltages (typically less than -200 V), corresponding to the smallest accessible electron densities, the sheet resistance increases as the temperature is decreased, a behavior indicating an insulating ground state. As the electron density is increased the system becomes a

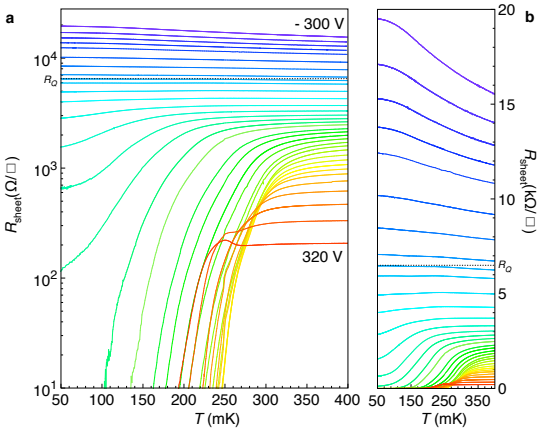

Figure 25: *Field effect modulation of the transport properties at the $LaAlO_3/SrTiO_3$ interface. Sheet resistance as a function of temperature for different applied gate voltages on a logarithmic (a) and on a linear (b) resistance scale.*

superconductor. A further increase in the electron density produces first a rise of the critical temperature to a maximum of 310 mK. For larger voltages the critical temperature decreases again. These experiments reveal the existence of a quantum phase transition between a superconducting and an insulating phase at the $LaAlO_3/SrTiO_3$ interface. In the insulating region of the phase diagram a large (40% at 8 T) negative magnetoresistance has been observed which has been interpreted as resulting from weak localization.

3 Quantum matter

3.1 Free-energy distribution functions for the randomly forced directed polymer (*G. Blatter*)

Directed polymers subject to a random potential exhibit non-trivial behavior deriving from the interplay between elasticity and disorder; numerous physical systems can be mapped onto this important model, among others the pinning of vortices in type II superconductors, with its obvious relevance for applications. We studied the $1+1$-dimensional random directed polymer problem, i.e. an elastic string subject to a Gaussian random force/potential and confined within a plane. We concentrate on three related and exactly solvable versions of this problem, the random force (or Larkin) problem, the shifted random force problem, and the harmonically correlated potential problem. Using the replica technique, we derive the distribution functions $\mathcal{P}_{L,y}(F)$ and $\mathcal{P}_L(F)$ of free energies F of a polymer of length L for fixed ($\phi(L) = y$) and free boundary conditions. We trace back the difficulties with the random harmonic problem to its non-spectral correlator and present a general criterion for physically admissible potential correlators. The work sheds light on the use of these models as a short-scale approximation of the generic random directed polymer problem.

a) *Directed random polymer* We consider an elastic string (elasticity c) directed along the x-axis within an interval $[0, L]$ and subject to a disorder potential $V(\phi, x)$ driving the displacement field $\phi(x)$; its energy is given by

$$H[\phi(x); V] = \int_0^L dx \Big\{ \frac{c}{2} \big[\partial_x \phi(x)\big]^2 + V[\phi(x), x] \Big\}.$$

The disorder average is carried out over a Gaussian distribution with zero mean $\langle V(x,\phi)\rangle_V = 0$ and a correlator $\langle V(\phi,x)V(\phi',x')\rangle_V = \delta(x-x')U(\phi-\phi')$. Here, we are interested in the Larkin model where the random potential is linearized on short scales, $V(\phi,x) = f(x)\phi(x)$, with $f(x)$ a (Gaussian) random force field with zero mean $\overline{f(x)} = 0$ and a correlator

$$\overline{f(x)f(x')} = u\,\delta(x-x').$$

Alternatively, we study the model where the correlator $U(\phi)$ (rather than the potential $V(\phi,x)$) is expanded; we then arrive at the random harmonic potential problem characterized by the parabolic correlator

$$U(\phi-\phi') \simeq U_p(\phi-\phi') = U_0 - \frac{1}{2}u(\phi-\phi')^2.$$

For a comparison of these two approximations, it is crucial to include a random shift in the Larkin model, $V(\phi,x) = V_0(x) + f(x)\phi(x)$, with $\overline{V_0(x)V_0(x')} = U_0\,\delta(x-x')$ and $\overline{V_0(x)f(x')} = 0$. Both models are used to describe the short-scale behavior of the generic short-range correlated random polymer problem [33][76].

b) *Replica theory* The standard procedure [77] leading to the distribution function $\mathcal{P}_L(F)$ starts from the partition function ($k_B = 1$)

$$Z(L,y;V) = \int_0^y \mathcal{D}[\phi(x)] \exp(-H[\phi(x);V]/T),$$

providing us with the free energy $F(L,y;V) = -T\ln Z$. n-fold replication and averaging over disorder realizations V map the problem to n quantum bosons with local interactions given by the correlator $U(\phi)$; for the (shifted) Larkin and random harmonic potential problems, the quadratic theories can be solved exactly. The replica partition function $Z_r(n;L,y) \equiv \overline{Z^n[L,y;V]} = \overline{\exp\left(-\beta n F[L,y;V]\right)}$ then can be constructed from the single-particle partition (or wave-) functions for the free problem and for the particle in the (inverted) harmonic potential.

Computing the replica partition function Z_r for arbitrary continuous replica parameters n allows us to reconstruct the full distribution function via the inverse Laplace transform ($\xi = n/T$)

$$\mathcal{P}_{L,y}(F) = \frac{1}{2\pi i}\int_{-i\infty}^{+i\infty} d\xi\, Z_r(\xi;L,y)\, \exp(\xi F), \tag{2.2}$$

where the integration goes over the imaginary axis $\xi = iy + \epsilon$, with ϵ chosen in such a way as to place all singularities in $Z_r(\xi;L,y)$ to its right.

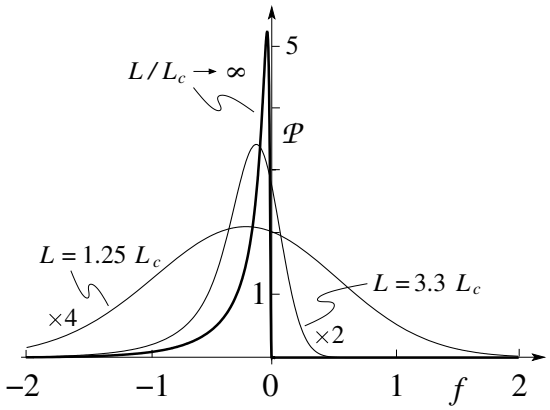

Figure 26: *Free-energy distribution function $\mathcal{P}(f)$ of the randomly forced directed polymer with free boundary conditions including the random shift $V_0(x)$. $f = F/F_f(L)$ with $F_f(L) = U_c(L/L_c)^2$.*

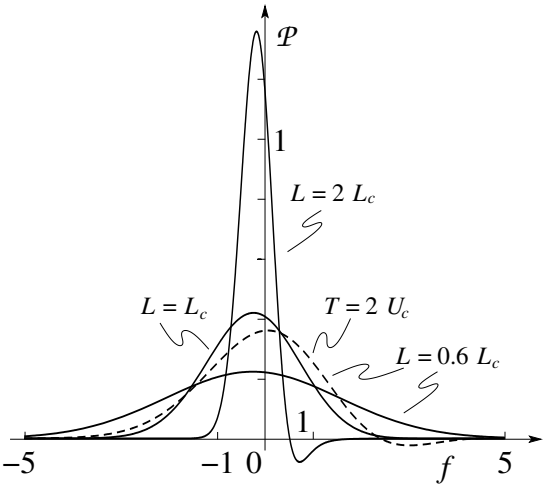

Figure 27: *Free-energy distribution function $\mathcal{P}(f)$ for the directed polymer with free boundary conditions subject to a random harmonic potential. $f = F/F_f(L)$ with $F_f(L) = U_c(L/L_c)^2$.*

c) *Results* The results for the shifted random force model and for the harmonic correlator model are shown in Figs. 26 and 27. The non-trivial distribution function of the Larkin-model (see the curve $L \to \infty$ in Fig. 26) has to be convoluted with the simple Gaussian distribution originating from the random shift $V_0(x)$. At short scales $L < L_c = (c^2U_0/u^2)^{1/3}$ where the Larkin model serves as an approximation of the random polymer problem, the distribution function is dominated by the trivial Gaussian part and it is difficult to observe the non-trivial random-force part.

Although the inverse Laplace transform can be performed for the harmonic correlator model, the resulting free-energy probability distribution develops a negative right tail at zero temperature and pronounced oscillations at finite temperatures (Fig. 27). The breakdown of the harmonic approximation is conveniently observed in the second moment: expanding $\tilde{Z}_r(s)$ for small values of s, we find that the second cumulant turns negative for $L > 2\sqrt{3/2}\,L_c$ and the results makes no longer any sense, hence the harmonic approximation to a random potential problem cannot be used on scales larger then $\xi = (U_0/u)^{1/2}$ (along the transverse direction) or L_c (along the longitudinal direction); at finite temperatures the regime of validity is further reduced.

Hence it appears that the harmonic approximation breaks down at those length scales ξ (transverse) and L_c (longitudinal), and energy scale $U_c = (cU_0^2/u)^{1/3}$, where the short scale approximation of the random polymer problem is expected to break down.

3.2 Effects of oxygen doping on $Bi_2Sr_2CuO_{6+\delta}$ vortex matter (*Ø. Fischer*)

Investigating the vortex phase diagram of layered superconductors is a key to unveil the nature of the coupling mechanisms between the superconducting Cu-O planes and the extremely anisotropic properties [78, 79]. The relatively low T_c ($\approx$ 15 K) and the difficulty of synthesizing the pure superconducting phase render the studies of the one-layer $Bi_2Sr_2CuO_{6+\delta}$ (Bi-2201) demanding. The successful growth of pure and large Bi-2201 single crystals allowed to study the vortex phase diagram over the whole overdoped regime. The effect of oxygen-doping results in both the irreversibility (H_{IL}) and second-peak (H_{SP}) lines shifting to higher temperatures and fields (Fig. 28) [34].

This suggests that the interlayer coupling between Cu-O layers increases with δ, similarly to $Bi_2Sr_2Ca_2Cu_3O_{10+\delta}$ [35, 36]. However, in striking contrast with the two and three-layer compounds, Bi-2201 exhibits a temperature-dependent H_{SP} line. We tested the relation $H_{SP} \propto \Phi_0/(s\gamma)^2$ (Josephson coupling) by using a temperature-dependent γ, fitted from our data with a phenomenological polynomial function. The excellent agreement is shown in the inset of Fig. 28. This finding constitutes strong evidence that in Bi-2201 $H_{SP}(T)$ is governed by the temperature-dependence of the anisotropy and that the pinning parameter is moderate.

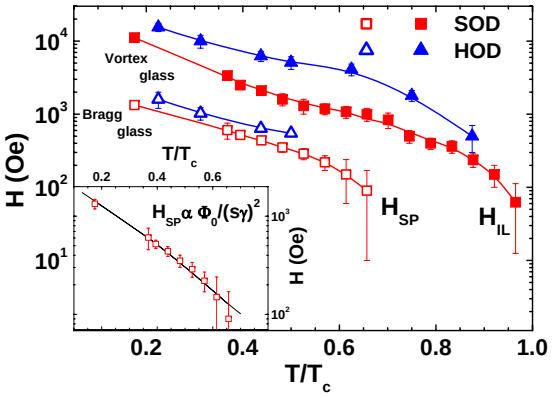

Figure 28: *$H_{IL}(T)$ (full symbols) and $H_{SP}(T)$ (open symbols) measured in the same Bi-2201 sample in the slightly (SOD) and highly-overdoped (HOD) regimes. Inset: fit of the $H_{SP}(T)$ using $\gamma(T)$ fitted from the measured data.*

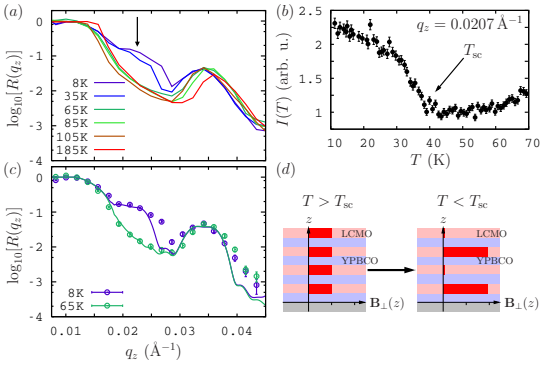

Figure 29: *Polarized neutron reflectometry spectra, temperature dependence of the half- and first-order superlattice Bragg peaks, and theoretical model to described the data.*

3.3 Competition between superconductivity and ferromagnetism in oxide-based superconductor/ferromagnet (SC/FM) superlattices (*C. Bernhard*)

We performed pulsed laser deposition (PLD) growth of oxide-based thin films and multilayers from cuprate high-T_c superconductors, like $YBa_2Cu_3O_7$ (YBCO) and ferromagnetic oxides like the manganite compound $La_{2/3}Ca_{1/3}MnO_3$ (LCMO). Their structural and magnetic properties have been investigated with polazised neutron reflectometry and X-ray diffraction.

By means of synchrotron X-ray diffraction and reflectometry measurements at the Swiss Light Source (SLS) we investigated the structural transitions of a $SrTiO_3$ substrate and their influence on a $Y_{0.6}Pr_{0.4}Ba_2Cu_3O_7$ /$La_{2/3}Ca_{1/3}MnO_3$ superlattice grown on top [37]. We found that rather than the well known antiferrodistortive cubic-to-tetragonal transition around 104 K, the tetragonal to orthorhombic transition around 65 K has the most pronounced impact on the superlattice. It is accompanied by the formation of micrometer-sized, anisotropic surface facets that are tilted with respect to one another by up to 0.5°. This tilting is transmitted into the superlattice.

The magnetic properties of this superlattice sample have been also investigated with the technique of polarized neutron reflectometry (PNR). To our surprise, these measurements provided evidence for a giant SC-induced modulation of the FM moment [38].

This is shown in Fig. 29 which displays our neutron reflectrometry data on this superlattice. In particular, from the T-dependence of the unpolarized spectra in Fig. 29a, it is evident that a peak appears at the position of the 0.5^{th} Bragg peak in the reflectivity curve right below the SC transition temperature of the $Y_{0.6}Pr_{0.4}Ba_2Cu_3O_7$ layers ($T_{sc} = 40$ K). Another unusual behavior concerns the evolution of the 1^{st} order Bragg peak which exhibits no corresponding anomalous change at T_{sc} showing that the average magnetic moment per LCMO layer remains almost constant. Fig. 29b and c shows that the data can be reasonably well reproduced with a model where the magnitude of the FM moment in the LCMO layers becomes modulated along the vertical direction with a periodicity of twice the one of the bilayers when the $Y_{0.6}Pr_{0.4}Ba_2Cu_3O_7$ layers enter the SC state. We only note that our data exclude the possibility of a modulation of the direction of the magnetic moments.

We have outlined a possible explanation of this unusual SC-induced phenomenon in terms of a gain in the SC condensation energy of the SC layers in the presence of very soft FM layers [38]. The latter behavior is ascribed to the versatile magnetic properties of the LCMO layers where the FM metallic states are nearly degenerate with a corresponding paramagnetic insulating one (that is stabilized by Jahn-Teller distortions). The required balance between the competing interactions in LCMO should be highly susceptible to the lattice strain. In agreement with this expectation, we find that the SC-induced anomaly strongly depends on the pressure that is applied to the substrate and the subsequent rearrangement of the structural domains.

This is seen in Fig. 30 which details off-specular neutron reflectometry maps where the sample was mounted under well controlled uniaxial pressures of (a) 0.4 MPa and (b) 0.1 MPa,

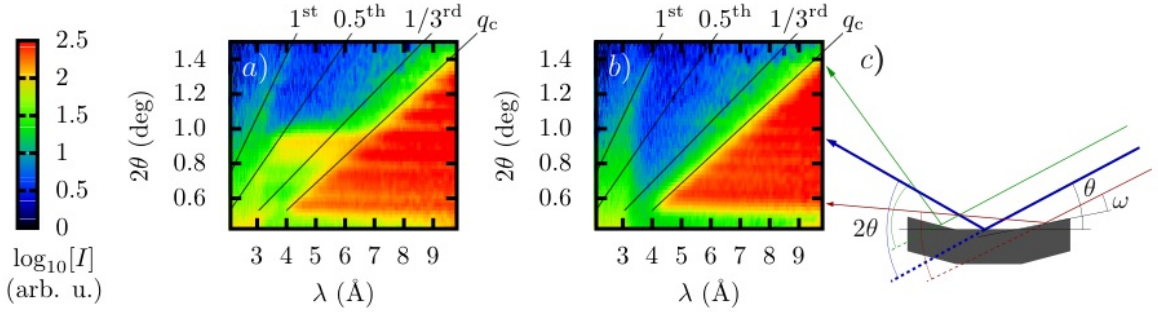

Figure 30: *Influence of the uniaxial pressure on the fractional-order Bragg peak and the structural and magnetic domains.*

respectively. The fractional-order Bragg-peak occurs here only at 0.4 MPa, while it is entirely absent at 0.1 MPa. As sketched in Fig. 30c, the reflection signals from the differently tilted micrometer-sized domains appear in these maps on horizontal lines that are spread along the 2θ-axis, where ω is the angle between the incident neutron beam and the domain surfaces. Accordingly, the map at 0.4 MPa reveals that the fractional-order Bragg peak occurs only for some of the structural domains. Furthermore, these maps directly show that the uniaxial pressure gives rise to a rearrangement of the structural domains. Our results call for more detailed investigations of this SC-induced phenomenon and its strong dependence on structural strain as transmitted from the substrate.

3.4 Superconductivity and magnetism in $YBa_2Cu_3O_7/PrBa_2Cu_3O_7$ multi-layers (*E. Morenzoni*)

Interlayer coupling effects in heterostructure systems consisting of magnetic and superconducting layers of $PrBa_2Cu_3O_7$ (PBCO) and $YBa_2Cu_3O_7$ (YBCO) have been studied intensely during recent years. We used the low energy muon spin rotation technique (LE-μSR) to determine the local magnetic fields and field distributions as a function of depth in different layers throughout such heterostructures.

In the last year we extended our studies of *c*-axis oriented multi-layers to asymmetric YBCO/PBCO/YBCO tri-layers with only a thin bottom YBCO-layer (thickness of 70/50/20 nm). These samples were grown by magnetron sputtering. We additionally investigated a PBCO/YBCO bi-layer system (70/70 nm) grown by pulsed laser deposition (PLD).

In zero field μSR experiments the PBCO layers of these heterostructures exhibit the known antiferromagnetic ordering of the Copper ($T_{N,Cu} \sim 285$ K) and the Praseodymium moments ($T_{N,Pr} \sim 17$ K). The characteristics of observed spontaneous muon spin precession proofs the good quality and *c*-axis epitaxy of the layers.

To investigate the superconducting properties of the films we conducted transverse field μSR measurements with a magnetic field applied parallel to the surface and measured the field profile as a function of the muon implantation depth and the temperature. We find a diamagnetic shift of the applied field in the PBCO buffer of the tri-layer, when the temperature is below the critical temperature of YBCO. This indicates a non-zero superfluid density in the PBCO layer which effectively couples the two adjacent YBCO layers but appears to be spatially separated from the coexisting intrinsic magnetism, which is only weakly affected by the onset of superconductivity. A small but sizable diamagnetic shift of the magnetic field is observed in the PBCO/YBCO bi-layer as well when muons are implanted in the PBCO top-layer of the structure (Fig. 31), indicating that

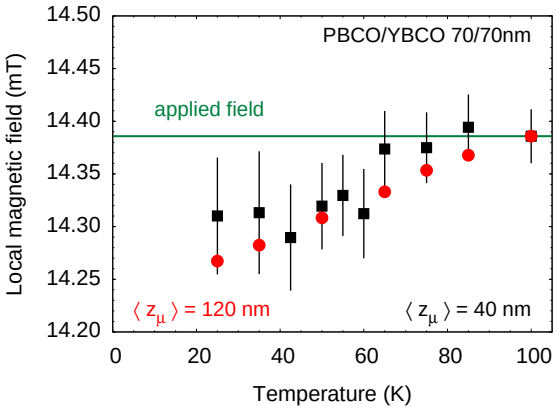

Figure 31: *Temperature dependence of the local magnetic fields measured in the PBCO ($\langle z_\mu \rangle$ = 40 nm, black squares) and the YBCO layer ($\langle z_\mu \rangle$ = 120 nm, red circles) of the PBCO/YBCO heterostructure.*

dissipation free supercurrents shielding the external field flow in the antiferromagnet. Overall, the results present the signature of an unusual and large proximity effect not expected in this material on the base of conventional proximity models. Especially important is the detection of the diamagnetic shift in the bilayer, because in this structure extrinsic effects such as microshorts or superconducting paths through the insulating barrier are absolutely excluded.

4 Collaborative efforts

A major component in the collaborative efforts is the study and discussion, by several groups in several other laboratories participating in the MaNEP network, of results which have been obtained on materials prepared at the ETHZ, EPFL, UniGE, and PSI. Several projects involve the work of junior collaborators at different institutions. RIXS experiments on cuprates and pnictides are carried out jointly between EPFL, UniGE and PSI. Infrared studies of iron pnictides are carried out jointly by members of ETHZ, PSI and UniGE. A joint project combining ARPES, STM and optics is being carried out by groups at UniGE, EPFL and PSI.

MaNEP-related publications

► [1] G. Ghiringhelli, A. Piazzalunga, C. Dallera, T. Schmitt, V. Strocov, J. Schlappa, L. Patthey, X. Wang, H. Berger, and M. Grioni, Physical Review Letters **102**, 027401 (2009).

[2] J. Chang, C. Niedermayer, R. Gilardi, N. B. Christensen, H. M. Rønnow, D. F. McMorrow, M. Ay, J. Stahn, O. Sobolev, A. Hiess, S. Pailhes, C. Baines, N. Momono, M. Oda, M. Ido, and J. Mesot, Physical Review B **78**, 104525 (2008).

[3] J. Chang, Y. Sassa, S. Guerrero, M. Månsson, M. Shi, S. Pailhés, A. Bendounan, R. Mottl, T. Claesson, O. Tjernberg, L. Patthey, M. Ido, M. Oda, N. Momono, C. Mudry, and J. Mesot, New Journal of Physics **10**, 103016 (2008).

[4] K.-Y. Yang, W.-Q. Chen, T. M. Rice, M. Sigrist, and F.-C. Zhang, arXiv:0807.3789 (2008).

► [5] M. Shi, J. Chang, S. Pailhés, M. R. Norman, J. C. Campuzano, M. Månsson, T. Claesson, O. Tjernberg, A. Bendounan, L. Patthey, N. Momono, M. Oda, M. Ido, C. Mudry, and J. Mesot, Physical Review Letters **101**, 047002 (2008).

[6] Ø. Fischer, M. Kugler, I. Maggio-Aprile, C. Berthod, and C. Renner, Reviews of Modern Physics **79**, 353 (2007).

[7] B. W. Hoogenboom, C. Berthod, M. Peter, Ø. Fischer, and A. A. Kordyuk, Physical Review B **67**, 224502 (2003).

► [8] G. Levy de Castro, C. Berthod, A. Piriou, E. Giannini, and Ø. Fischer, Physical Review Letters **101**, 267004 (2008).

[9] E. van Heumen, R. Lortz, A. B. Kuzmenko, F. Carbone, D. van der Marel, X. Zhao, G. Yu, Y. Cho, N. Barisic, M. Greven, C. C. Homes, and S. V. Dordevic, Physical Review B **75**, 054522 (2007).

[10] F. Carbone, A. B. Kuzmenko, H. J. A. Molegraaf, E. van Heumen, V. Lukovac, F. Marsiglio, D. van der Marel, K. Haule, G. Kotliar, H. Berger, C. S., P. H. Kes, and M. Li, Physical Review B **74**, 064510 (2006).

[11] F. Carbone, A. B. Kuzmenko, H. J. A. Molegraaf, E. van Heumen, E. Giannini, and D. van der Marel, Physical Review B **74**, 024502 (2006).

[12] G.-M. Zhao, H. Keller, and K. Conder, Journal of Physics: Condensed Matter **13**, R569 (2001).

[13] R. Khasanov, A. Shengelaya, E. Morenzoni, K. Conder, I. M. Savić, and H. Keller, Journal of Physics: Condensed Matter **16**, S4439 (2004).

[14] H. Keller, in *Superconductivity in Complex Systems*, K. A. Müller and A. Bussmann-Holder, eds. (Springer, Berlin, 2005), vol. 114, p. 143.

► [15] R. Khasanov, A. Shengelaya, D. Di Castro, E. Morenzoni, A. Maisuradze, I. M. Savić, K. Conder, E. Pomjakushina, A. Bussmann-Holder, and H. Keller, Physical Review Letters **101**, 077001 (2008).

[16] A. Bussmann-Holder and H. Keller, in *Polarons in Advanced Materials*, A. Alexandrov, ed. (Springer, Dordrecht & Canopus Publishing Ltd., Bristol, 2007), vol. 103, p. 599.

► [17] D. Eichenberger and D. Baeriswyl, *to be published in* Physical Review B (2009), arXiv:0808.0433.

[18] D. Eichenberger and D. Baeriswyl, Physical Review B **76**, 180504(R) (2007).

► [19] P. Chudzinski, M. Gabay, and T. Giamarchi, Physical Review B **78**, 075124 (2008).

► [20] C. Weber, A. Läuchli, F. Mila, and T. Giamarchi, Physical Review Letters **102**, 017005 (2009).

► [21] M. Ossadnik, C. Honerkamp, T. M. Rice, and M. Sigrist, Physical Review Letters **101**, 256405 (2008).

[22] J. Chang, M. Shi, S. Pailhés, M. Månsson, T. Claesson, O. Tjernberg, A. Bendounan, Y. Sassa, L. Patthey, N. Momono, M. Oda, M. Ido, S. Guerrero, C. Mudry, and J. Mesot, Physical Review B **78**, 205103 (2008).

[23] K.-Y. Yang, H. B. Yang, P. D. Johnson, T. M. Rice, and F.-C. Zhang, arXiv:0812.3045 (2008).

[24] N. D. Zhigadlo, S. Katrych, Z. Bukowski, S. Weyeneth, R. Puzniak, and J. Karpinski, Journal of Physics: Condensed Matter **20**, 342202 (2008).

[25] D. Daghero, M. Tortello, R. S. Gonnelli, V. A. Stepanov, N. D. Zhigadlo, and J. Karpinski, arXiv:0812.1141v1 (2008).

► [26] T. Yokoyama, C. Iniotakis, Y. Tanaka, and M. Sigrist, Physical Review Letters **100**, 177002 (2008).

[27] H. Kaneyasu, N. Hayashi, B. Gut, and M. Sigrist, arXiv:09xxxxx (2009).

► [28] M. Kenzelmann, T. Strässle, C. Niedermayer, M. Sigrist, B. Padmanabhan, M. Zolliker, A. D. Bianchi, R. Movshovich, E. D. Bauer, J. L. Sarrao, and J. D. Thompson, Science **321**, 1652 (2008).

[29] M. Brühwiler, S. M. Kazakov, J. Karpinski, and B. Batlogg, Physical Review B **73**, 094518 (2006).

[30] C. Dubois, A. P. Petrović, G. Santi, C. Berthod, A. A. Manuel, M. Decroux, Ø. Fischer, M. Potel, and R. Chevrel, Physical Review B **75**, 104501 (2007).

► [31] S. Gariglio, N. Reyren, A. D. Caviglia, and J.-M. Triscone, *to be published in* Journal of Physics: Condensed Matter (2009).

[32] N. Reyren, S. Thiel, A. D. Caviglia, L. F. Kourkoutis, G. Hammerl, C. Richter, C. W. Schneider, T. Kopp, A.-S. Ruetschi, D. Jaccard, M. Gabay, D. A. Muller, J.-M. Triscone, and J. Mannhart, Science **317**, 1196 (2007).

► [33] V. Dotsenko, L. B. Ioffe, V. B. Geshkenbein, S. E. Korshunov, and G. Blatter, Physical Review Letters **100**, 050601 (2008).

[34] A. Piriou, E. Giannini, Y. Fasano, and Ø. Fischer, *submitted to* Physical Review B (2009).

[35] A. Piriou, Y. Fasano, E. Giannini, and O. Fischer, Physica C **460-462**, 408 (2007).

[36] A. Piriou, Y. Fasano, E. Giannini, and Ø. Fischer, Physical Review B **77**, 184508 (2008).

► [37] J. Hoppler, J. Stahn, H. Bouyanfif, V. K. Malik, B. D. Patterson, P. R. Willmot, G. Cristiani, H. U. Habermeier, and C. Bernhard, Physical Review B **78**, 134111 (2008).

► [38] J. Hoppler, J. Stahn, C. Niedermayer, V. K. Malik, H. Bouyanfif, A. J. Drew, M. Rössle, A. Buzdin, G. Cristiani, H.-U. Habermeier, B. Keimer, and C. Bernhard, Nature Materials (2009), doi: 10.1038/nmat2383.

Other references

[39] L. Braicovich, L. J. P. Ament, V. Bisogni, F. Forte, C. Aruta, G. Balestrino, N. B. Brookes, G. M. De Luca, P. G. Medaglia, F. M. Granozio, M. Radovic, M. Salluzzo, J. van den Brink, and G. Ghiringhelli, arXiv:0807.1140v1 (2008).

[40] J. P. Hill, G. Blumberg, Y.-J. Kim, D. S. Ellis, S. Wakimoto, R. J. Birgeneau, S. Komiya, Y. Ando, B. Liang, R. L. Greene, D. Casa, and T. Gog, Physical Review Letters **100**, 097001 (2008).

[41] Q. Li, M. Hucker, G. D. Gu, A. M. Tsvelik, and J. M. Tranquada, Physical Review Letters **99**, 067001 (2007).

[42] E. Berg, E. Fradkin, E.-A. Kim, S. A. Kivelson, V. Oganesyan, J. M. Tranquada, and S. C. Zhang, Physical Review Letters **99**, 127003 (2007).

[43] H. F. Fong, P. Bourges, Y. Sidis, L. P. Regnault, A. Ivanov, G. D. Gu, N. Koshizuka, and B. Keimer, Nature **398**, 588 (1999).

[44] M. Eschrig and M. R. Norman, Physical Review Letters **85**, 3261 (2000).

[45] P. Monthoux and D. J. Scalapino, Physical Review Letters **72**, 1874 (1994).

[46] C. S. Owen and D. J. Scalapino, Physica **55**, 691 (1971).

[47] D. J. Scalapino, E. Loh, and J. E. Hirsch, Physical Review B **34**, 8190 (1986).

[48] A. J. Millis, H. Monien, and D. Pines, Physical Review B **42**, 167 (1990).

[49] T. A. Maier, D. Poilblanc, and D. J. Scalapino, Physical Review Letters **100**, 237001 (2008).

[50] M. R. Norman and A. V. Chubukov, Physical Review B **73**, 140501(R) (2006).

[51] D. Zech, H. Keller, K. Conder, E. Kaldis, E. Liarokapis, N. Poulakis, and K. A. Müller, Nature **371**, 681 (1994).

[52] G.-M. Zhao, M. B. Hunt, H. Keller, and K. A. Müller, Nature **385**, 236 (1997).

[53] G.-M. Zhao, K. Conder, H. Keller, and K. A. Müller, Journal of Physics: Condensed Matter **10**, 9055 (1998).

[54] A. Shengelaya, G.-M. Zhao, C. M. Aegerter, K. Conder, I. M. Savić, and H. Keller, Physical Review Letters **83**, 5142 (1999).

[55] P. W. Anderson, Science **235**, 1196 (1987).

[56] M. Abdel-Jawad, M. P. Kennett, L. Balicas, A. Carrington, A. P. Mackenzie, R. H. McKenzie, and N. E. Hussey, Nature Physics **2**, 821 (2006).

[57] H.-B. Yang, J. D. Rameau, P. D. Johnson, T. Valla, A. Tsvelik, and G. D. Gu, Nature **456**, 77 (2008).

[58] H. H. Ding, P. Richard, K. Nakayama, K. Sugawara, T. Arakane, Y. Sekiba, A. Takayama, S. Souma, T. Sato, T. Takahashi, Z. Wang, X. Dai, Z. Fang, G. Chen, J. Luo, and N. Wang, Europhysics Letters **83**, 47001 (2008).

[59] J. Hooper, Z. Q. Mao, K. D. Nelson, Y. Liu, M. Wada, and Y. Maeno, Physical Review B **70**, 014510 (2004).

[60] H. Yaguchi, K. Takizawa, M. Kawamura, N. Kikugawa, Y. Maeno, T. Meno, T. Akazaki, K. Semba, and H. Takayanagi, Journal of the Physical Society of Japan **75**, 125001 (2006).

[61] V. L. Ginzburg, Journal of Experimental and Theoretical Physics **4**, 153 (1957).

[62] D. Fay and J. Appel, Physical Review B **22**, 3173 (1980).

[63] S. S. Saxena, P. Agarwal, K. Ahilan, F. M. Grosche, S. R. Julian, P. Monthoux, G. G. Lonzarich, A. Huxley, I. Sheikin, D. Braithwaite, and J. Flouquet, Nature **604**, 587 (2000).

[64] Y. Ōnuki, S. W. Yun, I. Ukon, I. Umehara, K. Satoh, I. Sakamoto, M. Hunt, P. Meeson, P. A. Probst, and M. Springford, Journal of the Physical Society of Japan **60**, 2127 (1991).

[65] A. Huxley, I. Sheikin, E. Ressouche, N. Kernavanois, D. Braithwaite, R. Calemczuk, and J. Flouquet, Physical Review B **63**, 144519 (2001).

[66] C. Pfleiderer and A. D. Huxley, Physical Review Letters **89**, 147005 (2002).

[67] C. G. Oomi, T. Kagayama, and Y. Ōnuki, Journal of Alloys and Compounds **271-273**, 482 (1998).

[68] N. Tateiwa, K. Hanazono, T. C. Kobayashi, K. Amaya, T. Inoue, K. Kindo, Y. Koike, N. Metoki, N. Y. Haga, R. Settai, and Y. Onuki, Journal of the Physical Society of Japan **70**, 2876 (2001).

[69] E. J. Singley, C. P. Weber, D. N. Basov, A. Barry, and J. M. D. Coey, Physical Review B **60**, 4126 (1999).

[70] A. B. Shick and W. E. Pickett, Physical Review Letters **86**, 300 (2001).

[71] H. Yamagami, Journal of Physics: Condensed Matter **15**, S2271 (2003).

[72] A. D. Huxley, S. Raymond, and E. Ressouche, Physical Review Letters **91**, 207201 (2003).

[73] A. J. Millis and P. A. Lee, Physical Review B **35**, 3394 (1987).

[74] J. Kuneš, T. Jeong, and W. E. Pickett, Physical Review B **70**, 174510 (2004).

[75] K. Sasai, K. Hirota, Y. Nagao, S. Yonezawa, and Z. Hiroi, Journal of the Physical Society of Japan **76**, 104603 (2007).

[76] T. Halpin-Healy and Y. C. Zhang, Physics Reports **254**, 215 (1995).

[77] M. Kardar, Nuclear Physics B **290**, 582 (1987).

[78] G. Blatter, M. V. Feigel'man, V. B. Geshkenbein, A. I. Larkin, and V. M. Vinokur, Reviews of Modern Physics **66**, 1125 (1994).

[79] A. E. Koshelev and V. M. Vinokur, Physical Review B **57**, 8026 (1998).

Project 3 Crystal growth

Project leader: L. Forró (EPFL)

Participating members: J. Karpinski (ETHZ), D. van der Marel (UniGE), J. Mesot (PSI), G. Margaritondo (EPFL).

Summary and highlights: It is more true than ever that the bottle-neck for a serious research in novel electronic materials is the accessibility to unique and high quality single crystals. This fact was recognized from the beginning by MaNEP leaders and a strong effort was devoted to crystal growth. At the four participating laboratories (ETHZ, PSI, EPFL and UniGE) the major crystal growing techniques are implemented. These are self-flux and the chemical vapor transport methods, traveling solvent floating zone growth, Czochralski method using Hukin crucible and last but not least, high pressure crystal growth techniques. With all these developments we can make a safe statement that single crystal growth is the strength of MaNEP and of the Swiss solid state community.
The highlight of the last year was beyond any doubt the very fast synthesis of Iron-pnictide superconductors after their discovery, especially that of the 1111 phase with T_c of 54 K. Besides this family many others have been synthesized which can be consulted in the Single Crystal Catalog of MaNEP (see p. 69).
Some measurements on crystals grown in this project are already given in this short summary but the in-depth studies are reported in Projects 1 and 2.

Introduction

The main categories of single crystals are the following: 1. novel superconducting materials; 2. magnetic materials; 3. low-dimensional conductors; 4. materials beyond the foreseen plan. In the following the presentation of the activity is organized by the participating laboratories.

1 Single crystal growth at ETHZ

Group leader: J. Karpinski. *Researchers involved*: N. D. Zhigadlo, J. Karpinski, S. Katrych, Z. Bukowski.

1.1 Single crystals of LnFeAsO$_{1-x}$F$_x$

Single crystals of LnFeAsO$_{1-x}$F$_x$ (Ln = La, Pr, Nd, Sm, Gd) were grown from NaCl/KCl flux at pressure of 3.0 GPa and temperature of 1350 – 1450°C using cubic anvil high-pressure technique. Within this family the first free standing FeAs-pnictades crystals (SmFeAsO$_{1-x}$F$_y$) [1] were obtained. High pressure environment served to stabilize the structure of Ln-1111 at high temperature. Structural studies have confirmed the high structural perfection. Single crystals were used for electrical transport, structure, magnetic torque and spectroscopic studies. T_c of the single crystals varies between 45 and 53 K.
As a precursor for the synthesis of polycrystalline samples and single crystals, mixtures of LnAs, FeAs, Fe$_2$O$_3$, Fe, and LnF$_3$ powders have been used. The precursor to flux ratio varies between 1:1 and 1:3. By variation of nominal oxygen and fluorine content between 0.6 – 0.8 and 0.4 – 0.2 respectively, different doping levels were achieved. In a typical run, a pressure of 3 GPa was applied at room temperature. Temperature was increased within 1 h up to the maximum value of 1350 – 1450°C, kept for 4 – 85 h and decreased in 1 – 24 h to room temperature. Then pressure was released, sample removed and in the case of single crystal growth in NaCl/KCl the flux was dissolved in water. By optimization of the growth conditions SmFeAs(O,F) single crystals with the sizes in the range of 150 – 300μm and $T_c \approx 53$ K have been obtained (Figs. 1 and 2).
Single crystals were studied on a four-circle diffractometer equipped with CCD detector. Structure investigation confirmed high structural perfection and showed lower occupa-

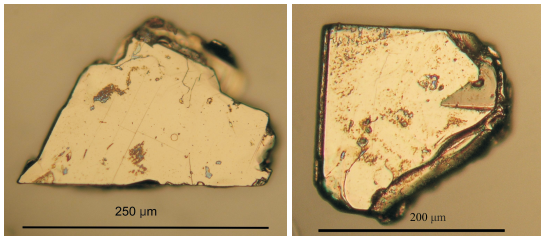

Figure 1: *Single crystals of SmFeAsO$_{1-x}$F$_y$.*

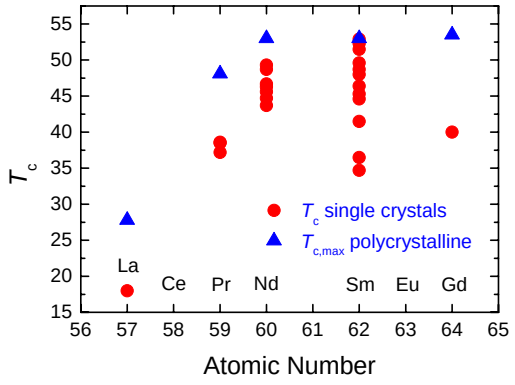

Figure 2: *T_c measured on single crystals with different doping level in comparison with $T_{c,max}$ from literature measured on polycrystalline samples.*

tion of (O,F) position in superconducting LnFeAsO$_{1-x}$F$_x$ crystals [1, 2].

Direct four-point resistivity measurements were performed on SmFeAsO$_{0.8}$F$_{0.2}$ (hereafter Sm-1111) single crystals in a magnetic field up to 13.5 T. Sm-1111 crystals smaller than 200μm were selected and contacted using Focused Ion Beam technique.

The magnetic field causes only a slight shift of the onset of superconductivity, but a significant broadening of the transition indicating weaker pinning and accordingly larger flux flow dissipation. The upper critical fields $H_{c2}^{\parallel ab}$ and $H_{c2}^{\parallel c}$ extracted from resistivity measurements (50% transition) are shown in Fig. 3. The temperature dependence of the magnetic moment was also measured for one single crystal of nominal content SmFeAsO$_{0.6}$F$_{0.35}$. The transition temperature of 48 K indicates that the crystal is underdoped. The critical current density at

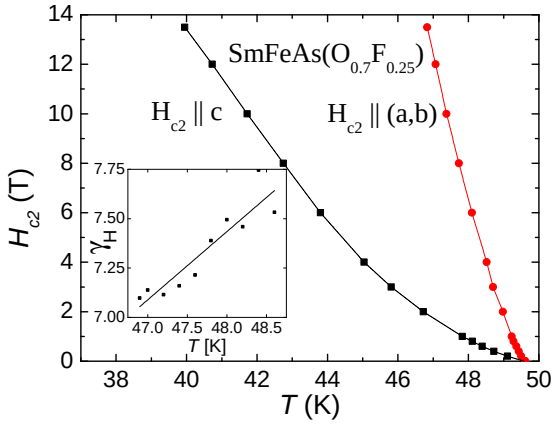

Figure 3: *Temperature dependence of the upper critical fields with $H_{c2}^{\parallel ab}$ and with $H_{c2}^{\parallel c}$. Inset: the upper critical field anisotropy $\gamma_H = H_{c2}^{\parallel ab}/H_{c2}^{\parallel c}$ in the vicinity of T_c [2].*

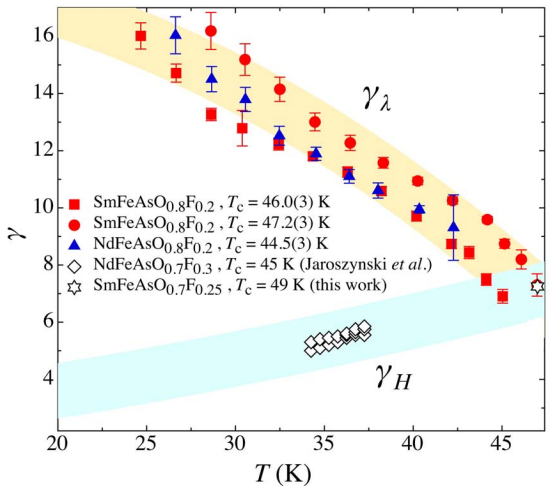

Figure 4: *Anisotropies obtained from the torque data [3], using fixed values for the upper critical field anisotropy after Jaroszynski et al. [14].*

2 K, 5 K and 15 K, estimated from the width of the hysteresis loop for SmFeAsO$_{0.8}$F$_{0.2}$, reaches values higher than 10^9 A/m^2. This is very promising for eventual applications. Slight increase of the critical current density for higher magnetic fields may indicate the increase of the effectiveness of pinning centers with increasing magnetic field.

Torque magnetometry has been applied to determine the penetration depth anisotropy γ_λ of several SmFeAsO$_{0.8}$F$_{0.2}$ and NdFeAsO$_{0.8}$F$_{0.2}$ single crystals.

By fixing the upper critical field anisotropy γ_H to the values obtained by Jaroszynski *et al.* [14], the magnetic penetration depth anisotropy γ_λ was found to be strongly temperature dependent and different from the upper critical field anisotropy γ_H (Fig. 4) [3].

Further investigations within MaNEP groups are in progress.

2 Single crystal growth at PSI

Group leader: J. Mesot. *Researchers involved*: K. Conder, K. Pomjakushina.

2.1 Spin state polarons and superstructure formation in cobaltites

Single crystals of layered and cubic cobaltites were investigated using single crystal synchrotron X-ray diffraction, muon-spin relaxation (μSR), inelastic neutron scattering (INS), electron spin resonance (ESR) and nuclear magnetic resonance (NMR).

By means of reciprocal space mapping and symmetry analysis of synchrotron diffraction data, we have shown that the first-

order structural transition in layered cobaltites RBaCo$_2$O$_{5.5}$ (R = Tb, Nd) accompanied by a metal-insulator transition (MIT) turns out to be a $Pmmm \leftrightarrow Pmma$ transformation. The detailed structural analysis shows that all four Co^{3+} sites, symmetrically inequivalent within the space-group $Pmma$, have different oxygen polyhedron distortions, thus indicating ordering in different spin states [4]. These results are in agreement with our muon-spin relaxation measurements on the magnetic structures of RBaCo$_2$O$_{5.5}$ (R = Y, Tb, Dy, Ho) [5], where three different magnetic phases below MIT have been identified, in agreement with different ordered spin state arrangements of cobalt.

Lightly hole doped cubic cobaltites La$_{1-x}$Sr$_x$CoO$_3$ ($x \leq 0.005$) were studied by means of INS, ESR and NMR in order to establish an origin of an unusually strong magnetic signal [6]. The obtained data give evidence for two regimes: $T < 35$ K dominated by spin polarons; $T > 35$ K dominated by thermally activated magnetic Co^{3+} ions.

2.2 Studies of superstructure formation at the metal-insulator transition in layered cobaltites RBaCo$_2$O$_{5.5}$

Great controversy has arisen regarding the Co spin state and the explanation of numerous physical properties (spin state and magnetic transitions, charge and orbital ordering) of the compounds belonging to the layered perovskite family RBaCo$_2$O$_{5+x}$ (R = rare earth element). These compounds display MIT (slightly above room temperature) accompanied by structural changes. The driving force of this transition is closely related to the Co spin state and the corresponding electronic structure. In the RBaCo$_2$O$_{5.5}$ structure, cobalt cations exist in two coordination environments – pyramidal CoO$_5$ and octahedral CoO$_6$, which both feature the oxidation state Co^{3+}. Superstructures in the RBaCo$_2$O$_{5.5}$ reported so far are classified as multiplied periodicity of the primitive cubic perovskite $a_c \times a_c \times a_c$.

We have undertaken neutron powder diffraction studies of the crystal structure across the MIT in HoBaCo$_2$O$_{5.5}$ [7]. Whereas the observed crystal symmetry was orthorhombic ($Pmmm$ ($a_c \times 2a_c \times 2a_c$)) in the whole investigated temperature range (250 – 400 K), the lattice constants undergo dramatic changes in the vicinity of the transition accompanied by an abrupt negative change of the unit cell volume and melting of the orbital order in the pyramids. Bragg intensities indicating multiplication of the unit cell are usually several orders of magnitude weaker than the main reflections for both neutron and X-ray diffractions, and so they are difficult to observe using powder diffraction.

In order to obtain reliable data on weak diffraction features in layered cobaltites over a wide temperature range ($100 < T < 375$ K) we have performed single crystal synchrotron X-ray diffraction study using reciprocal space mapping with an area detector. We made many attempts to grow such crystals trying different rare earth (Pr, Dy, Gd, Nd, Tb, Ho) and different growth conditions (varying growth atmosphere, growth rate, diameter of the feed and seed rods). Finally single crystals of RBaCo$_2$O$_{5+x}$ (R = Nd, Tb, Tb$_{0.9}$Dy$_{0.1}$) were successfully grown in our group [8] by the Travelling Solvent Floating Zone (TSFZ) method using a four-mirror furnace FZ-T-10000-H-VI-VP, Crystal System Corp., Japan.

For these crystals it was shown that the metal insulator transition is of the first order and that it is accompanied by a structural transition. Below T_{MIT}, a new $Pmma(2a_c \times 2a_c \times 2a_c)$ superstructure was observed. The present structural data are consistent with most general, symmetry-based analysis of the structure transformations in the perovskite based cobaltite crystals. The parametrization of the structural distortions do not tell which Co ion stays in which spin state. However, it clearly states that above MIT, there are two different Co sites in the unit cell located in pyramidal and octahedral coordinating polyhedrons while below there are four different Co sites. All four independent cobalt sites show different oxygen polyhedron distortions indicating ordering in different spin states. Thus, in contrast to conclusions of previous studies, it appears clearly that a structural transition creating four different Co ions takes place simultaneously with MIT and surely should be taken into account in all models of metal-insulator, as well as magnetic transitions of RBaCo$_2$O$_{5.5}$ related with the ordering of different Co states. Part of the reported results was included in the PhD thesis of Marian Stingaciu [9].

2.3 Spin state polarons in lightly hole-doped cubic cobaltites LaCoO$_3$

Lightly hole-doped La$_{1-x}$Sr$_x$CoO$_3$ ($x = 0.002$, 0.005 (Fig. 5)) with an estimated concentration of only two/five holes per thousand of Co^{3+} ions exhibits unusual paramagnetic properties at low temperatures; apparently a few embedded spins in a nonmagnetic matrix give

Figure 5: *A single crystal of* $La_{0.995}Sr_{0.005}CoO_3$.

an order of magnitude larger magnetic susceptibility than expected. In contrast to the parent compound $LaCoO_3$, where no excitations have been observed on zero field inelastic neutron spectra for $T < 30$ K [10], for the $La_{0.998}Sr_{0.002}CoO_3$ an inelastic peak at 0.75 meV was observed down to $T = 1.5$ K and another one at 0.6 meV at $T > 30$ K similar to that found in $LaCoO_3$. Electron spin resonance spectra also show intense excitations with large effective g factors, at the same time nuclear magnetic resonance data indicate the creation of extended magnetic clusters.

Combining inelastic neutron scattering data, obtained with and without magnetic field, with single crystal electron spin resonance and nuclear magnetic resonance measurements on $La_{0.998}Sr_{0.002}CoO_3$ single crystal, we find that the charges introduced by substitution of Sr^{2+} for La^{3+} do not remain localized at the Co^{3+} ions, transforming them to a higher spin state Co^{4+}. In fact the observed magnetic and spectroscopic properties (INS) can be explained assuming the creation of a magnetic seven-site (heptamer) polaron (see Fig. 6). The formation of the spin polarons may be a common mechanism present in other Co-based compounds. Spin-state polarons behave like magnetic nanoparticles embedded in an insulating nonmagnetic matrix.

Increasing of the spin-state polaron concentration with hole doping finally results in a metallic ferromagnetic state for $x > 0.3$.

We continue studying the $La_{1-x}Sr_xCoO_3$ system with higher Sr-content in order to follow the evolution of the spin polaron state into ferromagnetic state. A series of single crystals of $La_{1-x}Sr_xCoO_3$ ($x = 0.01$, 0.02, 0.05, 0.1) was grown by TSFZ method, preliminary chemical, structural and magnetic characterizations were made prior to neutron scattering experiments, which will be performed during 2009. Series of

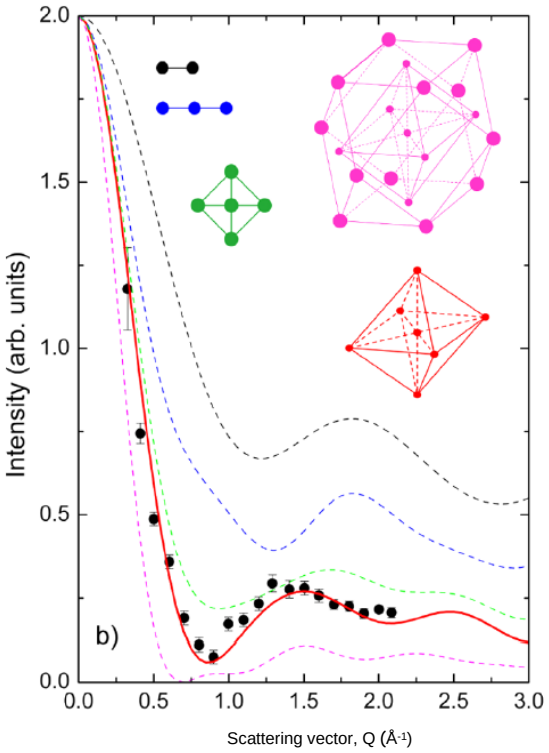

Figure 6: *Circles: experimental Q dependence of the intensity of the peak observed at 0.75 meV. Lines: calculated Q dependence of the neutron cross section for different Co multimers (visualized in the figure) in the cubic perovskite lattice of* $LaCoO_3$ *and for* $|S\rangle \Longrightarrow |S\rangle$ *transitions.*

synthesizes were performed in order to find a proper electron dopant (four valent cation on the La^{3+} site) in the $LaCoO_3$ matrix.

3 Crystal growth of superconducting and magnetic materials at the University of Geneva

Group leader: D. van der Marel. *Researcher involved*: E. Giannini.

The research activity focuses on two classes of materials in which strong electron correlations play a major role: unconventional metals with novel magnetic properties and new superconducting materials. The transition metal silicides with the "B20" FeSi-type structure are a playground for the study of band magnetism. Various magnetic ground states and quantum phase transitions are observed in (Mn,Co)Si, (Mn,Ni)Si and (Fe,Co)Si as a function of doping. Neutron scattering experiments are made possible on large single crystals grown in our laboratory. Magnetic quantum criticality and strong electron correlations are studied in $CeCoGe_{3-x}Si_x$ as well. Both poly- and single crystalline samples of this compound are being

processed.
One of the most exciting highlights of the year was certainly the discovery of superconductivity in quaternary oxi-pnictides (up to 56 K in SmOFeAs) and in many other related binary and ternary compounds with a similar tetrahedral structure. We have succeeded in growing large single crystals of $Fe_{1+x}Te$ and $Fe_{1+x}(Te,Se)$. The study of the Bi-based superconducting cuprates has continued and the focus has been put on the single-layer $Bi_2Sr_2CuO_{6+\delta}$ (Bi-2201) superconductor, whose vortex phase diagram has been deeply investigated. The search for novel properties, like superconductivity, in strongly correlated oxides has lead to the investigation of the Sr_2VO_4 compound, whose orbital transitions have been successfully studied by means of optical and thermal experiments. Single-crystals of the topological insulator $Bi_{1-x}Sb_x$ have been grown and spectroscopic studies are in progress.

3.1 Magnetic excitations in $Fe_{1-x}Co_xSi$

MnSi and $Fe_{1-x}Co_xSi$ have been subject of intense research. At low temperature, these systems order in a helimagnetic state, that can be driven into a conventional ferromagnet by applying either pressure or magnetic field. Inelastic neutrons scattering (INS) experiments on a broad energy range have revealed that the simple model of Stoner magnetism can account for the high energy excitations in MnSi. Whether such a description is also valid for the $Fe_{1-x}Co_xSi$ solid solution is still an open question we try to answer. We have grown the large single crystals needed for high energy INS experiments by using a Czochralski pulling technique from a levitating melt in a RF induction furnace.

3.2 Magnetic ground state of $Mn_{1-x}Co_xSi$

Doping the famous helimagnet MnSi with a small amount of other transition metals (Cr, Fe, Co) leads to a sharp decrease of the helimagnetic ordering temperature. Recent neutron diffraction experiments have confirmed that, in the doping range $0 < x < 0.06$, the materials still order helimagnetically. This is proved by the appearance of magnetic satellites around the [111] direction (inset in Fig. 7c). At the limit concentration $x = 0.06$ a zero temperature transition from the helimagnetic state to a completely different magnetic ground state takes place and is likely to mark a quantum critical point. Beyond this critical composition, transport measurements reveal a non-

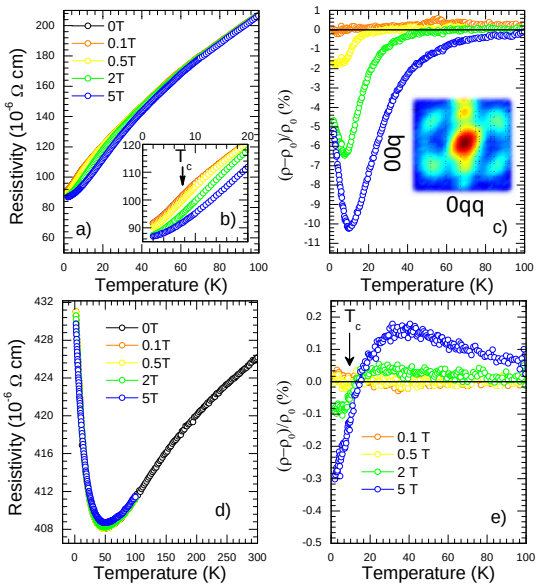

Figure 7: *Electrical resistivity and magnetoresistance of a, b, c) $Mn_{0.95}Co_{0.05}Si$ and d, e) $Mn_{0.5}Co_{0.5}Si$. The inset in panel c) shows the diffraction satellites due to the helimagnetic ordering along (111).*

monotonic temperature dependence of the resistivity with an upturn at a temperature that scales with the magnetic ordering T_c (Fig. 7d), thus revealing a possible transition to an insulating state. Anomalous changes of sign of the magnetoresistance are also observed in this doping range (Fig. 7e). Single crystals of the whole solid solution $Mn_{1-x}Co_xSi$ have being grown for unveiling the nature of this antiferromagnetic phase and the magnetic properties in the region close to the critical concentration.

3.3 Processing and crystal growth of $CeCoGe_{3-x}Si_x$

The pseudoternary $CeCoGe_{3-x}Si_x$ alloy is one of the few examples of strongly electron correlated systems whose physical properties close to a magnetic quantum critical point (QCP) can be studied under feasible experimental conditions. A long term proposal for neutron scattering experiments has been recently approved and aims at shedding light on such a complex magnetic system. For this project, both polycrystals and single crystals of $CeCoGe_{3-x}Si_x$ are needed. For processing polycrystalline samples, all the elements are first melted in an arc furnace at the stoichiometric amounts. Then the poly-phased polycrystalline material is annealed at 900°C for two weeks under pure Ar in sealed quartz tubes. Single crystals can be grown by the flux method using Bi flux. A dedicated setup has been built and the prelimi-

nary tests revealed the growth of small crystals with the wanted structure and stoichiometry. The availability of such a technique in our laboratory is very promising for the success of this project as well as for the growth of other novel materials.

3.4 Superconducting pnictides and chalcogenides

The discovery of superconductivity at 26 K in F-doped LaOFeAs at the beginning of the year 2008 [15] has put to the limelight a new class of superconducting materials. Either binary ("11"), or ternary ("122") or quaternary ("1111") compounds, all sharing a common structural feature, a layer of PbO structure type tetrahedra, can exhibit superconductivity up to quite high temperatures (56 K achieved so far in "1111" SmOFeAs). All these new superconductors contain a transition metal from the $VIIIA$ group (mainly Fe) and either a pnictogen or a chalcogen element (P, As, Sb, Bi, and Se, Te).

3.5 ROFePn (R = rare earth element, Pn = Sb, Bi)

It is not known yet if superconductivity exists in quaternary Fe-based pnictides with Sb or Bi. Our research is focussing on these compounds, with the aim of synthesizing superconductors containing no As, that is a particularly toxic element. Cubic RSb or RBi have been prepared by direct reaction between the pure metals in several steps between 500°C and 700°C and for several days. Preliminary experiments provided encouraging results for the synthesis of NdOFeSb under very high pressures (5 GPa) and high temperature (800 – 1000°C).

3.6 FeSe and FeTe

Recently, FeSe was reported to be superconducting when it crystallizes in the PbO-like $P4/nmm$ space group with an excess of Fe [16]. We have successfully synthesized superconducting polycrystalline samples of both FeSe and $FeSe_{1-x}Te_x$. We have succeeded in growing single crystals of FeTe (Fig. 8), in self flux under closed Ar atmosphere. FeTe does not exhibit superconductivity at ambient pressure down to 2 K.

3.7 BiIn

Other binary alloys with the same crystal structure as that of PbO may exhibit a superconducting state at low T. BiIn is isostructural to

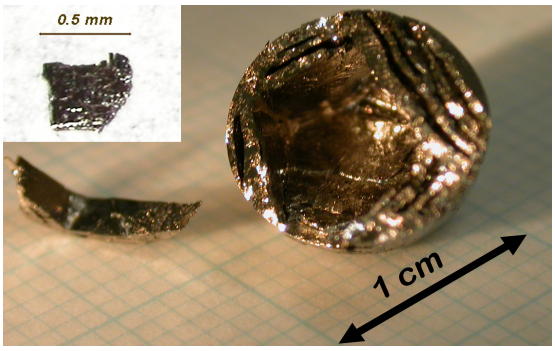

Figure 8: *Single Crystals of $Fe_{1+x}Te$.*

PbO, it is metallic and even becomes superconductor (T_c about 1.5 K) under high pressure, whereas all the $III-V$ compounds are semiconductors. Pure BiIn and doped $Bi_{1-x}M_x$In and $BiIn_{1-x}M'_x$ (M = Pb, Sb and M' = Ga, Sn) have been prepared and large crystals ($2 \times 1 \times 1$ cm^3) have been grown. The Sb doped compound was found to be single phase for $x < 0.05$ and was found to be superconducting below 8 K.

3.8 Bismuth-based cuprates

The growth of the Bi-based superconducting cuprates $Bi_2Sr_2Ca_{n-1}Cu_nO_{2n+4}$ (n = 1, 2, 3) is still one of the leading activities of our laboratory. Fruitful collaborations among various MaNEP partners have led to remarkable ARPES, STM and optical spectroscopy studies that are described in the report of Project 2 (see references therein). Highly pure crystals of Bi-2212 and Bi-2223 grown in Geneva have been used by F. Carbone at Caltech for time-resolved electron diffraction experiments that have provided a direct evidence of the role of the lattice in the transition to the superconducing state [11]. Particular attention has been devoted to the growth of the 1-layer compound $Bi_2Sr_2CuO_{6+\delta}$ with a controlled hole-doping level. The vortex phase diagram has been investigated as a function of doping in the overdoped regime.

3.9 Thallium-based cuprates

$Tl_2Ba_2CuO_6$ (Tl-2201) has the highest critical temperature among the cuprates with a single CuO_2 plane (92 K). In addition to the extreme sensitivity to the preparation conditions, the difficulties in processing this compound are enhanced by the high toxicity and volatility of Tl. We have developed a chemical approach to the synthesis of Tl-2201 ceramics. Starting from a solution of acetates in acetic acid, we

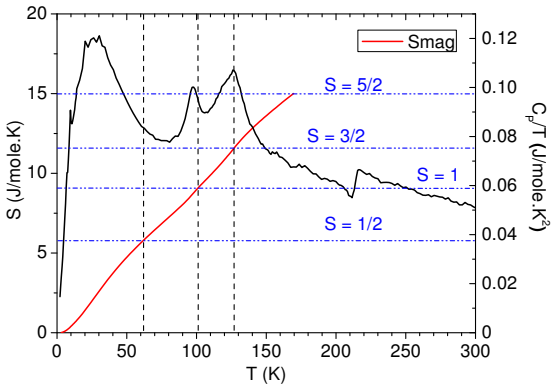

Figure 9: *Magnetic contribution to the heat capacity and magnetic entropy in tetragonal Sr_2VO_4.*

provoke a sudden precipitation of oxalates by adding an excess of oxalic acid ($H_2C_2O_4$). The homogeneous mixture of highly reactive oxalates is dried at 80°C (24 h) and calcined at 500°C (48 h), thus obtaining an homogeneous mixture of Tl_2O_3, $BaCO_3$, and CuO that is used for the final reaction step. By this method, the calcination and reaction temperatures are lowered and the Tl losses are reduced.

3.10 Orbital ordering transition in Sr_2VO_4

Sr_2VO_4 shares several structural and electronic features with La_2CuO_4, the parent compound of high-T_c superconducting cuprates. Despite the failure of any attempt to dope it and induce a superconducting transition, this compound was found to exhibit an interesting orbital ordering transition at 100 K [17]. Our results of optical and specific heat experiments on polycrystals show the nature of such a transition. We observe two transitions at about 125 K and 100 K, which should correspond to a tetragonal-orthorhombic and an orthorhombic-tetragonal transition, respectively, associated to the orbital ordering (Fig. 9).

3.11 The topological insulator $Bi_{1-x}Sb_x$

Single crystals of $Bi_{1-x}Sb_x$ have been grown for the optical investigations of the exciting electronic properties of this alloy, ranging from metal-semimetal transition, topological Dirac insulating behavior, spin-Hall state. Special care was taken in the preparation of the polycrystalline precursor, then crystals were grown by the floating zone method in a closed quartz mould. The most critical aspect, that is the homogeneity of the Sb doping, was overcome and highly homogeneous crystals were obtained.

4 Crystal growth of dichalcogenides and magnetic materials at the EPFL

Group leader: G. Margaritondo. *Researchers involved*: H. Berger, A. Magrez.

4.1 Synthesis of single crystals of $BaVSe_3$

The paramagnetic-ferromagnetic transition (PM-FM) in 3*d* transition metal compounds has received lot of attention because of its importance in applications, for example in colossal magnetoresistance compounds, or because of the exotic physics it can lead to, such as in the case of MnSi [18]. Like this latter compound, $BaVSe_3$, which has a structurally one-dimensional character, shows a PM-metal to FM-metal transition at 43 K. The in-depth investigation of this compound and its comparison to other 3*d* correlated systems has been precluded until now due to the lack of sizeable single crystals. During MaNEP phase II, we have succeeded in the synthesis of high quality crystals (Fig. 10). A further importance in studying $BaVSe_3$ is a recent interest in its sister-compound of $BaVS_3$, which has a very rich phase diagram (see reports of previous years), and whose high pressure magnetic ground state is poorly understood. Formally, because of the stronger interchain overlap due to the larger selenium atoms, $BaVSe_3$ [12, 13] could be considered as the high pressure counterpart of $BaVS_3$.

4.2 Synthesis of single crystals of transition metal dichalcogenides

In the transition metal dichalcogenides (TMD) one can study extensively the interplay between superconductivity and charge density wave (CDW) state either by doping/intercalation or by application of high pressures. Along these lines, a large number of TMD crystals was synthesized both in the pristine and intercalated forms. The intercalation was achieved by Cu and Nb.

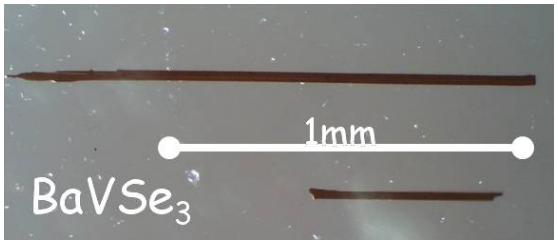

Figure 10: *Image of high quality single crystals of $BaVSe_3$.*

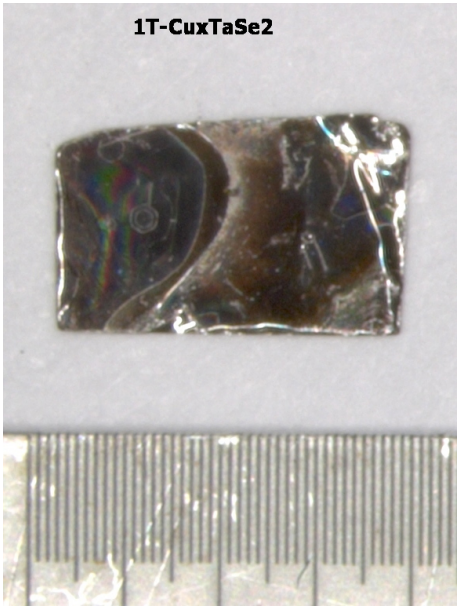

Figure 11: *Image of a large single crystals of 1T-Cu_xTaSe_2.*

The single crystals were grown by a conventional vapor transport method and the sample stoichiometry was verified by X-ray and resistivity measurements. A non-exhaustive list of systems synthesized in the last year is the following: 2H-$NbSe_2$, 1T-$TiSe_2$, 1T-$Ti_{1-x}Cu_xSe_2$, 1T-$TaSe_2$, 2H-$TaSe_2$. An exemple of a large crystal is shown in Fig. 11. Large number of studies within and outside MaNEP laboratories is in progress.

4.3 Synthesis of frustrated magnetic materials

In the last period we have prepared the $FeTe_2O_5Cl$ system which grows in a layered structure with a monoclinic unit cell, where individual layers are bonded by weak van der Walls forces. Each layer is then built of separate $[Fe_4O_{16}]_{20}$ tetramers, which are held together by $[Te_4O_{10}X_2]_6$ entities. In each individual tetramer two chemically inequivalent Fe^{3+} sites can be distinguished. The tetramer structure infers magnetically frustrated ($S = 5/2$) Fe^{3+} geometry. Along these lines we have prepared another member of the same family, namely $Fe_3Te_3O_{10}Cl$ (Fig. 12). Their structural and physical properties are currently studied in several laboratories.

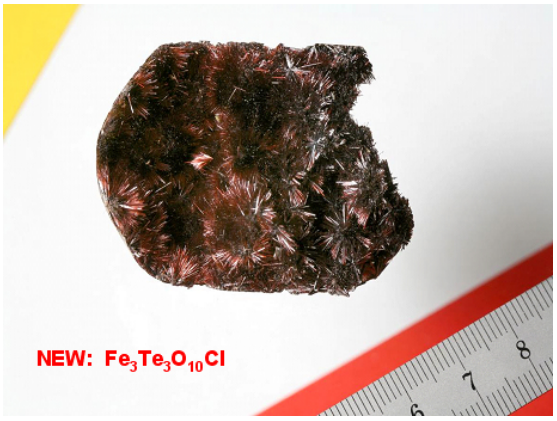

Figure 12: *A large assembly of single crystals of $Fe_3Te_3O_{10}Cl$.*

5 Collaborative efforts

During the project meetings and other MaNEP events the crystal growers and their collaborators have fruitful discussions and had exchanges of ideas. Single crystals grown in these four laboratories were intensively studied inside other MaNEP projects.

MaNEP-related publications

[1] N. D. Zhigadlo, S. Katrych, Z. Bukowski, S. Weyeneth, R. Puzniak, and J. Karpinski, Journal of Physics: Condensed Matter **20**, 342202 (2008).

[2] J. Karpinski, N. D. Zhigadlo, S. Katrych, Z. Bukowski, P. Moll, S. Weyeneth, H. Keller, R. Puzniak, M. Tortello, D. Daghero, R. Gonnelli, I. Maggio-Aprile, Y. Fasano, Ø. Fischer, and B. Batlogg, Physica C (2009), doi: 10.1016/j.physc.2009.03.048.

[3] S. Weyeneth, R. Puzniak, N. D. Zhigadlo, S. Katrych, Z. Bukowski, J. Karpinski, and H. Keller, Journal of Superconductivity and Novel Magnetism **22**, 347 (2009).

► [4] D. Chernyshov, V. Dmitriev, E. Pomjakushina, K. Conder, M. Stingaciu, V. Pomjakushin, A. Podlesnyak, A. A. Taskin, and Y. Ando, Physical Review B **78**, 024105 (2008).

► [5] H. Luetkens, M. Stingaciu, Y. G. Pashkevich, K. Conder, E. Pomjakushina, A. A. Gusev, K. V. Lamonova, P. Lemmens, and H.-H. Klauss, Physical Review Letters **101**, 017601 (2008).

► [6] A. Podlesnyak, M. Russina, A. Furrer, A. Alfonsov, E. Vavilova, V. Kataev, B. Büchner, T. Strässle, E. Pomjakushina, K. Conder, and D. I. Khomskii, Physical Review Letters **101**, 247603 (2008).

[7] E. Pomjakushina, K. Conder, and V. Pomjakushin, Physical Review B **73**, 113105 (2006).

► [8] M. Stingaciu, E. Pomjakushina, H. Grimmer, M. Trottmann, and K. Conder, Journal of Crystal Growth **310**, 1239 (2008).

[9] M. Stingaciu, Synthesis, crystal growth and investigation of layered cobaltites type $RBaCo_2O_{5+\delta}$, Ph.D. thesis, Technische Universität Braunschweig (2008).

[10] A. Podlesnyak, S. Streule, J. Mesot, M. Medarde, E. Pomjakushina, K. Conder, A. Tanaka, M. Haverkort, and D. I. Homskii, Physical Review Letters **97**, 247208 (2006).

[11] F. Carbone, D. Yang, E. Giannini, and A. H. Zewail, Proceedings of the National Academy of Science of the USA **105**, 20161 (2008).

[12] A. Akrap, V. Stevanović, M. Herak, M. Miljak, N. Barišić, H. Berger, and L. Forró, Physical Review B **78**, 235111 (2008).

[13] M. Herak, M. Miljak, A. Akrap, L. Forró, and H. Berger, Journal of the Physical Society of Japan **77**, 093701 (2008).

Other references

[14] J. Jaroszynski, F. Hunte, L. Balicas, Y. jung Jo, I. Raičević, A. Gurevich, D. C. Larbalestier, F. F. Balakirev, L. Fang, P. Cheng, Y. Jia, and H. H. Wen, Physical Review B **78**, 174523 (2008).

[15] Y. Kamihara, T. Watanabe, M. Hirano, and H. Hosono, Journal of the American Chemical Society **130**, 3296 (2008).

[16] F.-C. Hsuet, Proceedings of the National Academy of Science of the USA **105**, 14262 (2008).

[17] H. D. Zhou, B. S. Conner, and C. R. Wiebe, Physical Review Letters **99**, 136403 (2007).

[18] C. Pfleiderer, D. Reznik, L. Pintschovius, H. v. Löhneysen, M. Garst, and A. Rosch, Nature **427**, 227 (2004).

Single Crystal Catalog of MaNEP

Material	Growth technique	Furnace	Conductor	Insulator	Magnetic	Responsable
Various elemental metals	Bridgman, Zone melting	RF Induction, Electronic bombardement	yes			Giannini (022 3796076, enrico.giannini@physics.unige.ch)
MgB2	Mg-flux under HP	cubic anvil hot press	yes, Tc=39K			Giannini (022 3796076, enrico.giannini@physics.unige.ch)
TMSi (TM=Transition Metal: Co, Fe, Mn, ...)	Czochralski, TSFZ	RF Induction, Mirror image furnace	yes/no		some	Giannini (022 3796076, enrico.giannini@physics.unige.ch)
Sr14Cu24O41	TSFZ	Mirror image furnace	No			Giannini (022 3796076, enrico.giannini@physics.unige.ch)
(Sr,M1,M2)14Cu24O41-x (M1, M2 = Ca, Bi, Y...)	TSFZ	Mirror image furnace	No			Giannini (022 3796076, enrico.giannini@physics.unige.ch)
Bi2Sr2Ca2Cu3O10 Bi-2223	TSFZ	Mirror image furnace	Yes, Tc=110 K			Giannini (022 3796076, enrico.giannini@physics.unige.ch)
Bi2-xPbxSr2Ca2Cu3O10+d Bi,Pb-2223	TSFZ	Mirror image furnace	Yes, Tc=110 K			Giannini (022 3796076, enrico.giannini@physics.unige.ch)
Bi2Sr2CaCu2O8 Bi-2212	TSFZ	Mirror image furnace	Yes, Tc=91 K			Giannini (022 3796076, enrico.giannini@physics.unige.ch)
Bi2-xPbxSr2CaCu2O8 Bi,Pb-2212	TSFZ	Mirror image furnace	Yes, Tc=93 K			Giannini (022 3796076, enrico.giannini@physics.unige.ch)
Bi2Sr2CuO6 Bi-2201	TSFZ	Mirror image furnace	Yes, Tc=8 K			Giannini (022 3796076, enrico.giannini@physics.unige.ch)
REBa2Cu3O7	self flux	3-zone furnace, Top seeded growth	Yes, Tc=90 K			Giannini (022 3796076, enrico.giannini@physics.unige.ch)
MgB2	Mg-flux under HP	cubic anvil hot press	yes, Tc=39K			Karpinski(044 6332254, karpinski@phys.ethz.ch)
Mg(1-x)AlxB2	Mg-flux under HP	cubic anvil hot press	yes			Karpinski(044 6332254, karpinski@phys.ethz.ch)
MgB2-xCx	Mg-flux under HP	cubic anvil hot press	yes			Karpinski(044 6332254, karpinski@phys.ethz.ch)
Mg(1-x)MnxB2	Mg-flux under HP	cubic anvil hot press	yes			Karpinski(044 6332254, karpinski@phys.ethz.ch)
Mn(1-x)FexB2	Mg-flux under HP	cubic anvil hot press	yes			Karpinski(044 6332254, karpinski@phys.ethz.ch)
KOs2O6	ampoule method	resistive furnace	yes, Tc=9.6K			Karpinski(044 6332254, karpinski@phys.ethz.ch)
Na2Os2.5O6	HP	cubic anvil hot press	no			Karpinski(044 6332254, karpinski@phys.ethz.ch)
YBa2Cu4O8	HP	high O2 pressure	yes, Tc=80K			Karpinski(044 6332254, karpinski@phys.ethz.ch)
Ca(2-x)NaxCuO2Cl2	HP	cubic anvil hot press	yes, Tc=13-25K			Karpinski(044 6332254, karpinski@phys.ethz.ch)
YBa(2-x)SrxCu4O8	HP	high O2 pressure	yes			Karpinski(044 6332254, karpinski@phys.ethz.ch)
YMnO3	TSFZ	Mirror image furnace		stacked-triangular AF		kazimierz.conder@psi.ch
DyMnO3	TSFZ	Mirror image furnace		AF Tn~40K, ferroelectric T<19K		ekaterina.pomjakushina@psi.ch
LaCoO3	TSFZ	Mirror image furnace		magnetic and spin state transitions		Kazimierz Conder/Ekaterina Pomjakushina
La(1-x)SrxCoO3	TSFZ	Mirror image furnace		magnetic and spin state transitions		Kazimierz Conder/Ekaterina Pomjakushina
SrCu2(BO3)2	TSFZ	Mirror image furnace			2D spin system	Kazimierz Conder/Ekaterina Pomjakushina
EuNi2(Si(1-x)Gex)2	TSFZ	Mirror image furnace			valence transition in E	Kazimierz Conder/Ekaterina Pomjakushina
LaFeO3	TSFZ	Mirror image furnace		magneto-optical Faraday effect		Kazimierz Conder/Ekaterina Pomjakushina
La(1-x)SrxFeO3	TSFZ	Mirror image furnace		magneto-optical Faraday effect		Kazimierz Conder/Ekaterina Pomjakushina
ErFeO3	TSFZ	Mirror image furnace		magneto-optical Faraday effect		Kazimierz Conder/Ekaterina Pomjakushina
YFeO3	TSFZ	Mirror image furnace		magneto-optical Faraday effect		Kazimierz Conder/Ekaterina Pomjakushina
TbBaCo2O(5+x)	TSFZ	Mirror image furnace		magnetic, metal-insulator, spin state transitic		Kazimierz Conder/Ekaterina Pomjakushina
LuFe2O4	TSFZ	Mirror image furnace		ferroelectric, charge frustrated system		Kazimierz Conder/Ekaterina Pomjakushina
NaxCoO2 (x=0.7, 0.75, 1)	TSFZ	Mirror image furnace		FM, AFM, MI transitions		Kazimierz Conder/Ekaterina Pomjakushina
NdBaCo2O(5+x)	TSFZ	Mirror image furnace		magnetic, metal-insulator, spin state transitic		Kazimierz Conder/Ekaterina Pomjakushina
La(2-x)SrxCuO4	TSFZ	Mirror image furnace	superconductor			Kazimierz Conder/Ekaterina Pomjakushina
La2CuO4	TSFZ	Mirror image furnace		AFM		Kazimierz Conder/Ekaterina Pomjakushina
Nd1/3Sr2/3FeO3	TSFZ	Mirror image furnace		AFM, charge disproportionation		Kazimierz Conder/Ekaterina Pomjakushina
CaVO3	TSFZ	Mirror image furnace	metal below 1K			Kazimierz Conder/Ekaterina Pomjakushina
SmBaMn2O6	TSFZ	Mirror image furnace		charge ordering, orbital ordering		Kazimierz Conder/Ekaterina Pomjakushina
Al2-xNixO3	TSFZ	Mirror image furnace				Kazimierz Conder/Ekaterina Pomjakushina
SrTi1-xNixO3	TSFZ	Mirror image furnace				
YBa2Cu3O(6+x), x=0--1, 16O-18O	solid state synthesis		superconductor			Kazimierz Conder/Ekaterina Pomjakushina
LnBaCo2O5+x, x=0--1, 16O-18O	solid state synthesis			magnetic, metal-insulator, spin state transitic		Kazimierz Conder/Ekaterina Pomjakushina
Ln(2-x)SrxCuO4, 16O-18O	solid state synthesis		superconductor			Kazimierz Conder/Ekaterina Pomjakushina
Ca3Cu(3-x)Nix(PO4)4	solid state synthesis				quantum spin trimer	Kazimierz Conder/Ekaterina Pomjakushina
NdNi2B2C	arc melting		superconductor			Kazimierz Conder/Ekaterina Pomjakushina
(La(1-x)Prx)1-yCayMnO3, 16O-18O	solid state synthesis				AF, FM	Kazimierz Conder/Ekaterina Pomjakushina
FeSe1-x	solid state synthesis		superconductor, Tc~8.3 K			Kazimierz Conder/Ekaterina Pomjakushina
R1-x CaxBaMn2O6	solid state synthesis			charge ordering, orbital ordering		
Fe3O4	CVT	2-zone furnace	Yes Tc 123K			Berger 021 693 4484, helmuth.berger@epfl.ch)
CoS2	CVT	2-zone furnace	Yes Tc 121K		ferromagnetic	Berger 021 693 4484, helmuth.berger@epfl.ch)
BaVS3	Flux grown	1-zone furnace with temp.gradient	Yes	Insulator		Berger 021 693 4484, helmuth.berger@epfl.ch)
LiCu2O2	Flus grown	1-zone furnace with temp.gradient	No			Berger 021 693 4484, helmuth.berger@epfl.ch)
NbSe2	CVT	2-zone furnace	Yes Tc 7.2K			Berger 021 693 4484, helmuth.berger@epfl.ch)
Cu3TeO6	CVT and flux grown	2-zone furnace	No			Berger 021 693 4484, helmuth.berger@epfl.ch)
Na0.75CoO2	Flux grown	1-zone furnace with temp.gradient	Yes			Berger 021 693 4484, helmuth.berger@epfl.ch)

Single Crystal Catalog of MaNEP

Material	Growth technique	Furnace	Conductor	Insulator	Magnetic	Responsable
CuSb2O5	CVT	2-zone furnce	No			Berger 021 693 4484, helmuth.berger@epfl.ch)
CdCr2S4	CVT	2-zone furnace	Tc		ferromagnetic	Berger 021 693 4484, helmuth.berger@epfl.ch)
CdCr2Se4	CVT	2-zone furnace	Yes		ferromagnetic	Berger 021 693 4484, helmuth.berger@epfl.ch)
C-60	Sublimation	10-zone furnace	No	Insulator		Berger 021 693 4484, helmuth.berger@epfl.ch)
NbTe2	CVT	2-zone furnace	Yes Tc= 86K		ferromagnetic	Berger 021 693 4484, helmuth.berger@epfl.ch)
TaTe2	CVT	2-zone furnace	Yes Tc=130K		ferromagnetic	Berger 021 693 4484, helmuth.berger@epfl.ch)
TiTe2	CVT	2-zone furnace	Yes			Berger 021 693 4484, helmuth.berger@epfl.ch)
alpha TeVO4	CVT	2-zone furnace	No		magnetic properties	Berger 021 693 4484, helmuth.berger@epfl.ch)
beta TeVO4	CVT	2-zone furnace	No			Berger 021 693 4484, helmuth.berger@epfl.ch)
ZnO	CVT	2-zone furnace	No		magnetic properties	Berger 021 693 4484, helmuth.berger@epfl.ch)
Ni5(SeO3)4Cl2	CVT	2.zone furnace	No		magnetic properties	Berger 021 693 4484, helmuth.berger@epfl.ch)
Ni5(SeO3)4Br2	CVT	2-zone furnace	No		magnetic properties	Berger 021 693 4484, helmuth.berger@epfl.ch)
Cu2Te2O5Cl2	CTV	2-zone furnace	No		magnetic properties	Berger 021 693 4484, helmuth.berger@epfl.ch)
Cu2Te2O5Br2	CVT	2-zone furnace	No		magnetic properties	Berger 021 693 4484, helmuth.berger@epfl.ch)
Co6(TeO3)2(TeO6)Cl2	CVT	2-zone furnace	No		antiferromagnetic	Berger 021 693 4484, helmuth.berger@epfl.ch)
Co6(TeO3)2(TeO6)Br2	CVT	2-zone furnace	No		antiferromagnetic	Berger 021 693 4484, helmuth.berger@epfl.ch)
CdRe2O7	CVT	2-zone furnace	Yes Tc=1k			Berger 021 693 4484, helmuth.berger@epfl.ch)
Co2TeO3Cl2	CVT	2-zone furnace	No		magnetic properties	Berger 021 693 4484, helmuth.berger@epfl.ch)
Co2TeO3Br2	CVT	2-zone furnace	No		magnetic properties	Berger 021 693 4484, helmuth.berger@epfl.ch)
Ni5(TeO3)4Cl2	CVT	2-zone furnace	No		magnetic properties	Berger 021 693 4484, helmuth.berger@epfl.ch)
Ni5(TeO3)4Br2	CVT	2-zone furnace	No		magnetic properties	Berger 021 693 4484, helmuth.berger@epfl.ch)
Ni5(TeO3)4Br2-xClx	CVT	2-zone furnace	No		magnetic properties	Berger 021 693 4484, helmuth.berger@epfl.ch)
CuWO4	Flux grown and CVT	2-zone furnace	No		magnetic properties	Berger 021 693 4484, helmuth.berger@epfl.ch)
Co7Te4O12Br6	CVT	2-zone furnace	No		magnetic properties	Berger 021 693 4484, helmuth.berger@epfl.ch)
CuSbTeO3Cl2	CVT	2-zone furnace	No	Insulator		Berger 021 693 4484, helmuth.berger@epfl.ch)
Cu3(SeO3)4Cl2	CTV	2-zone furnace	No		magnetic properties	Berger 021 693 4484, helmuth.berger@epfl.ch)
CuTe2O5	CVT	2-zone furnace	No		magnetic properties	Berger 021 693 4484, helmuth.berger@epfl.ch)
CuSe2O5	CVT	2-zone furnace	No			Berger 021 693 4484, helmuth.berger@epfl.ch)
Pentacene	CTV	2-zone furnace	No	Insulator		Berger 021 693 4484, helmuth.berger@epfl.ch)
Rubrene	CTV	2-zone furnace	No	Insulator		Berger 021 693 4484, helmuth.berger@epfl.ch)
Coronene	CTV	2-zone furnace	No	Insulator		Berger 021 693 4484, helmuth.berger@epfl.ch)
Tetracene	CTV	2-zone furnace	No	Insulator		Berger 021 693 4484, helmuth.berger@epfl.ch)
Anthracene	CTV	2-zone furnace	No	Insulator		Berger 021 693 4484, helmuth.berger@epfl.ch)
TCNQ	CTV	2-zone furnace	No	Insulator		Berger 021 693 4484, helmuth.berger@epfl.ch)
TTF-TCNQ	CTV	2-zone furnace	No	Organic Conductor		Berger 021 693 4484, helmuth.berger@epfl.ch)
Perylene	CTV	2-zone furnace	No	Insulator		Berger 021 693 4484, helmuth.berger@epfl.ch)
TCNQ-Perylene complexe	CTV	2-zone furnace	No			Berger 021 693 4484, helmuth.berger@epfl.ch)
Copper Pthalocyanine	CTV	2-zone furnace	No	p-type semiconductor		Berger 021 693 4484, helmuth.berger@epfl.ch)
FeTe2O5Cl	CTV	2-zone furnace	No	Insulator	magnetic properties	Berger 021 693 4484, helmuth.berger@epfl.ch)
FeTe2O5Br	CTV	2-zone furnace	No	Insulator	magnetic properties	Berger 021 693 4484, helmuth.berger@epfl.ch)
Na0.70CoO2	Flux grown	1-zone furnace with temp.gradient			magnetic properties	Berger 021 693 4484, helmuth.berger@epfl.ch)
Ca3Co2O6	Flux grown	1-zone furnace with temp.gradient			magnetic properties	Berger 021 693 4484, helmuth.berger@epfl.ch)
Ca3Co4O9	Flux grown	1-zone furnace with temp.gradient			magnetic properties	Berger 021 693 4484, helmuth.berger@epfl.ch)
In2VO5	CTV	2-zone furnace			magnetic properties	Berger 021 693 4484, helmuth.berger@epfl.ch)
$Co_5Te_4O_{11}Cl_4$.	CTV	2-zone furnace	No			Berger 021 693 4484, helmuth.berger@epfl.ch)
$Co_5(TeO_3)_4X_2$ (X = Cl, Br).	CTV	2-zone furnace	No	Insulator	magnetic properties	Berger 021 693 4484, helmuth.berger@epfl.ch)
$Co_5(SeO_3)_4X_2$ (X = Cl, Br).	CTV	2-zone furnace	No	Insulator	magnetic properties	Berger 021 693 4484, helmuth.berger@epfl.ch)
$NiSeO_3$	CTV	2-zone furnace	No	Insulator	magnetic properties	Berger 021 693 4484, helmuth.berger@epfl.ch)
ZrS3	CTV	2-zone furnace	No	Semiconductor		Berger 021 693 4484, helmuth.berger@epfl.ch)
ZrSe3	CTV	2-zone furnace	No	Semiconductor		Berger 021 693 4484, helmuth.berger@epfl.ch)
ZrTe3	CTV	2-zone furnace	No	Semiconductor		Berger 021 693 4484, helmuth.berger@epfl.ch)
HfS3	CTV	2-zone furnace	No	Semiconductor		Berger 021 693 4484, helmuth.berger@epfl.ch)
HfTe3	CTV	2-zone furnace	No	Semiconductor		Berger 021 693 4484, helmuth.berger@epfl.ch)
TiOBr	CTV	2-zone furnace	No	Insulator	magnetic properties	Berger 021 693 4484, helmuth.berger@epfl.ch)
Pd3(PS4)2	CTV	2-zone furnace	No	Semiconductor	diamagnetic	Berger 021 693 4484, helmuth.berger@epfl.ch)
MnPS3	CTV	2-zone furnace	No	Semiconductor	magnetic properties	Berger 021 693 4484, helmuth.berger@epfl.ch)

Single Crystal Catalog of MaNEP

Material	Growth technique	Furnace	Conductor	Insulator	Magnetic	Responsable
MnPSe3	CTV	2-zone furnace	No	Semiconductor	magnetic properties	Berger 021 693 4484, helmuth.berger@epfl.ch)
NiPS3	CTV	2-zone furnace	No	Semiconductor	magnetic properties	Berger 021 693 4484, helmuth.berger@epfl.ch)
NiPSe3	CTV	2-zone furnace	No	Semiconductor	magnetic properties	Berger 021 693 4484, helmuth.berger@epfl.ch)
FePS3	CTV	2-zone furnace	No	Semiconductor	magnetic properties	Berger 021 693 4484, helmuth.berger@epfl.ch)
FePSe3	CTV	2-zone furnace	No	Semiconductor	magnetic properties	Berger 021 693 4484, helmuth.berger@epfl.ch)
Ni3TeO6	CTV	2-zone furnace	No	Semiconductor	magnetic properties	Berger 021 693 4484, helmuth.berger@epfl.ch)
Co3TeO6	Flux grown	1-zone furnace with temp.gradient	No	Semiconductor	magnetic properties	Berger 021 693 4484, helmuth.berger@epfl.ch)
Cu_2CoTeO_6	Flux grown	1-zone furnace with temp.gradient	No	Semiconductor	magnetic properties	Berger 021 693 4484, helmuth.berger@epfl.ch)
LiCu2O2	Flux grown	1-zone furnace with temp.gradient	No	Semiconductor	magnetic properties	Berger 021 693 4484, helmuth.berger@epfl.ch)
PbMo6S8	solid state synthesis		Yes Tc = 15K			Petrovic (022 3796287, Alexander.Petrovic@physics.unige.ch)
PbMo6S8 + 3% O2	solid state synthesis		Yes Tc = 11K			Petrovic (022 3796287, Alexander.Petrovic@physics.unige.ch)
SnMo6S8	solid state synthesis		Yes Tc = 14K			Petrovic (022 3796287, Alexander.Petrovic@physics.unige.ch)
Sn(1-x)PbxMo6S8	solid state synthesis		Yes Tc = 7-12K			Petrovic (022 3796287, Alexander.Petrovic@physics.unige.ch)
LaMo6S8	solid state synthesis		Yes Tc = 7K			Petrovic (022 3796287, Alexander.Petrovic@physics.unige.ch)
Mo6Se8	solid state synthesis		Yes Tc = 6K			Petrovic (022 3796287, Alexander.Petrovic@physics.unige.ch)
Mo6S8	solid state synthesis		Yes Tc = 1K			Petrovic (022 3796287, Alexander.Petrovic@physics.unige.ch)
Mo6S6Br2	solid state synthesis		Yes Tc = 13.5K			Petrovic (022 3796287, Alexander.Petrovic@physics.unige.ch)
InMo6S8	solid state synthesis		Yes			Petrovic (022 3796287, Alexander.Petrovic@physics.unige.ch)
Tl2Mo6Se6	solid state synthesis		Yes Tc = 4.2K			Petrovic (022 3796287, Alexander.Petrovic@physics.unige.ch)
In2Mo6Se6	solid state synthesis		Yes Tc = 2.9K	Metal-Insulator		Petrovic (022 3796287, Alexander.Petrovic@physics.unige.ch)
Na2Mo6Se6	solid state synthesis		No	Metal-Insulator		Petrovic (022 3796287, Alexander.Petrovic@physics.unige.ch)
K2Mo6Se6	solid state synthesis		No	Metal-Insulator		Petrovic (022 3796287, Alexander.Petrovic@physics.unige.ch)
Rb2Mo6Se6	solid state synthesis		No	Metal-Insulator		Petrovic (022 3796287, Alexander.Petrovic@physics.unige.ch)
Cs2Mo6Se6	solid state synthesis		No			Petrovic (022 3796287, Alexander.Petrovic@physics.unige.ch)
Mo6Se6	solid state synthesis		No			Petrovic (022 3796287, Alexander.Petrovic@physics.unige.ch)
CsMo12S14	solid state synthesis		Yes Tc = 7K			Fischer (022 3796270, Oystein.Fischer@physics.unige.ch)
Ba2Mo6S9	solid state synthesis		Yes Tc = 5K			Fischer (022 3796270, Oystein.Fischer@physics.unige.ch)
Rb(2n)Mo(6n+9)S(6n+13) (n = 1-4)	solid state synthesis		Yes Tc = 4-10K			Fischer (022 3796270, Oystein.Fischer@physics.unige.ch)
LnFeAs(O,F) (Ln=La,Pr,Nd,Sm,Gd)	NaCl/KCl flux at HP	cubic anvil	Yes Tc=15-53K			Karpinski(044 6332254, karpinski@phys.ethz.ch)
Ba(1-x)RbxFe2As2	Sn flux	ampoule method in resistive furnace	Yes Tc=23K			Karpinski(044 6332254, karpinski@phys.ethz.ch)
Various elemental metals	Bridgman, Zone melting	RF Induction, Electronic bombardement	yes			Giannini (022 3796076, enrico.giannini@physics.unige.ch)
Bi(1-x)Sbx	Zone melting	Mirror image furnace	yes	yes (depending on x)		Giannini (022 3796076, enrico.giannini@physics.unige.ch)
FeTe(1-x)Sex	self flux	1-zone vertical furnace	yes			Giannini (022 3796076, enrico.giannini@physics.unige.ch)
BiIn	self flux	1-zone vertical furnace	yes			Giannini (022 3796076, enrico.giannini@physics.unige.ch)
Fe3Te3O10Cl	CTV	2-zone furnace	No	Insulator	magnetic properties	Berger 021 693 4484, helmuth.berger@epfl.ch)
Fe8Te12O32Cl6	CTV	2-zone furnace	No	Insulator	magnetic properties	Berger 021 693 4484, helmuth.berger@epfl.ch)
Fe3Te12O32Br6	CTV	2-zone furnace	No	Insulator	magnetic properties	Berger 021 693 4484, helmuth.berger@epfl.ch)
Fe5(TeO3)6Cl2	CTV	2-zone furnace	No	Insulator	magnetic properties	Berger 021 693 4484, helmuth.berger@epfl.ch)
Fe1-xRuxTe2OCl	CTV	2-zone furnace	No	Insulator	magnetic properties	Berger 021 693 4484, helmuth.berger@epfl.ch)
Fe1-xRuxTe2O5Br	CTV	2-zone furnace	No	Insulator	magnetic properties	Berger 021 693 4484, helmuth.berger@epfl.ch)
Cu9O2(SeO3)4Cl6	CTV	2-zone furnace	No	Insulator	magnetic properties	Berger 021 693 4484, helmuth.berger@epfl.ch)
Cu5Se4O12Cl2	CVT	2-zone furnace	No	Insulator	magnetic properties	Berger 021 693 4484, helmuth.berger@epfl.ch)
Cu2-xMnxTe2O5Cl2	CTV	2-zone furnace	No	Insulator	magnetic properties	Berger 021 693 4484, helmuth.berger@epfl.ch)
Cu4Te5O12Cl4	CTV	2-zone furnace	No	Insulator	magnetic properties	Berger 021 693 4484, helmuth.berger@epfl.ch)
Fe2O(SeO3)2	CTV	2-zone furnace	No	Insulator	magnetic properties	Berger 021 693 4484, helmuth.berger@epfl.ch)
(VO)2SeO3)2	CTV	2-zone furnace	No	Insulator	magnetic properties	Berger 021 693 4484, helmuth.berger@epfl.ch)
Fe2SeO5	CTV	2-zone furnace	No	Insulator	magnetic properties	Berger 021 693 4484, helmuth.berger@epfl.ch)
Sr2CuO2Cl2	Flux grown	1-zone furnace with temp.gradient	No	Insulator	magnetic properties	Berger 021 693 4484, helmuth.berger@epfl.ch)
Sr2-xPrxCuO2Cl2	Flux grown	1-zone furnace with temp.gradient	No	Insulator	magnetic properties	Berger 021 693 4484, helmuth.berger@epfl.ch)
Fe3-xNiXO4	CTV	10-zone furnace	yes	metal	ferromagnetic	Berger 021 693 4484, helmuth.berger@epfl.ch)
Fe3-xAlxO4	CTV	10-zone furnace	Yes	metal	ferromagnetic	Berger 021 693 4484, helmuth.berger@epfl.ch)
Fe3-xMnxO4	CTV	10-zone furnace	Yes	metal	ferromagnetic	Berger 021 693 4484, helmuth.berger@epfl.ch)
Co3O4	CTV	10-zone furnace	Yes	metal	magnetic properties	Berger 021 693 4484, helmuth.berger@epfl.ch)
CuxZrTe3	CTV	2-zone furnace	Yes	metal		Berger 021 693 4484, helmuth.berger@epfl.ch)
Cux1T-TiSe2	CTV	2-zone furnace	Yes Tc 2.2-4.2K	metal		Berger 021 693 4484, helmuth.berger@epfl.ch)
Cux2H-TaS2	CTV	2-zone furnace	Yes Tc = 4.2K	metal		Berger 021 693 4484, helmuth.berger@epfl.ch)
CuxNbS2	CTV	2-zone furnace	Yes	metal		Berger 021 693 4484, helmuth.berger@epfl.ch)

Single Crystal Catalog of MaNEP

Material	Growth technique	Furnace	Conductor	Insulator	Magnetic	Responsable
Fe0.28TaS2	CTV	2-zone furnace	Yes	metal	magnetic properties	Berger 021 693 4484, helmuth.berger@epfl.ch)
Fe0.33TaSe2	CTV	2-zone furnace	Yes	metal	magnetic properties	Berger 021 693 4484, helmuth.berger@epfl.ch)
Cux1T-TaS2	CTV	2-zone furnace	Yes Tc 2.2K	metal		Berger 021 693 4484, helmuth.berger@epfl.ch)
2H-TaS2	CTV	2-zone furnace	Yes	charge density wave transition		Berger 021 693 4484, helmuth.berger@epfl.ch)
2Hb-TaS2	CTV	2-zone furnace	Yes	show 2 first order transition		Berger 021 693 4484, helmuth.berger@epfl.ch)
Cu2OSeO3	CTV	2-zone furnace	No	piezoelectric ferrimagnet		Berger 021 693 4484, helmuth.berger@epfl.ch)
CuSeO3	CTV	2-zone furnace	No	Insulator	antiferromagnetic	Berger 021 693 4484, helmuth.berger@epfl.ch)
BaVSe3	Flux grown	1-zone furnace with temp.gradient	Yes	metal	ferromagnetic	Berger 021 693 4484, helmuth.berger@epfl.ch)
NiCl2	CTV	2-zone furnace	No	Insulator	magnetic properties	Berger 021 693 4484, helmuth.berger@epfl.ch)
NiBr2	CTV	2-zone furnace	No	Insulator	magnetic properties	Berger 021 693 4484, helmuth.berger@epfl.ch)
TiOBr	CTV	2-zone furnace	No	Insulator	magnetic properties	Berger 021 693 4484, helmuth.berger@epfl.ch)
NiGa2S4	CTV	2-zone furnace			antiferromagnetic	Berger 021 693 4484, helmuth.berger@epfl.ch)
(Ni30Te32O90Cl3)Ni4Cl	CTV	2-zone furnace	No	Insulator	antiferromagnetic	Berger 021 693 4484, helmuth.berger@epfl.ch)
(Ni30Te32O90Br3)Ni4Br	CTV	2-zone furnace	No	Insulator	antiferromagnetic	Berger 021 693 4484, helmuth.berger@epfl.ch)
FeAs2	CTV	2-zone furnace			magnetic properties	Berger 021 693 4484, helmuth.berger@epfl.ch)
FeSb2	CTV	2-zone furnace			magnetic properties	

Project 4 Novel materials

Project leader: J. Hulliger (UniBE)

Participating members: L. Forró (EPFL), J. Hulliger (UniBE), J. Karpinski (ETHZ), R. Nesper (ETHZ), L. Schlapbach (Empa).

Summary and highlights: First single crystals of the $Ba_{1-x}Rb_xFe_2As_2$ superconductor were grown from a Sn flux. Magnetic measurements showed that doped $Ba_2Fe_2As_2$ is significantly more isotropic than the LnFeAsO family (Ln = La, Pr, Nd, Sm, Gd, see report on Project 3). Since the discovery of superconductivity in MgB_2, interest has grown in lattices providing similar structural features, namely intercalated graphene nets. Doping experiments for CaB_2C_6 were performed, but no indication for superconductivity was found. A new type of equipment for the measurement of T_c of small isolated superconducting grains distributed within non-superconducting particles was developed and applied to cuprates. Revisiting the Tl-2223 phase system revealed that only a very small number of grains $d > 10$ μm show a T_c of 125 K. Evidence for superconductivity up to 131 K was found by SQUID. A novel perovskite type material prepared by plasma assisted anionic substitution showed a memistor effect, i.e. resistance switching providing a high/low ratio of maximum 10. The hydrozincites method has produced single phase $Zn_{1-x}Mn_xO$ material, exhibiting ferromagnetism at $T_c = 35$ K.

1 Superconductors

1.1 Superconductivity in substituted $BaFe_2As_2$

Single crystals of $Ba_{1-x}Rb_xFe_2As_2$ were grown by the group of J. Karpinski (ETHZ) using a Sn flux method in quartz ampoules [1]. The Fe:Sn ratio (1:24) in a starting composition was kept constant in all runs while the Rb:Ba ratio was varied between 0.7 and 2.0. The appropriate amounts of Ba, Rb, Fe_2As, As, and Sn were placed in alumina crucibles and sealed in silica tubes under 1/3 atmosphere of Ar gas. Next, the ampoules were heated at 850°C for 3 hours until all components were completely melted, and cooled over 50 hours back to 500°C. At this temperature the liquid Sn was decanted from the crystals. The remaining thin film of Sn was dissolved at room temperature using liquid Hg, and finally the crystals were heated to 190°C in vacuum to evaporate traces of Hg. The single crystals of $Ba_{1-x}Rb_xFe_2As_2$ grow in a plate-like shape with typical dimensions $(1-3) \times (1-2) \times (0.05-0.1)$ mm^3 (Fig. 1). Depending on the starting composition, the crystals displayed a variety of properties from nonsuperconducting to superconducting with sharp transitions to the superconducting state. For further studies, single crystals grown from initial composition $Ba_{0.6}Rb_{0.8}Fe_2As_2$ were used. The composition of the crystals from this batch determined by EDX analysis leads to the chemical formula $Ba_{0.84}Rb_{0.10}Sn_{0.09}Fe_2As_{1.96}$. Crys-

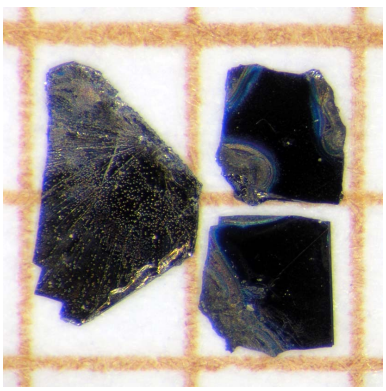

Figure 1: *Photograph of three single crystals of $Ba_{0.9}Rb_{0.1}Fe_2As_2$ on a millimeter grid.*

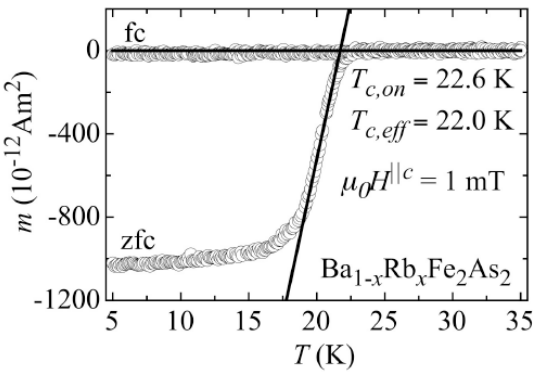

Figure 2: *Temperature dependence of the magnetic moment in a magnetic field of 1 mT applied parallel to the c-axis of the single crystal.*

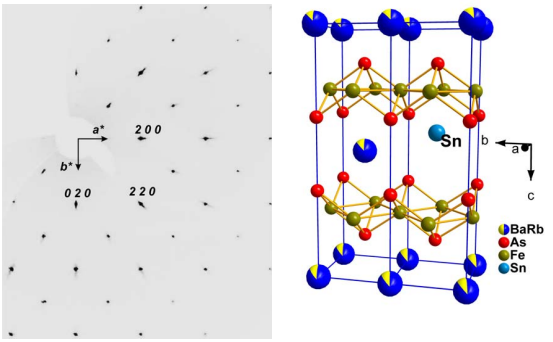

Figure 3: *a) The hk0 reciprocal space section of the $Ba_{1-x}Rb_xFe_2As_2$ crystal. b) Schematic illustration of two unit cells of $Ba_{0.89}Rb_{0.05}Sn_{0.06}As_2Fe_2$. Sn position is shown, for clarity, on one site only.*

tals from the selected batch exhibit T_c around $22-24$ K (Fig. 2). The crystals studied by X-ray diffraction (XRD) revealed good quality, and no additional phases (impurities, twins or intergrowing crystals) were detected by examining the reconstructed reciprocal space sections (Fig. 3a). Rb atoms substitute for Ba atoms therefore the Rb/Ba occupations have been refined simultaneously.

After several cycles of refinement the Fourier difference map showed two pronounced maxima of the electron density away from the Ba/Rb site. They located the Sn atoms on these sites, shifted towards the Fe_2As_2–layers. The resulting structure is shown on Fig. 3b. Compared to unsubstituted $BaAs_2Fe_2$ the lattice parameter a is slightly shorter, the c-parameter is longer and the volume of the unit cell is smaller. The increase of the c-parameter in $Ba_{0.89}Rb_{0.05}Sn_{0.06}As_2Fe_2$ is caused mainly by substitution of Ba^{2+} ions ($r = 1.42$ Å) by larger Rb^+ ($r = 1.61$ Å). Relatively large shortening of the a parameter (larger than expected from Vegard's law) seems to be the effect of Sn incorporation.

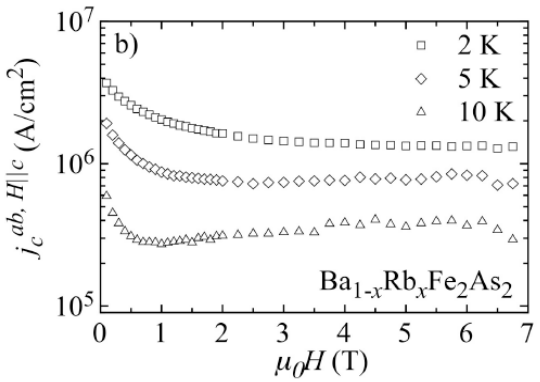

Figure 4: *The critical current density calculated from the hysteresis loops.*

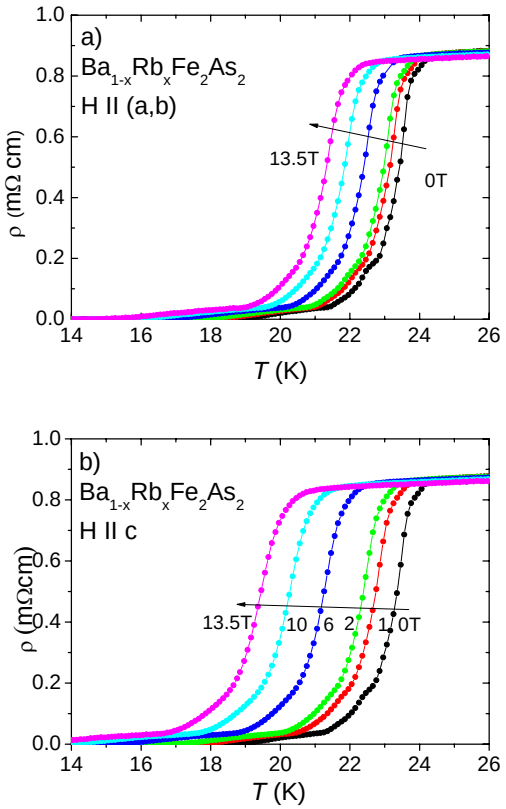

Figure 5: *$\varrho(T,H)$ dependences measured with the field applied (a) parallel to the Fe_2As_2–layers ($H \parallel ab$) and (b) perpendicular to them ($H \parallel c$) in magnetic fields of 0, 2, 4, 6, 8, 10, 12 and 13.5 T.*

A plate like single crystal with approximate dimensions of $125 \times 125 \times 10$ μm^3 was chosen for dc magnetization studies. A relatively strong pinning was confirmed in magnetic hysteresis loop measurements and by magnetic torque. The critical current density at 2 K, 5 K, and 10 K, estimated from the field dependence of the magnetic moment, reaches values higher than 10^6 A/cm^2 (see Fig. 4).

The resistance has been measured with the magnetic field applied parallel to the Fe_2As_2–layers ($H \parallel ab$, $I \parallel H$) and perpendicular to them ($H \parallel c$, $I \parallel ab$). Examples of $\varrho(T,H)$ are shown in Fig. 5. Particularly notable is the well defined shift of the resistance drop with increasing field, without a significant broadening due to flux flow dissipation. The upper critical field anisotropy in the vicinity of T_c, defined as $\gamma_H = H_{c2}^{\|ab}/H_{c2}^{\|c}$, is presented in the inset to the Fig. 6. The upper critical field anisotropy decreases with decreasing temperature. The slope of the upper critical field $H_{c2}^{\|c}$ of 4.2 T/K leads to very high value of $H_{c2}^{\|c}(0)$ (see Fig. 6).

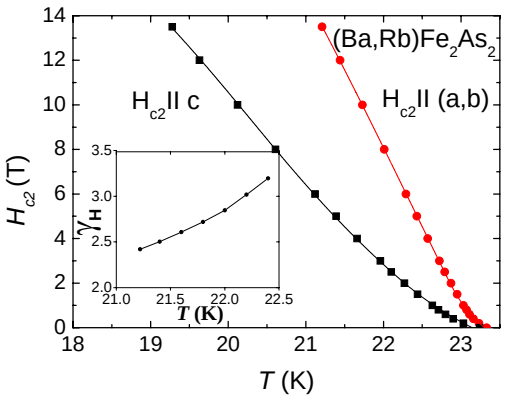

Figure 6: *Temperature dependence of the upper critical field with $H \parallel ab$ and with $H \parallel c$. Inset: the upper critical field anisotropy $\gamma_H = H_{c2}^{\parallel ab}/H_{c2}^{\parallel c}$ in the vicinity of T_c.*

1.2 $(CaB_2)C_n$ compounds with heterographite layers

Since the discovery of superconductivity in MgB_2 with a $T_c = 39$ K in 2001 [7] the interest in compounds having the similar structural features, namely intercalated graphene or hetero-graphene nets, has widely increased. In 2002, Rosner *et al.* [8] predicted high temperature superconductivity in hole-doped LiBC. However, all subsequent attempts to synthesize superconducting samples of $Li_{1-x}BC$ failed so far [9, 10, 11] [2, 3]. It seems that the Li–deintercalation, which is equivalent to hole doping, leads to local structural distortions that induce changes in the electronic band structure [12, 13]. Also high temperature superconductivity upon hole doping was predicted for the structurally related and isoelectronic compound MgB_2C_2 [14, 15, 16, 17, 18] but no superconducting samples could be obtained by deintercalation experiments [2]. The existence of a carbon richer compound CaB_2C_4 was reported first in 1964 by Markovskii *et al.* [19, 20]. The compound was structurally not characterized, however. During the work of Nesper's group (ETHZ) investigating the phase system Ca–B–C, they synthesized and characterized the two compounds CaB_2C_4 (Fig. 7) and CaB_2C_6, (Fig. 8) as described in the following. Both phases consist of hetero-graphene [B, C] nets intercalated by Ca atoms. $(CaB_2)C_n$ with $n = 4$ and $n = 6$ have been prepared from calcium hexaboride, calcium carbide and graphite according to $CaB_6 + 2\,CaC_2 + (3n-4)\,C \rightarrow 3\,(CaB_2)C_n$. The synthesis of $Ca_{0.921(2)}B_2C_4$ was optimized towards higher yield and purity. The crystal structure was determined from powder data by Rietveld

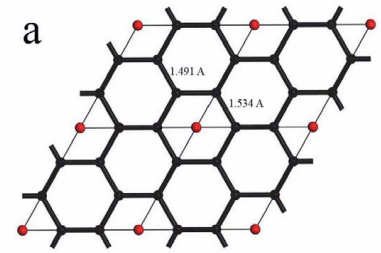

Figure 7: *Crystal structure of CaB_2C_4 in (001) projection. Ca atoms are depicted in red, B and C positions in black.*

analysis (P6/mmm (no.191), $a = 4.5597(1)$, $c = 4.4020(1)$ Å). Distances between Ca and B, C atoms are uniformly of 2.6830(6) Å but the hetero-graphene layer B–C bonds split into 1.534(1) and 1.491(2) Å. This widens the band gap of the intrinsic semiconductor even more. They were also able to optimize the synthesis of $Ca_{0.956}B_2C_6$ towards good yield and pure material. The refinement of the crystal structure (P6/mmm (no. 191), $a = 2.58390(5)$, $c = 4.43597(8)$ Å) shows that distances between Ca and B, C atoms are of 2.6730(6) Å and those in the hetero-graphene layers of 1.49183(3) Å, both a bit smaller than for the Ca–richer compound.

Doping experiments were performed through reaction with gaseous iodine and by hydrolysis with water. CaB_2C_6 is very air sensitive. The compound decomposes within minutes to a black powder while the volume increases drastically. The decomposition product was thoroughly washed with water and examined by

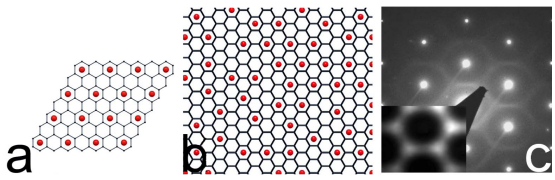

Figure 8: *Results for the simulation of the diffuse scattering (Program DISCUS [21]) as found by electron diffraction of CaB_2C_6. (a) Hypothetical ordered model for the composition CaB_2C_6 leading to superstructure reflections. But electron diffraction along (111) (c) and XRD powder diffraction show diffuse scattering only. Therefore, a disordered model based on (a) was developed, a section of which is shown in (b). (c) The electron diffraction pattern of a crystallite viewed along the [111] direction. The inset shows the simulated diffuse scattering based on this model (intensities at Bragg positions are not shown). Most likely the real crystal is composed of areas where ordered domains according to (a) exist, which exhibit stacking faults, leading to rods of diffuse intensities along the c^*-axis.*

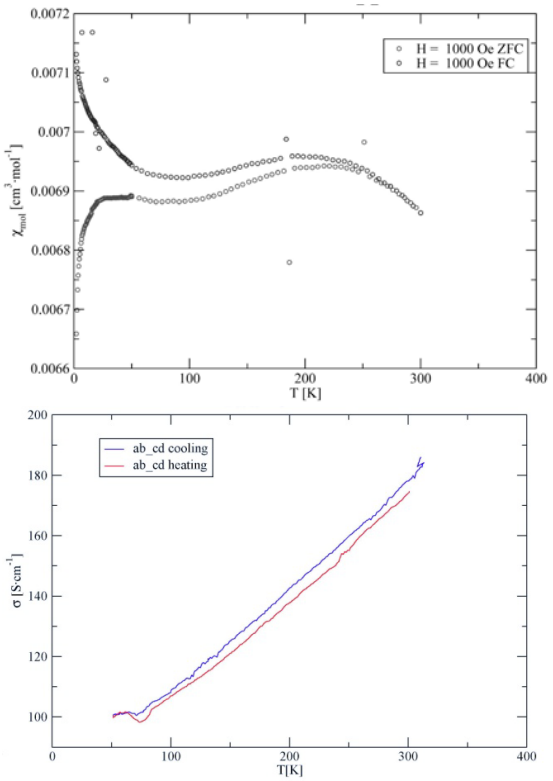

Figure 9: *(left) Magnetic measurement of CaB_2C_6 after treatment with iodine-vapor for 1 h at ambient conditions. The sample shows a history dependent behavior with a relatively high effective magnetic moment of 4.2 μ_B. We attribute the superconducting transition between 9.5 and 9 K to impurities of Nb-borides and -carbides arisen from side reactions with the container. (right) Temperature dependence of the electric conductivity of CaB_2C_6 (pressed powder). The behavior in the high temperature regime is clearly semiconducting with a linear relation to temperature, indicative of a very small band gap.*

transmission electron microscopy. The sample consisted of very thin sheets, which showed no Bragg scattering under electron diffraction. Clearly, loss of calcium must give rise to p-doping of the layers. The magnetic data (Fig. 9) do not show any indication for a superconducting transition of the hetero-graphene material, though.

1.3 Measuring single grains T_c's

A basic investigation of inhomogeneous reactions mixtures resulting from whatever solid-state reaction to produce oxide superconductors necessitates a physical method to i) detect superconductive grains and to ii) determine the T_c of individual grains [4]. Together with a conventional SQUID measurement of the bulk, magnetic separation can provide detailed information on the inhomogeneity of a ceramic sample, i.e. the distribution of T_c among grains

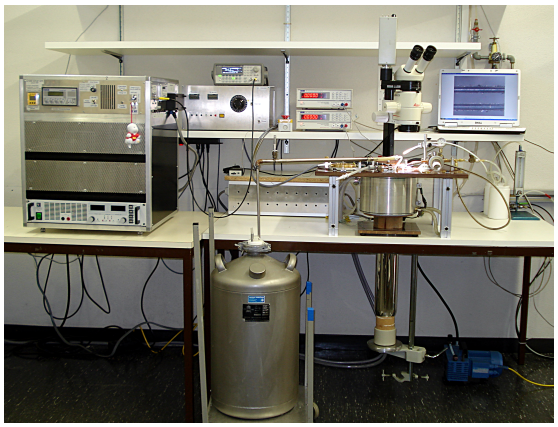

Figure 10: *Entire new set-up for magnetic separation at UniBE.*

as well as it can reveal ferromagnetic impurity phases. Most importantly it allows searching for grains featuring the highest T_c within a material class.

During the last years of MaNEP phase II, the group of J. Hulliger (UniBE) has accomplished a set-up, which allows to perform magnetic separation and measurements of T_c of individual grains as small as optical observation allows for (presently limited to about $d > 10\ \mu$m). Fig. 10 shows the entire set-up, including electronics for controlling field and temperature (all home designed and built). Some details about the performance are the following: max. field amplitude 1200 Gauss, pulse waves up to a frequency of 40 Hz and duty cycle of 85%, temperature range from 80 to 300 K using propane/ethane mixtures or other alkanes, absolute temperature precision $\delta T = 0.5$ K. The sample chamber is temperature controlled and allows observation of grains through a high quality quartz bar. Magnetic action on grains can be taken in two ways: i) by attracting them to a Fe-wire or ii) by moving them on a brass plate with buried Fe-wires.

The plate system (Fig. 11) is particularly suited for sorting superconductive matter from strongly para- or ferromagnetic impurities. Measurement of the $T_c(H)$ for individual grains is preferably done by the plate system and the observation of the torque movement due to a strong $\chi(T, H)$ anisotropy of layered superconductors. The comparison of single grains T_c's measured by SQUID and observation of torsion agreed within experimental error ($\delta T = 0.5$ K).

This was done for Bi-2223 ceramic grains and for a 'single crystal' of Bi-2223 from the group of E. Giannini in Geneva.

The analysis of the single crystal showed the unique strength of the present method. The ob-

Figure 11: *Brass plate with buried Fe-wires for magnetic separation and T_c measurements of small grains. The spring serves for vibrating the plate, thereby distributing grains over the buried wires.*

tained crystal was crashed into smaller pieces. Magnetic separation revealed that not more than about 50% of the volume was Bi-2223 (also Bi-2212 phase was present in this sample). Surprisingly ferromagnetic particles were observed. However, measurements of T_c of small crystallites in the new setup and by SQUID show an agreement of the methods.

In view of the general program of the group in Berne, the Tl-2223 system was analyzed by revisiting procedures of synthesis [22, 23, 24, 25, 26]. Their study has shown the following: i) most published procedures yield only a low fraction of superconducting 2223 phase, ii) the samples are generally very inhomogeneous, i.e. featuring a broad T_c distribution and iii) the number of grains featuring the highest T_c for each particular sample is very low. Among all samples produced by a method described in [22, 23, 24, 25, 26], only a few grains of $T_c = 125$ K were found.

Following the procedure of e.g. reference [22], interesting results from SQUID measurements where obtained. A field dependent diamagnetic contribution up to T about 131 K was found (Fig. 12). In order to compare data collected in different fields, they were normalized by the normal-state magnetization measured at $T = 163$ K. In this case, normal state paramagnetism results in a collapse of $M(T)$ data measured in different fields into a single curve. Divergence between the curves, which may be seen at $T < 131$ K corresponds to a superconducting diamagnetism. Although the critical temperatures of two samples were different, the onset of the diamagnetism occurs at approximately the same temperature.

After annealing the sample (6 days, 1023 K) in evacuated quartz tube, less superconducting phase was present, but an up-shift of the main transition was observed. Additionally a second transition at 115 K appeared (Tl-1234 phase).

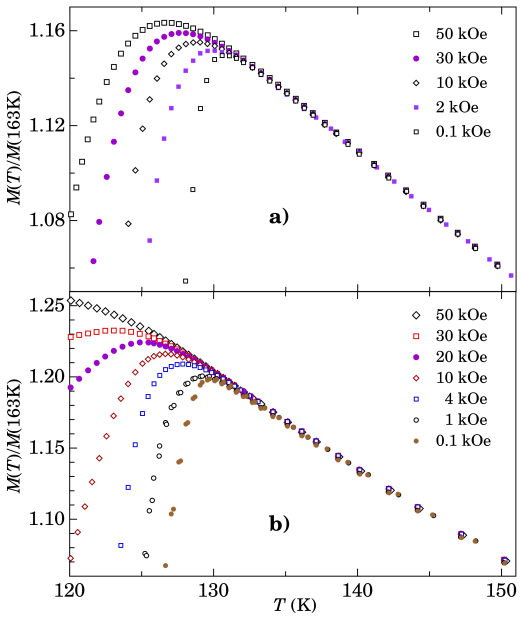

Figure 12: *Magnetization $M(T)$ curves for the samples a) Tl-2223 as synthesized at 1193 K for 3 hours, and b) Tl-2223 annealed at 1023 K for 6 days.*

Powder X-ray diffraction analysis on these samples revealed the presence of Tl-2223 as a majority phase with minor amount of ferromagnetic calcium copper oxide phase. At present, one may conclude that T_c of the Tl-2223 system is not yet properly known. Most likely, very small grains (below 5 to 10 μm) are responsible for a high temperature tail in χ. This agrees with magnetic separation results demonstrating a dying out of the population of grains showing T_c as reported of 125 K. Magnetic AFM studies are planned to investigate sub micrometer grains, because investigation by magneto-optics was limited to a size above a few micrometer [5].

In summary, the development of a chemistry producing intentionally inhomogeneous ceramic reaction mixtures and a very sensitive method to measure the T_c of micrometer sized grains offers new understanding for preparation procedures of cuprate superconductors.

2 Other materials

2.1 Perovskite-type oxynitride thin films by pulsed laser deposition

Investigations on the influence of the gas pulse used in pulsed reactive crossed beam laser ablation (PRCLA), and substrate temperature on

the films composition, crystallinity and properties led to a better understanding and control of the process and in the end to well defined products [27, 28, 29][6].

N-substituted $SrTiO_3$ thin films were deposited by the group of L. Schlapbach (A. Weidenkaff, Empa) in one step by PRCLA with nitrogen or ammonia gas pulses. The nitrogen content in the films deposited by PRCLA with ammonia is 3.5 times higher compared to the corresponding films deposited by classical Pulsed Laser Deposition (PLD). Ammonia is more active for the gas pulse than nitrogen due to the smaller bond energy in the molecule and the reducing behavior of NH_3. The N content in the films grown with ammonia gas pulse increased from 0.8 ± 0.3 to 4.1 ± 0.4 at.% with increasing the substrate temperature in the range of 570 – 720°C. During deposition with the nitrogen gas pulse the influence of the substrate temperature is more complex: in the range of 580 – 650°C the nitrogen concentration increases, while further heating results in a gradual decrease of the N content. All $SrTiO_3$:N films deposited by PRCLA as well as by classical PLD are reduced, i.e. they exhibit anionic deficiency accompanied by formation of Ti^{3+}.

Nitrogen incorporation into the crystal lattice of $SrTiO_3$ results in a change of the electronic structure: the localized N($2p$) levels are formed inside the band gap of $SrTiO_3$:N. The energy of these levels is about -2.7 eV with respect to the Fermi level. This results in the visible light absorption at the wavelength range of 367 – 460 nm, which is not the case for pure strontium titanate. Optical absorption in this region increases gradually with increasing the N content from 0.8 to 4.1 at.% (i.e. when the substrate temperature increases from 570 to 620°C during deposition with the ammonia gas pulse). At the same time, films with higher UV-vis transparency (in the range of 460 – 2000 nm) are obtained at higher substrate temperatures, which is most probably due the lower Ti^{3+} content in the films. Therefore, ammonia gas pulse and high substrate temperatures (above 700°C) are more favorable for deposition of $SrTiO_3$:N films for photocatalytic tests.

The studied films reveal a cubic perovskite-type structure. Deposition on $LaAlO_3$ (LAO) and $SrTiO_3$ (STO) substrates results in perfectly c-axis oriented films, whereas some of the films grown on MgO exhibit small (011) reflections, indicating not perfect out-of-plane orientation due to the relatively large lattice mismatch. For the same reason, mosaicity (in-plain orientation distribution) of the studied $SrTiO_3$:N films increases in the following raw: mosaicity (on STO) $<$ mosaicity (on LAO) $<$ mosaicity (on MgO). This indicates that the epitaxial quality and the number of non zero-order defects (i.e. dislocations, grain boundaries) is the worst in the films grown on MgO. Also films deposited in NH_3 gas pulse reveal a worse epitaxial quality compared to the films grown with nitrogen or in vacuum, i.e. mosaicity (in NH_3) $>$ mosaicity (in N_2) $>$ mosaicity (in vacuum). The epitaxial quality (i.e. in-plane and out-of-plane orientations) of the films is an important characteristic, which has a strong influence on the transport properties, as it will be shown later.

All studied $SrTiO_3$:N films exhibit electronic conductivity due to the presence of Ti^{3+}. The most important parameter affecting the conductivity of the films is their epitaxial quality, which has a great influence on the electron mobility, whereas the film composition (which mainly determines the electron concentration) plays only a secondary role. $SrTiO_3$:N grown on LAO and MgO exhibits semiconductor-like behavior or metal to-semiconductor/insulator transition. Films deposited on MgO substrates have larger mosaicity and, therefore, higher resistivities compared to films on LAO. Among the films grown on one of these substrates (LAO or MgO) the highest epitaxial quality and the lowest resistivity exhibit reference samples deposited in vacuum, followed by the films grown with nitrogen and ammonia gas pulse. Deposition of $SrTiO_3$:N on STO results in partial reduction of the substrate during film growth. The samples behave similar to $SrTiO_{3-\delta}$ single crystals, namely they reveal a metallic behavior of the resistance, and very high electron mobilities up to 10^4 $cm^2V^{-1}s^{-1}$ at temperatures below 10 K. In this temperature range the charge carriers are scattered from the ionized point defects (e.g. anionic vacancies), while at higher temperatures in the range 100 – 300 K electrons scatter from the longitudinal lattice phonons.

Further synthesis procedures were developed to grow successfully $LaTiO_{3-x}N_x$ and $SrMoO_xN_y$ thin films.

For deposition of the films with high nitrogen contents and good crystallinity, the PLD experimental conditions obtained from the model $SrTiO_3$:N system have been used. $LaTiO_{3-x}N_x$ perovskite-type thin films have been successfully grown by PRCLA with ammonia and nitrogen gas pulses. Deposition on MgO substrates yields films with mixed (112) and (001) out-of-plane orientations, whereas films grown on LAO exhibit only a (001) orientation along the c-axis. The N content can be tuned within 0.47 – 0.72 by adjusting the deposition con-

ditions. Ammonia gas pulses yielded films with more incorporated nitrogen. Increasing the substrate temperature in the range of 600 – 700°C resulted in the increase of the N content. The deposited films contain Ti^{3+}. This results in a lowered optical transparency of the films in the wavelength range of 500 – 1000 nm. At the same time, nitrogen incorporation resulted in a considerable decrease of the optical band gap from about 4.0 eV for $LaTiO_{3.5}$ down to about 2.3 – 2.6 eV for the $LaTiO_{3-x}N_x$ oxynitride films. The band gap gets smaller for higher nitrogen content.

$SrMoO_xN_y$ perovskite-type thin films have also been successfully deposited by PRCLA with ammonia and nitrogen gas pulses. As for other systems, ammonia gas pulse yields films with more incorporated nitrogen. Increasing the substrate temperature in the range of 600 – 650°C results in the increase of the N content, whereas further heating above 650°C leads to the film phase decomposition. The N content can be varied from 0.54 to 1.07, while the oxygen content ranges within 1.50 – 2.30 depending on the deposition conditions. Deposition on MgO substrates yields predominantly (011)–oriented films with some mixture of the (001) orientation. Films grown on LAO exhibit a predominant (001) orientation along the *c*-axis. Electrical characterization of the films is now in progress. The preliminary results reveal semiconductor-like type of conductivity in the samples.

2.2 Field induced resistance switching

The novel perovskite-type materials prepared by plasma assisted anionic substitutions show diverse interesting physical properties such as optical band gap reduction, photocatalytical activity, superconductivity and good thermoelectric properties (see also former MaNEP reports). Furthermore, resistance switching properties were investigated for the electronics application field by the Schlapbach group (Empa).

A memristor is a new electronic component besides capacitor, inductor and resistor. It exhibits a bistable resistance switching behavior. The "bistablity" of the memristor is characterized by two non-volatile resistance states, a high resistance state (HRS) and a low resistance state (LRS) denoting '0' and '1', respectively. In a typical configuration the memristor is a sandwich where a transition metal oxide is placed between two metal electrodes. In order to obtain bistable hysteretic $I-V$ behavior, voltages high enough for a resistance change (electroformation) have to be applied (typically reduction of resistance by orders of magnitude). In contrast, the $Al/SrTiO_{3-x}N_y/Al$ system reveals a much faster "electroformation". Here only one $I-V$ loop corresponding to 10 sec yield in high enough max voltage while published data for $SrTiO_3$:Cr are 8 hours. It was found that bistable (non-volatile) resistance switching develops at one of the Al electrodes used as anode and that the temperature of the $Al/SrTiO_{3-x}N_y$ anode interface rises to max. 210°C.

The local structure of the samples was investigated by transmission electron microscopy (TEM). The studies revealed that the samples with stacking fault show better switching properties compared to samples without stacking faults which can be related to differences in ion conductivity considering a memristor as a mixed-ionic-electronic-conductor (MIEC). Negligible degradation of the resistive states over the 106 sec time reveals good retention properties of the $Al/SrTiO_{3-x}N_y/Al$ system The ratio between high resistance and low resistance states of typically 2 to 10 decreases after 104 cycles.

2.3 Synthesis of diluted magnetic semiconductors

The science of spin electronics – spintronics [30, 31] – is based on a notion of a diluted ferromagnetic semiconductor [32], a material that merges widespread application of a semiconductor with ferromagnetic properties at room temperature. A ferromagnetic material at room temperature can serve as a reservoir of spins that can have their spin projection value modified by an applied electric field, a principle of spin-FET [33] or spin-LED diode [34]. The underlying theory based on the modified Zener model was developed by Dietl *et al.* [35] and Ohno *et al.* [36] predicting that the nominally antiferromagnetic diluted magnetic semiconductors (DMS) can become ferromagnetic in Transition Metal (TM) doped (II-VI) and (III-V) semiconductors (GaN and ZnO) with the excess of *p* carriers. The theory was extrapolated for *n*-type materials through the work of Coey *et al.* [37] by the introduction of the concept of shallow donor electrons that form bound magnetic polarons, which overlap to create a spin-split impurity band. The Achilles heel of the field of DMS-spintronics is a noticed lack of reproducibility [38]. The need for a quick, low-cost synthesis that produces room temperature ferromagnetic materials in a reproducible manner is therefore present.

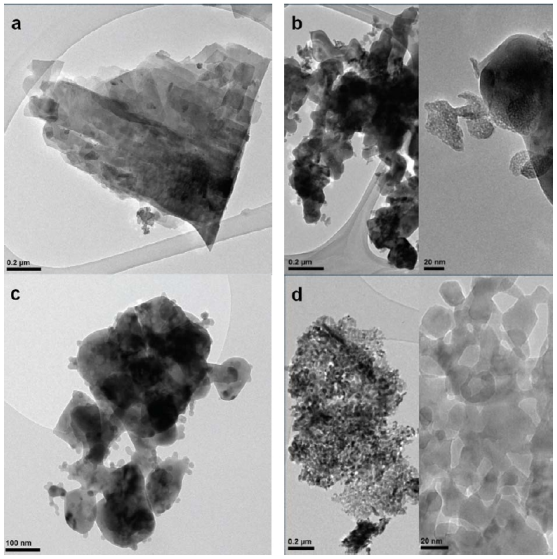

Figure 13: *(a) The Mn:hydrozincite precursor; (b) 200°C – Mn rich phases in the shape of fine particulate clusters; (c) 700°C – Mn rich phases in the shape of single crystal nodules; (d) decomposition under air at 400°C produces purely Mn-doped ZnO phase with grains around 20 nm in diameter.*

a) *Synthesis* The optimal synthesis parameters for the synthesis of $Zn_{1-x}Mn_xO$ $0.012 < x < 0.02$ samples were found to be the usage of hydrozincite precursors $(Zn_{1-x}Mn_x)_5(OH)_{6-2n}(CO_3)_{1+n}$, followed by their heat-treatment under forming gas N_2–H_2 at 400°C (HZ method). Temperatures other than 400°C induced formation of other phases, visible under TEM (Fig. 13). The hydrozincite precursors are made hydrothermally by the group of Forró (EPFL) at 125°C for 24 hours from stoichiometric mixture of Mn nitrate, Zn nitrate and urea, $CO(NH_2)_2$.

The $Zn_{1-x}Mn_xO$ $0.02 < x < 0.08$ phases have been alternatively synthesized by the decomposition of the melt-quenched stoichiometric mixture of Mn and Zn nitrates (N method). The NO_2 species coproduced during this particular synthesis are oxidative enough to invoke oxidation of Mn into higher oxidation states than 2+. This in turn causes the formation of a phase isomorphic to $ZnMnO_3$ which has only recently been identified by Blasco *et al.* [30] to be a cubic spinel $Mn_{3-x}Zn_xO_4$ $1.55 < x < 1.72$. The authors synthesized the material using low temperature ($T < 650$°C) synthesis. They have synthesized the $Mn_{3-x}Zn_xO_4$ phase by decomposition of the stoichiometric melt-quenched 1:1 Mn:Zn nitrate mixture in oxygen and it's further post-annealing under oxygen flow at 400°C for 11 hours.

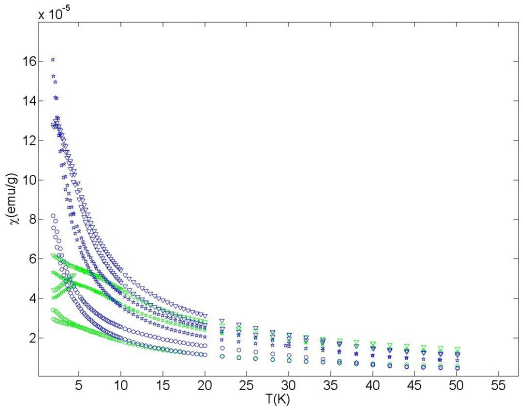

Figure 14: *Magnetic susceptibility at applied field of $H_{applied} = 1000$ Oe for $x = 0.012$ (circles), $x = 0.017$ (stars) and $x = 0.02$ (downward pointing triangles) of $Zn_{1-x}Mn_xO$, prepared from nitrate (green) and hydrozincite (blue) precursors.*

b) *Magnetic properties* The zero-field cooled – field cooled (ZFC – FC) measurements were performed using a SQUID magnetometer. The scans on $Zn_{1-x}Mn_xO$ $0.012 < x < 0.02$ made by both the HZ and N methods are given in Fig. 14. The samples produced by HZ method (blue) show properties strongly dependent on the atmosphere of the synthesis – the samples produced in forming gas, N_2-H_2, show ferromagnetism below 35 K, while the samples produced in air atmosphere did not show the ferromagnetic transition. This indicates the intrinsic nature of the ferromagnetism observed in these materials, most probably related to the oxygen vacancy content. Furthermore, the samples produced by N method (green) show ZFC – FC splitting at 5 K due to the presence of the $Mn_{3-x}Zn_xO_4$ phase. The presence of this phase was confirmed by TEM. To ascertain whether the small quantity of the parasitic phase is the one causing splitting at 5 K we have measured the magnetic properties of the $Mn_{3-x}Zn_xO_4$ using SQUID. The resulting material had the splitting at 5 K and a Curie-Weiss constant of -45 K (antiferromagnetic interactions). They have hence demonstrated fundamental differences in the magnetic behavior of the two sets of samples depending on the presence of second phases and the atmosphere in which the syntheses were performed.

Room temperature electron spin resonance (ESR) measurements of the N samples and HZ samples can provide an information on the local environment of the TM ions, providing that they are spin active. Mn^{2+} has a half-filled $3d$ shell, with a high spin $S = 5/2$ configuration and the orbital angular momentum $L = 0$. In the simplest picture, when

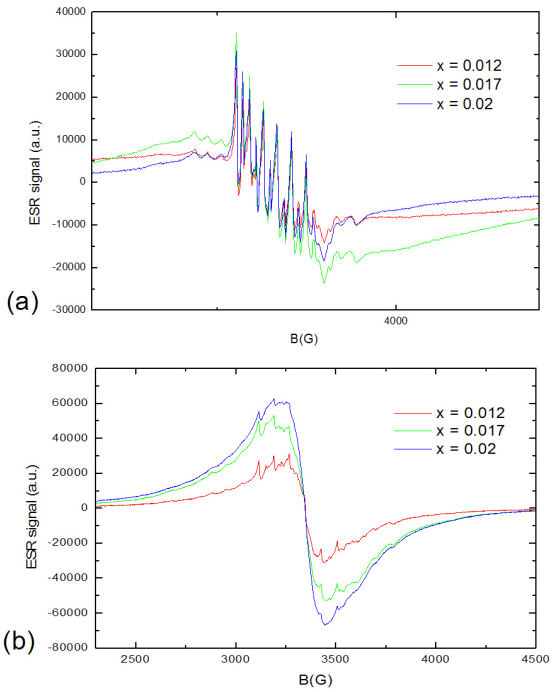

Figure 15: *Electron spin resonance measurements performed on $Zn_{1-x}Mn_xO$, $x = 0.012$ (red), $x = 0.017$ (green), $x = 0.02$ (blue) made by (a) N method and (b) HZ method.*

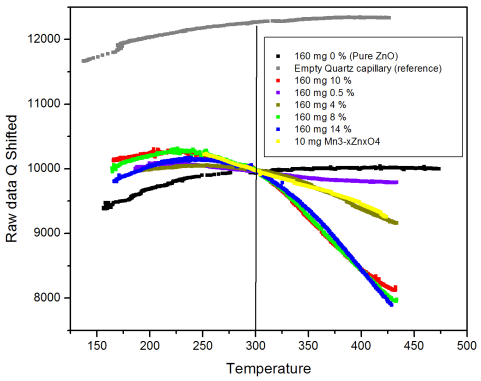

Figure 16: *Microwave conductivity on the $Zn_{1-x}Mn_xO$ made by the N method. The grey line is the reference signal of the empty cavity. The color-concentration correspondence is the following: $x = 0$ (undoped ZnO) – black, $x = 0.05$ – purple, $x = 0.04$ – army green, $x = 0.08$ – green, $x = 0.1$ – red, $x = 0.14$ – blue, $Mn_{3-x}Zn_xO_4$ – yellow.*

placed in magnetic field, the sixfold degeneration of the Mn^{2+} ground state is lifted resulting with five possible electronic transition energies. This is known as the fine structure. The electron-nucleus ($I = 5/2$) interaction further lifts the $(2I + 1)$ degeneracy of each of the 6 lines. Hence an isolated Mn^{2+} in the Zn site in ZnO in an ESR experiment will show 30 lines. In powder samples, due to the spatial distribution of magnetization easy-axes in the samples the signal can be somewhat more complex.
For the same concentrations x of Mn in the $Zn_{1-x}Mn_xO$ HZ and N samples, Forró's group has observed the smeared out hyperfine structure in the case of the HZ samples, and a non-smeared out hyperfine structure in the case of the N samples (Fig. 15). The difference is attributed to an increase in "communication" between the Mn^{2+} ions in the HZ samples, finally leading to the paramagnetic-ferromagnetic transition at 35 K.

c) *Electronic properties* The nature of magnetism in diluted magnetic semiconductors is closely related to the energy band scheme of the host semiconductor heavily influenced by doping with TM ions. In $Zn_{1-x}Mn_xO$ we do not expect net doping in the material "properly" doped with Mn, i.e. with Mn replacing Zn on Zn sites (substitutional Mn). In that case $Zn[3d^{10}4s^2] \rightarrow Mn\ [3d^5 4s^2]$. The *d* electrons are localized and do not contribute to conductivity. Forró's group has performed microwave conductivity measurements using a conventional X-band ESR spectrometer with the possibility of heating the sample. The quality factor of the cavity Q is directly proportional to the grain resistivity of the powder sample within the cavity. Hence the $Q(T)$ curves are analogous to the $R(T)$ grain resistivity curves of polycrystalline ZnO. The results for samples made by the N method are shown on Fig. 16.
A semiconducting nature of the $R(T)$ is confirmed with R decreasing with increasing T. A strong increase in conductivity in the $Zn_{1-x}Mn_xO$ has been measured for $0.005 < x < 0.1$ samples. The experiment was repeated with $Mn_{3-x}Zn_xO_4$ synthesized as described in the synthesis section. The $Mn_{3-x}Zn_xO_4$ (yellow curve) with mass $m(Mn_{3-x}Zn_xO_4)$ being equal to $\sim$ 6.25% of the mass of $Zn_{1-x}Mn_xO$ powders (all the other colors except grey) induced the same order of magnitude conductivity increase as in $Zn_{1-x}Mn_xO$ with $x = 0.04$. This points out that $Mn_{3-x}Zn_xO_4$ is the phase responsible for the conductivity increase in $Zn_{1-x}Mn_xO$. Independently, no increase in conductivity was measured for HZ samples produced in air, which fits well with the former assertion.

2.4 Doping studies on Sr_2VO_4:

In the collaborative project between the groups of J. Hulliger (UniBE) and D. van der Marel (UniGE), Sr_2VO_4 was successfully synthesized

using the conventional solid-state route starting from $SrCO_3$ and V_2O_5 at 1073 K to form $Sr_4V_2O_9$, with intermittent grindings. $Sr_4V_2O_9$ was then reduced without metallic zirconium under pure hydrogen flow at 1273 K to form Sr_2VO_4. The purity was confirmed by powder X-ray diffraction. The SQUID measurements displayed a ferromagnetic transition for Sr_2VO_4 at around 10 K, in contrast to the earlier reports of an anti-ferromagnetic transition [39].

Furthermore, reactions were carried out to prepare doped ceramic samples of Sr_2VO_4. Isovalent ions were selected to replace for V^{4+} and heterovalent sodium for Sr^{2+} at similar reaction conditions. The elements explored were 5%, 10% Ti^{4+}; 5%, 10% Ge^{4+}; 5%, 10% Sn^{4+} and 5%, 10% Na^{1+}.

No substantial shift was observed in the X-ray diffractograms of the doped samples as compared to pure Sr_2VO_4. The magnetic transition of the Na doped sample remained unchanged. This affirms the rigidity of this phase to incorporate any element in the parent structure. Possibly, high-pressure experiments may facilitate to form doped ceramic samples of Sr_2VO_4. In essence, no indication for a strong change in the conductivity was found.

3 Collaborative efforts

As mentioned in last report, the collaborations within MaNEP involving members of Project 4 are the following: (i) Hulliger and Karpinski cooperate in the field of high pressure syntheses, (ii) Nesper and Flükiger work on MgB_2 wire formation, (iii) Nesper and Fischer cooperate on the development of sensor materials. The new collaboration between van der Marel and Hulliger gave the first results, as mentioned in section 2.4.

MaNEP-related publications

[1] Z. Bukowski, S. Weyeneth, R. Puzniak, P. Moll, S. Katrych, N. Zhigadlo, J. Karpinski, H. Keller, and B. Batlogg, *to be published in* Physical Review B (2009).

[2] I. S. Costanza, Synthesis and Structures of Selected Layered Materials, and their Magnetic and electrochemical Properties, Ph.D. thesis, ETH-Zürich (2006).

[3] D. Widmer, Hochdruck- und Hochtemperatur-Reaktionen von Boridcarbiden und Boridnitriden, Ph.D. thesis, ETH-Zürich (2007).

► [4] J. B. Willems, D. Pérez, G. Couderc, B. Trusch, L. Dessauges, G. Labat, and J. Hulliger, Solid State Sciences **11**, 162 (2009).

► [5] J. B. Willems, J. Albrecht, I. L. Landau, and J. Hulliger, Superconductor Science & Technology **22**, 045013 (2009).

[6] F. La Mattina, Insulator-to-metal Transition and Resistive Memory Switching in Cr-doped $SrTiO_3$: Charge-transfer Processes Involving the Cr Ions, Ph.D. thesis, University of Zurich (2008).

Other references

[7] J. Nagamatsu, N. Nakagawa, T. Muranaka, Y. Zenitani, and J. Akimitsu, Nature **410**, 63 (2001).

[8] H. Rosner, A. Kitaigorodsky, and W. E. Pickett, Physical Review Letters **88**, 127001 (2002).

[9] A. Bharathi, S. J. Balaselvi, M. Premila, T. N. Sairam, G. L. N. Reddy, C. S. Sundar, and Y. Hariharan, Solid State Communications **124**, 423 (2002).

[10] A. M. Fogg, J. B. Claridge, G. R. Darling, and M. J. Rosseinsky, Chemical Communications **12**, 1348 (2003).

[11] Y. Nakamori and S. I. Orimo, Journal of Alloys and Compounds Letters **L7**, 370 (2004).

[12] A. M. Fogg, J. Meldrum, G. R. Darling, J. B. Claridge, and M. J. Rosseinsky, Journal of the American Chemical Society **128**, 10043 (2006).

[13] A. M. Fogg, G. R. Darling, J. B. Claridge, J. Meldrum, and M. J. Rosseinsky, Philosophical Transactions of the Royal Society A **366**, 55 (2008).

[14] A. K. Verma, P. Modak, D. M. Gaitonde, R. S. Rao, B. K. Godwal, and L. C. Gupta, Europhysics Letters **63**, 743 (2003).

[15] T. Mori and E. Takayama-Muromachi, Current Applied Physics **4**, 276 (2004).

[16] N. Emery, C. Herold, M. d'Astuto, V. Garcia, C. Bellin, J. F. Mareche, P. Lagrange, and G. Loupias, Physical Review Letters **95**, 087003 (2005).

[17] T. Breant, D. Pensec, J. Bauer, and J. Debuigne, Comptes rendus hebdomadaires des séances de l'Académie des Sciences. Série C **287**, 261 (1978).

[18] B. Albert and K. Schmitt, Inorganic Chemistry **38**, 6159 (1999).

[19] L. Y. Markovskii, N. V. Vekshina, and G. F. Pron, in *High Temperature Inorganic Compounds*, G. V. Samsonov, ed. (Kiev, 1965), p. 547.

[20] L. Y. Markovskii and N. V. Vekshina, Zhurnal Prikladnoi Khimii **37**, 2126 (1964).

[21] T. Proffen and R. B. Neder, Journal of Applied Crystallography **30**, 171 (1997).

[22] C. C. Torardi, M. A. Subramanian, J. C. Calabrese, J. Gopalakrishnan, K. J. Morrissey, T. R. Askew, R. B. Flippen, U. Chowdhry, and A. W. Sleight, Science **240**, 631 (1988).

[23] S. S. P. Parkin, V. Y. Lee, E. M. Engler, A. I. Nazzal, T. C. Huang, G. Gorman, R. Savoy, and R. Beyers, Physical Review Letters **60**, 2539 (1988).

[24] G. M. Phatak, R. M. Iyer, K. Gangadharan, R. M. Kadam, P. V. P. S. S. Sastry, M. D. Sastry, and J. V. Yakhmi, Bulletin of Materials Science **14**, 241 (1991).

[25] A. Maignan, C. Martin, V. Hardy, C. Simon, M. Hervieu, and B. Raveau, Physica C **219**, 407 (1994).

[26] K. Kawano, T. Takao, K. Hirano, and T. Kimura, Journal of the Society of Inorganic Materials, Japan **7**, 117 (1994).

[27] D. S. Jeong, H. Schroeder, U. Breuer, and R. Waser, Journal of Applied Physics **104**, 123716 (2008).

[28] R. J. D. Tilley, *Defects in Solids* (Hoboken, N.J.: Wiley, 2008).

[29] I. Riess, Journal of Electroceramics **17**, 247 (2006).

[30] J. Blasco and J. García, Journal of Solid State Chemistry **179**, 2199 (2006).

[31] I. Žutić, J. Fabian, and S. Das Sarma, Reviews of Modern Physics **76**, 323 (2004).

[32] J. Furdyna and J. Kossut, *Diluted Magnetic Semiconductors*, vol. 25 of *Semiconductors and Semimetals* (Academic Press, 1988).

[33] S. Datta and B. Das, Applied Physics Letters **56**, 665 (1990).

[34] R. Fiederling, M. Keim, G. Reuscher, W. Ossau, G. Schmidt, W. A., and M. L. W., Nature **402**, 787 (1999).

[35] T. Dietl, H. Ohno, F. Matsukura, J. Cibert, and D. Ferrand, Science **287**, 1019 (2000).

[36] H. Ohno, Science **281**, 951 (1998).

[37] J. M. D. Coey, M. Venkatesan, and C. B. Fitzgerald, Nature Materials **4**, 173 (2005).

[38] J. M. D. Coey, Current Opinion in Solid State and Materials Science **10**, 83 (2006).

[39] M. Cyrot, B. Lambert-Andron, J. L. Soubeyroux, M. J. Rey, P. Dehauht, F. Cyrot-Lackmann, G. Fourcaudot, J. Beille, and J. L. Tholence, Journal of Solid State Chemistry **85**, 321 (1990).

Project 5 Thin films, artificial materials and novel devices

Project leader: J.-M. Triscone (UniGE)

Participating members: P. Aebi (UniNE and UniFr), Ø. Fischer (UniGE), D. van der Marel (UniGE), A. Morpurgo (UniGE), P. Paruch (UniGE), A. Schilling (UniZH), J.-M. Triscone (UniGE).

Highlights: Ultrathin $PbTiO_3$ ferroelectric films have been studied using X-ray photoemission spectroscopy. It is shown that changes in the surface/contamination layer induce modifications in the core level energy shifts, highlighting the complexity of the screening mechanism at ferroelectric surfaces. It is also shown that a one unit cell thick $PbTiO_3$ film is pyroelectric. In $PbTiO_3/SrTiO_3$ superlattices, it is found that the ferroelectric properties can be tuned. At short wavelength, a new type of improper ferroelectricity is observed. Domain walls in multiferroic $BiFeO_3$ have been investigated using piezoforce microscopy. A dynamic different from the one observed in ferroelectric $Pb(Zr,Ti)O_3$ is found as well as an in-plane piezoresponse due to the domain wall itself. In $EuTiO_3$ ceramics, a very large Faraday rotation is observed due to a magnetic circular dichroism for magnetic excitations. In manganite/ferroelectric structures, a charge mediated direct electric field control of the magnetization has been achieved.

Summary and highlights

Photoemission from oxide surfaces – finite size effects (*P. Aebi, J.-M. Triscone*)

Using the chemical sensitivity of X-ray photoemission spectroscopy and the angular intensity distribution of core level emission lines, ultrathin ferroelectric $PbTiO_3$ films grown on Nb-$SrTiO_3$ have been studied at the atomic scale. As a function of film thickness, the tetragonality of the films (related to the polarization via polarization-strain coupling) evolves in the same way as energy shifts in the photoemission core level emission lines, suggesting an identical origin of the energy shifts.

Since the standard electrostatic model for the potential drop accross a screened ferroelectric film with the substrate as bottom electrode and the surface/contamination-layer as top electrode under short circuit boundary conditions results in exactly the opposite sign of the shift (in contradiction with the above suggestion), we have investigated the influence of top-electrode-modification and temperature on the tetragonality and core level energy shifts.

We find that the core level energy shifts exhibit a complicated behavior as a function of surface/contamination-layer modification suggesting an important role of charge states at the surface. However, the behavior of the tetragonality with temperature appears to be in agreement with what is expected from the temperature dependence of the polarization.

Artificially layered ferroelectric superlattices: tailored properties and "new" ferroelectricity (*J.-M. Triscone*)

We have explored the properties of ferroelectric/paraelectric $PbTiO_3/SrTiO_3$ superlattices. We find for relatively thick individual layers that the critical temperature T_c and the polarization P can be tuned and predicted using a simple electrostatic model. The key parameter controlling T_c and P is the $PbTiO_3$ volume fraction. For very thin layers, one or a few unit cells thick, a new type of improper ferroelectricity has been observed which reflects a very unusual coupling of antiferrodistortive and polar modes. We also find that the polarization becomes very unstable for short wavelength superlattices when prepared on $SrRuO_3$ electrodes. The use of interfaces to allow for order parameter coupling is a promising route to the design of new functionalities.

Nanoscale studies of domains and domain walls in ferroelectric and multiferroic materials (*P. Paruch*)

We study the static and dynamic behavior of ferroelectric domain walls, both as a useful model system for elastic interfaces in disordered media, and to understand domain switching and stability at the nanoscopic scales required by current and future technological applications. Piezoresponse force microscopy (PFM) studies of domain walls in multiferroic $BiFeO_3$ thin films have shown increased roughening and slower dynamic response compared to domain walls in pure ferroelectric materials

such as $Pb(Zr_{0.2}Ti_{0.8})O_3$. We have studied the effects of domain walls on in-plane and out-of-plane PFM signals in this material, which show a clear signature in phase and amplitude of d_{35} coupling. We are currently working on ultrahigh-vacuum, variable temperature measurements of domain walls in the two systems.

Spin-lattice coupling and magnetic circular dichroism of $EuTiO_3$ (*D. van der Marel*)

The tight proximity of $EuTiO_3$ to both a ferroelectric ordered state and a ferromagnetic ordered state makes it a promising candidate in the quest for magneto-electrics and multiferroics which are interesting materials for future applications.
The THz transmission of ceramic $EuTiO_3$ has been determined for energies between 0.15 and 2.5 meV, between 3.0 K and 300 K and in magnetic fields up to 1.65 T. Our data show a gigantic Faraday rotation of 170° per tesla per mm of the THz light which is due to a magnetic circular dichroism for *magnetic* excitations within the Zeeman split Eu $4f$ levels. In addition, we find that $EuTiO_3$ has a prominent spin-lattice coupling manifested by the ferroelectric soft mode dependence on the magnetic order.

Nano-electronics with novel materials (*A. Morpurgo*)

Last year we have worked on the installation of new nano-fabrication facilities (electron-beam lithography and electron-beam evaporation), an important step for the development of nano-electronics with novel materials.

Magnetoelectric effects in complex oxides with competing ground states (*J.-M. Triscone*)

We have used ferroelectric/manganite $Pb(Zr_{0.2}Ti_{0.8})O_3/La_{0.8}Sr_{0.2}MnO_3$ bilayers to obtain large, charge controlled, magnetoelectric effects. Switching the ferroelectric polarization produces a change in carrier density in the thin $La_{0.8}Sr_{0.2}MnO_3$ channel, modifying the magnetic properties of the manganite layers. *E-M* loops are obtained demonstrating directly the electric field control of the magnetization.

Superconducting nanostructures and single-photon detectors (*A. Schilling*)

In the report period we have successfully continued the development of our nano-lithography process. Applying this process to a 5 nm thick NbN-film we have produced single-photon detectors with varying strip widths. The detectors have quantum efficiencies up to about 9% and intrinsic detection efficiencies $>$ 65%.

Patterning of YBCO thin films for SSPDs applications (*Ø. Fischer*)

With the aim of manufacturing high-T_c superconducting single-photon detector (SSPD), we grew 12 nm thick YBCO films and patterned 500 nm wide structures, gaining a downscaling factor of 4 as compared to last year's best performances. A dipstick was also designed and built to carry out optical characterization.

1 Photoemission from oxide surfaces – finite size effects (P. Aebi, J.-M. Triscone)

1.1 Introduction

The thin, single crystalline, *c*-axis oriented $PbTiO_3$ (PTO) perovskite films used here, were grown and characterized by X-ray diffraction (XRD) in Geneva [1]. We apply photoemission based, surface sensitive and atom specific spectroscopy, i.e. X-ray photoemission (XPS) and X-ray photoelectron diffraction (XPD), to these, only a few unit cells thick, epitaxial films to probe the important question of finite size effects in ferroelectrics [2, 3].

In the past the evolution of the tetragonality (c/a ratio) as a function of film thickness has been measured, showing the same evolution for bulk sensitive XRD [1] and surface sensitive XPD [4]. The fact that the XPD c/a ratio is larger than the one from XRD is not explained so far. For thicknesses not accessible with XRD, the XPD measurement shows a continuous decrease of tetragonality down to the thickness of one unit cell implying, via the polarization-strain coupling, that the films have a finite – progressively reduced – spontaneous polarization.

At the same time XPS measurements have shown energy shifts for the core level photoemission lines of the PTO films as a function of thickness. Such shifts are related to changes of the electrostatic potential of the films (band bending, charging states). It was striking to see that the evolution was identical to the one observed for the tetragonality suggesting to link the shifts to the electrostatic potential drop created by the ferroelectric polarization across the screened ferroelectric films depending on

the particular electrodes and their screening lengths. However, it appears that the standard model of continuous ferroelectricity gives an energy shift of opposite direction. Therefore, in order to learn more about the origin of these effects, several parameters of the system were varied.

Two main approaches were followed during the past year, namely measurements to investigate the influence of electrode composition and temperature.

1.2 Electrode dependence

As part of the electrostatic potential system, the electrodes play a significant role in stabilizing and enhancing the ferroelectricity inside the film. To test the effects of changes made to the electrode, multiple approaches were used.

In the past, the bottom electrode was changed between Nb-$SrTiO_3$ and $SrRuO_3$ and the top electrode was removed completely using a plasma treatment. Since the effect of the application of plasma is not entirely clarified, e.g. with respect to film damaging, a different approach was now chosen to manipulate the electrode. The film's top electrode was modified *ex situ* by a heating procedure in an organic solvent. This leads to an increase and change of the surface/contamination-layer (top electrode). The measurement with X-rays leads to a slight increase of the sample temperature, resulting in a desorption process within the electrode. A continuous shift of the core level energies to higher binding energies during this desorption is observed. The question whether the tetragonality changes with the shift of the core levels could not be answered since the desorption process takes place at the same time scale as the diffraction measurement.

To test the liability of the short circuit boundary conditions under UHV conditions, a thick film of $PbTiO_3$ is cooled to 20 K while argon is adsorbed on its surface to form an Ar film. At the same time an Ar film is formed on the Cu sample holder next to the $PbTiO_3$. The comparison of the core level energies of the Ar $2p$ orbital of the film on $PbTiO_3$ and the one on copper showed a significant shift to lower binding energy on Cu, indicating that the Ar films are not on the same potential and questioning the short circuit boundary conditions of the ferroelectric system.

However, in general, since the photon penetration depth is much larger than the electron escape depth, we have to consider that charges through direct photoemission and through secondary electrons are injected between neighboring layers with a rate that is certainly material dependent. Therefore, we may have to deal with a *dynamical* equilibrium of charges leading to a particular value of the electrostatic potential.

1.3 Temperature dependence

In general, ferroelectrics display a temperature dependence of their polarization, called pyroelectriciy, which is comparable to the Curie-Weiss behavior for ferromagnets. At a critical temperature (T_c), the system undergoes a second order phase transition at which, due to kinetic excitations of phonons, the polar distortion inside the unit cell is reduced to zero. The T_c for thin films is strongly dependent on the film's thickness. Films with a thickness larger than 100 Å have a transition temperature close to the bulk value, whereas the T_c for thinner films shows a significant drop of several hundred Kelvin, with an extrapolation indicating a limit of two unit cells for a pyroelectric ground state [15].

The presence of pyroelectricity does not necessarily signify the presence of ferroelectricity whereas the absence of pyroelectricity rules out the possibility of a ferroelectric ground state. Therefore, the critical thickness of pyroelectricity gives a lower limit for the critical thickness for ferroelectricity.

With the help of XPD measurements, the relative change in lattice tetragonality between a thick (297 Å) and a thin (4 Å) $PbTiO_3$ film on Nb-$SrTiO_3$ was compared upon cooling.

The thick sample shows a room temperature tetragonality close to the expected value of bulk $PbTiO_3$ [4] and a slight increase during cooling.

The results of the one unit cell film measurements indicate a stronger change of the unit cells tetragonality (Fig. 1, top). This suggests the presence of pyroelectricity in films as thin as one unit cell and a T_c which is lower than for the 297 Å film. The diffraction pattern of the film's substrate was also measured as a reference. It shows no sign of a temperature dependence (Fig. 1, bottom) strengthening the argument for a pyroelectric nature of the film.

What is necessary to do now is to establish the precise behavior of the tetragonality with temperature in order to see wether a T_c can be determined. This would then allow us to study T_c as a function of thickness down to the unit cell level.

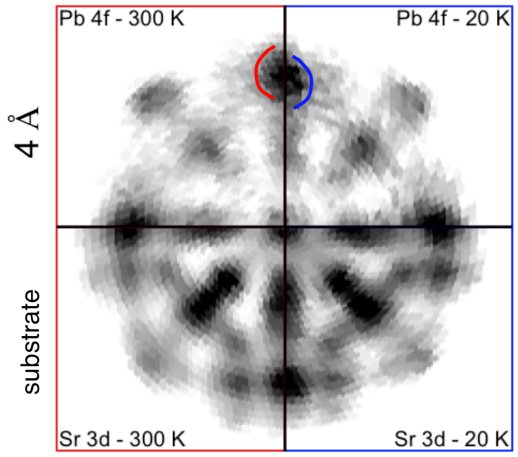

Figure 1: *Pb 4f photoelectron diffraction patterns from a 4 Å thick $PbTiO_3$ film on Nb-$SrTiO_3$ at 300 K and 20 K (top left and right, respectively). Sr 3d photoelectron diffraction pattern from the Nb-$SrTiO_3$ substrate below the 4 Å thick $PbTiO_3$ film at 300 K and 20 K (bottom left and right, respectively). High intensities are in black and low intensities in white. The center of the plot represents the normal emission direction whereas the border of the pattern approaches grazing emission. Black, high intensity maxima represent forward focusing maxima representative for atom-atom directions. Note that the topmost maximum of the Pb 4f emission pattern is contracting towards normal emission while going from 300 K to 20 K (red and blue markers), indicating an increase of the c/a ratio with lowering the temperature.*

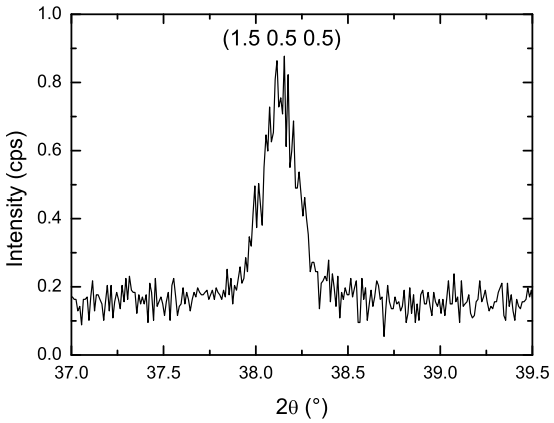

Figure 2: *X-ray scan around the (1.5 0.5 0.5) reflection (with respect to the pseudocubic perovskite unit cell), showing a peak and confirming the doubling of the unit cell in-plane in a 2/2 superlattice on $SrTiO_3$.*

2 Artificially layered ferroelectric superlattices: tailored properties and "new" ferroelectricity (J.-M. Triscone)

Artificial superlattices and complex heterostructures are exciting systems where one hopes to develop controlled properties and/or new functionalities. Here we have studied $PbTiO_3/SrTiO_3$ superlattices and discovered that, in this a priori simple combination of paraelectric and ferroelectric materials, the properties can be tuned over a wide range of thicknesses, but also that, for short wavelength superlattices, a new type of ferroelectricity arises at the interfaces.

Experimentally we have developed the ability to produce superlattice structures of high crystalline and surface quality. We have demonstrated that the key ferroelectric parameters, polarization and critical temperature, can be tuned over a very wide range. Polarization can be varied on demand from $0 - 60\mu C/cm^2$ and the transition temperature from room temperature to 700°C, while maintaining a perfect crystal structure and low leakage currents in these heterostructures [5, 6]. Furthermore, we developed a simple model based on Landau theory that would guide straightforward production of samples with ferroelectric properties designed for particular applications. As electrostatic considerations force the two materials in the superlattice to have near identical polarizations, the $PbTiO_3$ volume fraction, $x = l_p/(l_p + l_s)$, where l_p and l_s are the thicknesses of the $PbTiO_3$ and $SrTiO_3$ layers respectively in the superlattice, is the key parameter in controlling the properties of the system.

For short wavelength superlattices, however, we have discovered a different behavior with striking "ferroelectric" properties: a polarization that evolves linearly in temperature and a dielectric constant that does not diverge at T_c. *Ab initio* calculations performed in the group of P. Ghosez in Liège have allowed us to show that this anomalous behavior is a signature of improper ferroelectricity (the polarization is not the main order parameter) driven by a very special coupling of three instabilities, two antiferrodistortive and one polar mode [7].

The new properties of these artificial materials, in particular the high and temperature independent dielectric constant, might be interesting for applications. Oxide superlattices also provide a new approach to designing material properties by the coupling of instabilities at interfaces. Such interface engineering might be another way of realizing new ferroelectrics and multiferroic materials.

Structural measurements employing X-ray diffraction have also played a central role in identifying the microscopic mechanism of improper ferroelectricity. The antiferrodistortive instabilities at the interfaces lead to unit cell doubling, thus producing weak diffraction

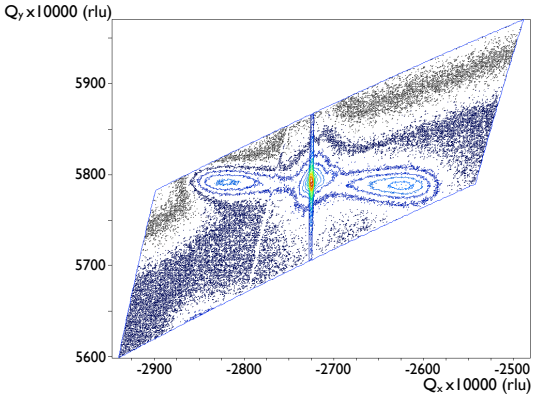

Figure 3: *Reciprocal space map around the (-113) superlattice reflection showing a sharp Bragg peak and two broad satellite features due to ferroelectric stripe domains. Domain structure can provide invaluable information about surface boundary conditions and interlayer electrical coupling.*

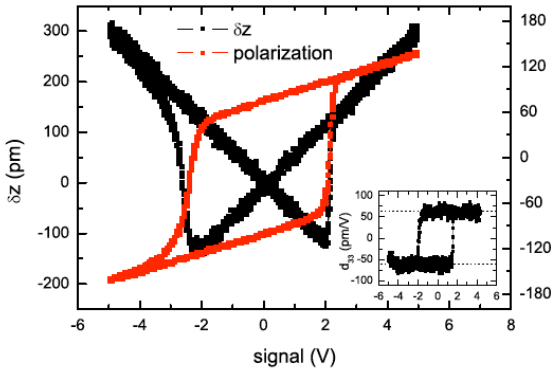

Figure 5: *Vertical displacement versus voltage and polarization loops measured simultaneously at 16 Hz on a $Pb(Zr_{0.2}Ti_{0.8})O_3$ thin film. The matching between coercive voltages for the two cases is excellent.*

peaks at half-integer *hkl* values (as can be seen on Fig. 2 for a 2 unit cell/2 unit cell superlattice). Further synchrotron measurements have just been completed on ultra-short wavelength superlattices and data analysis is underway to accurately reconstruct the atomic positions as a function of depth and hence observe directly the various contributing instabilities. In parallel the ferroelectric domain structure is being examined, which should shed some light on the electrical coupling between the $PbTiO_3$ and $SrTiO_3$ layers. Fig. 3 for instance shows satellite peaks indicative of a stripe domain structure.

Understanding in details improper ferroelectricity occurring in a relatively simple system is certainly very important before to move to more complex materials. We are therefore pursuing intensively several research directions aimed at a better understanding of this system. It has been found, for example, that the stability of the ferroelectric polarization is sensitive to the type of electrodes used, with $SrRuO_3$, which is a better metal than Nb doped $SrTiO_3$, leading to vanishingly small coercive fields and hence a loss of polarization at room temperature. Stabilization of the polarization could, however, be achieved upon cooling and a full electrical characterization was performed over a temperature range from 4.2 to 500 K.

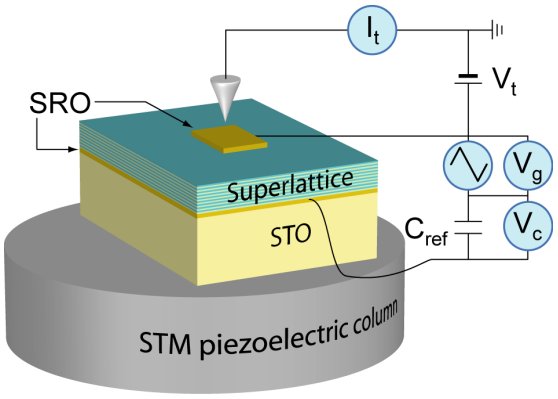

Figure 4: *Setup for STM measurement of piezoelectric properties, with an integrated Sawyer-Tower circuit.*

To investigate the piezoelectric response, we have developed a new set-up combining a scanning tunnelling microscope (STM) with a Sawyer-Tower circuit (Fig. 4). This not only allows simultaneous recording of the piezoelectric butterfly loops and polarization-voltage hysteresis curves, but also has clear advantages over conventional piezoforce microscopy measurements. Being a non-contact method, problems associated with tip or cantilever hardness are eliminated, while at the same time giving excellent vertical resolution (we were able to measure the tip displacement to 7 pm precision). The system was tested on high-quality epitaxial $Pb(Zr_{0.2}Ti_{0.8})O_3$ films (Fig. 5) and subsequently was used to measure the piezoelectric d_{33} coefficients of $PbTiO_3/SrTiO_3$ superlattices (Fig. 6).

Such oxide superlattices provide a new approach to designing material properties by the coupling of instabilities at interfaces. Such interface engineering might be another way of realizing new ferroelectrics and multiferroic materials and this route will be pursued.

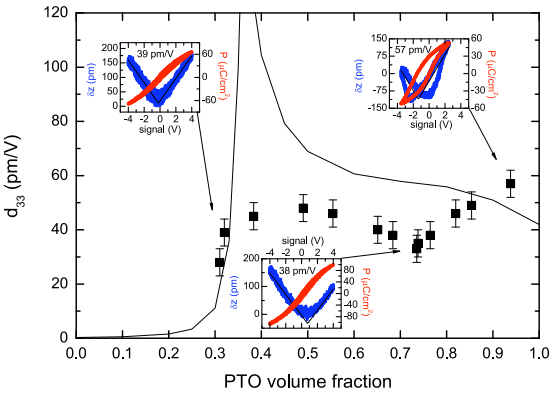

Figure 6: *Piezoelectric coefficients of $PbTiO_3/SrTiO_3$ superlattices, with $n_{SrTiO_3} = 3$ and n_{PbTiO_3} in the range 2 to 47. Solid black-line: prediction from the Landau theory. Examples of "strain" and polarization loops are inset for 47/3, 7/3 and 2/3 superlattices.*

3 Nanoscale studies of domains and domain walls in ferroelectric and multiferroic materials (P. Paruch)

3.1 Investigation of ferroelectric domain walls in $Pb(Zr_{0.2}Ti_{0.8})O_3$ thin films

Piezoresponse force microscopy (PFM) is the primary technique for nanoscale imaging of ferroelectric domains by applying a small ac bias with an AFM tip to locally induce a mechanical oscillation in the underlying ferroelectric sample by inverse piezoelectric effect. By measuring the vertical deflection and the lateral torsion of the AFM cantilever resulting from this oscillation, out-of-plane (OP) and in-plane (IP) components of the spontaneous polarization can be accessed, coupling to the electric field via the d_{33} and d_{35} piezoelectric coefficients. However, the presence of domain walls can complicate this relatively simple model of PFM. To understand their effects on PFM we have carried vertical and lateral measurements on purely tetragonal $Pb(Zr_{0.2}Ti_{0.8})O_3$ (PZT) in which the spontaneous polarization is aligned along the [001] direction. A purely vertical signal is therefore expected.

However, as can be seen on Fig. 7(a), we observe not only a finite vertical but also a lateral response in PZT after writing an array of ferroelectric circular nanodomains in a uniformly polarized background. In our measurements, opposite lateral contrast features (light vs dark) appear at the domain walls, with a zero lateral response signal (similar to the background) at the center of the domain, visible in Fig. 7(b) – (d). However, the fact that the observed features remain identical regardless of the cantilever's orientation indicates the absence of any

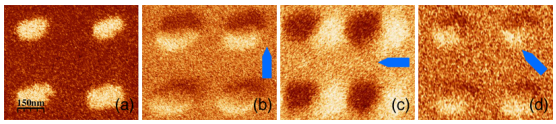

Figure 7: *2×2 array of circular ferroelectric nanodomains, written with 1 s, +12 V voltage pulses applied with the AFM tip. In parallel to the OP phase signal (a), the IP phase signal was recorded with the tip cantilever set at (b) 0°, (c) 90° and (d) 45° with respect to the horizontal. Dark and bright colors correspond to nonzero opposite responses.*

spontaneous polarization in-plane component. Indeed, as the tip cantilever can only twist sideways, lateral signal can only be detected in directions perpendicular to it. Thus, as the angle of the cantilever is changed with respect to the nanodomain array, the observed patterns would be expected to exhibit different features in presence of in-plane polarization. We observe similar edge effects at domain walls in PZT measured under ultrahigh-vacuum. In addition, the cleaner signals obtained during vacuum measurements allow us to image PFM amplitude showing the expected vertical signal decrease at domain walls, and an unexpected lateral increase at the domain walls.

The mechanism behind these observations could be explained by recent theoretical calculations [16] of the d_{33} and d_{35} coefficients for PFM. In a tetragonal ferroelectric with purely OP polarization, the d_{33} coefficient undergoes a sign change, going locally to zero directly at the domain wall. On the other hand, while the d_{35} coefficient is forbidden by symmetry in a bulk tetragonal structure, the opposite piezoelectric deformations at the domain wall yield a local shear, characterized by a maximal d_{35} coefficient at the wall. Following this model, during a scan over a circular ferroelectric domain, two opposite domain walls are encountered, yielding two opposite nonzero contributions to the lateral signal at the domain borders, as is observed in our measurements.

3.2 Investigation of ferroelectric domain wall behavior in epitaxial $BiFeO_3$ thin films

To look for evidence of magnetoelectric coupling in the nanoscale behavior of ferroelectric domain walls in $BiFeO_3$ (BFO), we measured the static configuration and dynamic response of domain walls using PFM at ambient temperature. The phase and amplitude of the piezoresponse in the normal and lateral directions provide information about OP and IP polarization present in the material. A nanoscale control of the ferroelectric polarization by the conduct-

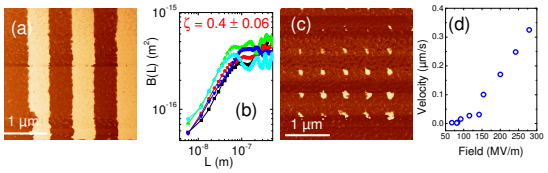

Figure 8: *Sample of BFO(70 nm)/(La,Sr)MnO_3/ $SrTiO_3$(111): out-of-plane PFM phase response measured after writing domain stripes (a) and dots with different pulse duration (c). (b) Correlation function of the relative displacements from an elastically ideal flat configuration for the domain walls measured in (a). (d) Evolution of the domain wall velocity as a function of electric field, extracted from (c).*

ing tip of the PFM allows both large (Fig. 8a) and small (Fig. 8c) domains to be written, by sweeping the tip during voltage application or by applying a voltage pulse of fixed duration to a stationary tip, respectively.

Within the framework of disordered elastic systems theory, the analysis of the static configuration of domain walls in Fig. 8a allows the critical roughness exponent ζ to be determined. We observed values of around 0.4 – 0.5 for ζ in 70 nm BFO films deposited on (111)- and (001)-oriented $SrTiO_3$, higher than the 0.25 value obtained for comparable pure ferroelectric $Pb(Zr,Ti)O_3$ films [8], possibly due to greater domain wall thickness and thus decreased dimensionality as compared to 180° domain walls in a pure ferroelectric. In addition, the analysis of domain size as a function of the pulse duration allows domain wall velocity to be calculated, and correlated with the applied electric field which drives the domain wall motion. The observed non-linear behavior (Fig. 8d) is typical of the creep regime for subcritical driving forces observed and predicted for elastic interfaces moving through a random pinning potential. Preliminary analyses of the dynamical exponent μ governing this behavior suggest its value, like that of the characteristic roughness exponent, is different in BFO as compared to a purely ferroelectric material.

The present PFM measurements were performed on BFO thin films grown by pulsed laser deposition in the team of Agnès Barthélémy in the Unité Mixte de Physique CNRS/Thales (France). We are currently optimizing in-house epitaxial growth of BFO thin films using RF-magnetron sputtering.

4 Spin-lattice coupling and magnetic circular dichroism of $EuTiO_3$ (D. van der Marel)

The rare-earth perovskite $EuTiO_3$ has been recently highlighted for possible exceptionally strong magneto-electrical coupling which should occur in in-plane strained $EuTiO_3$ [17]. In this prediction, a strong spin-lattice coupling will soften the ferroelectric phonon mode entirely in a modest magnetic field. Although never directly observed experimentally, recent quasi-static dielectric studies claim the spin-lattice coupling to be also present in unstrained bulk $EuTiO_3$ [18]. Here we report about our magneto-optical study in the THz range in order to directly probe the behavior of the ferroelectric soft mode. Fig. 9 shows the measured time dependence of a 1 ps wide THz electromagnetic pulse transmitted through a 315 μm thin $EuTiO_3$ slab as a function of an externally applied magnetic field B. The used geometry consists of a linearly polarized source and a linearly polarized detector which are parallel to each other. The data show a strong decrease of the transmission with increasing magnetic field for the straight transmission (first peak), whereas the echos (second and third peak) also show a zero crossing and eventually become negative. The fact that the intensity change of the first echo goes much faster than the main peak suggests that the incident linearly polarized light is subject of a rotation by passing through the sample. This so-called Faraday rotation is linear with both the magnetic field and the transmission path length and changes the projection of the transmission like $n \cdot \cos^{-1}[I(B)/I(0)]$, where $I(B)$ is the transmitted intensity in a magnetic field B and

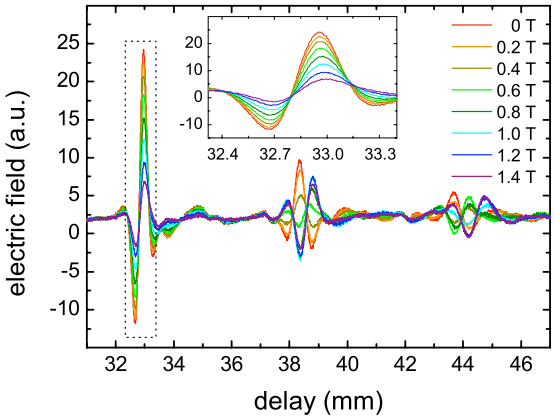

Figure 9: *THz time-domain transmission of 315 μm thick $EuTiO_3$ as a function of magnetic field at 3.0 K. The inset shows a magnification of the straight transmission pulse.*

n is the number of passages through the sample (e.g. three for the first echo). The experimental data show that this approximately holds for the straight transmission and first echo. The deviation from linearity will be discussed below. Based on the straight transmission, we find a gigantic rotation of about 170° per tesla per mm in the range from 0.15 to 2.5 meV at 3 K. This rotation is orders of magnitude too large to originate from an electric dipole transition, but enters the right ballpark of one which is due to a magnetic dipole excitation within the purely Zeeman split $4f$ multiplet. Circularly polarized light can transfer a spin or orbital angular momentum quantum to the system upon absorption, although the probability is different for each chirality. Therefore, linearly polarized light will be turned into elliptically polarized light when leaving the sample, for which the main axis is rotated by an angle θ.

As mentioned before, the suppression of the measured transmission as a function of the magnetic field is about 30% larger than what one would expect for a Faraday rotation. After correction for the Faraday rotation [1] and subsequent Drude-Lorentz modeling, it turns out that the extra suppression is due to the magnetic field dependence of the ferroelectric soft mode, as shown in Fig. 10. In agreement with previous studies [19], the mode softens in the paramagnetic state from 12.5 meV to 9.1 meV at 10 K following a Curie-Weiss behavior. Below 5.5 K $EuTiO_3$ orders antiferromagnetically (AFM) which is shown by a the soft mode *hardening* of 0.10 meV. A modest magnetic field of 1.5 T aligns the Eu spins and induces a ferromagnetic (FM) ordering as shown by the magnetic susceptibility. Optically this is seen by a mode *softening* of about 0.17 meV. Our THz data evidence the coupling between the magnetic ordering and the ferroelectric soft mode behavior. Previously, quasi-static (1 kHz) dielectric measurements were utilized to infer a similar scenario for the behavior of the soft mode. However, the energy scale of the data and of the soft mode are 6 orders of magnitude apart, and moreover, in between these two scales, Maxwell-Wagner polarization effects that strongly influence the behavior of ϵ_1 have been observed, even for single crystals [18, 19].

[1] To a first order approximation, the rotation effect can be cancelled by iteratively scaling the intensity upon the observed time delay, in a Kramers-Kronig consistent way. Direct inversion of the Fourier transformed THz spectra provides the dielectric function.

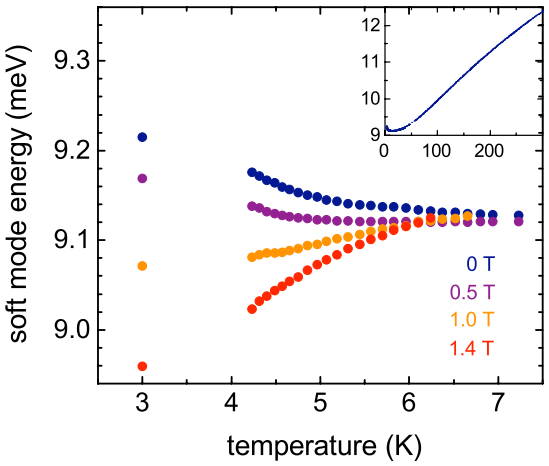

Figure 10: *Temperature dependence of the ferroelectric soft mode energy of $EuTiO_3$ as a function of the applied magnetic field. The inset shows the temperature dependence of the soft mode energy in zero magnetic field.*

5 Nano-electronics with novel materials (A. Morpurgo)

Research on nano-electronics requires state of the art nano-fabrication facilities and considerable effort during this initial period at the University of Geneva has been devoted to install the required instrumentation. We took advantage of the clean-room existing within DPMC, which enables all resist preparation processes (spinning, backing, inspection, etc.), as well as conventional photolithography. With the support of MaNEP, the University of Geneva, and the Swiss National Science Foundation (through a Re-Equip grant), we have purchased and installed a system for electron-beam lithography and one for electron-beam evaporation. In addition, a RF magnetron sputtering has been moved from Delft. Together with the existing clean-room, these systems allow the fabrication of devices with features down to $\approx$ 50 nm, and form a solid basis for the nano-fabrication of devices with novel materials in Geneva.

Since the fabrication of nano-devices is, for the most part, a new direction within MaNEP and at the University of Geneva, it is worth spending a few words to describe the capabilities of the new instrumentation. The electron-beam lithography system is a Raith50 model (Fig. 11). It comprises a motorized stage capable of holding 2-inch wafers, a laser interferometer for accurate overlay and stitching with a nominal precision close to 50 nm, automatic markers recognition, writing capability down to the 50 nm scale for smallest feature. In less technical terms, it is possible to write patterns on 2-

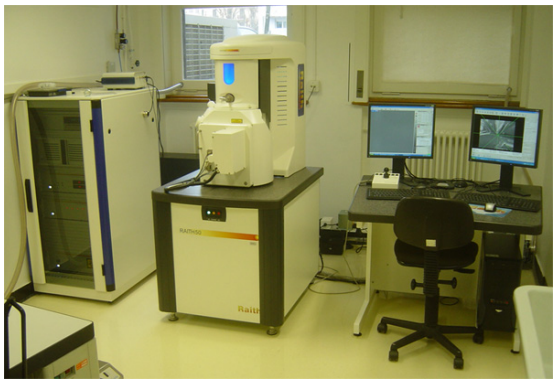

Figure 11: *The Raith50 electron-beam writer recently installed at UniGE.*

inch substrates coated by an electron-sensitive resist with features as small as 50 nm, and to subsequently write one or more different patterns aligned to the initial one with a precision of approximately 50 nm. We are currently testing the system. The results so far suggest that, upon careful optimization, performance exceeding the official machine specifications may be achievable if needed. We expect that devices for actual experiments will be fabricated during the first months of 2009.

For metal evaporation we have installed an electron-beam evaporator (Fig. 12) bought from the company Plassys (France). Key features are: fast turnaround time (the system has a load-lock and a eight-pocket crucible), background pressure of 10^{-8} mbar, possibility to heat the substrate to temperatures higher than 700°C and to cool it to liquid Nitrogen temperature, high-precision substrate rotation around two axes for shadow evaporation, ion-gun for precleaning of the substrate surface. The system will mainly be used for the evaporation of common metals, typically in combination with a lift-off process. A main goal is the fabrication of metallic electrodes for nano-devices, including contacts of superconducting and ferromagnetic materials. The RF magnetron sputtering – a older system purchased from the company Alliance (Annecy-France) – possesses a load-lock and four independent targets. It is a flexible machine that can be used to deposit many different materials; in the past we have used this system mainly to deposit films of insulating oxides, including Ta_2O_5, Al_2O_3, HfO_2, etc., essential for our research on organic transistors.

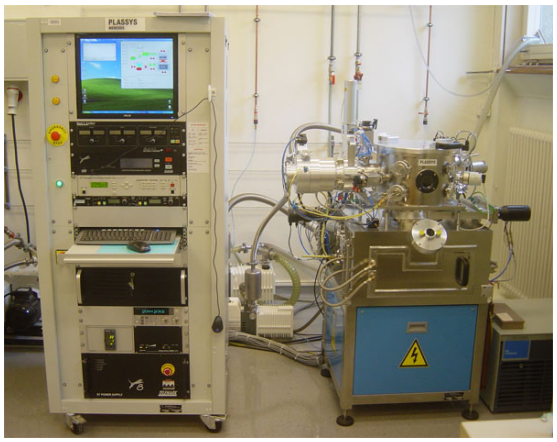

Figure 12: *The new e-gun evaporator enabling the deposition of metallic films, as it is needed for the fabrication of nano-electronic devices.*

6 Magnetoelectric effects in complex oxides with competing ground states (J.-M. Triscone)

The drive to develop materials with new multifunctional capabilities has rekindled interest in multiferroics systems which are characterized by the simultaneous presence of magnetic and electric order parameters. In naturally occurring multiferroics the magnetoelectric coupling is weak and new classes of artificially structured composites that combine dissimilar magnetic and ferroelectric materials are being developed to optimize order parameter coupling. Here, we describe direct, charge-mediated (via the electric field) magnetoelectric coupling in a heterogeneous multiferroic that takes advantage of the sensitivity of a strongly correlated magnetic system to competing electronic ground states. Using magneto-optic Kerr effect (MOKE) magnetometry, we observe large magnetoelectric coupling in ferroelectric/Lanthanum manganite heterostructures, including electric field-controlled on/off switching of magnetism.

Doped Lanthanum manganites are complex oxides characterized by a strong interplay between electron transport, magnetism and crystal lattice distortions, leading to a rich variety of electronic behavior, including magnetic and charge ordered states, colossal magnetoresistance (CMR), and a diversity of electron transport behavior.

In this study we use off-axis magnetron sputtering to grow a continuous 250 nm $Pb(Zr_{0.2}Ti_{0.8})O_3$/4.0 nm $La_{0.8}Sr_{0.2}MnO_3$ bilayer structure on a $SrTiO_3$(001) single crystal. We choose $La_{0.8}Sr_{0.2}MnO_3$, since the bulk compound lies near the boundary between metallic and insulating ferromagnetic ground states; the paramagnetic-magnetic Curie temperature occurs at 300 K [2]. To provide

[2]The critical temperature is slightly reduced in films

the electric field, we use the spontaneous electric polarization of $Pb(Zr_{0.2}Ti_{0.8})O_3$, which can generate polarizations of the order of 50 $\mu C/cm^2$. For the bilayer structures, X-ray diffraction reveals that the $Pb(Zr_{0.2}Ti_{0.8})O_3$ is *c*-axis oriented, with the polarization lying perpendicular to the film surface. The polarization is switched by applying a voltage across the $Pb(Zr_{0.2}Ti_{0.8})O_3$ layer, using a gold top electrode and the $La_{0.8}Sr_{0.2}MnO_3$ layer as the bottom electrode. The contact was made large enough (400×600 μm^2) to accommodate the focused laser beam for the MOKE magnetometry measurements, while thin enough to be transparent to the laser beam ($\sim$ 1 mW power, $\lambda = 633$ nm). Polarization-electric field ($P - E$) hysteresis measurements reveal a square loop with a remanent polarization of ~ 45 $\mu C/cm^2$.

To probe the local magnetic state of the $La_{0.8}Sr_{0.2}MnO_3$ as a function of the $Pb(Zr_{0.2}Ti_{0.8})O_3$ polarization state, we employ MOKE magnetometry. In this technique, the sample magnetization gives rise to changes in the polarization of light reflected off the surface. We measure the Kerr rotation and ellipticity, both of which are proportional to the magnetization. For the reflection geometry used here, optical effects originating from the birefringence of the $Pb(Zr_{0.2}Ti_{0.8})O_3$ and $SrTiO_3$ substrate (which becomes tetragonal below $\sim$ 100 K) are negligible. For these measurements, the sample was placed in a high-vacuum cryostat with optical apertures for longitudinal MOKE measurements. The light polarization was modulated using a photoelastic modulator operating at 50 kHz, while the signal at the detector was fed to a lock-in amplifier locked either to the fundamental harmonic (signal proportional to the Kerr ellipticity) or to the second harmonic (signal proportional to the Kerr rotation). The magnetic field is applied parallel to the remanent magnetization lying in the plane of the sample, and is generated by a coreless electromagnet that provides magnetic field capable of generating up to 30 Oe at room temperature and up to 80 Oe at 20 K in the frequency range from 0 to $\sim$ 120 Hz. Two types of MOKE measurements were performed: (i) in the dc mode, the Kerr rotation or ellipticity are measured as a function of the slowly varying (quasi-static) magnetic field (0.005 Hz), yielding ordinary $M - H$ characteristics; (ii) in the ac mode, an oscillating magnetic field (12 Hz) is applied to the sample and the Kerr rotation or ellipticity is measured by a second lock-in amplifier

thinner than 10 nm.

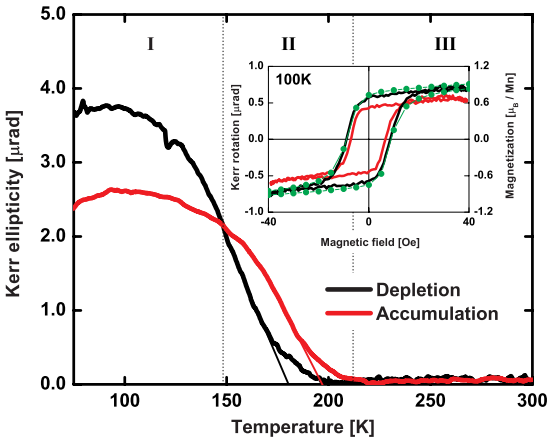

Figure 13: *Temperature dependence of the $La_{0.8}Sr_{0.2}MnO_3$ magnetization for the two polarization states of the $Pb(Zr_{0.2}Ti_{0.8})O_3$ layer. A shift in T_c of about 20 K is observed. The inset shows quasi-static $M - H$ loops measured at 100 K for the accumulation and depletion states; full lines: MOKE data; symbols: SQUID data (depletion state); y-axis corresponds to the magnetic moment obtained from SQUID magnetometry, used to calibrate the MOKE Kerr signal.*

locked at the field excitation frequency. The latter technique, where the output signal is proportional to the saturation magnetization amplitude averaged over many field cycles, has the advantage that the non-magnetic optical contributions are automatically filtered from the output signal. With this set-up, the Kerr rotation and ellipticity are measured with a precision of better than 50 nrad.

In Fig. 13 we show how the magnetization of the structure evolves as a function of temperature and ferroelectric polarization. The red and black curves correspond to the states where the ferroelectric adds and removes charges from the magnetic hole doped $La_{0.8}Sr_{0.2}MnO_3$ layer; these are termed the accumulation and depletion states, respectively. We distinguish three different temperature regimes for the magnetization curves. At high temperatures (region III, $T > 212$ K) we find that the $La_{0.8}Sr_{0.2}MnO_3$ is in a paramagnetic state for both polarization states and shows no magnetic response. For intermediate temperatures (region II, $147 < T < 212$ K), we observe a vertical and horizontal split in the magnetization curves, where the accumulation state becomes magnetic at higher temperatures and has a larger magnetization than in the depletion state. A crossover in behavior is observed at 147 K, where a reversal in the relative position of the magnetization curves occurs: the magnetization for the depletion state becomes larger than that for the accumulation state. Region I, $T < 147$ K, is charac-

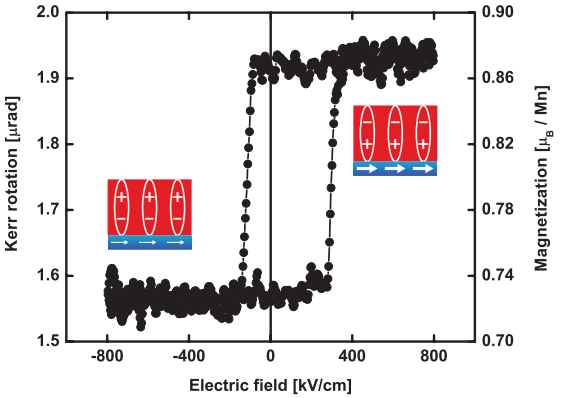

Figure 14: *Magnetoelectric hysteresis curve at 100 K showing the magnetic response of the $Pb(Zr_{0.2}Ti_{0.8})O_3/La_{0.8}Sr_{0.2}MnO_3$ system as a function of the applied electric field. Insets represent the magnetic and electric states of the $La_{0.8}Sr_{0.2}MnO_3$ and $Pb(Zr_{0.2}Ti_{0.8})O_3$ layers, respectively. The size of the arrows indicates qualitatively the magnetization amplitude.*

terized by the gradual increase of the magnetization towards a constant ground state value [3]. The decrease in the ground state magnetization with increasing doping level, observed in region I of Fig. 13 and also in the hysteresis loops, may at first seem surprising since it implies that the material with the higher T_c has a lower magnetization. However, this trend is exactly what is expected in the ferromagnetic phase of the bulk CMR manganites, where the magnetic moment varies with hole concentration x as $(4-x)\mu_B$ per Mn: as the hole concentration (doping) increases, a larger fraction of the Mn cations changes from the $S = 2$ (Mn^{3+}) to the $S = 3/2$ (Mn^{4+}) spin state.

This competition between ground states and their sensitivity to the charge carrier density can be exploited to achieve large magnetoelectric couplings driven directly by charge and electric field. A striking illustration of this magnetoelectric coupling is given in Fig. 14, where we show the *magnetic* response of the system as a function of the applied *electric* field, displaying abrupt modulation of the $La_{0.8}Sr_{0.2}MnO_3$ magnetization as the $Pb(Zr_{0.2}Ti_{0.8})O_3$ polarization switches. In contrast to traditional $M-H$ and $P-E$ loops, which reveal how the parameter (magnetism M, polarization P) of an individual ferroic material responds to its corresponding driving field (magnetic field H, electric field E), this $M-E$ loop demonstrates cross-coupling between ferroic ground states, showing a hysteretic magnetic response as a function of the electric field. In our system, the magnetoelectric coupling is achieved via modulation of the charge carrier concentration, and is directly linked to the gate oxide surface bound charge. $\alpha = \Delta M/\Delta\mathcal{E}$, which corresponds to the relative change in magnetization for an applied electric field, can be chosen as the figure of merit that characterizes the strength of the magnetoelectric coupling in our system. Using the width of the $M-E$ hysteresis, we obtain $\alpha = 0.8\times10^{-3}$ Oe cm V^{-1} (0.8 ns/m in S.I. units) at 100 K. Values for homogeneous multiferroics are typically 2 – 4 orders of magnitude smaller, while for magneto- and piezoelastically coupled composites, values up to 25×10^{-3} Oe cm V^{-1} have been reported, showing that the route demonstrated here may allow the development of novel magnetoelectric devices with large charge mediated coupling between the electric and magnetic degrees of freedom.

[3] The drop in magnetization for temperatures below $\sim$ 90 K is due to an increase in coercivity beyond the applied field amplitude.

7 Superconducting nanostructures and single-photon detectors (A. Schilling)

7.1 Lithography

The properties of superconducting nanowire single-photon detectors (SNPD) depend crucially on the quality of the NbN starting film and the structuring process. We have further optimized our mix & match photo- and e-beam lithography process [9] and are now able to produce state-of-the-art single-photon detectors. Starting from 5 nm thick NbN film [10] with a $T_c \approx 14$ K we have prepared several detectors with different strip widths and filling factors. In Fig. 15 a scanning electron microscope (SEM) picture is shown that depicts

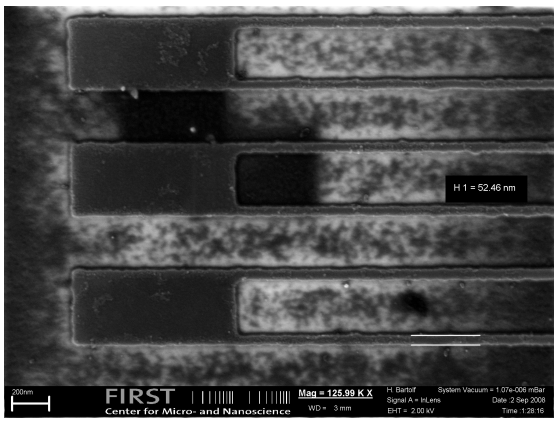

Figure 15: *SEM picture of a meander with approximately 50 nm strip width. The filling factor was around 15%.*

part of a meander structure with a strip width of only $\sim$ 50 nm.

7.2 Detector characterization

The detector characteristics were thoroughly tested for three of the prepared meander structures. After the nano-lithography the critical temperatures dropped slightly to about 12.5 K. The transitions were smooth and relatively sharp indicating very homogeneous meanders. The optical measurements were performed in a ^{4}He-bath cryostat, with the detectors cooled to $\sim$ 5.5 K. The detectors were biased with a custom-built, battery-powered constant voltage source and shielded from electro-magnetic interferences as much as possible. The continuous spectrum from the light source was passed through a prism monochromator and directed onto the meander through the optical access of the cryostat.

The wavelength dependence of the quantum efficiency (QE) shows the typical behavior expected for SNPD: nearly constant QE for wavelengths shorter than a device dependent cut-off wavelength and an approximately exponential decrease for longer wavelengths (Fig. 16). The cut-off wavelength for the 170 nm wide meander lies outside our accessible spectral range as one would expect based on the refined detection model [11, 12]. With the 80 nm wide meander we obtained a QE of up to 9%. Numerically calculating the absorbance of this meander, we can conclude that about 65% of the absorbed photons are detected. We have also obtained a similar value for this intrinsic detection efficiency for the 50 nm wide meander, which is one of the narrowest SNPDs produced so far.

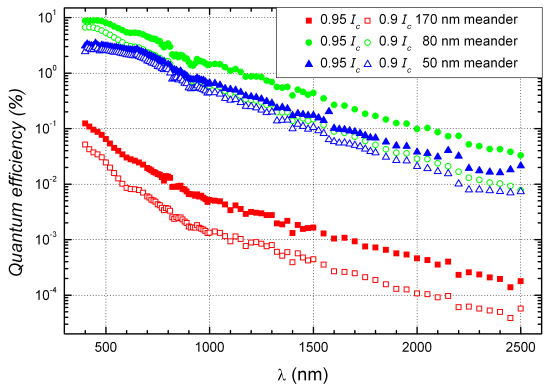

Figure 16: *Quantum efficiency of three meanders with different strip width as a function of incident photon wavelength.*

8 Patterning of YBCO thin films for SSPDs applications (Ø. Fischer)

8.1 Motivation

The field of single-photon detection is extensively investigated inside the optics community [13]. In this framework, superconducting single photon detectors (SSPDs) are a type of device combining ultimate sensitivity (single photon) with a good quantum efficiency and counting rates $>$ GHz [20], making them an excellent candidate for single-photon telecommunication and applications such as quantum cryptography [21]. This work focuses on high-T_c superconductors in order to provide alternative materials to current state-of-the-art NbN SSPDs.

8.2 Thin films

For this project, we grew $YBa_2Cu_3O_{7-\delta}$ (YBCO) ultra-thin (10 to 15 nm) films by RF magnetron sputtering deposition on (100) $SrTiO_3$ substrates, to which were added *in situ* gold contacts and a protective amorphous PBCO cap layer on top (see last year's report). It is worth noting that our sputtering process allowed us to create films whose high quality was well suited for muons measurements [14], and ultra-thin films ($\leq$ 5 nm) to study the first superconducting layers with synchrotron radiations.

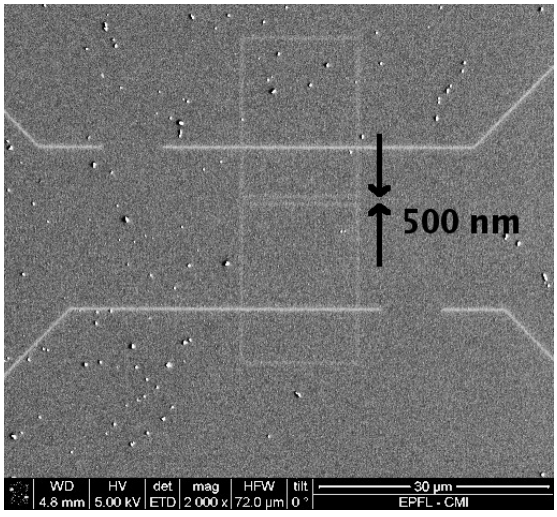

Figure 17: *SEM micrograph of a 12 nm thick, 15 µm long, 500 nm wide stripe patterned with a focused Ga^{3+} ion beam (FIB). The structure has been written on an area where surface particles are relatively sparse.*

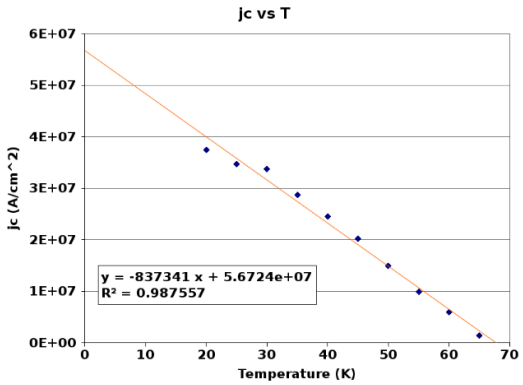

Figure 18: *Critical current density vs temperature for a 2 μm wide YBCO meander. The points are extrapolated to $j_c(0\,K) = 57\ MA/cm^2$.*

8.3 FIB-driven patterning protocol

Following the 2-step protocol designed last year, involving a preliminary chemical etching followed by a focused Ga^{3+} ion beam (FIB), we patterned superconducting meanders down to 1 μm wide, and stripes down to 500 nm wide (Fig. 17). Various patterned geometries exhibit similar transport properties, demonstrating that this particular protocol works down to this scale.

8.4 Critical current density measurements

Critical current density j_c was measured for a number of samples, at various temperatures (Fig. 18 provides an example), and voltage responses of the samples to bias current were successfully modeled by power laws, hence giving good estimations of the power dissipated in the sample after a S/N switch.

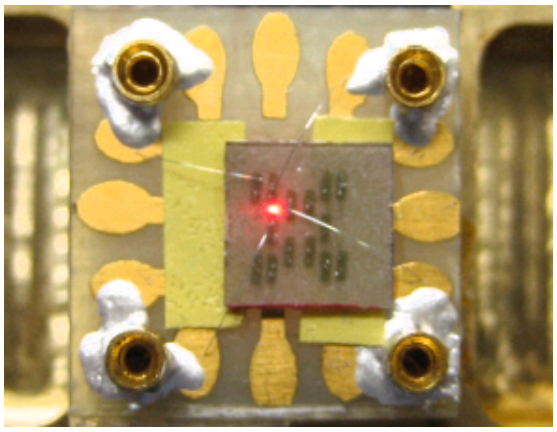

Figure 19: *Sample located on the head of the dipstick, illuminated by a 650 nm laser. The spot is focused on the FIB-patterned nanostructure.*

8.5 Optical characterization

A dipstick was specially designed and built to carry out optical characterization of the samples. Light emitted by a 650 nm CW laser is transported through a fiber incorporated in the dipstick to illuminated the samples cooled in a liquid He cryostat (Fig. 19). First measurements have been taken and show that the light may act upon the critical current density of the devices. Others experiments have still to be performed with different substrates and geometries.

9 Collaborative efforts

In the area of ferroelectric thin films and heterostructures, active collaboration between the Aebi, Paruch and Triscone groups took place to study thin films and superlattices using advanced characterization techniques. On oxide interfaces, new collaboration between the Aebi, Morpurgo, Paruch, van der Marel and Triscone groups is developing to study low T domain dynamics, polarization at surfaces, optical spectroscopy, and new techniques to pattern oxide heterostructures.

MaNEP-related publications

[1] C. Lichtensteiger, J.-M. Triscone, J. Junquera, and P. Ghosez, Physical Review Letters **94**, 047603 (2005).

[2] L. Despont, D. Naumovic, F. Clerc, C. Koitzsch, M. G. Garnier, F. J. Garcia de Abajo, M. A. Van Hove, and P. Aebi, Surface Science **600**, 380 (2006).

[3] L. Despont, C. Lichtensteiger, F. Clerc, M. G. Garnier, F. J. Garcia de Abajo, M. A. Van Hove, J.-M. Triscone, and P. Aebi, The European Physical Journal B **49**, 141 (2006).

[4] L. Despont, C. Koitzsch, F. Clerc, M. G. Garnier, P. Aebi, C. Lichtensteiger, J.-M. Triscone, F. J. Garcia de Abajo, E. Bousquet, and P. Ghosez, Physical Review B **73**, 094110 (2006).

[5] M. Dawber, C. Lichtensteiger, M. Cantoni, M. Veithen, P. Ghosez, K. Johnston, K. M. Rabe, and J.-M. Triscone, Physical Review Letters **95**, 177601 (2005).

[6] M. Dawber, N. Stucki, C. Lichtensteiger, S. Gariglio, P. Ghosez, and J.-M. Triscone, Advanced Materials **19**, 4153 (2007).

► [7] E. Bousquet, M. Dawber, N. Stucki, C. Lichtensteiger, P. Hermet, S. Gariglio, J.-M. Triscone, and P. Ghosez, Nature **452**, 732 (2008).

[8] P. Paruch, T. Giamarchi, and J.-M. Triscone, Physical Review Letters **94**, 197601 (2005).

► [9] H. Bartolf, A. Engel, L. Gómez, and A. Schilling, Multi-project wafer scale process for productive research and development, Raith application note, Physics Institute of the University of Zurich, Switzerland (2008).

[10] K. Il'in, M. Siegel, A. Engel, H. Bartolf, A. Schilling, A. Semenov, and H.-W. Huebers, Journal of Low Temperature Physics **151**, 585 (2008).

[11] A. Engel, A. D. Semenov, H.-W. Hübers, K. Il'in, and M. Siegel, Physica C **444**, 12 (2006).

[12] A. Semenov, A. Engel, H.-W. Hübers, K. Il'in, and M. Siegel, The European Physical Journal B **47**, 495 (2005).

[13] R. T. Thew, N. Curtz, P. Eraerds, N. Walenta, J.-D. Gautier, E. Koller, J. Zhang, N. Gisin, and H. Zbinden, Nuclear Instruments and Methods in Physics Research A (2009).

[14] B. M. Wojek, E. Morenzoni, D. G. Eshchenko, A. Suter, T. Prokscha, E. Koller, E. Treboux, Ø. Fischer, and H. Keller, Physica B (2009), doi: 10.1016/j.physb.2008.11.189.

Other references

[15] S. K. Streiffer, J. A. Eastman, D. D. Fong, C. Thompson, A. Munkholm, M. V. Ramana Murty, O. Auciello, G. R. Bai, and G. B. Stephenson, Physical Review Letters **89**, 067601 (2002).

[16] A. N. Morozovska, S. V. Svechnikov, E. A. Eliseev, and S. V. Kalinin, Physical Review B **76**, 054123 (2007).

[17] C. J. Fennie and K. M. Rabe, Physical Review Letters **97**, 267602 (2006).

[18] T. Katsufuji and H. Takagi, Physical Review B **64**, 054415 (2001).

[19] S. Kamba, D. Nuzhnyy, P. Vanek, M. Savinov, K. Knizek, Z. Shen, E. Santava, K. Maca, M. Sadowski, and J. Petzeltm, Europhysics Letters **80**, 27002 (2007).

[20] G. N. Gol'tsman, O. Okunev, G. Chulkova, A. Lipatov, A. Semenov, K. Smirnov, B. Voronov, A. Dzardanov, C. Williams, and R. Sobolewski, Applied Physics Letters **79**, 705 (2001).

[21] D. Stucki, N. Walenta, F. Vannel, R. T. Thew, N. Gisin, H. Zbinden, S. Gray, C. Towery, and S. Ten, *submitted to* New Journal of Physics (2009).

Project 6 Industrial applications and pre-application development

Project leader: Ø. Fischer (UniGE)

Participating members: M. Abplanalp (ABB), D. Eckert (Bruker BioSpin), Ø. Fischer (UniGE), R. Flükiger (UniGE), L. Forró (EPFL), M. Hasler (EPFL), J. Mesot (PSI – ETHZ), R. Nesper (ETHZ), C. Renner (UniGE), J.-M. Triscone (UniGE), K. Yvon (UniGE).

Introduction: This project explores opportunities of applications of MaNEP materials as well as technical know-how present in MaNEP. Projects on applied superconductivity are based on long-term collaborations with two important companies, Bruker BioSpin and ABB. In the domains of sensors and thin film applications we established new collaborations in the second phase of MaNEP (Mecsens, Metrolab, Phasis and Swissneutronics). We have further explored collaborations with new industrial partners, especially as a preparation for the third phase. Thus projects with Vacheron Constantin and Swatch Group have been concluded and we are continuing discussions with other Swiss companies.

Summary and highlights

Applied superconductivity

During the last year several important results have been obtained in the domain of applied superconductivity concerning both classical superconductors like MgB_2 and high-temperature superconducting cuprates as well as the new iron pnictides. These projects are carried out in collaboration with the companies Bruker BioSpin and ABB

MgB_2 is now progressing towards a real alternative to HTS for certain applications. Research in R. Flükiger's group has shown that important improvements of the critical current can be achieved by "cold high pressure densification". A remarkable result is that at 20 K and 4 Tesla the critical current was increased by 300%. In MgB_2 wires alloyed with malic acid J_c was even enhanced by a factor 8, thus reaching a new upper limit for J_c in this class of wires. This result is related to an enhanced connectivity between the grains. In this context we can also note that the group of R. Nesper has developed a new method for synthesizing nanoscopic boron of high purity with a narrow size distribution which may turn out to be a good starting point for nanoscopic MgB_2 production.

A number of new results have been obtained in MaNEP on the new iron pnictide superconductors. In connection with possible future applications of these materials the results obtained in R. Flükiger's group are particularly important. By measuring the specific heat in a magnetic field they could show that the upper critical fields of these materials are well above 100 Tesla, thus making these compounds potential candidates for high field applications. However, weak grain boundaries in the same sample show that this may turn out to become a problem for obtaining high critical currents.

The properties of YBCO coated conductors from different producers have been investigated by the groups of Flükiger and Fischer/Decroux. R. Flükiger's group studied the relation between the T_c distribution and the magnetic relaxation in such coated conductors and found a correlation showing that the larger the T_c distribution the slower the magnetic relaxation, concluding that pinning is enhanced by the T_c inhomogeneities. The Fischer/Decroux group has investigated coated conductors in view of their use in fault current limiters. A key property in such applications is the normal zone propagation (NZP) velocities in such conductors. An unexpected low value for these velocities was measured in tapes from the two producers studied so far. In fact, values two orders of magnitude lower than what was obtained earlier in epitaxial YBCO films deposited on sapphire, were found. Simulations based on an adiabatic model showed that considerably higher values should be expected. Thus a challenge for the continuation of this project will be to understand this behavior and to find ways to improve this situation. A more sophisticated simulation of this NZP behavior is being carried out by the Hasler group. First results applied on coated conductors show that the NZP velocities depend strongly on the substrate properties.

Finally, the actively shielded 16 T split-coil magnet is on track to be delivered in the sum-

mer 2009. After the design review in January 2008, the magnet system has been manufactured and will be tested in the 2^{nd} quarter 2009 both at Bruker and at PSI (group of J. Mesot) before its shipment to the USA.

MaNEP sensors and security applications

During this year L. Forró's group has continued at a low financial level the search for a material which can give extremely narrow ESR line so that it can be used for precise low magnetic field measurements (collaboration with Metrolab). Several candidates have been found and the problems to be solved identified. Although the collaboration with the company Mecsens is at a hold because of financial problems, L. Forró's group continued to prepare for a stronger project in phase III. Using nanorods they have found ways which will open the road towards very fast gas detectors.
Last year Ø. Fischer's group introduced the marking technology inspired by STM and using nanoparticles in a suspension to write a given compound into the surface of a conducting material. This year they have identified the key parameters which govern the out of equilibrium process of forming and incrusting the various alloys and compounds which have been investigated. Several companies are interested in this technology and for the third phase a CTI project has been submitted with the company Vacheron Constantin.
This year two new sensor activities are presented. The first has been developed in C. Renner's group in collaboration with other institutions. It is strain gauge based on a contact between silicon and a metal. For given geometrical conditions one obtains a very sensitive strain gauge. Although the practical use of this device is limited by the corresponding very low voltages new applications are now being investigated. A second new approach is the use of intermetallic hydrides, showing a metal insulator transition upon uptake of hydrogen, as sensitive hydrogen sensors. This will be a subproject in phase III in collaboration between K. Yvon, Ø. Fischer, and the Swatch Group. In the present report K. Yvon presents preliminary investigations, showing that compounds of the type $LaMg_2Ni–H_x$ and $LaMg_2Pd–H_x$ are excellent candidates for such detectors.

Thin film preparation and applications

The PSI (J. Mesot's group) – Swissneutronics collaboration successfully tested a bender-prototype that was developed for the neutron spin analysis of the HYSPEC-spectrometer at the SNS (Oak Ridge, USA). The device consists of an optimized polarizing supermirror based on $FeCoV/TiN_x$ multilayers and achieved a beam polarization of $\sim$ 95% for the neutron wavelengths between 3 Å and 6 Å . In addition, they designed and built a parabolically shaped reflector with a Ni/Ti-multilayer coating which is graded along the length of the device. They obtained a reflectivity of $>$ 96% for a 8 mm wide parallel beam focused down to 0.8 mm. The wavelength band was 4.7 Å $\pm$ 5% and the focal point was 250 mm behind the device.
A key goal of phase II was to be able to master the growth of epitaxial high quality perovskite films on silicon. This has been achieved by a few groups in the world and it is an essential technological step for a number of potential applications, especially of piezoelectric materials. This year the group of J.-M. Triscone succeeded in growing epitaxial $SrTiO_3$ buffer layers on silicon. PTZ/SRO/STO/silicon heterostructures have been realized and processed in collaboration with N. de Rooij (Institute of Micro Technology (IMT), Neuchâtel) for test MEMs.

1 Applied superconductivity

1.1 Wires for high field applications (*R. Flükiger*)

a) *Enhanced J_c in* in situ *MgB_2 wires by cold high pressure densification* Besides quality and size of the Magnesium and Boron powder particles and the addition of Carbon, another important factor for the enhancement of J_c in MgB_2 wires is the connectivity between neighbor grains, characterized by the electric resistivity. The latter is also influenced by the considerable amount of voids in the filaments of *in situ* wires, the mass density of the filaments being usually $\leq$ 50% of the theoretical density of MgB_2. We have introduced a new way to enhance J_c by means of cold high pressure densification (Fig. 1) [1]. At 20 K, pressure of 1.85 GPa on a binary Fe/MgB_2 wire raised $J_c^{\parallel}$ by more than 300% at 5 T, and the irreversibility field B_{irr} by 0.7 T. After pressing of a MgB_2 wire alloyed with 10 wt.% malic acid, the highest J_c values reported so far were obtained (Fig. 1) [2]. After applying 6.5 GPa, the mass density d_m of the unreacted (B + Mg) filaments reached 96% of theoretical density, which corresponds

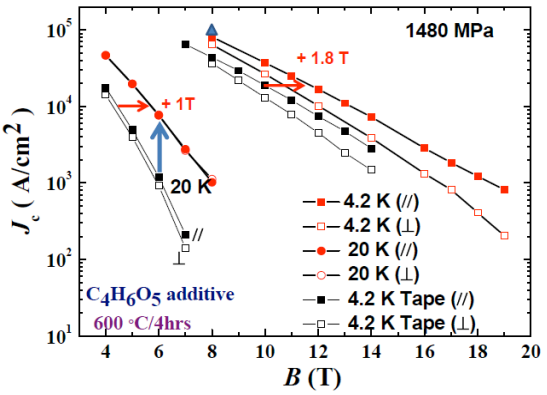

Figure 1: *J_c enhancement in densified alloyed MgB_2 wires.*

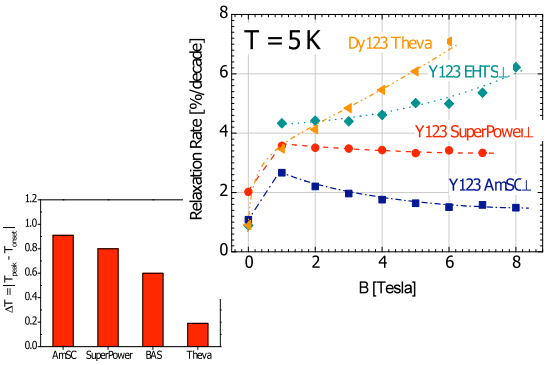

Figure 3: *Relaxation rates at 5 K and width ΔT in Y123 tapes.*

to a mass density of MgB_2 filaments of 73% (Fig. 2). Densified wires exhibit lower electrical resistivity values, thus reflecting an improved connectivity [1].

b) *T_c distribution and relaxation rates in industrial Y123 coated conductors* The T_c distribution in industrial Y123 coated conductor tapes from various manufacturers produced by different methods has been studied by means of zero field cooling (ZFC) magnetization vs T data, in order to probe the compositional and structural homogeneity of the superconducting layer. The time decay of the non-equilibrium magnetization has been performed in dc fields up to 9 T at 5 K $\leq T \leq$ 50 K. The presence of non-uniformities in the Y123 layer leads to a broadening of the T_c distribution. The very thin layer of the Y123 tapes allows investigating the T_c distribution from the M vs T curves, getting rid of screening effects. If a magnetic field $B_0 < B_{c1}(T)$ is applied parallel to the *ab*-plane after zero field cooling, the screening currents flow in the bulk of the superconducting layer, the field penetration length λ_c being comparable to the film thickness. The theoretical derivative dM/dT for a thin homogenous film in parallel field goes discontinuously to zero at $T = T_c$ [3], while the experimental dM/dT for coated conductors has a maximum at T_{peak} and decreases smoothly to zero for $T_{peak} < T < T_c$. This is the signature of a T_c distribution in the layer. The difference $\Delta T = |T_{peak} - T_c|$ can be approximately interpreted as the width of the T_c distribution. The histogram in Fig. 3 shows the width ΔT for the Y123 tapes of Theva, Bruker Adv. Supercon, SuperPower and AMSC. In order to compare the ability of these tapes to operate in persistent mode, we have measured the relaxation rates of the irreversible magnetization as a function of magnetic field, as shown in Fig. 3 for $T = 5$ K [3]. The Y123 tape from AMSC exhibits the lowest relaxation rates in the examined field and temperature ranges. In Fig. 4, the values of the relaxation rate at a given magnetic field $B = 5$ T at various temperatures are associated to the width of the T_c distribution. A correlation is observed: the inhomogeneities leading to the broadening of the superconducting tran-

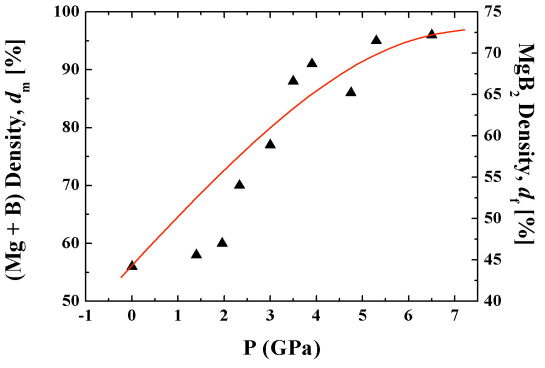

Figure 2: *Mass density in MgB_2 wires after compression.*

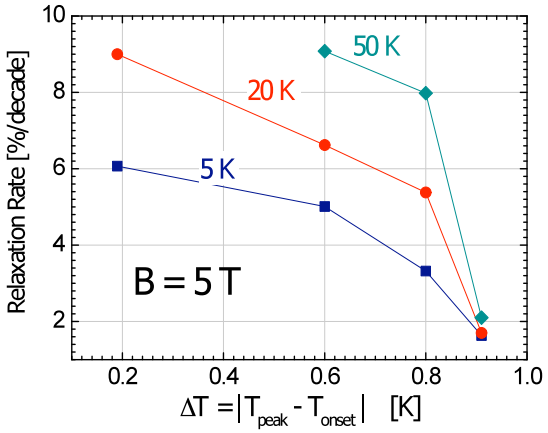

Figure 4: *Relaxation rates vs ΔT at various T for Y123 tapes.*

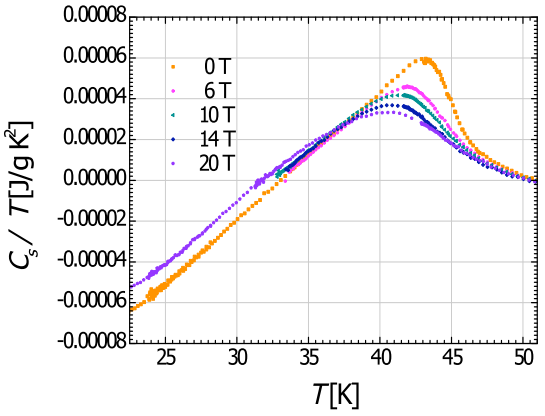

Figure 5: *Specific heat measurements of $SmFeAsO_{0.85}F_{0.15}$ at various fields up to 20 T.*

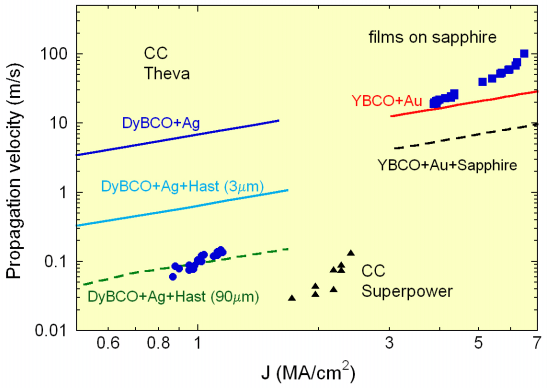

Figure 6: *Propagation velocity of the normal zone as a function of the applied current density for the CC (circle: from Theva, triangle: from Superpower) and the film on saphhire (square). The lines represent the simulations by the Dresner's model.*

sition are also responsible for the improvement of the pinning properties.

c) *Upper critical fields well above 100 T for $SmFeAsO_{0.85}F_{0.15}$ with $T_c = 46$ K* The dependence $B-T$ for a polycrystalline $SmFeAsO_{0.85}F_{0.15}$ sample was studied by means of high field calorimetry and by magnetization measurements. Specific heat measurements at magnetic fields up to 20 T (Fig. 5) allowed the determination of the $B_{c2}(T)$ curve [4]. The slope $|dB_{c2}/dT|_{T_c}$, extracted from the $B_{c2}(T)$ data for T_{max} is -5 T/K. The $B_{c2}(T=0)$ value derived from the WHH formula is 150 T, thus exceeding the BCS paramagnetic limit $B_p \approx 85$ T. The low value of the superconducting magnetic moment suggests the presence of "weak links", i.e. the current does not circulate through the entire sample, the observed granular behavior being analogous to that of high-T_c compounds. The granular behavior of our sample renders the correct estimation of J_c quite difficult, due to the uncertainties in the current carrying length.

1.2 Thin film based fault current limiter (*Ø. Fischer/M. Decroux*)

a) *Introduction* The fault current limiter (FCL) is a device which limits the current in the electrical network during a short circuit. Thanks to the fast superconducting to normal transition the FCL can limit the current in less than a ms. We have studied and successfully tested a FCL made of YBCO thin films grown onto sapphire. Since the production costs of this type of FCL are too expensive for a commercialization, we have shifted our activities on the study of FCL made of coated conductors (CC). The CC have a poor thermal behavior leading to very low quench mechanism and very low electric field, typically below 1 V/cm, compared to 20 – 40 V/cm in film on sapphire. To improve these characteristics one need to understand the behavior of the CC at high current densities and to compare it to the measurements of film on sapphire.

b) *Measurements and simulation* During this year we have tested CC produced by Theva, Ag(40 nm)/DyBCO(300 nm)/Hastelloy(90 μm) with $J_c = 0.9 - 1.8$ MA/cm^2, and by Superpower, Ag(2 μm)/YBCO(1 μm)/Hastelloy(100 μm) with $J_c = 2 - 3$ MA/cm^2. We have already reported some important differences between the CC and the film on sapphire, Au(50 nm)/YBCO(300 nm)/sapphire(0.5 mm) with $J_c = 2 - 3$ MA/cm^2. The flux flow resistivities in CC are almost 3 orders of magnitude higher than in the film on sapphire [5]. This might be explained by a different variety of interfaces present in these films. The switching behavior observed is also different; the film on sapphire stays in a very low dissipative state until a quick transition into a the normal state appears whereas in CC the line is in a high flux flow state and then there is a heating of the line up to the normal state [6]. The other important difference between the CC and the film on sapphire we have observed is the propagation velocity of the normal zone. This velocity is one of the key parameter of the FCL, fast quench propagation is a crucial issue for the homogenization of the dissipated power distribution along the tape. We have measured the propagation velocities in CC (from Theva and Superpower) and in the film on sapphire as a function of the applied current (scaled to DyBCO cross section) (Fig. 6) [6].
For the films on sapphire the velocities are

ranging from 20 to 100 m/s. On CC samples we have observed velocities which are 2 orders of magnitude smaller. In both CC samples, these velocities are ranging from around 4 to 14 cm/s. To simulate these velocities we have used an adiabatic model developed by Dresner [15] – we have checked that during our measurements the CC (Theva) and the film on sapphire are indeed in the adiabatic regime. The results from this model are presented in Fig. 6. For the DyBCO/Ag (CC) the simulated velocities are almost 2 orders of magnitude higher than the experimental results whereas for YBCO/Au the simulated values are close to the experimental results for current around J_c, but are too low for higher current densities. If the substrate is added (dashed line in Fig. 6) the simulated velocities decrease. For the CC the results fall right on the experimental values, but this is a pure coincidence since the penetration of the heat into the Hastelloy substrate at the front heat is only of the order of few μm. For instance the simulation with a thickness of the Hastelloy corresponding to a penetration depth of 3 μm is reported in Fig. 6. In this case the calculated velocities are almost one order of magnitude higher than the measured values. Since the thermal coupling between the substrate and the superconducting line is not perfect, we expect the results to be in between the YBCO and YBCO + Ag + Hastelloy (3 μm) curve. These simulations indicate that the Hastelloy substrate acts mainly as a heat sink which slows down the relatively high intrinsic velocities of the conducting bilayer. We clearly need to carry out more realistic simulations in order to highlight which parameter is susceptible to improve the experimental propagation velocities in CC and therefore to make possible to increase the electric field that a CC can sustain.

1.3 Modeling coated conductor fault current limiters (*M. Hasler*)

a) *Introduction* Up to now, second generation HTS, made of coated conductors (CCs), seem the most promising design for efficient resistive fault current limiters (FCLs). However, a detailed knowledge about their thermal and electromagnetic behaviors in the presence of over-critical currents is crucial for their improvement. In this context, we performed finite element modeling of coated conductors under over-critical current on several geometries. Accordingly, we have investigated the influence of the physical properties of the substrate on the quench propagation in CCs to improve the HTS-FCL design. By measuring the temporal increase of the voltage along CCs, it is possible to estimate the very slow normal zone propagation (NZP) velocity observable in these tapes [5, 6]. For the year 2008 we tried to compared experimental data with some coupled-FEM models made in the commercial package COMSOL multiphysics.(www.comsol.com).

b) *Simulation* Our geometrical model was based on commercial coated conductors available from Theva. The coated HTS tapes are made of four layers. A thick conductive substrate layer made of Hastelloy C276, which is usually electrically isolated from the HTS; a MgO buffer layer; a superconductive film made of $DyBa_2Cu_3O_7$ (DyBCO) and a silver stabilizer in electrical contact with the superconductor.
Heat diffusion through coated conductors should be as fast as possible in order to avoid apparition of burned spots with local destruction of the superconductor. However experimental measurements in YBCO tapes have shown that the NZP velocity in CC is not as fast as expected (in the range of 0.1 to 4 cm/s) and have poor thermal properties from a diffusion point of view [16, 17]; other recent experiments demonstrate that NZP in CC are strongly dependent on substrate thermal properties [5, 6]. Our simulations were done using a strictly-thermal model, i.e. we compute the temperature rise resulting from Joule heating in a nonlinear resistivity material (DyBCO), without considering Faraday's law and eddy current effects, which is easily justified here since the DyBCO layer is in a very resistive flux flow state even at time $t = 0$.
The thermal diffusivity is defined as:

$$\alpha = \frac{k}{\rho_m C_p} \qquad [m/s^2]. \tag{2.1}$$

To observe the effect of thermal substrate parameters on the NZP velocity (NZPV), we simulated substrates having the same mass density $\rho_m = 10'000$ kg m^{-3} but with different values of C_p and k, hence, having different thermal diffusivity α. Table 2.1 summarizes these thermal substrate parameters effects.
By studying the 3D temperature profile evolution for these different substrates, we have shown that low C_p values are responsible for a fast transition of the tape – facility to raise the temperature over the critical temperature – and high k values result in a faster spreading of heat (ability to conduct heat).
Table 2.1 proposed NZPV value that seems in disagreement with the last statement concerning k. As a matter of fact, for $C_p = 10$ J/kg K,

α (m^2/s)	C_p (J/kg K)	k (W/mK)	NZPV (cm/s)
1×10^{-5}	100	10	26
1×10^{-5}	**10**	**1**	**548**
1×10^{-5}	1000	100	4
1×10^{-3}	**10**	**100**	**381**
1×10^{-3}	1	10	1224
1×10^{-3}	100	1000	38

Table 2.1: *Effect of substrate thermal parameters on the NZP.*

we see that the NZPV is less important for $k = 100$ W/mK than for $k = 1$ W/mK. With $k = 1$ W/mK, the thermal conductivity of the substrate is seven times smaller than the thermal conductivity of the superconductor. In this case, heat travels mostly in the DyBCO layer until a sufficient temperature gradient is reached in the substrate, allowing heat transfer from the conducting layers (heat source) to the substrate.

In an attempt to understand by simulation the results obtained by Antognazza *et al.* [6], we compared the effect of two different substrates, i.e. sapphire and Hastelloy, on their switching behavior. Sapphire has a thermal diffusivity that is more than 1000 times larger than Hastelloy. With sapphire, both $\rho_m C_p$ and k increase the diffusion coefficient, i.e. $\rho_m C_p$ is smaller and k is larger than for Hastelloy. By comparing the NZP of these two tapes, we observed a NZPV approximately 20 times larger for the tape made of sapphire substrate.

Fig. 7 allows to observe the temperature and resistivity profiles in the z0y-plane for these two cases at the instant where complete transition of the tape made of sapphire occurred. The initial temperature in each case was that of liquid nitrogen, i.e. 77 K. As shown in (1-a), for sapphire, heat spread much more easily along the wire, heating up DyBCO, than for the tape made of Hastelloy (2-a), where heat is generated more locally. Fig. 7 (1-b) and (2-b) shows the resistivity map for both substrates. In the case of Hastelloy, only a partial transition is achieved in comparison to the sapphire case.

As expected from experiments realized in the Fischer/Decroux group [6], heat generated in the sapphire case remains low until a fast transition occurs. Once the heat generated reaches a threshold value, the low heat capacity of sapphire increases the temperature of the tape almost instantaneously to the critical value and to the maximum power generation ($t_{Sc}\rho_{Sc}]^2 = 3.9$ kW/cm^2). Then it seems that the fast spreading of heat in sapphire helps to uniformly switch the tape to the normal state. For the Hastelloy case, heat is generated almost directly after the beginning of the simulation but the full transition takes more time to reach. In fact, as we have shown in Fig. 7, the low diffusivity of Hastelloy results in a very localized heat generation. In this case, even if the tape has not completely transited (lower power generation), the local temperature could be high enough to induce damage in the superconductor.

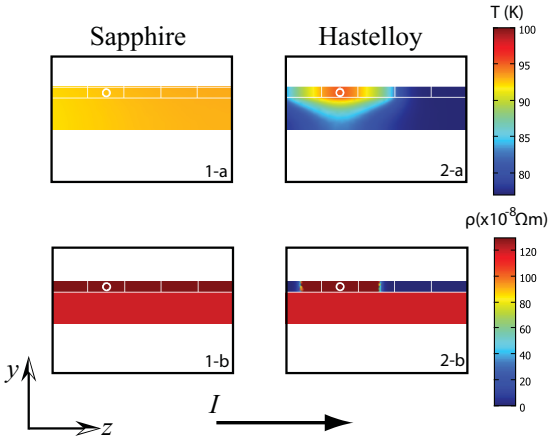

Figure 7: *Temperature (a) and resistivity (b) comparisons in the z0y-plane for tapes made of sapphire (1) and Hastelloy (2) once the full-transition is reached in the tape made of sapphire ($t = 2.6$ ms). For sapphire, heat spreads easily along the tape, avoiding local heating (1-a). The low heat capacity value of sapphire ensures a rapid transition of the whole tape (1-b). The initial normal zone is the white circle in each figure.*

1.4 Synthesizing Nanoscopic Boron (*R. Nesper*)

The fabrication of superconducting wires for industrial applications is always a challenge, which changes with each new superconducting material. Through exchange with R. Flükiger, we learned that nano particles would be the optimal basic ingredients for wire filling and pulling. The target compound is MgB_2. Therefore a two stage task was formulated: 1. synthesis of very pure nanoscopic boron; 2. if possible proceed to synthesize nanoscopic MgB_2.

The commercially available boron is useless for our undertaking. The synthesis of elemental boron in very pure form is an obstacle of its own as boron eagerly reacts with numerous elements and compounds forming very stable products. Especially oxygen impurities have to be reduced to the technically lowest possible content because all oxygen introduced into the MgB_2 formation process will lead to insulating

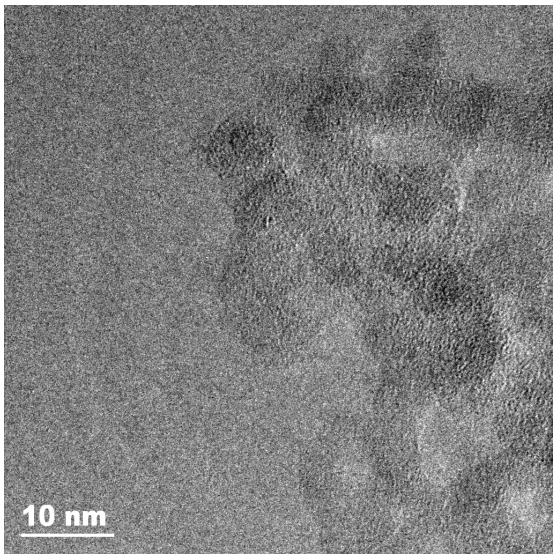

Figure 8: *Transmission electron micrograph of as synthesized nanoscopic boron (average diameter < 10 nm).*

MgO grains being nearly impossible to be extracted from the superconducting matrix. The first milestone has three goals: (A) high purity boron; (B) nano particles; (C) large homogeneity of particle size distribution. There are several textbook methods:

1. reduction by metals at high temperature (B_2O_3 + 3Mg $\rightarrow$ 2B + 3MgO) $\rightarrow$ 95 – 98% purity;
2. electrolytic reduction of fused borates or tetrafluroborates (KBF_4 in molten KCl/KF) $\rightarrow$ 95% purity;
3. reduction of volatile boron compounds by H_2 (BBr_3 + H_2)$\rightarrow$ highest purity;
4. thermal decomposition of boron hydrides and halides $\rightarrow$ highest purity.

Boron hydrides and boron halides have been chosen and tested as precursors but these routes have the disadvantage of employing highly reactive chemicals! To avoid Oswald ripening we investigated reactions of BBr_3 at room temperature:

1. using organic solvents such as hexanes: Na+BBr_3 $\rightarrow$ 3NaBr + B. This reaction delivers only very small yields;
2. without solvent: Na:K alloy + BBr_3 $\rightarrow$ B + NaBr + KBr.

Although the separation form the halides is not trivial we gain the targeted product in good yield (Fig. 8).

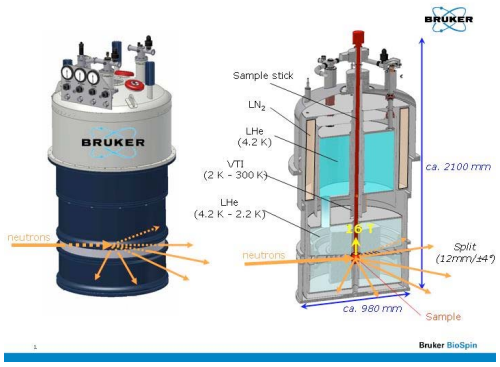

Figure 9: *Layout of the self-shielded 16 T split coil magnet system.*

An alternative way for purifying commercial boron was developed through our patented process [1]. Reaction of boron and lithium to LiB and successive extraction of lithium by use of benzophenone.
A successful route for the synthesis of nanoscopic MgB_2 was not developed in this research period.

1.5 Actively shielded 16 T magnet (*J. Mesot*)

Self-shielded solenoid magnets for high magnetic fields are today readily available for NMR with maximum fields up to 21 T and a room temperature bore of some centimeter diameter. However, for scattering methods (X-rays and neutrons), an axial access and room temperature is by far not satisfactory since these techniques and the associated science ask for access to most of the horizontal scattering plane and temperatures far below or above room temperature. Often, such magnets have to be operated in an environment with many other field-sensitive instruments which can only tolerate very low stray fields. Moreover, magnetic parts from the neutron source and instrument shielding might cause environmental magnetic forces that can lead to a significant degradation of unshielded magnets. "Off-the-shelf" split coil magnets nowadays reach 15 T but in most of the cases can only be operated at fields well below the maximum field due to the reasons mentioned above.
The close collaboration between a neutron laboratory with a large experience in magnetic scattering experiments and a manufacturer of commercial self-shielded NMR magnets provides a unique possibility to realize this demanding combination of self-shielding, high

[1] *Method for producing a superconducting material made of MgB_2*, WO 02071499, Sept. 2002

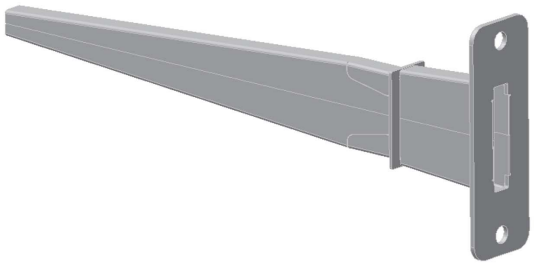

Figure 10: *Layout of the Cd-tunnel.*

magnetic fields and access to the scattering plane by a split coil arrangement.
During the design engineering phase, the specific problems of such a magnet, which is different from previously manufactured NMR or non-shielded split coil magnets, have been investigated and solved: split region (design, stability, radiation shielding, neutron transparency, activation), coil design (magnetic shielding, asymmetric mode, field distribution, stay fields) and the variable temperature inset (VTI) which has to be able to accommodate a wide range of custom made inserts (high and low temperatures). In Fig. 9 the layout of the magnet system is shown.
During the last year, many efforts have been done to reduce the neutron activation of the magnet system. Instead of the neutron absorbing coating (which encountered some technical problems) it has been decided to build a Cd-tunnel for the incoming neutron beam (Fig. 10), which allows a strong reduction of the neutron activation (Fig. 11).
The first magnet of this kind will be installed at the first 3^{rd} generation neutron source (SNS, Oak Ridge, USA) and will be available for Swiss users. The delivery of the magnet system is expected in summer 2009.

2 MaNEP sensors and security applications

2.1 Status quo in material preparation with narrow ESR line (*L. Forró*)

We have continued to look for an organic material suitable for measuring low magnetic field by electron spin resonance (ESR). This project is the fruit of a collaboration with Metrolab SA (which has a commercial product for high-field sensors) for elaborating a low magnetic field sensor based on ESR technique. Just to recall, the criteria for having a good ESR probe with narrow ESR line are the following:

- ESR linewidth < 100 mG (ideal 20 mG)
- Spin density $\geq 10^{26}$ m^{-3}
- Sample quantity 1 – 10 mm^3
- Isotropic line
- Working temperature 10 – 40°C
- Stable composition: Δg is defined better than 10 ppm
- Time stability (but it is not a high priority)
- Price $<$ 1000 CHF

The best candidates to satisfy these requirements are organic conductors, because of the weak spin-orbit coupling, the spin relaxation is slow. The promising candidate has been found in the family of quasi-onedimensional organic metals, Perylene-AsF_6 which have an ESR linewidth of 0.07 G . One single crystal

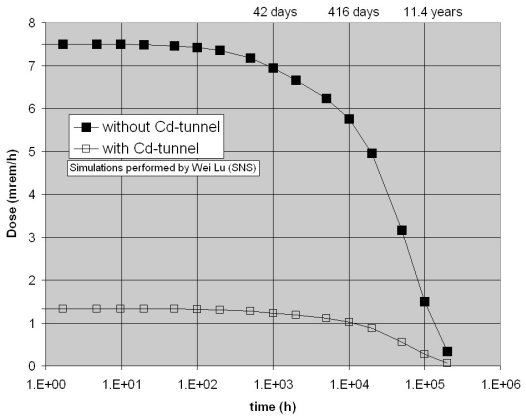

Figure 11: *Simulated neutron activation with/without Cd-tunnel (1-foot dose for the split magnet plates after 3 years of irradiation at SNS for a beam power of 2 MW).*

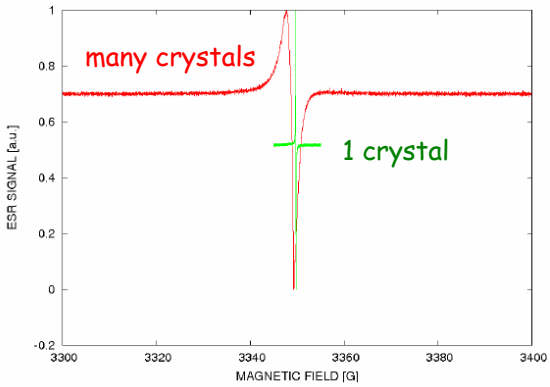

Figure 12: *ESR linewidth of a large number of Perylen-AsF_6 crystals (red) which shows a considerably broader line than one crystal of the batch (green) with a peak-to-peak linewidth of 0.07 G.*

has no sufficient intensity (Fig. 12) at 300 K to use it for sensing, so one needs to align hundreds of crystals. Unfortunately, the alignment is not perfect, and the resulting linewidth is 0.35 G. We have tried to synthesize a sister compound Fluoranthene-AsF_6, which has a starting linewidth of 0.02, and hoping that even unperfect alignment of a large quantity of crystals will give an overall linewidth narrower than 0.1 G. However, because of the incorporation of THF as a solvent in the crystals, it needs a low temperature synthesis ($-30°C$) which is getting installed in the laboratory. This issue will be fully addressed in the last six months of the project. This synthesis will be performed by a guest scientist, Dr. Rita Smajda from University of Szeged (Hungary).
We have tested graphene, the highlight of the last three years in condensed matter physics, if it has a suitable ESR signal for sensor applications. Despite the light, mono-component composition, its linewidth is too broad (4 G) at room temperature.

2.2 Gas detection with semiconducting oxides (*Ø. Fischer*)

There is a growing demand for devices performing selective and rapid detection of pollutants, both in urban and industrial environments. Resistive gas sensors are based on gas-induced changes in the electronic properties. Several sensing materials are available within the MaNEP network, and within this project we have studied the MoO_3 compound which is available in the shape of nanorods [7]. We have found that MoO_3 nanorods are very sensitive to a number of oxidizing and reducing gases, at temperatures between 250°C and 300°C. The response time is fast due to the large surface to volume ratio. In this report we point out another interesting feature of these 1D structures, namely the possibility of fabricating very small sensing structures by dip-pen lithography. The idea is to further minimize the thermal mass producing a connected but well-spaced array of nanowires. A very thin array of nanowires should allow for a quick penetration to the sensing interfaces and for a fast diffusion out of the device. The nanorods-based transducer was elaborated by combining 1) dip-pen lithography and 2) a mechanism based on flow-driven deposition of nanoparticles at the edges of drying drops [18]. Diluted solutions of nanorods have been deposited on alumina substrates with interdigital transducer gold electrodes. As the deposited liquid evaporates, the nanorods are driven to the edges by an outward liquid flow. This process produces a fine continuous pattern at the edge of the dried region (Fig. 13). A micropositioning XYZ stage was used to bring a fine capillary in close contact with the substrate and to monitor the deposition of the nanorods between the electrodes.
The measurement circuit uses an amplifier system that maintains a constant voltage on the nanorods pattern. We have found that the response time of these structures, from baseline to 90% signal saturation, is faster (less than 3 s) compared to dense layers of nanorods (about 6 s). The recovery time still appears to be much longer than the response time (Fig. 14). While the good accessibility of the nanorod/nanorod junctions may be responsible for the fast response time [19], these experiments suggest that the desorption process is intrinsically longer. However, for most applications, it is the gas detection that matters. And

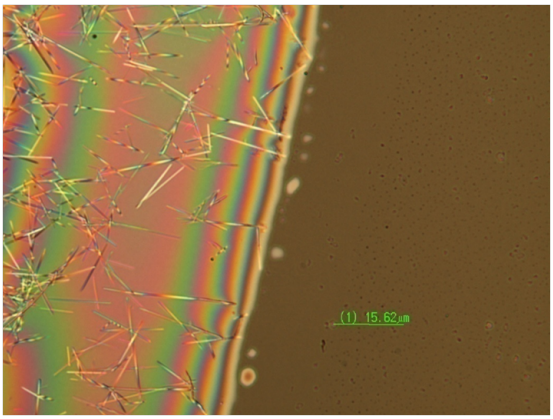

Figure 13: *Edge of a drying drop of distilled water containing MoO_3 nanorods. Flow-driven alignment of nanorods can be observed at the edge.*

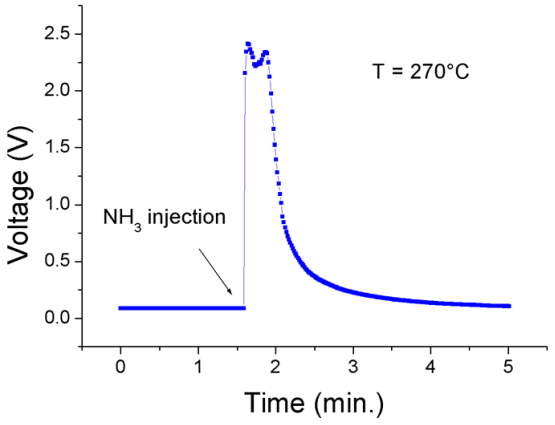

Figure 14: *Response of the MoO_3 nanorods-based transducer to the injection of NH_3 vapors. The sharp increase of the output voltage corresponds to a drop in the resistance of the sensing structure.*

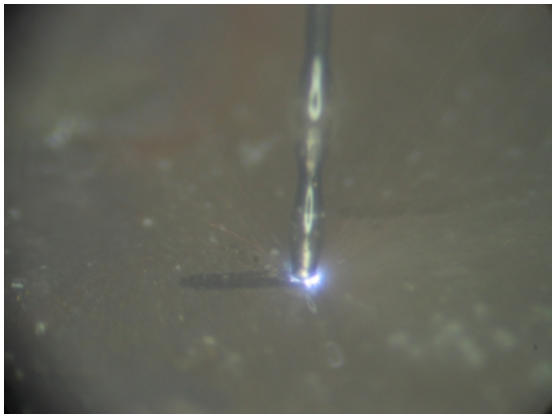

Figure 15: *A metal tip is brought to a well-defined distance of the surface of the sample. The process leaves a nanopowder-printed mark on the surface.*

the small thermal masses of nanorod transducers make them good candidates for battery powered portable devices.

2.3 Marking technology (CTI feasibility project)

This project uses a STM-inspired experimental setup to chemically mark small metal objects. Such parts (watches components, medical devices) remain difficult to mark by traditional methods because of the risk of structural or functional damage. In the studied technology [2], the applied voltage between the metal tip and the sample surface is monitored to produce electrical breakdown across a thin layer of a composite dielectric. We have been able to produce composite dielectrics with the required dielectric strength and marking properties. This was mainly achieved by doping with 1D metallic nanomaterials that are known to dramatically reduce the dielectric strength in insulators [20]. A close view of the process is shown in Fig. 15. We have demonstrated the feasibility of the technique, and constructed a working laboratory prototype.
The main physical parameters (voltage, current levels, gap sizes) driving the process have been identified. Hydrocarbon-based dielectrics (gels) mixed with several types of nanomaterials have been tested on various substrates. While the concentration of metallic additives has to be kept below the percolation threshold of conductivity, insulating compounds can be added in combination with small amounts of metallic dopants. This makes the range of possible compositions to achieve chemically encrypted signatures very large. Also, several technical alloys (stainless steel, Be-Cu, hard metals, gold alloys) have been successfully

[2] CTI feasibility project N° 8897.1

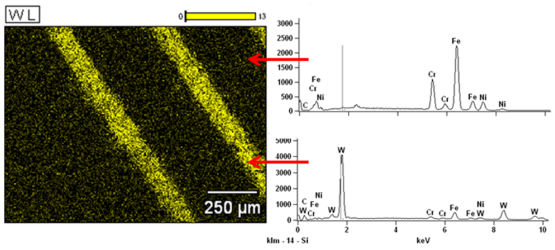

Figure 16: *Fine tungsten lines printed on a stainless steel surface. The lines are printed by horizontally scanning the tip over the surface.*

marked. Computer-driven scans of the tip over the surface result in continuous paths of a 'printed' alloy on the treated surface (Fig. 16).
The availability of modern, software controllable micropositioning tools, and the non-contact nature of the marking method, make the technology particularly appropriate for small, precise metal objects. This project will be continued as a regular CTI project with one industrial partner.

2.4 Giant piezoresistance in a metal-semiconductor hybrid (*C. Renner*)

a) *Sensitive strain gauge* The race for miniaturization demands ever smaller sensors of all kinds, including stress sensors. The demand for miniature sensors with the ability to measure minute strain is particularly acute for MEMS devices. The ability to measure very weak stresses is essential for atomic force microscopy (AFM) and AFM-derived biomechanical assays.
The automotive industry is also on the lookout for novel sensors. In this case an important requirement is to drastically reduce power dissipation. This requirement can be matched through more sensitive piezoresistive gauges with large signal to noise ratio enabling their operation at lower bias compared to state-of-the art devices.

b) *Giant piezoresistance metal silicon hybrid* The metal silicon hybrid (MSH) strain gauge we developed [8, 9] is shown in Fig. 17. It is a planar device fabricated using standard lithography from a boron implanted ($p = 1 \times 10^{17}\mathrm{cm}^{-3}$) silicon (001) wafer. The dimension b defines the distance from the four point measurement leads to the metal shunt (aluminum in the present case). The crystalline [110] direction is along the y-axis of Fig. 17. This is also the direction along which the mechanical tensile stress X is applied.
A number of devices with b ranging from 1 μm to 20 μm were fabricated and measured. The

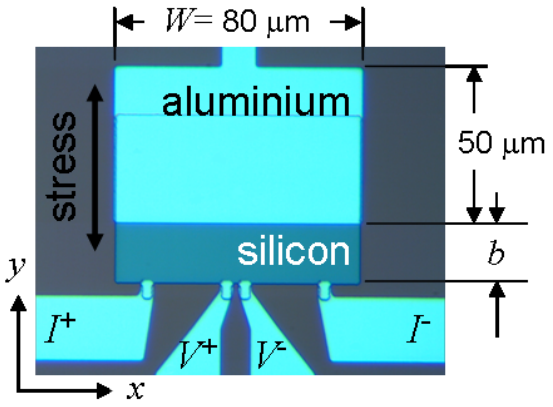

Figure 17: *False color SEM picture of a metal semiconductor hybrid strain gauge. x and y point along the* $[1\bar{1}0]$ *and* $[110]$ *silicon crystal axes respectively.*

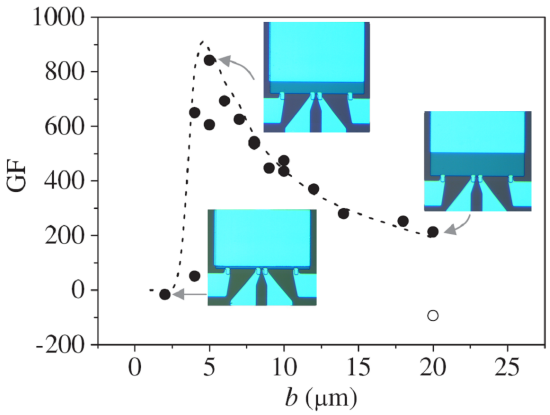

Figure 19: *Measured GF as a function of silicon width b. The dashed line is the calculated GF with no adjustable parameters.*

total resistance of the unstrained devices is monotonically increasing with b from about 200 Ω to 2000 Ω. The change in resistance ΔR as a function of strain for selected devices is shown in Fig. 18.

The gauge factor $GF = \frac{\Delta R}{R_0}\frac{1}{\varepsilon}$ as a function of device geometry shown in Fig. 19 exhibits a very non linear behavior. Note that it does not interpolate linearly between the values for silicon ($GF \approx -100$) and aluminum ($GF \approx 2$), but reaches a maximum value in excess of 800 for $b = 5$ µm.

The absolute value of the gauge factor is entirely controlled by the aspect ratio of the device. It stems from the silicon conductivity tensor $\tilde{\sigma}$ which becomes anisotropic under stress, a fact well known since the early 50's [21].

$\tilde{\sigma} = \sigma_0 \begin{pmatrix} 1+\delta & 0 \\ 0 & 1-\delta \end{pmatrix}$ where $\delta \approx \frac{X}{2}\pi_{44}$.

X is the stress applied along [110] and $\pi_{44} = 138.1 \times 10^{-11}\text{Pa}^{-1}$. The device works somewhat like a switch: a small fraction of the total current is directed away from the metal shunt as the stress on the silicon is increased. The effect on the resistance will be most pronounced when the current flow is concentrated along the silicon/metal shunt interface. This explains the sensitivity to the dimension b for a given width W of the device.

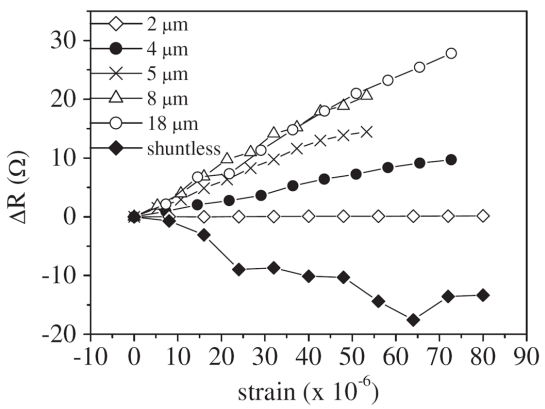

Figure 18: *Change in resistance ΔR as a function of strain for a number of devices with different b dimensions.*

c) *Prospects and caveat* The above experiments hold promise to enable the electric detection of sub-nanometer scale deflection of a micron sized cantilever typically used in AFM or biomechanical assays [22]. However, there is a caveat. The device relies on a four probe measurement: the closer the voltage probes are together, the larger the relative change in voltage drop becomes as a function of stress. But simultaneously, the voltage drop becomes very small, with the unfortunate consequence that it is very difficult to measure. This experimental observation was recently confirmed in a theoretical paper [23] which shows that the boost in gauge factor is always outweighed by the loss of signal to noise ratio in such a device, making it impractical for applications. There are nevertheless possibilities to use this device as a sensitive strain gauge in a two terminal setup which we are currently exploring.

The MSH strain gauge [8] did attract significant interest from the specialized press and the industry. A. Rowe, one of the key partner in the project, will do a theoretical proof of concept study for a specific device for *Freescale*. In Geneva we are actively seeking an industrial partner to develop an all electrical readout scheme for MEMS cantilever in collaboration with CSEM (*Centre suisse d'électronique et de microtechnique*, Neuchâtel). Such a development would be a major breakthrough in atomic force microscopy and biomechanical assays.

2.5 Hydrogen induced metal-insulator transitions (*K. Yvon*)

a) *Aim of project* Materials undergoing hydrogen induced metal-insulator (MI) transitions have the potential of being used as active elements in hydrogen detectors. Such devices will play a key role in mass markets of a future hydrogen economy, such as hydrogen powered fuel-cell vehicles and hydrogen production units for residential areas. This project aims at developing tailored sensing devices that are cheaper and more selective than those currently available. This will be achieved by preparing novel multi-component materials based on transition and rare-earth elements.

b) *Known materials* There exist essentially two groups of materials undergoing hydrogen induced MI transitions, rare-earth elements (R) such as Lanthanum, and transition metal (T) compounds such as Mg_2Ni and the recently discovered $LaMg_2Ni$ and La_2MgNi_2. The characteristics and mechanisms of their MI transitions are quite different. In the R–H systems the MI transition occurs at non-stoichiometric compositions (e.g. LaH_x: metallic for $x < 2.8$, insulating for $x > 2.8$) and generally lead to thermally rather stable hydrides, at least in the bulk (decomposition temperature at 1 bar hydrogen pressure $> 300°C$), whereas in the T-metal systems they lead to the formation of stoichiometric hydrides such as Mg_2NiH_4, $LaMg_2NiH_7$ [10] and $La_2MgNi_2H_8$ [11] that are thermally less stable (decomposition temperatures at 1 bar hydrogen pressure $< 280°C$). The reason why a MI transition in the La–H_x system occurs at the off-stoichiometric composition $LaH_{2.8}$ rather than at the stoichiometric composition LaH_3 as expected from simple bonding considerations is still under debate. A possibility that has not yet been explored is the occurrence of structural changes around H vacancies leading to the local formation of La^{2+}– La^{2+} bonds. As to d-metal systems, their MI transition correlates with the formation of hydrido-complexes having closed-shell electron configurations (mostly 18 electrons), such as $[NiH_4]^{4-}$ ($LaMg_2NiH_7$), or $[Ni_2H_7]^{7-}$ and $[Ni_2H_{12}]^{12-}$ ($La_2MgNi_2H_8$). For practical applications hydrogen-induced MI transitions need to occur at useful temperatures ($-20 - 50°C$) and hydrogen pressures (< 1 bar), and the transitions should be reversible. From this point of view, multi-component d-metal systems are of greater interest than R metal systems because the former are generally less stable (weak T–H bonds) than the latter (strong R–H bonds) and have a greater freedom for elemental substitution. Thus, in order to gain insight into the ways how the hydrogen induced MI transitions can be tailored to suit practical environments, attempts were made to model the metal environment of H vacancies in binary LaH_3, and to prepare quaternary RMg_2TH_7 analogues based on other rare-earth (R = La, Ce, Pr, Nd) and transition elements (T = Ni, Pd, Pt) in order to study their structural, electronic and thermodynamic properties.

T/R	La	Ce	Pr	Nd
Ni	x		x	x
Pd	x	x	x	
Pt	x			

Table 2.2: *Known RMg_2TH_7 analogues*

c) *$La_{32}H_{94}$ ($LaH_{2.94}$)* In order to investigate the influence of H vacancies on the electronic structure of stoichiometric LaH_3, total energy calculations by the density functional theory (DFT) formalism were performed on a cubic $2 \times 2 \times 2$ superstructure in collaboration with a group in Vienna [12]. Various hydrogen vacancy configurations were tested by allowing the metal atoms to relax around the vacancies. The lowest energy was found for a pair of hydrogen vacancies situated across the edge of adjacent metal octahedra, corresponding to the composition $La_{32}H_{94}$ (= $LaH_{2.94}$). Surprisingly, and in agreement with experiment, the band structure of this model displayed an energy gap. Furthermore, the electron density of the two upper most occupied bands showed maxima at the sites of the H vacancies. This result is consistent with La–La bond formation across the H vacancies, i.e. the presence of La^{2+}. The La^{2+}– La^{2+} bonds in H deficient LaH_{3-y} are reminiscent of the Ti^{3+}– Ti^{3+} and V^{4+}– V^{4+} bonds forming as a function of temperature in the Mott systems Ti_2O_3 and VO_2 .

d) *MI transition in $LaMg_2Pd$–H system and search for analogues* Attempts to prepare analogues to the nickel compound $LaMg_2NiH_7$ by substitution of Nickel by Palladium and Platinum, and of Lanthanum by other rare earths were successful (Table 2.2).
The palladium system $LaMg_2Pd$–H_x was studied in more detail with respect to electric resistivity and hydrogen absorption [13]. While the intermetallic compound is metallic, its hydride $LaMg_2PdH_7$ is insulating and contains tetrahedral $[PdH_4]^{4-}$ complexes. DFT calculations suggest a band gap of $\sim$1.0 eV and the presence of four 2-center-2-electron Pd–H bonds consistent with an 18 electron

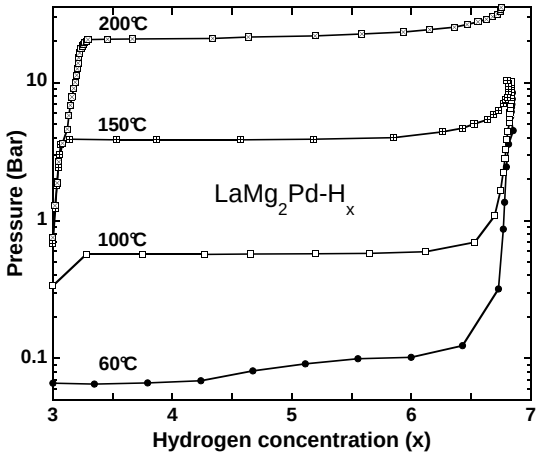

Figure 20: *Pressure-composition isotherms of $LaMg_2Pd$–H_x system for $3 < x < 7$ as measured during absorption.*

hydrido-complex centered by Pd in a d^{10} configuration. The enthalpy of hydride formation was measured from pressure-composition isotherms and found to be in a range suitable for applications (Fig. 20).
Interestingly, the data show the presence of an intermediate hydride phase at the approximate composition $LaMg_2PdH_{\sim 3}$. Its existence is an important asset for the design of hydrogen detectors because it tends to decrease the hydrogen concentration range over which the MI transition occurs, and thus has the potential of increasing the sensitivity of the detector.

e) *Conclusions and perspectives* The hydrogen induced MI transitions in the systems La–H_x and $R$$Mg_2T$–$H_x$ are associated with chemical bond formation (La^{2+}– La^{2+} bonds in LaH_{3-y}, T–H bonds in RMg_2TH_7). For the La–H_x system the persistence of a band gap at non-stoichiometric compositions LaH_{3-y} is presumably due to structural relaxations around hydrogen vacancies. These relaxations (and the concomitant presence of La^{2+} in the structure) will be confirmed by experiment. For the palladium system $LaMg_2Pd$–H_x the Pd–H bonds are associated with $[PdH_4]^{4-}$ complexes that form at temperature-pressure conditions that are closer to applications than those of the $[NiH_4]^{4-}$ complexes in the nickel system. Further members of the RMg_2TH_7 series will be investigated at lower temperatures and hydrogen pressures in order to explore their full potential for use in hydrogen detection devices.

3 Thin film preparation and applications

3.1 Neutron supermirrors (*J. Mesot*)

Polarizing supermirrors based on multilayer systems such as FeCoV/TiN_x are used in neutron instrumentation to provide a polarized neutron beam and to analyze the polarization of the scattered beam. An application of our optimized FeCoV/TiN_x supermirrors [24] is the polarization-analyzer for the HYSPEC spectrometer at the SNS (Oak Ridge, USA). The polarization analysis allows to distinguish between magnetic excitations and phonons. For polarization analysis covering the entire scattering region, a novel neutron optical system that covers a large angular range is required. We used a novel design consisting of a wedge-shaped stack of bend polarizing supermirrors. The analyzer-prototype consists of 30 glass-substrates coated on both sides with FeCoV/TiN_x polarizing supermirrors ($m = 3$) and was successfully tested on the instrument AMOR at SINQ, PSI (Figs. 21 and 22). For the

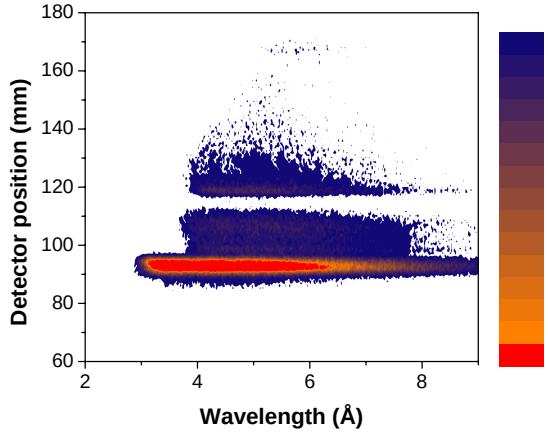

Figure 21: *Spin-up neutron intensity as function of position y and wavelength λ. The color bar express the neutron intensity in arbitrary units.*

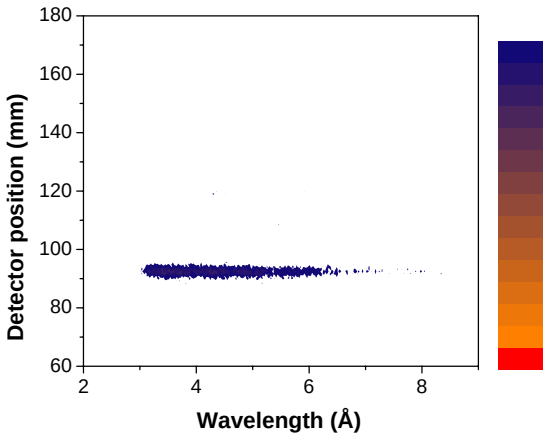

Figure 22: *Spin down neutron intensity as function of position y and wavelength λ. The color bar express the neutron intensity in arbitrary units.*

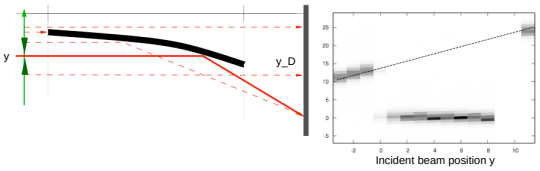

Figure 23: *Experimental characterization of the focusing device: For the fixed parabolic reflector the neutron beam was scanned along the y direction and measured by an area detector. The figure on the right side shows the corresponding map with intensities (white means zero, black maximum intensity) as a function of the incident beam position y and the position on the detector y_D.*

neutron wavelengths between 3 Å and 6 Å we obtained a beam polarization of ∼95%.

In addition, we designed and built a parabolically shaped reflector with a Ni/Ti-multilayer coating which is graded along the length of the device. Laterally graded mirrors have led to a marked improvement of X-ray diffractometers [25]. Neutron optics usually require a vertical thickness gradient to account for the variation of the incident angle given by the focusing geometry. These *supermirror* coatings provide a beam acceptance up to four times the total reflection of Ni. A drawback is their limited reflectivity for increasing angle of incidence: This is caused by non-specular scattering at rough interfaces and by absorption in the layers *on top* of the region in the supermirror actually fulfilling the scattering condition. If the neutrons to be focused have energies within a narrow band one can substitute a laterally graded multilayer with vertically non-varying layer thickness for the laterally homogenous supermirror. Usually the interface roughness increases from the substrate towards the interface with the number of layers. Thus with a multilayer one gains twice: only few interfaces might lead to diffuse scattering and these are even less rough compared to a supermirror. For this work we have designed and fabricated a parabolically bent device coated with a linearly graded multilayer. The bilayer thickness follows the varying angle of incidence to match the Bragg condition.

Measurements showed that this leads to higher reflectivity for monochromatic neutrons compared to the conventional supermirror coating. The measurements on the focusing properties of the device have been performed on the neutron reflectometer Morpheus at spallation neutron source SINQ (PSI). The beam was scanned in y direction relative to the parabola to get information of the reflectivity along x. In order to image the focused beam, a 2D detector with 256 × 128 pixels was used. Fig. 23 shows a sketch of the experimental set-up and a map with gray-scale encoded intensity as a function of the y-position of the incoming beam and the y_D-position of the reflected/direct beam. Due to the scanning the direct beam forms an inclined streak. For this measurement the wavelength was $\lambda = 4.7$ Å and the detector was located at the focal distance. A more quantitative analysis of the focusing effect includes the width and the divergence of the incoming beam: the device can focus a 8 mm wide parallel beam down to less than 0.8 mm at the focal point at $l = 250$ mm.

3.2 Epitaxial oxides on silicon (*J.-M. Triscone*)

Epitaxial oxides grown onto silicon have attracted considerable attention over the past decade, in part because of the need to replace SiO_2 as the dielectric layer in field effect transistors. Crystalline oxide–Si heterostructures can also be a way to integrate the variety of properties which is found in crystalline oxides, such as magnetism, ferroelectricity, and superconductivity, with modern Si device technology. The idea we are exploring here is to combine epitaxial piezoelectric heterostructures with silicon microfabriction techniques to provide a unique platform to realize piezo micro- and nano-electromechanical-systems (MEMS and NEMS).

To grow epitaxial perovskite thin films with robust piezoelectric response directly onto silicon, proper intermediate layers are required. Indeed, to fully realize the potential of this heterostructure, the interface must be atomically abrupt between the silicon and the oxide material despite their differences in bonding, chemistry, and coordination. Following the procedure developed by McKee *et al.* [26], we first grow an epitaxial $SrTiO_3$ (STO) layer on silicon by molecular beam epitaxy (MBE). The key point is the chemical passivation of the Si surface to oxygen: this is achieved by the deposition of half a mono-layer of alkaline Sr or Ba at high temperature. On this buffer layer, STO was grown in an oxygen pressure of 2×10^{-9} mbar by co-evaporation at low temperature and crystallized at 300 – 400°C in vacuum. The control of the deposition sequence is achieved by following the evolution of the surface reconstructions measured by reflection high energy electron diffraction (RHEED) [27]. This very complex process which includes sub-mono layer control and different surface reconstructions has been

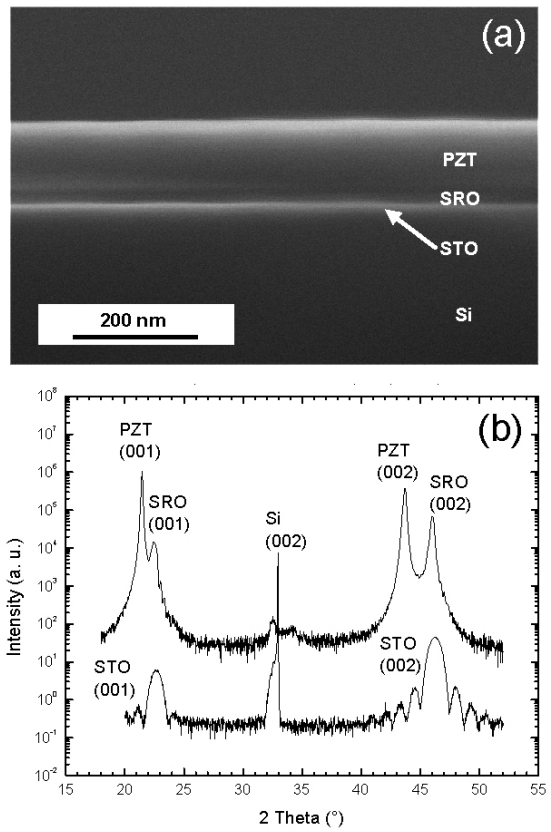

Figure 24: *Cross-sectional SEM image of epitaxial PZT/SRO/STO thin films grown on a Si(001) substrate; (b) $\Theta - 2\Theta$ X-ray diffractogram of such a structure.*

successfully implemented in Geneva. We thus control the whole material growth with the silicon buffer layers and the subsequent growth of metallic and piezoelectric layers on 2, 3 or 4 inches silicon wafers.

In a typical structure necessary for realizing MEMS, we first grow a 10 – 20 unit-cell thick STO layer onto 2" (001) Si wafers using MBE. Successively, we grow using off-axis magnetron sputtering a $SrRuO_3$ (SRO) film used as a bottom electrode and then a ferroelectric $Pb(Zr_{0.2}Ti_{0.8})O_3$ (PZT) layer [14]. A SEM picture of the typical final stack, PZT (200 nm)/SRO (30 nm)/STO (10 nm)/Si, is shown in Fig. 24a. X-ray Θ-2Θ diffraction spectra (Fig. 24b) display only (00l) peaks, confirming the c-axis orientation of the oxide structure and revealing a PZT c-axis lattice parameter of 4.13 Å. Finite size oscillations around (001) and (002) SRO reflections attest the high crystalline coherence of the bottom electrode. Rocking curve measurements reveal the good crystalline quality of the piezoelectric layer with a full width half maximum of 0.5° for the (001) PZT peak. Detailed diffraction

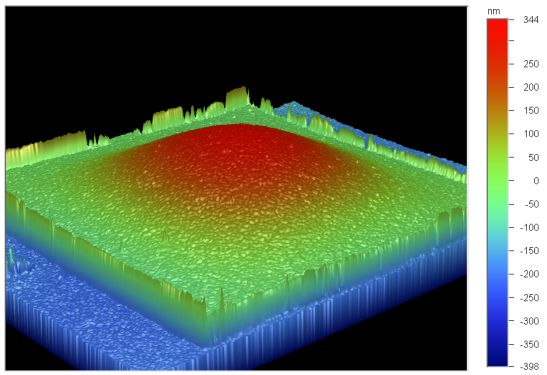

Figure 25: *3D reconstruction of a piezoelectric membrane under application of 3 V obtained with an optical interferometer microscope.*

analyses confirm the epitaxial relationship between the oxide layers and the substrate: PZT(001)‖SRO(001)‖STO(001)‖Si(001) and PZT[100]‖SRO[100]‖STO[100]‖Si[110]. Local measurements of the d_{33} piezoelectric coefficient [28], performed with an atomic force microscope, revealed that the piezoelectric coefficient d_{33} is of the order of 50 pm/V and the coercive field around 2 V. The same atomic force microscope allowed domains to be written and imaged in the ferroelectric PZT layer.

In collaboration with the Institute of Micro Technology (IMT) at the University of Neuchâtel (now EPFL), piezoelectric membranes were realized as proof-of-concept systems. The microfabrication steps have been optimized for such heterostructures allowing the processing of the front side (piezoelectric layer) and of the back side (silicon substrate). Fig. 25 shows an optical microscope view of a square membrane under an applied voltage of 3 V across the piezoelectric layer: the membrane deflects upwards from the flat 0 V position, demonstrating the successful realization of epitaxial MEMS. Since the growth of the materials and processing are now under control, we foresee a rapid development of several test MEMS.

4 Collaborative efforts

The collaborative efforts mentioned in the precedent report remained active for the last year of MaNEP phase II. We note however the new participation of K. Yvon in the domain of sensors. In the framework of Project 6, we can outline collaborative work between MaNEP teams as follows

- Superconducting wires: R. Flükiger (UniGE), R. Nesper (ETHZ) and D. Eckert,

Bruker BioSpin.

- Fault Current Limiter: Ø. Fischer, M. Decroux (UniGE), M. Hasler (EPFL) and M. Abplanalp, ABB.
- Sensors: Ø. Fischer (UniGE), J. Cors (UniGE), K. Yvon (UniGE), G. Patzke (UniZH) and Mecsens SA. L. Forró and Metrolab SA
- Thin film preparation: J. Mesot (PSI), J.-M. Triscone and Swissneutronics, J.-M. Triscone (UniGE), N. de Rooij (IMT-Neuchâtel) and the HES-EIG in Geneva.

MaNEP-related publications

[1] R. Flükiger, M. S. A. Hossain, and C. Senatore, arXiv:0901.4546 (2009).

[2] M. Hossain, C. Senatore, R. Flükiger, M. A. Rindfleisch, M. J. Tomsic, J. H. Kim, and S. X. Dou, *to be published in* Superconductor Science & Technology (2009).

[3] C. Senatore and R. Flükiger, *to be published in* Superconductor Science & Technology (2009).

[4] C. Senatore, M. Cantoni, G. Wu, R. H. Liu, X. H. Chen, and R. Flükiger, Physical Review B **78**, 054514 (2008).

► [5] M. Therasse, M. Decroux, L. Antognazza, M. Abplanalp, and Ø. Fischer, Physica C **468**, 2191 (2008).

► [6] L. Antognazza, M. Therasse, M. Decroux, F. Roy, B. Dutoit, M. Abplanalp, and Ø. Fischer, *to be published in* IEEE Transactions on Applied Superconductivity (2009).

[7] G. R. Patzke, A. Michailovski, F. Krumeich, R. Nesper, J. Grunwaldt, and A. Baiker, Chemistry of Materials **16**, 1126 (2004).

► [8] A. C. H. Rowe, A. Donoso-Barrera, C. Renner, and S. Arscott, Physical Review Letters **100**, 145501 (2008).

[9] A. C. H. Rowe, C. Renner, and S. Arscott, Piezoresistive strain sensor, French Patent #05 12740 (2005).

[10] K. Yvon, G. Renaudin, C. M. Wei, and M. Y. Chou, Physical Review Letters **94**, 066403 (2005).

[11] J.-N. Chotard, Y. Filinchuk, B. Revaz, and K. Yvon, Angewandte Chemie International Edition **45**, 7770 (2006).

[12] G. Schöllhammer, W. Wolf, P. Herzig, K. Yvon, and P. Vajda, Journal of Alloys and Compounds (2008), doi:10.1016/j.jallcom.2008.10.009.

[13] K. Yvon, J.-P. Rapin, N. Penin, Z. Ma, and M. Y. Chou, Physical Review Letters **446-447**, 34 (2007).

[14] S. Gariglio, N. Stucki, J.-M. Triscone, and G. Triscone, Applied Physics Letters **90**, 202905 (2007).

Other references

[15] L. Dresner, *Stability of Superconductors* (Plenum press, New York, 1995).

[16] J. W. Lue, M. J. Gouge, R. C. Duckworth, D. F. Lee, D. M. Kroeger, and J. M. Pfotenhauer, Advances in Cryogenic Engineering **614**, 321 (2002).

[17] X. Wang, U. P. Trociewitz, and J. Schwartz, Journal of Applied Physics **101**, 053904 (2007).

[18] R. D. Deegan, O. Bakajin, T. F. Dupont, G. Huber, S. R. Nagel, and T. A. Witten, Nature **389**, 827 (1997).

[19] J. W. Gardner, Sensors and Actuators B: Chemical **1**, 166 (1990).

[20] P. D. Beale and P. M. Duxbury, Physical Review B **37**, 2785 (1988).

[21] C. S. Smith, Physical Review **94**, 42 (1954).

[22] R. A. McKendry, J. Zhang, Y. Arntz, T. Strunz, M. Hegner, H.-P. Lang, M. K. Baller, U. Certa, H.-J. Guntherodt, and C. Gerber, Proceedings of the National Academy of Science of the USA **99**, 9783 (2002).

[23] O. Hansen, K. Reck, and E. V. Thomsen, Journal of Applied Physics **104**, 114510 (2008).

[24] M. S. Kumar, V. R. Shah, C. Schanzer, P. Böni, T. Krist, and M. Horisberger, Physica B **350**, e241 (2004).

[25] C. Morawe, P. Pecci, C. Peffen, and E. Ziegler, Review of Scientific Instruments **70**, 3227 (1999).

[26] R. A. McKee, F. J. Walker, and M. F. Chisholm, Physical Review Letters **81**, 3014 (1998).

[27] J. W. Reiner, K. F. Garrity, F. J. Walker, S. Ismail-Beigi, and C. H. Ahn, Physical Review Letters **101**, 105503 (2008).

[28] A. Lin, X. Hong, V. Wood, A. A. Verevkin, C. H. Ahn, R. A. McKee, F. J. Walker, and E. D. Specht, Applied Physics Letters **78**, 2034 (2001).

3 Knowledge and technology transfer

During year 8, we focused our efforts on attracting new research partners on board. New companies like Sécheron joined us and other ones for which collaboration seemed possible led to new opportunities which are currently being investigated. All collaborations with current partners will extend over to MaNEP Phase III, including Rolex. The bonds with the Geneva Economic Promotion generated positive results such as meetings, publications and invitations to events. The same is true with the other Geneva based NCCRs with whom excellent relationships exist. Two major future collaborations with industries are being discussed: one with ASULAB, the new cleantech arm of the Swatch Group and one with the CSEM which is still at an early stage. As this report indicates, intense networking continued to take place.

3.1 Knowledge transfer to the research community

3.1.1 MaNEP E-Newsletter

In the February 2009 issue of the MaNEP E-Newsletter several KTT related announcements were made:

MaNEP Alumnis. The launch of the MaNEP Alumni Group on LinkedIn (www.LinkedIn.com) was announced. This initiative aims at allowing all PhDs, Postdocs and Professors participating in MaNEP projects to connect on this popular social networking platform. LinkedIn was elected over other systems (Facebook, Friendster, Hi Five, etc.) for it is mainly used professionally. We also believe that this is an opportunity for the MaNEP management to connect with alumnis who are now in the industry.

Sécheron SA. A new collaboration with Sécheron SA was engaged, holding interesting promises for the future; MaNEP is helping Sécheron to develop a new generation of contacts for circuit breakers. If successful in this endeavor, MaNEP may, by means of a spin-off, be allowed to become a supplier for such contacts.

New MaNEP technology. The new Piezo-pinch technology developed by Prof. Renner of MaNEP was announced. This is a co-development between University of Geneva, the CNRS (France) and the *Ecole Polytechnique* (France).

Ozone sensor. Dr Jorge Cors presented the achievements of a inter-regional (Interreg IIIA) collaboration project about Ozone sensors for food quality applications.

Figure 1: *Editorial page of the fall issue of the WHY Geneva magazine with highlight on the chapter dedicated to the three Geneva based NCCRs*

3.1.2 WHY Geneva magazine

Thanks to the excellent relationships built by MaNEP KTT with the Geneva Economic Promotion authorities, MaNEP is now an integral part of the state of Geneva marketing policy to attract industries in the canton of Geneva . This awareness about our activities was initiated during year 7 together with the other two Geneva based NCCRs: *Frontiers in Genetics* and *Affective Science*. From the beginning it was our belief that there are useful synergies to leverage in different fields. As a consequence of the above, a full page of the 2008 issue of the *WHY Geneva* magazine (about Research and Education) was dedicated to MaNEP (Fig. 1).

3.1.3 Interview in Agefi magazine

In the March 2009 issue of the *Agefi* magazine, an interview of Matthias Kuhn was published, where he was asked to elaborate about applications of superconductivity in the field of Information and Communication Technologies (ICT). The Agefi is read by 118000 people (fr.wikipedia.org/wiki/Agefi_SA).

3.1.4 Industry seminars

We initiated MaNEP Industry seminars starting with a presentation of Schlumberger by Dr Claude Signer, Research Director Geology and Rock Physics on August 13, 2008. About 20 people (Professors, PhDs and Post-Docs) attended the seminar. The feedback was excellent with the following average scores on a 1 (extremeley poor) to 10 (excellent) scale: general impression: 8.4, usefulness: 8.4, speaker presentation skills: 9.1. The whole audience was interested in having more of such seminars.

3.1.5 MaNEP Posters

Two posters were prepared during year 8, the first for the Review panel visit in May 2008 (Fig. 2) and the second to advertise the Schlumberger Industry seminar(Fig. 3).

3.1.6 Participation in EU programs

The MaNEP research groups are involved in many European (EU) Programs. During year 8, at least ten EU Projects were in progress.

- Prof. G. Blatter
  ESF Research Networking Programme on

Figure 2: *Site visit: KTT poster (some logos were removed for confidentiality reasons)*

Figure 3: *Announcement poster for the Schlumberger industry seminar*

"Nanoscience and Engineering in Superconductivity" (NES), 2007 – 2012.

- Prof. G. Büttiker
  EU Marie Curie RTN "Fundamentals of Nanoelectronics", MCRTN-CT-2003-504574, May 2004 – May 2008.
  EU STREP project on "Sub kT Low Energy Transistors", SUBTLE, Oct. 2006 – Oct. 2009.

- Prof. T. Giamarchi
  Member of the steering committee of an ESF network (INSTANS) on strongly correlated systems.

- Prof. H. Keller
  "Controlling Mesoscopic Phase Separation" (CoMePhS), NMPS-CT-2005-517039, Contract Number 517039, June 2005 – May 2008 (36 months). Remark: This project has been extended till November 2008.

- Prof. J.-M. Triscone and Prof. P. Paruch
  STREP European Commission Project: "Manipulating the Coupling in Multiferroic Films" (Acronym: MaCoMUFi). Group of Agnès Barthélémy of the Unité Mixte CNRS-Thales, Palaiseau, Paris, France. Group of Josep Fontcuberta, Institut de Ciencia de Materials de Barcelona Campus, Universitat Autonoma de Barcelona Bellaterra, Barcelona Catalunya, Spain.

- Prof. C. Renner
  Collaboration with the London Centre for Nanotechnology, University College London, 2005 – 2008.

- Prof. J.-M. Triscone
  Project NANOXIDE, 2007 – 2009.
  Project TIOX (ESF) "Thin Films for Novel Oxides", 2003 –

- Prof. M. Sigrist
  COST Emergent behavior if Correlated Matter (ECOM), Cost (EU).

- Prof. D. van der Marel
  Project COST P16 - ECOM, 2005 – 2008

- Prof. Ø. Fischer
  ESF Research Networking Program – NES Nanoscience and Engineering in Superconductivity. "Single-photon nanostructured detectors for advanced optical applications", Sinphonia.

3.2 Knowledge transfer with the economy

3.2.1 Spin offs: Phasis Sàrl

Epitaxial gold thin films. PHASIS elaborates thin films with simplified machines inspired from research equipment, to produce cutting-edge microscopy substrates needed by industry. PHASIS high-quality thin films have attracted interest from chemists and biologists from around the world. At the atomic scale, a traditional glass or metal microscope slide would look like a pitted road, making the study of, say, a gene impossible. Instead, genomics labs use slides of epitaxially grown gold-coated thin films. Thin films developed by PHASIS are increasingly in demand by R&D labs. There are very few companies in the world making these films and PHASIS has an added advantage in the fact that it has grown out of a National Centre of Competence in Research (MaNEP) with an excellent reputation in the field of thin films and nanoscience.

Anti-counterfeit applications. PHASIS is also developing anti-counterfeit applications. Luxury goods of all kinds are subject to counterfeiting. PHASIS is working on ways to protect these goods, for example, fine watches, by engraving ultra-small, codified identification marks on the objects themselves. This technique uses tools and materials from nanotechnology, and provides a track-and-trace signature for authentication purposes.

3.2.2 Industrial mandates

Sécheron SA. Two mandates were performed by the team of Prof. Van der Marel for Sécheron SA. They consisted in investigating materials which had undergone failure. Based on this ongoing need, a service contract is being negotiated.

Bosch, Schott, BASF and Umicore. The group of Prof. Schlapbach at Empa is currently performing heat and electrical transport measurements for these companies.

3.2.3 Current industrial collaborations

ABB. The project on superconducting fault current limiters (SFCL) continued successfully

with the study of the behavior and the performance of superconducting tapes (coated conductors). As mentioned in the year 7 report, coated conductors perform much more poorly than the SFCL built on a sapphire substrate, mainly because they switch more slowly from the superconducting state to the resistive state. The latter generates a rapid heating of the SFCL which can lead to the destruction of the device. The research group is currently looking at solutions to allow a more uniform switching of SFCL made of such coated conductors.

Bruker BioSpin AG. The collaboration with Bruker continued with regard to the development of superconducting cables. Topics covered during year 8 where: (i) cold pressure densification of MgB_2 wires (Fig. 4) to increase the critical current density J_c and (ii) relaxation analysis of Y-123 coated conductors. A new CTI project was accepted and a patent was filed indicating the high level of inventiveness of the group of Prof. René Flükiger.

Swiss Neutronics AG. This collaboration continued well over year 8, with rewarding results in relation to the application of polarized neutron super mirrors. A Bruker Hybrid Spectrometer (HYSPEC) is currently being built at the spallation neutron source (SNS) of the Oak Ridge National Laboratory in Tennessee. The HYSPEC comprises a polarization analyzer which is the result of a cooperation between the Paul-Scherrer-Institute and the SNS. This analyzer uses polarized neutron supermirrors developed with Swiss Neutronics AG in the frame of MaNEP. SNS is an accelerator-based neutron source which, when at full power, will provide the most intense pulsed neutron beams in the world. It will be used for scientific research and industrial developments. With its polarization analyzer, HYSPEC will be the first polarized beam spectrometer in the SNS instrument suite (Fig. 5), and the first successful polarized neutron inelastic instrument at a pulsed spallation source in the world (neutrons.phy.bnl.gov/HYSPEC/).
Another important development in collaboration with Bruker is the actively shielded 16 T split-coil magnet for scattering methods (X-ray and neutrons): after the design review in January 2008, the magnet system has been manufactured and will be tested in the 2^{nd} quarter of 2009 both at Bruker and at PSI before its shipment to the USA. This will be the first magnet of this kind. It will be installed at the first 3^{rd} generation neutron source (SNS, Oak Ridge, USA) and will be available for Swiss users. The delivery of the magnet system is expected in summer 2009.

Figure 4: *Perioding cold pressing equipment at UniGE*

3.2.4 New industrial collaborations

Sécheron SA. Several meetings and visits took place. Sécheron SA is active in the area of dc and ac circuit-breakers for the rail industry. They expressed a need to improve contact materials in their devices. A collaboration contract has been signed in January 2009, worth CHF 17'839.

Rolex SA. During year 8, 3 extensions to the year 7 contract were signed. A 12 months col-

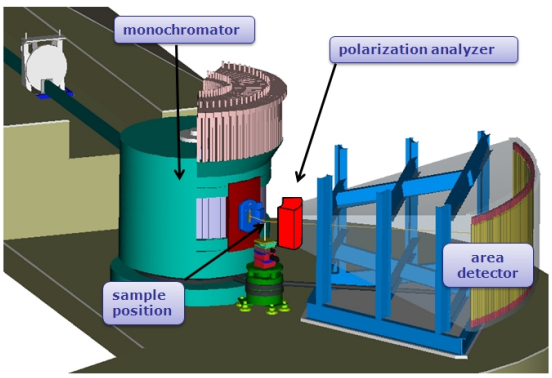

Figure 5: *In red, between the sample and the detector optionally a polarization analyzer can be installed which is part of a collaboration between SNS and PSI in the frame of MaNEP.*

laboration contract was also signed. It aims at optimizing industrialization parameters in relation to the materials studied in previous projects. The principal investigator is Dr E. Giannini, in the group of Prof. van der Marel.

3.2.5 Industry prospective iniatitives and outcome

Freescale. Several meeting with Freescale Semiconductors took place with the aim to identify fields for collaborative research. Freescale expressed a strong interest for our piezo-pinch technology (see section 3.3.2). This technology was developped together by three institutions: UniGE, CNRS (France) and *Ecole Polytechnique* (France); from the last meeting in November 2008, it looks like a collaboration will take place between Freescale and one of the other partners. The topic chosen, i.e. benchmarking automotive sensors, is best dealt in this way. MaNEP is more interested in developping the technology in the area of atomic force microscopy, biomedical assays and micro- and nano-balances. The CSEM (*Centre Suisse d'Electronique et de Microtechnique*, Neuchâtel), with whom discussions are actively taking place, looks like an excelent partner to this end.

CSEM. Discussions about a collaboration started in September 2008 on the topic of atomic force microscopy, biomedical assays and micro- and nano-balances based on the piezo-pinch technology mentioned above. The main reason why CSEM is very insterested in our sensor technology is that it provides a sensitivity level never achieved before and is both cost effective and energy efficient. A confidentiality agreement was signed in February 2009. The common goal is to find an industrial partner and start a triangular collaboration to develop the technology.

DuPont de Nemours. A visit on the DuPont de Nemours site in Genenva was organized in summer 2008 to discuss possible interests for a collaboration. Matthias Kuhn met the heads of the business units and presented MaNEP. As a follow up, a visit of MaNEP will be organized. A provisional brief was also received from DuPont to perform a high resolution SEM analysis of a polymer. Unfortunately, MaNEP is not equiped with such a device.

ABB. Several meetings took place to define the scope and the scale of our collaboration over MaNEP Phase III.

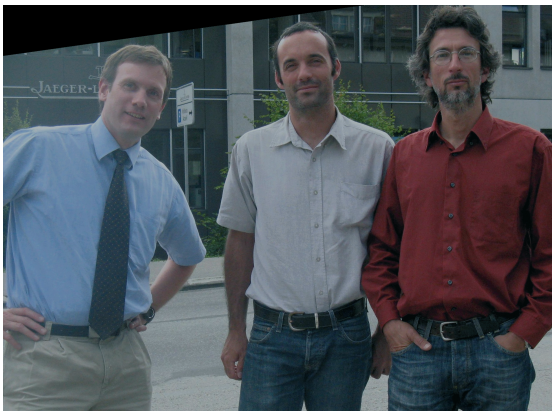

Figure 6: *Left to right: M. Kuhn, Dr J. Teyssier and Dr E. Giannini during visit at Jaeger-LeCoultre in Le Sentier*

Vacheron Constantin. The watchmaker has shown keen interest in MaNEP's surface and coating technologies. A project for Phase III has been elaborated.

ASULAB (Swatch Group). Several meetings took place to define a common project about hydrogen sensors. Swatch Group is now well aware of the expertise of Prof. Klaus Yvon of MaNEP in this domain. As an independent counselor to the European Union, Prof. Yvon is an ideal partner for the Swatch Group, both for research and for consulting. A large CTI project is being negotiated.

Jaeger-LeCoultre. During the summer of 2008, a visit of MaNEP was organized for the watch maker Jaeger-LeCoultre. Following a strong interest from their part in our expertise in thermal treatments, MaNEP received a research mandate which was discussed at the Jaeger-LeCoultre facilities in Le Sentier (Fig. 6). Jaeger-LeCoultre eventually decided to take another route to optimize their product.

Micronarc. This intercantonal promotion platform for micro- and nano- technologies in West Switzerland is active through the organization of forums and conferences. Micronarc also attends industry fairs, allowing member industries and academia to showcase their product under an attractive and uniform umbrella. MaNEP met with Edward Byrne, project leader at Micronarc to confirm our mutual interest to collaborate. A visit of MaNEP was organized in February 2009.

3.2.6 CTI projects

The following CTI projects went on or ended during year 8

- Prof. R. Flükiger – CTI project "Nb_3Sn strands with enhanced properties at high field for economically viable 1 GHz magnetic resonance magnets"
  Industrial partner: Bruker BioSpin, Fällanden (ZH).
  Start: 01.09.2007, end: 30.06.2010.

- Prof. Ø. Fischer – CTI Discovery Projects 8897.1 "Faisabilité d'une technique de marquage pour l'authentification d'objets métalliques".
  Start: 01.08.2007, end: 31.07.2008.

3.2.7 Seminars and conferences

CCMX Annual conference in Bern, April 2008. The aim of participating in the CCMX (Competence Centre for Materials Science and Technology) Annual Conference was to better understand how this consortium operates, especially from the KTT stand point. CCMX performs more applied research than MaNEP and thus is able to attract a larger number of industrial partners. CCMX offers various levels of participation to its industry partners: interested industries can either buy research tickets or become members of Club CCMX. At MaNEP, we obtain good results by selectively agreeing upon short term mandates based on industry needs. For larger scale research collaborations, we allow our partners to attend our Forum meetings; this gives them a deep insight into the latest developments taking place within MaNEP. Occasionally, we also organize MaNEP visits to selected industries or groups of industries (example in year 7: ADAEV, the *Association pour le Développement des Activités Economiques de la Vallée de Joux*).

Energissima Fair, Fribourg, April 2008. MaNEP was invited through the Alliance Consortium (www.alliance-tt.ch) to participate in this technology fair. The underlying goal for the organizers was to offer the opportunity to research institutions to rent a boot for the next editions.

TechConnect Boston, June 2008. Matthias Kuhn participated to the TechConnect meeting in Boston to promote University of Geneva technologies. During this trip, he seized the opportunity to present MaNEP at SwissNex in front of about 15 guests from the local industries and academia and to visit the research laboratory of Schlumberger, a global oilfield and information services company with a major focus on energy.

Toyota seminar, July 2008. This seminar was organized by Prof. Klaus Yvon of MaNEP. The speakers presented the impressive japanese hydrogen road map. One of the takeaways was that Japan is the only country in the world following simultaneously the various hydrogen storage routes: pressurized vessels, liquid hydrogen, solid hydrogen and composite solutions.

Micronarc Forum at Y-Park, October 2008. Micronarc is an intercantonal promotion platform for industries and academies of western Switzerland in the area of micro- and nanotechnologies. There is a mutual interest in closer collaboration. MaNEP is a major source of innovation and expertise. Micronarc aims at connecting companies and academic institutions.

Forum de l'innovation at EPFL, November 2008. This one day meeting gathers key players of the technology transfer arena in Western Switzerland and aims at discussing topics of interest to all. This year's topic was: *Le transfert de technologie académique: un service public ou un commerce ?*

Inforum, Hewlett-Packard, Geneva, March 15-17, 2009. MaNEP was invited by the Office of Economic Development and AlpICT (ICT cluster of Western Switzerland) to present a talk about superconductivity in telecom applications. It was an opportunity for Prof. Michel Decroux and Dr Louis Antognazza of MaNEP to explain that MaNEP is a key player at the national and international level in superconductivity research.

CEA visit, Grenoble. In August 2008, Matthias Kuhn joined a group of Technology Transfer specialists, including Mr Le Goff, head of CERN Technology Transfer and Laurent Miéville, President of the Association of European Science & Technology Transfer Professionals (ASTP), to visit *CEA-Valorisation*, the technology transfer agency of the CEA in Grenoble, France. There, the group met with the Director of CEA, Mr. Jean-Claude Guibert (Fig. 7). The CEA technology transfer pol-

Figure 7: *KTT visitors at CEA Valorisation visit. Mr J.C. Guibert is the third from the left.*

icy is entirely focused on bringing in new industrial partners. Means of achieving this include: keeping patents reserved for future industrial partners, launching spin-offs which will become future partners (example: ST-Microelectronics).

3.3 Applications, exploitation and commercialization of new ideas

3.3.1 Applications

ALPS software. The group of Matthias Troyer at ETHZ released the new versions 1.3.3 and 1.3.4 of the ALPS (Algorithms and Libraries for Physics Simulations) software together with open source licenses.

Flow cryostat mounte invention. On June 18, 2008, a new invention was announced, entitled "Flow cryostat mounte ultra compact superconducting magnet with THz radiation access". This invention was announced based on a working prototype. It stems from the group of Prof. D. van der Marel.

Nano-marking of metal parts. A STM inspired working laboratory prototype was built by Dr J. Cors and D. Matthey from the Prof. Fischer group at UniGE. This prototype, through a novel technique, allows the nano-marking of metal parts. This technology which is developed in the frame of a CTI project, is of high interest to various companies in the field of micro-technologies.

Epitaxial PZT on silicon for MEMS applications. The team of Prof. Triscone at UniGE optimized the process of epitaxially depositing PZT on silicon wafers to the point where quality is not an issue any more. With this major result, the team was able to produce 4 inch wafer prototypes from which MEMS can be made. This work is done in collaboration with the IMT (*Institut de Microtechnique*) in Neuchâtel which is now part of EPFL.

High-T_c superconducting single photon detector (SSPD) for telecom applications. A high-T_c superconducting (YBCO) single photon detector prototype was built by members of the Fischer group in Geneva. Rapid development of test MEMS are foreseen.

Low-T_c SSPD. The group of A. Schilling at the University of Zurich is also working on a SSPD. The group is now able to produce state-of-the-art single-photon detectors made of NbN. Starting from 5 nm thick NbN film with a T_c of 14 K this group prepared several detectors with different strip widths and filling factors. Such SSPD can detect photons in the wave length range from 500 to 2500 nm at least.

Cold high pressure densification of MgB_2 wires. The group of Prof. Flükiger at UniGE invented a new technology to increase the critical current J_c in MgB_2 superconducting wires. The method is called "cold high pressure densification". A working prototype was built.

3.3.2 Aquired intellectual property rights

Piezo-pinch strain sensor invention. On June 5, 2008 a European patent application (EP 07117587) was filled between University of Geneva, *Ecole Polytechnique* (France) and CNRS (France) entitled "Strain sensor with high gauge factor". A co-ownership agreement was consequently signed between the same institutions, defining the commercialization modus-operandi.

Procedure of Densifying Filaments for a Superconductive Wire. As an inventor, Prof. R. Flükiger filed this European patent for Bruker BioSpin AG, on October 1, 2008. Patent application number: SP09659EP

Material comprising finely layered heterostructures of oxide materials. An international PCT application was filed under the application number: CT/EP2008/061109. Filing date: August 26, 2008.

3.3.3 Miscellaneous

Jury MOT. November 2008: Matthias Kuhn was called as a juror at the Management of Technology (MOT) Masters Exam in Entrepreneurship at EPFL.

Jury Prix de l'Industrie Genève. January 2008: Matthias Kuhn was elected as a member of the Jury for the *Prix de l'industrie* from the *Chambre de Commerce et d'Industrie de Genève* (CCIG).

4 Education, training and advancement of women

4.1 Education and training

4.1.1 Doctoral School

The Geneva staff of PhD students

2008 was a year of renewal for the staff of PhD students in MaNEP-Geneva. Six of our students have obtained their PhD degree in 2008. Out of the remaining twenty-one students, ten were in their first year of studies at the end of 2008. This situation is due for one half to the establishment of three new research groups (Prof. Morpurgo, three students starting in 2008, Prof. Paruch, one student, Prof. Renner, one student). Apart from these new forces, seven students will in principle finish their studies in 2009. This means that during 2009 nearly 80% of the PhD students will be in their first or second year.

Teaching activities

In the 2008 autumn semester we have started our teaching program with two courses. The main course given by Dr C. Berthod is entitled *Applications of the Many-Body Formalism in Condensed-Matter Physics*. This course will last three semesters with the aim to realize the various idea developed in the previous progress report, in short: establish as tight a link as possible between the general many-body formalism and the various experimental techniques used within MaNEP. The first semester is just ending now, and has been devoted to the basic formalism itself. This part was followed by ten PhD students and five post-docs, who learned (or repeated) the concept of correlation functions, and the way to express and calculate them using the tools of second quantization and perturbation theory in imaginary time. This semester was actually too short to contain all the material the teacher wanted to put in, and some of this material will be distributed over the two next semesters. The second semester has started by a lesson of Claude Monney (UniNE and UniFR) about angle-resolved photo-emission spectroscopy (ARPES) and inelastic neutron scattering (INS), two experimental methods widely used within MaNEP, followed by a theoretical description of these techniques.
The second course was a one-semester course given by Prof. Markus Müller, visiting professor in the Department of Theoretical Physics at UniGE, and was entitled *Transport and Magnetism in Disordered Systems*. The ten to fifteen people who attended this course learned various important concepts governing transport and glassy ordering phenomena in disordered systems, such as Anderson localization, Coulomb gap and Coulomb glass, spin glass and random ferromagnets.
Aside from these courses, two tutorials have been organized over the last period. The first by Prof. René Monnier from ETHZ was entitled *Elements of Bandstructure Theory in a Nutshell*, and was followed by twenty people. The second, given by Dr Alexey Kuzmenko from UniGE, was an *Introduction to Infrared Spectroscopy of Solids*, and was attended by fourteen participants.
Finally, let us mention that twelve of the Geneva PhD students attended the MaNEP Saas-Fee Winter School in January 2009.

Recruitment

One of the purposes of the doctoral program is to attract students for a PhD thesis within MaNEP. Indeed, among the ten students who started in Geneva during 2008, only two obtained their Master degree from UniGE. In order to increase our chances of finding outstanding students, we made a first international call for applications in February 2008. We received forty-three applications from which we selected five candidates who were invited

for an interview. Unfortunately only three of them came, and none was finally hired. The main reason was some inadequacy between the personal affinities of the candidates and the research conducted in our labs. A second call launched in October 2008 is ongoing and promise to give better results. For this second call we received eighty-eight applications and invited four candidates of which three came for an interview. There are good chances that these three students will eventually perform their PhD studies in Geneva.

4.1.2 PhysiScope Genève

Summary

The PhysiScope was inaugurated on October 3, 2008, in the presence of state and University officials, including the Minister in charge of the Geneva department of public education and the Rector of the University of Geneva, and about 150 invited guests. This event concluded two years of preparation and marked the official exploitation debut of this unique communication and education tool, whose aim is to sway the younger generations into embracing a scientific career.

From PhysicsPark to PhysiScope

The past twelve months have been very eventful for MaNEP's education and communication initiative: the PhysicsPark was renamed PhysiScope, it received an original visual identity (Fig. 1) and a website (www.physiscope.ch). It all culminated in a festive official inauguration of the PhysiScope on October 3, 2008.
The purpose of the PhysiScope is to show junior high-school and high-school students from Geneva and beyond how fascinating science is via a hands on and playful discovery

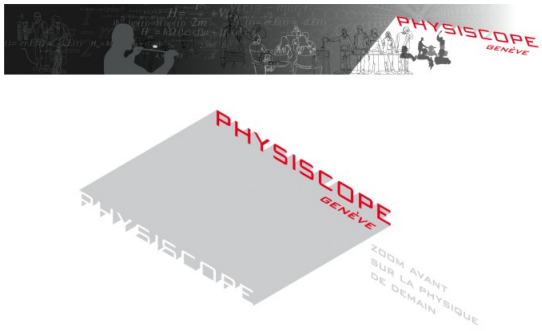

Figure 1: *Visual identity and logo designed by Judith Behar, l'Artichaut, Geneva.*

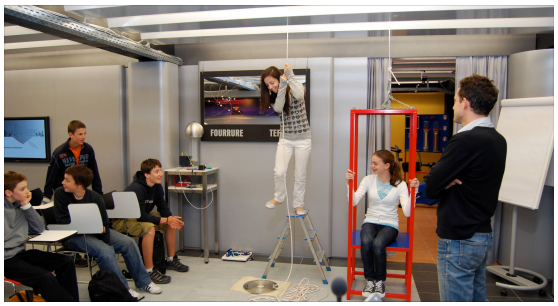

Figure 2: *Students playing with pulleys and forces.*

of Physics (Fig. 2). The aim is to contribute to halt the tendency of dwindling numbers in students embracing scientific studies observed world-wide [1].
The PhysiScope is operated and funded jointly by MaNEP and the Physics Section of the University of Geneva. Further funding is provided by private foundations, and we have the pleasure to report the continued support of the H. Dudley Wright foundation for the coming three years. We also secured a new sponsor, namely the Mark Birkigt foundation which is supporting two specific educational projects of the PhysiScope.
In 2008, the PhysiScope joined EuroPhysics Fun (EPF), a European network promoting the communication of Physics to the public in an original and entertaining fashion. EPF members meet once a year and the next workshop will be organized by the PhysiScope in Geneva from March 31 till April 4, 2009. These conferences give the opportunity to share experiences and discuss different ways of talking about physics to the general public.

Inauguration Day

On October 3, 2008, numerous invited personalities converged to the Physics Section to celebrate the official inauguration of the PhysiScope. The ceremony was organized in two stages. First, twenty-five selected guests were invited to the PhysiScope to live through a shortened version of a typical session. Distinguished guests included Charles Beer (Fig. 3), Minister in charge of the Geneva department of public education (DIP), Jean-Dominique Vassalli, Rector of the University of Geneva, Jean-Marc Triscone, Dean of the Faculty of Science, as well as members of the local government, schools, industry, funding agencies and the media. Subsequently, the PhysiScope was presented to over 120 guests in the main lecture

[1] C. Renner, *Hands-on inspiration for science*, Nature Materials **8**, 245 (2009).

Figure 3: *(left) Charles Beer, Minister in charge of the Geneva department of public education and (right) Gilles Marchand, director of the Télévision Suisse Romande (TSR) experiencing superconducting levitation on two distinct occasions.*

hall by Martin Pohl, president of the Physics Section. After an enthusiastic pitch about the future of MaNEP and its implication for the Physics Section by Øystein Fischer, the discussions continued around an aperitif. The inauguration was also a great opportunity to raise the public awareness of this initiative as well as MaNEP and the Geneva physics altogether, through several reports by the press and live interviews on *Radio Suisse Romande* and *World Radio Switzerland*.

Full steam ahead

During January 2009, the PhysiScope visitor count already passed the 1000 mark. The target audience of the PhysiScope are 12–19 year old students and so far about 40% of them were girls. We also performed for small children and adults (Fig. 3), and they all had a great time.
The immediate tasks awaiting the PhysiScope team are to develop novel presentations and activities dedicated to such a broad audience. In addition to the content, the team will also focus on issues such as presentation skills, show format and look of the demonstrations. This work is currently carried out by a team of seven PhD and postdoctoral assistants, in collaboration with four teachers. The latter are given half a day off every other week by the DIP to contribute to the PhysiScope, a most welcome support we hope to maintain in the future.
During the coming year, particular emphasis will be placed on building up new experiments and activities that are both original and attractive. We are also investigating ways to develop the communication skills of our presentation team to ensure a memorable and entertaining experience to all our visitors. Another task will be to establish and develop contacts with similar initiatives in Switzerland and abroad. Such interactions, initiated in 2008/2009 with *L'Espace des Inventions* in Lausanne and *Expo-Vision* in Fribourg, will enable the exchange of valuable know-how and ideas and possibly even some demonstrations. New funding will be sought to carry out all these tasks whose implementation is paramount to a successful long term operation of the PhysiScope.

Acknowledgements

The PhysiScope is very grateful to the H. Dudley Wright, Mark Birkigt and E. Boninchi foundations for their financial support. We also thank the Faculty of Science and the Geneva department of public education for their continued and encouraging support.

The PhysiScope team 2008/2009

Christoph Renner (president), Øystein Fischer, Martin Pohl, Jean-Gabriel Bosch, Olivier Gaumer, Anne Rougemont, Céline Corthay, Gauthier Alexandre, Augustin Baas, Elisa Fenu, Olivier Landry, Dook van Mechelen, Lidia Favre-Quattropani, Stefano Gariglio, Ruxandra Achimescu, Arnault Bardiot, Denis Boehm and Bernard Gisin.

4.1.3 Topical meeting

This year, on May 16, 2008 in the afternoon, one Topical meeting on *Iron Pnictides* was organized at the University of Fribourg. About 50 scientists participated in this informal and informative meeting, with scientific contributions from researchers at the ETHZ, UniFR, UniGE, UniBE, UniZH, and from PSI. The diverse results presented in this meeting covered many aspects of materials synthesis, single crystal preparation, spectroscopy, electronic structure and engineering strategies for novel superconducting materials. The discussions resulted in fruitful collaborations. These collaborations concern collaborative study and development of new materials sharing of experimental know-how and technologies. These collaborations are continuing until today and will be continued in the coming time.

4.1.4 MaNEP Winter School Saas-Fee 2009

Beginning of 2009, we organized the third MaNEP school. The first two schools hold in summer, but for the first time we organized it in winter since available dates in Saas-Fee were

Figure 4: *The building which welcomed the 2009 MaNEP winter school under a nice blue sky.*

Figure 6: *All the students listening with great attention to the lectures.*

in conflicts with the modification of the starting new academic year. Before the beginning of the school, one concern remained about the whether. Generally, January is quite dry and sunny. That rule was confirmed all over the week since a perfect blue sky has illuminated this school (Fig. 4).

The scope of this school was focused on the physics investigation of new electronic phases. This is a quite large scope, which has the advantage to cover almost all the scientific activities within MaNEP. From the survey realized after the second school in 2006, the participants made the statement that the MaNEP school had to be a school, not a conference. For this edition, we took care of these remarks and proposed a more compact school in term of subjects treated during the lectures (Fig. 5), with a substantially reduced number of lecturers. To achieve that, we identified within the scope of the school three basic courses where the lecturer got more time to developed in detail the basic concepts required for a good understanding. Profs. B. Battlog, M. Sigrist and J. Manhart did this job in a fantastic way. These basic courses were complements by three dedicated lectures, with the aim to present the state-of-the-art in this domain, given by Profs. K. Ensslin, A. Morpurgo and M. Rice. Finally our previous survey told us that the participants would appreciate some kind of practice. Therefore a practical lecture on band structure calculation was given by Prof. R. Valenti and the majority of the participants got for the first time the possibility to participate to the development of a band structure calculation.

The survey realized right at the end of this school showed that all the participants had

Figure 5: *Poster for the announcement of the 2009 MaNEP winter school in Saas-Fee.*

Figure 7: *Participants to the 2009 MaNEP winter school in Saas-Fee.*

greatly appreciate this school. Minors objections were made about organization and accommodation, but a large majority found that the winter school was just fantastic and that its organization in winter was a good idea that they would like repeated. The success of this edition came essentially form the high level of the lectures given during the week. Therefore we would like once again to thank warmly all the lecturers for the quality of the lectures they present during the school.
The school started on Sunday January 11 and ended on Friday January 16, 2009. Seventy students, postdocs and professors (Fig. 7) followed this school given by the seven lecturers. In addition three person from MaNEP administrative team took care of all the inherent problems related to the organization of such events. Mrs Marie Bagnoud and Mrs Sophie Griessen, new members of our administrative staff, took this opportunity to establish links within the MaNEP community.

4.2 Advancement of women

4.2.1 Summer internships

For the fifth year, the MaNEP internship program was organized for all the female students working in the institutions related to the MaNEP network (Fig. 8). In 2008 eleven candidates carried out their internship during the summer time; five at the EPFL, one at Empa, one at UniFR, and four at UniGE. All these internships were very successful since these young students were able to carry out very interesting projects. For several female students, the internship has convinced both parties to continue their collaboration at the PhD level. We would like to underline the effort made by all the project leaders and their collaborators and to thank them for their implication in this program for the promotion of women in sciences.
As it has been pointed out in the previous report, we intentionally do not restrict these internships to candidate interested to continue in domains related to MaNEP activities, but we offer this opportunity to all the female students. Our experience during the four previous years has shown that an indirect but very valuable impact of this program is also to give a chance to a candidate to test if the human and scientific environment of a research group corresponds to her expectation.
As in 2007, we asked the candidates to write down a short text describing their personal experience during this stay. For instance, did it improve their self confidence to manage research? Did it modify their career strategy? Many candidates think that these internships changed the vision they had before. Other candidates have continued an academic career in other domains outside of those covered by MaNEP. Nevertheless, we have a strong feeling that these internships give a unique opportunity to all these young talented female students to think themselves about their future. These internships correspond to a clear need. We are sure that all these students will keep in mind the chance that MaNEP gave to them.
Hereafter we summarize parts of the texts sent by 2008 internship students:

- How this will affect my future career is very clear to me: the fact that I now know how little I know makes it a logical choice to study more after my physics study. I already learned a lot from this internship, therefore I am confident that I will manage to learn enough to do scientific research.

Figure 8: *English version of the posters for the announcement of the Advancement of Women program.*

And thus, at the moment, I choose to apply for a PhD position, and not to be a very small part of a very large company.

- The internship did not change my career strategy very much, since I already had a very strong feeling that I would like to become PhD. I think that this internship will mostly attract women like me as this program is a very good step in choosing a career, but mostly in choosing a University, group and research topic for future scientific development.

Finally, all the female students who have participated to the 2008 internship received the new *Agenda 2009 des femmes/der Frauen* to remind them during 2009 that MaNEP did something specially dedicated for the women.

4.2.2 New developments

This year, we also started a deep thinking about what we could do more for the advancement of women. We have identified three levels at which we can play a part. First, at the high school level, we would like to arouse girl curiosity for sciences and in particular physics by specific programs, for instance in the frame of the PhysiScope. The second action addresses to the physics students at the universities and is already operating in the form of the summer internships. Thirdly we would like to think about female PhD students and Postdocs, in order to help them to conciliate professional and family life. To achieve this we need to have a quite precise overview about the way they are viewing these difficulties. Together with the Equality Office of the University of Geneva, we are preparing a survey that we will be send this spring to all the women researchers in MaNEP. The results of this survey are expected for the beginning of the summer and will guide us on the choice of further specific actions.

5 Communication & outreach

Year 8 has clearly marked an important shift in MaNEP's communication policy to a more strategic level: while maintaining a strong emphasis on public outreach activities, specific steps have also been taken to reach decision-makers and key-stakeholders, especially in Geneva. This shift reflects the challenges that go with the necessity for MaNEP to build a solid, supportive ground in order to pursue the scientific achievements in the coming 'post-SNF' era, while developing even closer connections with the community and the economy.

5.1 Stakeholders Management

5.1.1 Identification of stakeholders

At the beginning of 2008, the management and communication team engaged in a process of "stakeholders analysis" in order to have a clearer view of MaNEP's environment in terms of strengths, opportunities and potential 'threats'. This analysis provided precious data that are currently being processed in a new data base system (namely FileMaker Pro) that constitutes a tool for the management in its mission to find supports for MaNEP's activities in phase III and the 'post-SNF' era. The database has already been used during the organization of a first stakeholders-oriented event: the launch of the PhysiScope, on October 3, 2008.

5.1.2 Launch of the PhysiScope

The official launch of the PhysiScope (refer to section 4.1.2 for further details on the PhysiScope project) provided a great opportunity to reach many of the identified key-stakeholders. It took place in the presence of the minister in charge of the Geneva department of public education (DIP)(Fig. 1), the rector of the University of Geneva and some 150 other local and national 'VIPs' from different fields (public administration, media, politics, economics, education, fundraising, etc.). The event provided MaNEP's management with the opportunity – both through speech and one-to-one interactions – to not only point out MaNEP's pro-active attitude in its public outreach policy with the PhysiScope initiative, but also to focus on the crucial need to support the development of physics in the future, including the research, technology transfer and public outreach dimensions. Several of the contacts established during the launch have been followed by further meetings and discussions.

5.1.3 Networking

The shift to strategic communication also implies an increased need for networking for the management, for instance by taking part in

Figure 1: *The minister in charge of the Geneva department of public education (DIP) Charles Beer speaks at the PhysiScope's launch event.*

special events in innovation like the *Forum des 100*, on May 22, 2008. This event is organized by the Swiss weekly magazine *L'Hebdo* and takes place once a year. It gathers several hundreds key-players from different fields to discuss innovation issues in Switzerland.

5.2 Public outreach

5.2.1 New Art-Science Project

Over the last years, MaNEP's Communication and Outreach projects have intended to reflect the same creative attitude that is key to MaNEP's scientific achievements. So, after the *SupraFête* and the PhysiScope, MaNEP has initiated a new, original Art-Science Project. The project involves Swiss sculptor Etienne Krähenbühl, who is known for his special interest in metals with outstanding properties. This time, he is willing to try his talent at creating an unprecedented piece of art based on superconductors that will be set up at the Geneva School of Physics, where MaNEP has its headquarters. Etienne will be supported in his creative process by MaNEP physicists and one engineer. In addition a documentary will be filmed to immortalize these unique encounters between MaNEP science and Etienne's art. In 2008, three meetings have taken place to evaluate the project's feasibility on both sides (Fig. 2). An important launch event should be organized in December 2009, to conclude UniGE's 450^{th} anniversary celebrations

5.2.2 Partnerships with CERN

In 2008, MaNEP was a partner to two major public events at CERN. On April 4–6, the CERN organized Open Doors to celebrate the start of the Large Hadron Collider (LHC). Over 76'000 visitors gathered among which an estimated 15'000 enjoyed MaNEP's demonstration devices on superconductors: the new levitating SuperScooter (Fig. 3), the model Maglev train, the kids' levitating workshop, the superconducting bike, as well as the movie and the Mix & Remix exhibition created by MaNEP in 2007 to popularize superconductivity. In October, the whole set was again at CERN and starred during an interactive exhibition at the Globe (CERN's visitors center) called "Superconductivity: science or magic?". It lasted over 3 months (opening 2 days a week) and gathered some 3000 visitors, especially school chil-

Figure 2: *When art meets science: sculptor Etienne Krähenbühl discovers the magic of levitation with MaNEP physicist Dr Lidia Favre-Quattropani, in front of the cameras.*

Figure 3: *Young visitor enjoying the MaNEP levitating scooter at CERN's Open Doors, in April 2008. Source: CERN.*

dren and families.

5.2.3 Several other outreach activities in year 8

Prof. Jürg Hulliger at UniBE organized a special day on superconductivity for high-school students on November 22, 2008, using some of MaNEP's demonstration devices. It gathered about 90 people.
Several MaNEP experts were invited to give talks for the general public, like Prof. René Flükiger (Conference at the *Institut National Genevois*, October 7, 2008 – *Développement durable – Supraconductivité : fascination et applications réelles*) or Prof. Christoph Renner (Conference at the *Collège Rousseau*, Geneva, November 20, 2008 - *Nanotechnologies* and Conference at the *Institut National Genevois*, March 18, 2009 – *Les nanotechnologies sont parmi nous*).
MaNEP supported an exhibition on the 17^{th} and 18^{th} century Geneva scientists that was displayed at UniMail (Geneva), from April 8 to May 8, 2008.

5.3 MaNEP in the media

In 2008, we had two special highlights in our media coverage. The first one occurred in April 2008, with a press conference set up to present an important breakthrough on "improper ferroelectricity" published in *Nature* [1] by one of Prof. Jean-Marc Triscone's teams at UniGE. The media coverage was very satisfying, with newspapers as well as the radio and Swiss television showing interest. Though potentially rewarding, it is common knowledge that press conferences must only be held on rare occasions, as they are both time-consuming for all parts and only successful if used for truly appealing subjects in the view of journalists who have their own criteria in the matter – the discovery has to be accessible to non-specialist audiences, who must see how it might affect them and/or be an added-value for their day-to-day life/knowledge/entertainment, etc. – which are not easy to meet with fundamental research issues. This is also true with press releases, which have to be sent only on carefully chosen occasions.
These criteria were met again with the official launch of the PhysiScope (also read above in "Stakeholders Management"). Journalists requested to cover the event before and all had specific demands (visits, interviews, etc.) This resulted in numerous articles, as well as radio and Swiss television (*TSR*) coverage (the latter being usually the most difficult to obtain), all very positive and creating immediate reactions, with people calling/writing to express their approval, suggestions and/or interest in visiting the PhysiScope.
On another occasion, one feature published in MaNEP's e-Newsletter attracted the attention of the ATS (Swiss news agency) which resulted in several news items in the media. There again, the topic was clearly adapted to a general audience: it concerned new sensors based on nanomaterials studied at MaNEP, which were used to set up a new process to prolong the self-life of fruits and vegetables, a key issue for the food industry.

[1] E. Bousquet, M. Dawber, N. Stucki, C. Lichtensteiger, P. Hermet, S. Gariglio, J.-M. Triscone, and P. Ghosez, "Improper ferroelectricity in perovskite oxide artificial superlattices" Nature **452**, 732 (2008)

5.4 Website and e-Newsletter

As usual, MaNEP's website has undergone continuous improvements (in design and content) during year 8, although the French translation had to be postponed until spring 2009. This delay is due to a strong implication in important communication & outreach projects, as well as new strategic issues and target-audiences, all of which requested the communication officer's special attention. This also impacted on the frequency of the e-Newsletters in 2008. Two issues were sent during year 8, but we should be back to normal in year 9 with 4 to 6 issues. The last e-Newsletter (published on February 3, 2009) was longer in order to catch up on news and top publications.

6 Management

6.1 Activities

The NCCR MaNEP management bodies are the Forum assembly, the Evaluation Board, the Advisory Board and the Management Committee in Geneva.

- The **Forum** consists of all group leaders participating in the research projects in MaNEP. There are currently 34 members of the Forum. This year Alberto Morpurgo was appointed professor in Geneva and joined MaNEP in September 2008. At the end of last year, we appointed Professor Klaus Yvon as a new member. He is a specialist in hydrates and hydrogen storage. He joined the new collaboration planned with Swatch Group in Phase III.
  The Forum meets normally twice a year and is sometimes consulted by email by the MaNEP Director to gather suggestions or ideas concerning scientific topics, names of speakers for conferences, etc.

- The **Internal Evaluation Board** units all of the 6 scientific projects leaders plus 3 experienced members in an advisory capacity. This board met twice this year the last time on December 19, 2008 to discuss the plans for Phase III.

- The **Advisory Board** is composed of six well-known scientists for their specialized knowledge in the MaNEP fields. It was consulted for the pre-proposal and a next meeting is planned for autumn 2009.

- The MaNEP **Management Committee** in Geneva meets regularly to organize the various events.

Important changes took place in the MaNEP management during this year. After seven years as administrative manager, Isabelle Bretton decided to give her career a new orientation and left MaNEP in the autumn 2008. A new administrative manager, Marie Bagnoud, joined MaNEP on December 1, 2008. We also appointed a new executive assistant, Sophie Griessen and Pascal Cugni has taken care of MaNEP accounting on a temporary basis during most of this year. Anne Rougemont, the communication officer, shall leave MaNEP on May 1, 2009 and we are presently looking for a replacement. Anne will continue to look after certain communication projects for MaNEP until the end of 2009.
The main special tasks for MaNEP management this year has been to prepare the third phase. In addition to this, MaNEP has together with the Physics Section completed and inaugurated the new communication tool PhysiScope. This inauguration took place on Friday October 3, 2008 in the presence of the the Minister in charge of the Geneva department of public education, Mr Charles Beer, and the Rectorat of the University as well as numerous other personalities of Geneva. The PhysiScope has been financed mainly by private foundations: the H. Dudley Wright Foundation, the Ernest Boninchi Foundation and the Marc Birkigt Foundation. This ambitious realization is described in details in section 4.1.2.
The MaNEP management committee has organized the different following scientific meetings:

- The **Review Panel Meeting** took place in Geneva on May 20 and 21, 2008. The preproposal for the third phase was presented at that meeting.

- MaNEP **Internal Workshops** (one per MaNEP scientific project) were organized from Monday January 19 through Friday January 23, 2009 in Neuchâtel to discuss the progress of the six MaNEP projects. The MaNEP group leaders as well as some senior scientists well informed about their groups' contribution attended these workshops. These meetings also served as a

basis for the scientific reports written by the six project leaders in this 8^{th} MaNEP Progress Report.

- The 2009 MaNEP **Winter School** was organized from Sunday January 10 through Friday January 16, 2009 with sixty-five students and seven teachers. Besides eight members of the Management Committee were present.
- The management is actually preparing the next **Swiss Workshop on Materials with Novel Electronic Properties** to take place in Les Diablerets from Wednesday August 26 through Friday August 28, 2009. The Advisory Board is invited to be present at this meeting.

6.2 Experiences, recommendations to the SNSF

The combination of MaNEP hiring a new administrative manager on December 1, 2008 and the transition to NIRA 2 completed only end of February 2009 made it impossible to deliver the NIRA part (lists) together with this report.

As soon as we have been able to start introducing the data into NIRA 2, we shall contact the secretariat to find a date for the delivery of the NIRA part. We anticipate that NIRA 2 will produce more administrative efforts for MaNEP.

7 Reactions to the recommendations of the Review Panel

MaNEP thanks the Review Panel for the thorough analysis of MaNEP's activities. We are of course pleased and encouraged by the many remarks which show that we are on the right track. We have also extracted several points in the report where improvement can be realized and we comment on these below.

Added value

The documentation of added value is not straight forward since the reference point – the activity of the groups without MaNEP – is not available. We have this year added a separate list of publications common to two or several groups. Out of 304 publications, 30 are publications resulting from collaborations. This number is encouraging but could also be higher. The point here is that it takes time to build new relations which finally result in real collaborations. Of the many attempts of the groups to work together, not all result immediately in collaborations and common publications.
We believe that the reaction of our members to the reduced available funding is a strong signature of the added value of MaNEP. One can indeed think of a center as MaNEP in two ways.

1. MaNEP is a funding source like any other and only a way for the individual groups to get additional funds for their activity. From this perspective the natural thing to do when only very little funds become available as in the third phase of MaNEP, would be to loose interest in MaNEP and not use self funding to replace the lost SNSF funding, but to forget MaNEP and search for funds somewhere else. This was by the way the attitude adopted by the presidencies of ETHZ and EPFL when we approached them to get some extra funds to support the MaNEP network.

2. MaNEP is an essential organization, providing added value to the groups even in the absence of significant SNSF funding. Note that in the third phase the small SNSF funding would not justify the relatively heavy reporting duties for each group if seen only from a purely financial point of view.

The MaNEP members from all institutions have clearly chosen between these two views. First, all present members want to stay in MaNEP even if their financial funds from MaNEP are only about 35'000 Fr. per year, and, in some cases, zero. Second, a large number of external excellent scientists want to join MaNEP even if the financial benefits for each of them are also very small. Third, the groups have not only compensated the missing SNSF Funding but have actually added even more self funding so that the overall budget of MaNEP has strongly increased in Phase III in spite of the loss of about 9 MFr. SNSF funding. Thus the vote of the MaNEP members is clear: they consider the added value of MaNEP as an essential asset.

Collaboration with industry

MaNEP appreciates the positive comments about its efforts to establish collaborations with industry. But MaNEP is also aware of the weakness of the situation in that only very few group leaders actually contribute to this activity and that the retirement of Professor Flükiger represents a strong loss in this sense. His formal successor – Alberto Morpurgo – is for obvious reasons focused on advanced, more basic research, than the more applied activity of Prof. Flükiger. The *Département de physique de la matière condensée*, MaNEP's leading house, has started a process to find a thematic successor to Prof. Flükiger who will hopefully become the driver of future collaboration with industry in Geneva.

Advancement of women

The starting point of MaNEP in 2001 was that condensed matter science/electronic materials science in Switzerland did not have a top level

female scientist who would fit into MaNEP thematically. Thus from the point of view of advancement of women, MaNEP started from as low a level as possible. At the time there were also very few women at the intermediate level as well as at the student level. Compared to that, we are proud that we shall have three female professors among the full members in the third phase (Professor Patrycja Paruch, Professor Greta Patzke and Professor Anke Weidenkaff).

We are of course aware to be far from an optimal situation and that progress is slow. We shall thus continue the actions already launched and stimulate the students to take advantage of these opportunities, in particular the internships for women. The establishment of the PhysiScope we believe shall in the long run be an even stronger motor in promoting women careers in science.

As discussed with the review panel last year we have started a process to give a special mandate to a person with experience in advancement of women to give us advice for other actions and how to proceed to be even more efficient in promoting women in MaNEP. We are presently working with the Equality Office of the University of Geneva to search for such a person, possibly from outside Switzerland. We have put aside funds to hire such a person, which should happen sometimes this summer or at latest at the beginning of the autumn.

Recommendations to MaNEP

Future hirings We are fully aware that a strengthening of MaNEP should come through the hiring of a top scientist at the interface between fundamental and applied science. It is an area where it is difficult to find excellent candidates and we anticipate that it may take some time before the process in this direction can be successfully concluded.

Interaction between theorists and experimentalists Our new structure has been made to foster interaction between theorists, experimentalists and material scientists (crystal growth, thin films, ...). We shall try to make even more use of the Topical meetings, mixing these categories to further stimulate these interactions.

8 Lists

8.5 Publications over the last period

The following lists cover the period from April 1st, 2008 to March 31st, 2009:

1. Scientific articles in journals with peer review
2. Scientific articles in journals without peer review
3. Publications from lists 1 and 2 involving several groups

The fist two lists are sorted by the name of the group leaders. The most important publications are outlined by a red mark.

8.5.1 Scientific articles in journals with peer review

Group of Ph. Aebi

▶ C. Battaglia, K. Gaál-Nagy, C. Monney, C. Didiot, E. F. Schwier, M. G. Garnier, G. Onida, and P. Aebi
New Structural Model for the Si(331)-(12 x 1) Surface Reconstruction
Physical Review Letters **102**, 066102 (2009).
Group: Aebi / Project: 1

C. Battaglia, K. Gaál-Nagy, C. Didiot, C. Monney, E. F. Schwier, M. G. Garnier, G. Onida, and A. P.
Elementary structural building blocks encountered in silicon surface reconstructions
Journal of Physics: Condensed Matter **21**, 013001 (2009).
Group: Aebi / Project: 1

▶ C. Monney, H. Cercellier, F. Clerc, C. Battaglia, E. F. Schwier, C. Didiot, M. G. Garnier, H. Beck, P. Aebi, H. Berger, L. Forró, and L. Patthey
Spontaneous exciton condensation in $1T-TiSe_2$: BCS-like approach
Physical Review B **79**, 045116 (2009).
Groups: Margaritondo, Aebi, Forró / Projects: 1, 3

C. Battaglia, P. Aebi, and S. C. Erwin
Stability and structure of atomic chains on Si(111)
Physical Review B **78**, 075409 (2008).
Group: Aebi / Project: 1

C. Battaglia, H. Cercellier, C. Monney, M. G. Garnier, L. Despont, and P. Aebi
Unveiling new systematics in the self-assembly of atomic chains on Si(111)
Journal of Physics: Conference Series **100**, 052078 (2008).
Group: Aebi / Project: 1

Group of D. Baeriswyl

▶ D. Eichenberger and D. Baeriswyl
Superconductivity in the 2D Hubbard model: Electron doping is different
to be published in Physical Review B (2009), arXiv:0808.0433.
Group: Baeriswyl / Project: 2

Group of Ch. Bernhard

▶ A. J. Drew, J. Hoppler, L. Schulz, F. L. Pratt, P. Desai, P. Shakya, T. Kreouzis, W. P. Gillin, A. Suter, N. A. Morley, V. K. Malik, A. Dubroka, K. W. Kim, H. Bouyanfif, F. Bourqui, C. Bernhard, R. Scheuermann, G. J. Nieuwenhuys, T. Prokscha, and E. Morenzoni

Direct measurement of the electronic spin diffusion length in a fully functional organic spin valve by low-energy muon spin rotation

Nature Materials **8**, 109 (2009).

Groups: Bernhard, Keller / Project: 2

- J. Hoppler, J. Stahn, C. Niedermayer, V. K. Malik, H. Bouyanfif, A. J. Drew, M. Rössle, A. Buzdin, G. Cristiani, H.-U. Habermeier, B. Keimer, and C. Bernhard
  Giant superconductivity-induced modulation of the ferromagnetic magnetization in a cuprate-manganite superlattice
  Nature Materials (2009), doi: 10.1038/nmat2383.
  Group: Bernhard / Project: 2

C. Bernhard, L. Yu, A. Dubroka, K. W. Kim, M. Rössle, D. Munzar, J. Chaloupka, C. T. Lin, and T. Wolf
Broad-band infrared ellipsometry measurements of the c-axis response of underdoped $YBa_2Cu_3O_{7-\delta}$: Spectroscopic distinction between the normal state pseudogap and the superconducting gap

Journal of the Physics and Chemistry of Solids **69**, 3064 (2008).

Group: Bernhard / Project: 2

- A. J. Drew, F. L. Pratt, J. Hoppler, L. Schulz, V. Malik-Kumar, N. A. Morley, P. Desai, P. Shakya, T. Kreouzis, W. P. Gillin, K. W. Kim, A. Dubroka, and R. Scheuermann
  Intrinsic Mobility Limit for Anisotropic Electron Transport in Alq_3
  Physical Review Letters **100**, 116601 (2008).
  Group: Bernhard / Project: 2

- A. J. Drew, F. L. Pratt, T. Lancaster, S. J. Blundell, P. J. Baker, R. H. Liu, G. Wu, X. H. Chen, I. Watanabe, V. K. Malik, A. Dubroka, K. W. Kim, M. Rössle, and C. Bernhard
  Coexistence of Magnetic Fluctuations and Superconductivity in the Pnictide High Temperature Superconductor $SmFeAsO_{1-x}F_x$ Measured by Muon Spin Rotation
  Physical Review Letters **101**, 097010 (2008).
  Group: Bernhard / Project: 2

- A. Dubroka, K. W. Kim, M. Rössle, V. K. Malik, A. J. Drew, R. H. Liu, G. Wu, X. H. Chen, and C. Bernhard
  Superconducting Energy Gap and c-Axis Plasma Frequency of (Nd,Sm) FeAs $O_{0.82}F_{0.18}$ Superconductors from Infrared Ellipsometry
  Physical Review Letters **101**, 097011 (2008).
  Group: Bernhard / Project: 2

- V. Hinkov, D. Haug, B. Fraunqué, P. Bourges, Y. Sidis, A. Ivanov, C. Bernhard, L. C. T., and B. Keimer
  Electronic Liquid Crystal State in the High Temperature Superconductor $YBa_2Cu_3O_{6.45}$
  Science **319**, 597 (2008).
  Group: Bernhard / Project: 2

- J. Hoppler, J. Stahn, H. Bouyanfif, V. K. Malik, B. D. Patterson, P. R. Willmot, G. Cristiani, H. U. Habermeier, and C. Bernhard
  X-ray study of structural domains in the near surface region of $SrTiO_3$ substrates with $Y_{0.6}Pr_{0.4}Ba_2Cu_3O_7/La_{2/3}Ca_{1/3}MnO_3$ superlattices grown on top
  Physical Review B **78**, 134111 (2008).
  Group: Bernhard / Project: 2

- K. W. Kim, G. D. Gu, C. C. Homes, and T. W. Noh
  Bound Excitons in Sr_2CuO_3
  Physical Review Letters **101**, 177404 (2008).
  Group: Bernhard / Project: 2

- A. S. Mishchenko, N. Nagaosa, Z.-X. Shen, G. De Filippis, V. Cataudella, T. P. Devereaux, C. Bernhard, K. W. Kim, and J. Zaanen
  Charge Dynamics of Doped Holes in High T_c Cuprate Superconductors: A Clue from Optical Conductivity
  Physical Review Letters **100**, 166401 (2008).
  Group: Bernhard / Project: 2

- S. J. Moon, H. Jin, K. W. Kim, W. S. Choi, Y. S. Lee, J. Yu, G. Cao, A. Sumi, H. Funakubo, C. Bernhard, and T. W. Noh
  Dimensionality-Controlled Insulator-Metal Transition and Correlated Metallic State in 5d Transition Metal Oxides $Sr_{n+1}Ir_nO_{3n+1}$ (n=1, 2, and inf*)*
  Physical Review Letters **101**, 226402 (2008).
  Group: Bernhard / Project: 2

- L. Yu, D. Munzar, A. V. Boris, P. Yordanov, J. Chaloupka, T. Wolf, C. T. Lin, B. Keimer, and C. Bernhard
  Evidence for Two Separate Energy Gaps in Underdoped High-Temperature Cuprate Superconductors from Broadband Infrared Ellipsometry
  Physical Review Letters **100**, 177004 (2008).
  Group: Bernhard / Project: 2

Group of G. Blatter

- F. Hassler and S. D. Huber
  Coherent pumping of a Mott insulator: Fermi golden rule versus Rabi oscillations

Physical Review A **79**, 021607 (2009).
Group: Blatter / Project: 1

- S. D. Huber and A. Rüegg
  Dynamically Generated Double Occupancy as a Probe of Cold Atom Systems
  Physical Review Letters **102**, 065301 (2009).
  Group: Blatter / Project: 1

A. F. Albuquerque, H. G. Katzgraber, M. Troyer, and J. Blatter
Engineering exotic phases for topologically-protected quantum computation by emulating quantum dimer models
Physical Review B **78**, 014503 (2008).
Groups: Troyer, Blatter / Project: 1

- V. Dotsenko, L. B. Ioffe, V. B. Geshkenbein, S. E. Korshunov, and G. Blatter
  Joint Free-Energy Distribution in the Random Directed Polymer Problem
  Physical Review Letters **100**, 050601 (2008).
  Group: Blatter / Project: 1

- A. U. Thomann, V. B. Geshkenbein, and G. Blatter
  The dynamically asymmetric SQUID: Münchhausen effect
  Physica C **468**, 705 (2008).
  Group: Blatter / Project: 2

Group of M. Büttiker

- H. Förster and M. Büttiker
  Fluctuation Relations Without Microreversibility in Nonlinear Transport
  Physical Review Letters **101**, 136805 (2008).
  Group: Büttiker / Project: 1

- M. Moskalets, P. Samuelsson, and M. Büttiker
  Quantized Dynamics of a Coherent Capacitor
  Physical Review Letters **100**, 086601 (2008).
  Group: Büttiker / Project: 1

S. E. Nigg and M. Büttiker
Quantum to Classical Transition of the Charge Relaxation Resistance of a Mesoscopic Capacitor
Physical Review B **77**, 085312 (2008).
Group: Büttiker / Project: 1

- S. Ol'khovskaya, J. Splettstoesser, M. Moskalets, and M. Büttiker
  Shot Noise of a Mesoscopic Two-Particle Collider
  Physical Review Letters **101**, 166802 (2008).
  Group: Büttiker / Project: 1

- J. Splettstoesser, S. Ol'khovskaya, M. Moskalets, and M. Büttiker
  Electron counting with a two-particle emitter
  Physical Review B **78**, 205110 (2008).
  Group: Büttiker / Project: 1

Group of L. Degiorgi

- M. Lavagnini, M. Baldini, A. Sacchetti, D. Di Castro, B. Delley, R. Monnier, J. H. Chu, N. Ru, I. R. Fisher, P. Postorino, and L. Degiorgi
  Evidence for coupling between charge density waves and phonons in two-dimensional rare-earth tritellurides
  Physical Review B **78**, 201101(R) (2008).
  Group: Degiorgi / Project: 1

M. Lavagnini, A. Sacchetti, L. Degiorgi, E. Arcangeletti, L. Baldassarre, P. Postorino, S. Lupi, A. Perucchi, K. Shin, and I. R. Fisher
Pressure dependence of the optical properties of the charge-density-wave compound $LaTe_2$
Physical Review B **77**, 165132 (2008).
Group: Degiorgi / Project: 1

F. Pfuner, L. Degiorgi, K. Y. Shin, and I. R. Fisher
Optical properties of the charge-density-wave polychalcogenide compounds R_2Te_5 (R = Nd, Sm and Gd)
The European Physical Journal B **63**, 11 (2008).
Group: Degiorgi / Project: 1

Group of Ø. Fischer

- L. Antognazza, M. Therasse, M. Decroux, F. Roy, B. Dutoit, M. Abplanalp, and Ø. Fischer
  Comparison between the behavior of HTS thin film grown on sapphire and coated conductors for fault current limiter applications
  to be published in IEEE Transactions on Applied Superconductivity (2009).
  Groups: Fischer, Abplanalp, Hasler / Project: 6

J. Karpinski, N. D. Zhigadlo, S. Katrych, Z. Bukowski, P. Moll, S. Weyeneth, H. Keller, R. Puzniak, M. Tortello, D. Daghero, R. Gonnelli, I. Maggio-Aprile, Y. Fasano, Ø. Fischer, and B. Batlogg
Single crystals of $LnFeAsO_{1-x}F_x$ (Ln=La, Pr, Nd, Sm, Gd) and $Ba_{1-x}Rb_xFe_2As_2$: growth, structure and superconducting properties
Physica C (2009), doi:

10.1016/j.physc.2009.03.048.
Groups: Karpinski, Keller, Fischer / Projects: 2, 3, 4

F. Roy, M. Therasse, B. Dutoit, F. Sirois, L. Antognazza, and M. Decroux
Numerical studies of the quench propagation in coated conductors for fault current limiters
to be published in IEEE Transactions on Applied Superconductivity (2009).
Groups: Fischer, Hasler / Project: 6

R. T. Thew, N. Curtz, P. Eraerds, N. Walenta, J.-D. Gautier, E. Koller, J. Zhang, N. Gisin, and H. Zbinden
Approaches to Single Photon Detection
Nuclear Instruments and Methods in Physics Research A (2009).
Group: Fischer / Project: 5

B. M. Wojek, E. Morenzoni, D. G. Eshchenko, A. Suter, T. Prokscha, E. Koller, E. Treboux, Ø. Fischer, and H. Keller
Magnetism and superconductivity in cuprate heterostructures studied by low energy μSR
Physica B (2009), doi: 10.1016/j.physb.2008.11.189.
Groups: Fischer, Keller / Projects: 2, 5

► C. Dubois, G. Santi, I. Cuttat, C. Berthod, N. Jenkins, A. P. Petrović, A. A. Manuel, Ø. Fischer, S. M. Kazakov, Z. Bukowski, and J. Karpinski
Scanning Tunneling Spectroscopy in the Superconducting State and Vortex Cores of the β-pyrochlore KOs_2O_6
Physical Review Letters **101**, 057004 (2008).
Groups: Giamarchi, Fischer, Karpinski / Projects: 2, 3, 4

► P. Legendre, Y. Fasano, I. Maggio-Aprile, Ø. Fischer, Z. Bukowski, S. Katrych, and J. Karpinski
Unexpectedly wide reversible vortex region in β-pyrochlore $RbOs_2O_6$: Bulk magnetization measurements
Physical Review B **78**, 144513 (2008).
Groups: Fischer, Karpinski / Projects: 2, 3, 4

► G. Levy de Castro, C. Berthod, A. Piriou, E. Giannini, and Ø. Fischer
Preeminent Role of the Van Hove Singularity in the Strong-Coupling Analysis of Scanning Tunneling Spectroscopy for Two-Dimensional Cuprates Superconductors
Physical Review Letters **101**, 267004 (2008).
Groups: Giamarchi, Fischer, van der Marel / Project: 2

A. Piriou, Y. Fasano, E. Giannini, and Ø. Fischer
Effect of oxygen-doping on $Bi_2Sr_2Ca_2Cu_3O_{10+\delta}$ vortex matter: crossover from electromagnetic to Josephson interlayer coupling
Physical Review B **77**, 184508 (2008).
Groups: Fischer, van der Marel / Projects: 2, 3

► S. Seiro, Y. Fasano, I. Maggio-Aprile, E. Koller, O. Kuffer, and Ø. Fischer
Polaronic signature in the metallic phase of $La_{0.7}Ca_{0.3}MnO_3$ films detected by scanning tunneling spectroscopy
Physical Review B **77**, 020407(R) (2008).
Group: Fischer / Project: 1

► M. Therasse, M. Decroux, L. Antognazza, M. Abplanalp, and Ø. Fischer
Electrical characteristics of DyBCO coated conductors at high current densities for fault current limiter application
Physica C **468**, 2191 (2008).
Groups: Fischer, Abplanalp / Project: 6

Group of R. Flükiger

M. Hossain, C. Senatore, R. Flükiger, M. A. Rindfleisch, M. J. Tomsic, J. H. Kim, and S. X. Dou
Enhancement of J_c and B_{irr} of in situ MgB_2 wires and tapes alloyed with $C_4H_6O_5$ (malic acid) after cold densification
to be published in Superconductor Science & Technology (2009).
Group: Flükiger / Project: 6

C. Senatore and R. Flükiger
Correlation between superconducting transition width and relaxation rates in various industrial Y123 coated conductors
to be published in Superconductor Science & Technology (2009).
Group: Flükiger / Project: 6

R. Flükiger, C. Senatore, M. Cesaretti, F. Buta, D. Uglietti, and B. Seeber
Optimization of Nb_3Sn and MgB_2 wires
Superconductor Science & Technology **21**, 054015 (2008).
Group: Flükiger / Project: 6

R. Flükiger, D. Uglietti, C. Senatore, and F. Buta
Microstructure, composition and critical current density of superconducting Nb_3Sn wires
Cryogenics **48**, 293 (2008).
Group: Flükiger / Project: 6

C. Scheuerlein, M. Di Michiel, G. Arnau Izquierdo, and F. Buta

Phase transformations during the reaction heat treatment of internal tin Nb_3Sn Strands with high Sn content

IEEE Transactions on Applied Superconductivity **18**, 1754 (2008).

Group: Flükiger / Project: 6

C. Senatore, M. Cantoni, G. Wu, R. H. Liu, X. H. Chen, and R. Flükiger

Upper critical fields well above 100 T for the superconductor $SmFeAsO_{0.85}F_{0.15}$ with T_c = 46 K

Physical Review B **78**, 054514 (2008).

Group: Flükiger / Project: 6

Group of L. Forró

- C. Monney, H. Cercellier, F. Clerc, C. Battaglia, E. F. Schwier, C. Didiot, M. G. Garnier, H. Beck, P. Aebi, H. Berger, L. Forró, and L. Patthey

  Spontaneous exciton condensation in $1T-TiSe_2$: BCS-like approach

  Physical Review B **79**, 045116 (2009).

  Groups: Margaritondo, Aebi, Forró / Projects: 1, 3

- A. Akrap, R. Gaal, and L. Forró

  Resistive switching in β-SrV_6O_{15}

  The European Physical Journal B **61**, 287 (2008).

  Group: Forró / Project: 1

- A. Akrap, A. Rudolf, F. Rullier-Albenque, H. Berger, and L. Forró

  Influence of point defects on the metal-insulator transition in $BaVS_3$

  Physical Review B **77**, 115142 (2008).

  Groups: Forró, Margaritondo / Projects: 1, 3

M. Herak, M. Miljak, A. Akrap, L. Forró, and H. Berger

Magnetic anisotropy of paramagnetic and ferromagnetically ordered state of single crystal $BaVSe_3$

Journal of the Physical Society of Japan **77**, 093701 (2008).

Groups: Forró, Margaritondo / Projects: 1, 3

T. Ivek, T. Vuletić, S. Tomić, A. Akrap, H. Berger, and L. Forró

Collective charge excitations below the metal-to-insulator transition in $BaVS_3$

Physical Review B **78**, 035110 (2008).

Groups: Forró, Margaritondo / Projects: 1, 3

- B. Sipos, A. F. Kusmartseva, A. Akrap, H. Berger, L. Forró, and E. Tutiš

  From Mott state to superconductivity in 1T-TaS_2

  Nature Materials **7**, 960 (2008).

  Groups: Forró, Margaritondo / Projects: 1, 3

Group of T. Giamarchi

T. Jarlborg

Properties of high-T_c Copper Oxides from Band Models of Spin-Phonon Coupling

Journal of Superconductivity and Novel Magnetism **22** (2009).

Group: Giamarchi / Project: 2

- B. Thielemann, C. Rüegg, K. Kiefer, H. M. Rønnow, B. Normand, P. Bouillot, C. Kollath, E. Orignac, R. Citro, T. Giamarchi, A. M. Läuchli, D. Biner, K. Krämer, F. Wolff-Fabris, V. S. Zapf, M. Jaime, J. Stahn, N. B. Christensen, B. Grenier, D. F. McMorrow, and J. Mesot

  Field-controlled Magnetic Order in the Quantum Spin-Ladder System $(Hpip)_2CuBr_4$

  Physical Review B **79**, 020408(R) (2009).

  Groups: Giamarchi, Mesot / Project: 1

- C. Weber, A. Läuchli, F. Mila, and T. Giamarchi

  Orbital Currents in Extended Hubbard Models of High-T_c Cuprate Superconductors

  Physical Review Letters **102**, 017005 (2009).

  Groups: Giamarchi, Mila / Projects: 1, 2

- B. Barbiellini and T. Jarlborg

  Importance of Local Band Effects for Ferromagnetism in Hole-Doped La_2CuO_4 Cuprate Superconductors

  Physical Review Letters **101**, 157002 (2008).

  Group: Giamarchi / Project: 2

- E. Berg, E. G. Dalla Torre, T. Giamarchi, and E. Altman

  Rise and fall of hidden string order of lattice bosons

  Physical Review B **77**, 245119 (2008).

  Group: Giamarchi / Project: 1

- P. Chudzinski, M. Gabay, and T. Giamarchi

  Orbital current patterns in doped two-leg Cu-O Hubbard ladders

  Physical Review B **78**, 075124 (2008).

  Group: Giamarchi / Project: 2

- C. Dubois, G. Santi, I. Cuttat, C. Berthod, N. Jenkins, A. P. Petrović, A. A. Manuel, Ø. Fischer, S. M. Kazakov, Z. Bukowski, and J. Karpinski

Scanning Tunneling Spectroscopy in the Superconducting State and Vortex Cores of the β-pyrochlore KOs_2O_6

Physical Review Letters **101**, 057004 (2008).

Groups: Giamarchi, Fischer, Karpinski / Projects: 2, 3, 4

▶ M. Klanjšek, H. Mayaffre, C. Berthier, M. Horvatić, B. Chiari, O. Piovesana, P. Bouillot, C. Kollath, E. Orignac, R. Citro, and T. Giamarchi

Controlling Luttinger Liquid Physics in Spin Ladders under a Magnetic Field

Physical Review Letters **101**, 137207 (2008).

Group: Giamarchi / Project: 1

A. Kleine, C. Kollath, I. P. McCulloch, T. Giamarchi, and U. Schollwöck

Excitation in two-component Bose-gases

New Journal of Physics **10**, 045025 (2008).

Group: Giamarchi / Project: 1

▶ G. Levy de Castro, C. Berthod, A. Piriou, E. Giannini, and Ø. Fischer

Preeminent Role of the Van Hove Singularity in the Strong-Coupling Analysis of Scanning Tunneling Spectroscopy for Two-Dimensional Cuprates Superconductors

Physical Review Letters **101**, 267004 (2008).

Groups: Giamarchi, Fischer, van der Marel / Project: 2

G. León, C. Berthod, T. Giamarchi, and A. J. Millis

Hall effect on the triangular lattice

Physical Review B **78**, 085105 (2008).

Group: Giamarchi / Project: 1

▶ G. Roux, T. Barthel, I. P. McCulloch, C. Kollath, U. Schollwöck, and T. Giamarchi

Quasiperiodic Bose-Hubbard model and localization in one-dimensional cold atomic gases

Physical Review A **78**, 023628 (2008).

Group: Giamarchi / Project: 1

▶ C. Rüegg, K. Kiefer, B. Thielemann, D. F. McMorrow, V. Zapf, B. Normand, M. B. Zvonarev, P. Bouillot, C. Kollath, T. Giamarchi, S. Capponi, D. Poilblanc, D. Biner, and K. W. Krämer

Thermodynamics of the Spin Luttinger Liquid in a Model Ladder Material

Physical Review Letters **101**, 247202 (2008).

Groups: Giamarchi, Mesot / Project: 1

Group of M. Grioni

▶ G. Ghiringhelli, A. Piazzalunga, C. Dallera, T. Schmitt, V. Strocov, J. Schlappa, L. Patthey, X. Wang, H. Berger, and M. Grioni

Observation of Two Nondispersive Magnetic Excitations in NiO by Resonant Inelastic Soft-X-Ray Scattering

Physical Review Letters **102**, 027401 (2009).

Groups: Grioni, Margaritondo / Projects: 2, 3

M. Grioni, S. Pons, and E. Frantzeskakis

Recent ARPES experiments on quasi-1D bulk materials and artificial structures

Journal of Physics: Condensed Matter **21**, 023201 (2009).

Group: Grioni / Project: 1

▶ C. R. Ast, D. Pacilé, L. Moreschini, M. C. Falub, M. Papagno, K. Kern, M. Grioni, J. Henk, A. Ernst, S. Ostanin, and P. Bruno

Spin-orbit split two-dimensional electron gas with tunable Rashba and Fermi energy

Physical Review B **77**, 014007(R) (2008).

Group: Grioni / Project: 1

▶ E. Frantzeskakis, S. Pons, H. Mirhosseini, J. Henk, C. R. Ast, and M. Grioni

Tunable spin gaps in a quantum-confined geometry

Physical Review Letters **101**, 196805 (2008).

Group: Grioni / Project: 1

L. Moreschini, A. Bendounan, C. R. Ast, F. Reinert, M. Falub, and M. Grioni

Effect of rare-gas adsorption on the spin-orbit split bands of a surface alloy: Xe on Ag(111)−$(\sqrt{3}\times\sqrt{3})R30°$-Bi

Physical Review B **77**, 115407 (2008).

Group: Grioni / Project: 1

▶ D. Pacilé, M. Papagno, A. Fraile-Rodríguez, M. Grioni, L. Papagno, C. O. Girit, J. C. Meyer, G. E. Begtrup, and A. Zettl

Near-edge x-ray absorption fine-structure investigation of graphene

Physical Review Letters **101**, 066806 (2008).

Group: Grioni / Project: 1

Group of M. Hasler

▶ L. Antognazza, M. Therasse, M. Decroux, F. Roy, B. Dutoit, M. Abplanalp, and Ø. Fischer

Comparison between the behavior of HTS thin film grown on sapphire and coated conductors for fault current limiter applications

to be published in IEEE Transactions on Applied Superconductivity (2009).

Groups: Fischer, Abplanalp, Hasler / Project: 6

F. Roy, M. Therasse, B. Dutoit, F. Sirois, L. Antognazza, and M. Decroux
Numerical studies of the quench propagation in coated conductors for fault current limiters
to be published in IEEE Transactions on Applied Superconductivity (2009).
Groups: Fischer, Hasler / Project: 6

▶ F. Roy, B. Dutoit, F. Grilli, and F. Sirois
Magneto-thermal finite element modeling of 2nd generation HTS for FCL design purposes
Journal of Physics: Conference Series **97**, 012286 (2008).
Group: Hasler / Project: 6

F. Roy, B. Dutoit, F. Grilli, and F. Sirois
Magneto-Thermal Modeling of Second-Generation HTS for Resistive Fault Current Limiter Design Purposes
IEEE Transactions on Applied Superconductivity **18**, 29 (2008).
Group: Hasler / Project: 6

▶ F. Sirois, M. Dione, F. Roy, F. Grilli, and B. Dutoit
Evaluation of two commercial finite element packages for calculating AC losses in 2-D high temperature superconducting strips
Journal of Physics: Conference Series **97**, 012030 (2008).
Group: Hasler / Project: 6

Group of J. Hulliger

▶ J. B. Willems, J. Albrecht, I. L. Landau, and J. Hulliger
Superconducting phase formation in random neck syntheses: a study of the Y-Ba-Cu-O system by magneto-optics and magnetometry
Superconductor Science & Technology **22**, 045013 (2009).
Group: Hulliger / Project: 4

▶ J. B. Willems, D. Pérez, G. Couderc, B. Trusch, L. Dessauges, G. Labat, and J. Hulliger
Magnetic extraction of superconducting grains from ceramic combinatorial syntheses
Solid State Sciences **11**, 162 (2009).
Group: Hulliger / Project: 4

I. Landau
Comparison of the scaling analysis of mixed-state magnetization data with direct measurements of the upper critical field for $YBa_2Cu_3O_{7-x}$
Journal of Physics: Condensed Matter **20**, 275229 (2008).
Group: Hulliger / Project: 4

I. L. Landau, J. B. Willems, and J. Hulliger
Detailed magnetization study of superconducting properties of $YBa_2Cu_3O_{7-x}$ ceramic spheres
Journal of Physics: Condensed Matter **20**, 095222 (2008).
Group: Hulliger / Project: 4

Group of J. Karpinski

Z. Bukowski, S. Weyeneth, R. Puzniak, P. Moll, S. Katrych, N. Zhigadlo, J. Karpinski, H. Keller, and B. Batlogg
Superconductivity at 23K and low anisotropy in Rb-substituted $BaFe_2As_2$ single crystals
to be published in Physical Review B (2009).
Group: Karpinski / Projects: 3, 4

J. Karpinski, N. D. Zhigadlo, S. Katrych, Z. Bukowski, P. Moll, S. Weyeneth, H. Keller, R. Puzniak, M. Tortello, D. Daghero, R. Gonnelli, I. Maggio-Aprile, Y. Fasano, Ø. Fischer, and B. Batlogg
Single crystals of $LnFeAsO_{1-x}F_x$ (Ln=La, Pr, Nd, Sm, Gd) and $Ba_{1-x}Rb_xFe_2As_2$: growth, structure and superconducting properties
Physica C (2009), doi: 10.1016/j.physc.2009.03.048.
Groups: Karpinski, Keller, Fischer / Projects: 2, 3, 4

S. Katrych, Q. F. Gu, Z. Bukowski, N. D. Zhigadlo, G. Krauss, and J. Karpinski
A new triclinic modification of the pyrochlore-type KOs_2O_6 superconductor
Journal of Solid State Chemistry **182**, 428 (2009).
Group: Karpinski / Projects: 3, 4

▶ T. Mertelj, V. V. Kabanov, C. Gadermaier, N. D. Zhigadlo, S. Katrych, J. Karpinski, and D. Mihailovic
Distinct Pseudogap and Quasiparticle Relaxation Dynamics in the Superconducting State of Nearly Optimally Doped $SmFeAsO_{0.8}F_{0.2}$ Single Crystals
Physical Review Letters **102**, 117002 (2009).
Group: Karpinski / Projects: 3, 4

▶ V. Moshchalkov, M. Menghini, T. Nishio, Q. H. Chen, A. V. Silhanek, V. H. Dao, L. F. Chibotaru, N. D. Zhigadlo, , and J. Karpinski
Type-1.5 Superconductivity
Physical Review Letters **102**, 117001 (2009).
Group: Karpinski / Projects: 3, 4

P. Parisiades, E. Liarokapis, N. D. Zhigadlo, S. Katrych, and J. Karpinski
Raman invesigations of C-, Li- and Mn-doped MgB_2
Journal of Superconductivity and Novel Magnetism **22**, 169 (2009).
Group: Karpinski / Projects: 3, 4

A. Schilling, R. Dell'Amore, J. Karpinski, Z. Bukowski, M. Medarde, E. Pomjakushina, and K. A. Müller
$LaBaNiO_4$: A Fermi glass
Journal of Physics: Condensed Matter **21**, 015701 (2009).
Groups: Karpinski, Schilling / Projects: 3, 4, 5

S. Weyeneth, R. Puzniak, U. Mosele, N. D. Zhigadlo, S. Katrych, Z. Bukowski, J. Karpinski, S. Kohout, J. Roos, and H. Keller
Anisotropy of superconducting single crystal $SmFeAsO_{0.8}F_{0.2}$ studied by torque magnetometry
Journal of Superconductivity and Novel Magnetism **22**, 325 (2009).
Groups: Karpinski, Keller / Projects: 2, 3, 4

S. Weyeneth, R. Puzniak, N. D. Zhigadlo, S. Katrych, Z. Bukowski, J. Karpinski, and H. Keller
Evidence for two distinct anisotropies in the oxypnictide superconductors $SmFeAsO_{0.8}F_{0.2}$ and $NdFeAsO_{0.8}F_{0.2}$
Journal of Superconductivity and Novel Magnetism **22**, 347 (2009).
Groups: Karpinski, Keller / Projects: 2, 3, 4

► C. Dubois, G. Santi, I. Cuttat, C. Berthod, N. Jenkins, A. P. Petrović, A. A. Manuel, Ø. Fischer, S. M. Kazakov, Z. Bukowski, and J. Karpinski
Scanning Tunneling Spectroscopy in the Superconducting State and Vortex Cores of the β-pyrochlore KOs_2O_6
Physical Review Letters **101**, 057004 (2008).
Groups: Giamarchi, Fischer, Karpinski / Projects: 2, 3, 4

J. Karpinski, N. D. Zhigadlo, S. Katrych, K. Rogacki, B. Batlogg, M. Tortello, and R. Puzniak
MgB_2 single crystals substituted with Li and with Li-C: Structural and superconducting properties
Physical Review B **77**, 214507 (2008).
Group: Karpinski / Projects: 3, 4

► R. Khasanov, K. Conder, E. Pomjakushina, A. Amato, C. Baines, Z. Bukowski, J. Karpinski, S. Katrych, H.-H. Klauss, H. Luetkens, A. Shengelaya, and N. D. Zhigadlo
Evidence of nodeless superconductivity in $FeSe_{0.85}$ from a muon-spin-rotation study of the in-plane magnetic penetration depth
Physical Review B **78**, 220510(R) (2008).
Groups: Karpinski, Mesot / Projects: 3, 4

► P. Legendre, Y. Fasano, I. Maggio-Aprile, Ø. Fischer, Z. Bukowski, S. Katrych, and J. Karpinski
Unexpectedly wide reversible vortex region in β-pyrochlore $RbOs_2O_6$: Bulk magnetization measurements
Physical Review B **78**, 144513 (2008).
Groups: Fischer, Karpinski / Projects: 2, 3, 4

C. Martin, M. D. Vannette, R. T. Gordon, R. Prozorov, J. Karpinski, and N. D. Zhigadlo
Effect of C and Li doping on the rf magnetic susceptibility in MgB_2 single crystals
Physical Review B **78**, 14512 (2008).
Group: Karpinski / Projects: 3, 4

A. Mattila, J. A. Soininen, S. Galambosi, T. Pylkkaenen, S. Huotari, N. D. Zhigadlo, J. Karpinski, and K. Hämäläinen
Electron-hole counts in Al-substituted MgB_2 superconductors from x-ray Raman scattering
Physical Review B **78**, 064517 (2008).
Group: Karpinski / Projects: 3, 4

K. Oganisian, K. Rogacki, C. Sulkowski, N. D. Zhigadlo, S. Katrych, and J. Karpinski
Thermoelectric power of MgB_2 single crystals doped with holes and electrons
Acta Physica Polonica A **114**, 191 (2008).
Group: Karpinski / Projects: 3, 4

P. Parisiades, D. Lampakis, D. Palles, E. Liarokapis, N. D. Zhigadlo, S. Katrych, and J. Karpinski
Two-mode behavior for the E_{2g} broad band in $Mg(B_{1-x}C_x)_2$
Physica C **468**, 1064 (2008).
Group: Karpinski / Projects: 3, 4

K. Rogacki, K. Oganisian, C. Sulkowski, N. Zhigadlo, S. Katrych, and J. Karpinski
Transport properties of MgB_2 single crystals doped with electrons and holes
Journal of the Physics and Chemistry of Solids **69**, 3202 (2008).
Group: Karpinski / Projects: 3, 4

J. Schoenes, A. M. Racu, K. Doll, Z. Bukowski, and J. Karpinski

Phonons and crystal structures of the beta-pyrochlore superconductors KOs_2O_6 and $RbOs_2O_6$ from micro-Raman spectroscopy

Physical Review B **77**, 134515 (2008).

Group: Karpinski / Projects: 3, 4

T. F. SCHULZE, M. BRÜHWILER, P. S. HÄFLIGER, S. M. KAZAKOV, C. NIEDERMAYER, K. MATTENBERGER, J. KARPINSKI, AND B. BATLOGG

Spin fluctuations, magnetic long-range order, and Fermi surface gapping in Na_xCoO_2

Physical Review B **78**, 205101 (2008).

Group: Karpinski / Projects: 3, 4

S. WEYENETH, T. SCHNEIDER, Z. BUKOWSKI, J. KARPINSKI, AND H. KELLER

3D-xy critical properties of $YBa_2Cu_4O_8$ and magnetic-field-induced 3D to 1D crossover

Journal of Physics: Condensed Matter **20**, 345210 (2008).

Groups: Karpinski, Keller / Projects: 2, 3, 4

S. WU, J. ZHANG, A. BELOUSOV, J. KARPINSKI, AND R. SOBOLEWSKI

Dynamics of intervalley transitions and propagation of coherent acoustic phonons in GaN single crystals studied by femtosecond pump-probe spectroscopy

Proceedings of SPIE **6894**, 68940K (2008).

Group: Karpinski / Projects: 3, 4

► N. D. ZHIGADLO, J. KARPINSKI, S. WEYENETH, R. KHASANOV, S. KATRYCH, P. WÄGLI, AND H. KELLER

Synthesis and bulk properties of oxychloride superconductor $Ca_{2-x}Na_xCuO_2Cl_2$

Journal of Physics: Conference Series **97**, 012121 (2008).

Groups: Karpinski, Keller / Projects: 2, 3, 4

N. D. ZHIGADLO, S. KATRYCH, Z. BUKOWSKI, S. WEYENETH, R. PUZNIAK, AND J. KARPINSKI

Single crystals of superconducting $SmFeAsO_{1-x}F_y$ grown at high pressure

Journal of Physics: Condensed Matter **20**, 342202 (2008).

Group: Karpinski / Projects: 3, 4

Group of H. Keller

► A. J. DREW, J. HOPPLER, L. SCHULZ, F. L. PRATT, P. DESAI, P. SHAKYA, T. KREOUZIS, W. P. GILLIN, A. SUTER, N. A. MORLEY, V. K. MALIK, A. DUBROKA, K. W. KIM, H. BOUYANFIF, F. BOURQUI, C. BERNHARD, R. SCHEUERMANN, G. J. NIEUWENHUYS, T. PROKSCHA, AND E. MORENZONI

Direct measurement of the electronic spin diffusion length in a fully functional organic spin valve by low-energy muon spin rotation

Nature Materials **8**, 109 (2009).

Groups: Bernhard, Keller / Project: 2

D. G. ESHCHENKO, V. G. STORCHAK, E. MORENZONI, AND D. ANDREICA

High-pressure muon spin rotation studies of magnetic semiconductors: EuS

Physica B (2009), doi:10.1016/j.physb.2008.11.140.

Group: Keller / Project: 2

D. G. ESHCHENKO, V. G. STORCHAK, E. MORENZONI, T. PROKSCHA, A. SUTER, X. LIU, AND J. K. FURDYNA

Low Energy μSR studies of semiconductor interfaces

Physica B (2009), doi:10.1016/j.physb.2008.11.148.

Group: Keller / Project: 2

J. KARPINSKI, N. D. ZHIGADLO, S. KATRYCH, Z. BUKOWSKI, P. MOLL, S. WEYENETH, H. KELLER, R. PUZNIAK, M. TORTELLO, D. DAGHERO, R. GONNELLI, I. MAGGIO-APRILE, Y. FASANO, Ø. FISCHER, AND B. BATLOGG

Single crystals of $LnFeAsO_{1-x}F_x$ (Ln=La, Pr, Nd, Sm, Gd) and $Ba_{1-x}Rb_xFe_2As_2$: growth, structure and superconducting properties

Physica C (2009), doi: 10.1016/j.physc.2009.03.048.

Groups: Karpinski, Keller, Fischer / Projects: 2, 3, 4

T. PROKSCHA, E. MORENZONI, D. G. ESHCHENKO, H. LUETKENS, G. J. NIEUWENHUYS, AND A. SUTER

Near-surface muonium states in germanium

Physica B (2009), doi:10.1016/j.physb.2008.11.150.

Group: Keller / Project: 2

V. G. STORCHAK, O. E. PARFENOV, J. H. BREWER, P. L. RUSSO, S. L. STUBBS, R. L. LICHTI, D. G. ESHCHENKO, , E. MORENZONI, S. P. COTTRELL, J. S. LORD, T. G. AMINOV, V. P. ZLOMANOV, A. A. VINOKUROV, R. L. KALLAHER, AND S. VON MOLNÁR

Electron localization into magnetic polaron in EuS

Physica B (2009), doi:10.1016/j.physb.2008.11.142.

Group: Keller / Project: 2

V. G. STORCHAK, O. E. PARFENOV, J. H. BREWER, P. L. RUSSO, S. L. STUBBS, R. L. LICHTI, D. G. ESHCHENKO, E. MORENZONI,

V. P. Zlomanov, A. A. Vinokurov, and V. G. Bamburov
Novel muonium centers – magnetic polarons – in magnetic semiconductors
Physica B (2009), doi:10.1016/j.physb.2008.11.141.
Group: Keller / Project: 2

S. Weyeneth, R. Puzniak, U. Mosele, N. D. Zhigadlo, S. Katrych, Z. Bukowski, J. Karpinski, S. Kohout, J. Roos, and H. Keller
Anisotropy of superconducting single crystal $SmFeAsO_{0.8}F_{0.2}$ studied by torque magnetometry
Journal of Superconductivity and Novel Magnetism **22**, 325 (2009).
Groups: Karpinski, Keller / Projects: 2, 3, 4

S. Weyeneth, R. Puzniak, N. D. Zhigadlo, S. Katrych, Z. Bukowski, J. Karpinski, and H. Keller
Evidence for two distinct anisotropies in the oxypnictide superconductors $SmFeAsO_{0.8}F_{0.2}$ and $NdFeAsO_{0.8}F_{0.2}$
Journal of Superconductivity and Novel Magnetism **22**, 347 (2009).
Groups: Karpinski, Keller / Projects: 2, 3, 4

B. M. Wojek, E. Morenzoni, D. G. Eshchenko, A. Suter, T. Prokscha, E. Koller, E. Treboux, Ø. Fischer, and H. Keller
Magnetism and superconductivity in cuprate heterostructures studied by low energy μSR
Physica B (2009), doi: 10.1016/j.physb.2008.11.189.
Groups: Fischer, Keller / Projects: 2, 5

A. Bussmann-Holder and H. Keller
Unconventional isotope effects, multi-component superconductivity and polaron formation in high temperature cuprate superconductors
Journal of Physics: Conference Series **108**, 012019 (2008).
Group: Keller / Project: 2

► A. Bussmann-Holder, H. Keller, A. R. Bishop, A. Simon, and K. A. Müller
Polaron coherence as origin of the pseudogap phase in high temperature superconducting cuprates
Journal of Superconductivity and Novel Magnetism **21**, 353 (2008).
Group: Keller / Project: 2

D. Di Castro, P. Dore, R. Khasanov, H. Keller, P. Mahadevan, S. Ray, D. D. Sarma, and P. Postorino
Pressure effects on the magnetic transition temperature in ordered double perovskites
Physical Review B **78**, 184416 (2008).
Group: Keller / Project: 2

R. Khasanov, P. W. Klamut, A. Shengelaya, Z. Bukowski, I. M. Savić, C. Baines, and H. Keller
Muon-spin rotation measurements of the penetration depth of the Mo_3Sb_7 superconductor
Physical Review B **78**, 014502 (2008).
Group: Keller / Project: 2

► R. Khasanov, T. Kondo, S. Strässle, D. O. G. Heron, A. Kaminski, H. Keller, S. L. Lee, and T. Takeuchi
Evidence for a competition between the superconducting state and the pseudogap state of $(BiPb)_2(SrLa)_2CuO_{6+\delta}$ from muon spin rotation experiments
Physical Review Letters **101**, 227002 (2008).
Group: Keller / Project: 2

► R. Khasanov, A. Shengelaya, D. Di Castro, E. Morenzoni, A. Maisuradze, I. M. Savić, K. Conder, E. Pomjakushina, A. Bussmann-Holder, and H. Keller
Oxygen isotope effects on the superconducting transition and magnetic states within the phase diagram of $Y_{1-x}Pr_xBa_2Cu_3O_{7-\delta}$
Physical Review Letters **101**, 077001 (2008).
Groups: Keller, Mesot / Project: 2

► R. Khasanov, A. Shengelaya, A. Maisuradze, D. Di Castro, I. M. Savić, S. Weyeneth, M. S. Park, D. J. Jang, S. I. Lee, and H. Keller
Nodeless superconductivity in the infinite-layer electron-doped cuprate superconductor $Sr_{0.9}La_{0.1}CuO_2$
Physical Review B **77**, 184512 (2008).
Group: Keller / Project: 2

► R. Khasanov, S. Strässle, K. Conder, E. Pomjakushina, A. Bussmann-Holder, and H. Keller
Universal correlations of isotope effects in $Y_{1-x}Pr_xBa_2Cu_3O_{7-\delta}$
Physical Review B **77**, 104530 (2008).
Groups: Keller, Mesot / Project: 2

► E. Morenzoni, H. Luetkens, T. Prokscha, A. Suter, S. Vongtragool, F. Galli, M. B. S. Hesselberth, N. Garifianov, and K. R.
Depth-Dependent Spin Dynamics of Canonical Spin-Glass Films: A Low-Energy Muon-Spin-Rotation Study
Physical Review Letters **100**, 147205 (2008).
Group: Keller / Project: 2

- V. G. Storchak, D. G. Eshchenko, E. Morenzoni, T. Prokscha, A. Suter, X. Liu, and J. K. Furdyna
  Spatially resolved inhomogeneous ferromagnetism in (Ga,Mn)As diluted magnetic semiconductors: A microscopic study by muon spin relaxation
  Physical Review Letters **101**, 027202 (2008).
  Group: Keller / Project: 2

- S. Strässle, J. Roos, M. Mali, and H. Keller
  Lack of evidence for orbital-current effects in the high-temperature $Y_2Ba_4Cu_7O_{15-\delta}$ superconductor using ^{89}Y nuclear magnetic resonance
  Physical Review Letters **101**, 237001 (2008).
  Group: Keller / Project: 2

  S. Weyeneth, T. Schneider, Z. Bukowski, J. Karpinski, and H. Keller
  3D-xy critical properties of $YBa_2Cu_4O_8$ and magnetic-field-induced 3D to 1D crossover
  Journal of Physics: Condensed Matter **20**, 345210 (2008).
  Groups: Karpinski, Keller / Projects: 2, 3, 4

- N. D. Zhigadlo, J. Karpinski, S. Weyeneth, R. Khasanov, S. Katrych, P. Wägli, and H. Keller
  Synthesis and bulk properties of oxychloride superconductor $Ca_{2-x}Na_xCuO_2Cl_2$
  Journal of Physics: Conference Series **97**, 012121 (2008).
  Groups: Karpinski, Keller / Projects: 2, 3, 4

Group of D. van de Marel

- J. L. M. van Mechelen, D. van der Marel, C. Grimaldi, A. B. Kuzmenko, N. P. Armitage, N. Reyren, H. Hagemann, and I. I. Mazin
  Electron-Phonon Interaction and Charge Carrier Mass Enhancement in $SrTiO_3$
  Physical Review Letters **100**, 226403 (2008).
  Group: van der Marel / Project: 5

  F. Carbone, D. Yang, E. Giannini, and A. H. Zewail
  Direct role of structural dynamics in electron-lattice coupling of superconducting cuprates
  Proceedings of the National Academy of Science of the USA **105**, 20161 (2008).
  Group: van der Marel / Project: 3

- J. Deisenhofer, I. Leonov, M. V. Eremin, C. Kant, P. Ghigna, F. Mayr, V. V. Iglamov, V. I. Anisimov, and D. van der Marel
  Optical Evidence for Symmetry Changes above the Néel Temperature of $KCuF_3$
  Physical Review Letters **101**, 157406 (2008).
  Group: van der Marel / Project: 1

- V. A. Gasparov, I. Sheikin, F. Levy, J. Teyssier, and G. Santi
  Study of the Fermi Surface of ZrB_{12} Using the de Haas-van Alphen Effect
  Physical Review Letters **101**, 097006 (2008).
  Group: van der Marel / Project: 1

  V. Guritanu, N. P. Armitage, R. Tediosi, S. S. Saxena, A. Huxley, and D. van der Marel
  Optical spectra of the heavy fermion uniaxial ferromagnet UGe_2
  Physical Review B **78**, 172406 (2008).
  Group: van der Marel / Projects: 1, 2

  E. van Heumen, A. B. Kuzmenko, and D. van der Marel
  Optics clues to pairing glues in high T_c cuprates
  Journal of Physics: Conference Series **150**, 052278 (2009).
  Group: van der Marel / Project: 2

- M. M. Koza, M. R. Johnson, R. Viennois, H. Mutka, L. Girard, and D. Ravot
  Breakdown of phonon glass paradigm in La- and Ce-filled Fe_4Sb_{12} skutterudites
  Nature Materials **7**, 805 (2008).
  Group: van der Marel / Projects: 1, 3

- A. B. Kuzmenko, E. van Heumen, F. Carbone, and D. van der Marel
  Universal Optical Conductance of Graphite
  Physical Review Letters **100**, 117401 (2008).
  Group: van der Marel / Project: 1

- G. Levy de Castro, C. Berthod, A. Piriou, E. Giannini, and Ø. Fischer
  Preeminent Role of the Van Hove Singularity in the Strong-Coupling Analysis of Scanning Tunneling Spectroscopy for Two-Dimensional Cuprates Superconductors
  Physical Review Letters **101**, 267004 (2008).
  Groups: Giamarchi, Fischer, van der Marel / Project: 2

  A. Piriou, Y. Fasano, E. Giannini, and Ø. Fischer
  Effect of oxygen-doping on $Bi_2Sr_2Ca_2Cu_3O_{10+\delta}$ vortex matter: crossover from electromagnetic to Josephson interlayer coupling
  Physical Review B **77**, 184508 (2008).
  Groups: Fischer, van der Marel / Projects: 2, 3

R. Tediosi, F. Carbone, A. B. Kuzmenko, J. Teyssier, D. van der Marel, and J. A. Mydosh
Charge ordering in three-dimensional $RE_5Ir_4Si_{10}$ compounds
arXiv:0812.1214 (2008).
Group: van der Marel / Project: 1

J. Teyssier, R. Lortz, A. Petrovic, D. van der Marel, V. Filippov, and N. Shitsevalova
Effect of electron-phonon coupling on the superconducting transition temperature in dodecaboride superconductors: A comparison of LuB_{12} with ZrB_{12}
Physical Review B **78**, 134504 (2008).
Group: van der Marel / Projects: 1, 2, 3

J. Teyssier, R. Viennois, J. Salamin, E. Giannini, and D. van der Marel
Experimental and first principle calculation of $Co_xNi_{1-x}Si$ solid solution structural stability
Journal of Alloys and Compounds **465**, 462 (2008).
Group: van der Marel / Projects: 1, 3

Group of G. Margaritondo

K.-Y. Choi, H. Nojiri, N. S. Dalal, H. Berger, W. Brenig, and P. Lemmens
Anomalous frequency and intensity scaling of collective and local modes in a coupled-spin tetrahedral system $Cu_2Te_2O_5Cl_2$
Physical Review B **79**, 024416 (2009).
Group: Margaritondo / Project: 3

▶ G. Ghiringhelli, A. Piazzalunga, C. Dallera, T. Schmitt, V. Strocov, J. Schlappa, L. Patthey, X. Wang, H. Berger, and M. Grioni
Observation of Two Nondispersive Magnetic Excitations in NiO by Resonant Inelastic Soft-X-Ray Scattering
Physical Review Letters **102**, 027401 (2009).
Groups: Grioni, Margaritondo / Projects: 2, 3

▶ M. Hoesch, A. Bosak, D. Chernyshov, H. Berger, and M. Krisch
Giant Kohn anomaly and the phase transition in charge density wave $ZrTe_3$
Physical Review Letters **102**, 086402 (2009).
Group: Margaritondo / Project: 3

A. A. Kordyuk, S. V. Borisenko, V. B. Zabolotnyy, R. Schuster, D. S. Inosov, D. V. Evtushinsky, A. I. Plyushchay, R. Follath, A. Varykhalov, L. Patthey, and H. Berger
Nonmonotonic pseudogap in high$-T_c$ cuprates
Physical Review B **79**, 020504 (2009).
Group: Margaritondo / Project: 3

▶ C. Monney, H. Cercellier, F. Clerc, C. Battaglia, E. F. Schwier, C. Didiot, M. G. Garnier, H. Beck, P. Aebi, H. Berger, L. Forró, and L. Patthey
Spontaneous exciton condensation in $1T-TiSe_2$: BCS-like approach
Physical Review B **79**, 045116 (2009).
Groups: Margaritondo, Aebi, Forró / Projects: 1, 3

M. Pregelj, A. Zorko, O. Zaharko, R. Bousier, H. Berger, H. A. Katori, and D. Arčon
Magnetic phase diagram of the two-dimensional antiferromagnet $Ni_5(TeO_3)_4Br_2$
Physical Review B **79**, 064407 (2009).
Group: Margaritondo / Project: 3

R. Schuster, R. Kraus, M. Knupfer, H. Berger, and B. Büchner
Negative plasmon dispersion in the transition-metal dichalcogenide $2H-TaSe_2$
Physical Review B **79**, 045134 (2009).
Group: Margaritondo / Project: 3

I. Živković, V. P. S. Awana, and H. Berger
Nonlinear magnetic response in ruthenocuprates
The European Physical Journal B **62**, 423 (2008).
Group: Margaritondo / Project: 3

▶ A. Akrap, A. Rudolf, F. Rullier-Albenque, H. Berger, and L. Forró
Influence of point defects on the metal-insulator transition in $BaVS_3$
Physical Review B **77**, 115142 (2008).
Groups: Forró, Margaritondo / Projects: 1, 3

A. Akrap, V. Stevanović, M. Herak, M. Miljak, N. Barišić, H. Berger, and L. Forró
Transport and magnetic properties of $BaVSe_3$
Physical Review B **78**, 235111 (2008).
Group: Margaritondo / Project: 3

S. Bernu, P. Foury-Leylekian, J. P. Pouget, A. Akrap, H. Berger, L. Forró, G. Popov, and M. Greenblatt
Influence of chemical substitutions on the charge instability of $BaVS_3$
Physica B **403**, 1625 (2008).
Group: Margaritondo / Project: 3

M. Bimbi, G. Allodi, R. De Renzi, C. Mazzoli, and H. Berger

Muon spin spectroscopy evidence of a charge density wave in magnetite below the Verwey transition

Physical Review B **77**, 045115 (2008).

Group: Margaritondo / Project: 3

- S. V. Borisenko, A. A. Kordyuk, A. N. Yaresko, V. B. Zabolotnyy, D. S. Inosov, R. Schuster, B. Büchner, R. Weber, R. Follath, L. Patthey, and H. Berger
  Pseudogap and Charge Density Waves in Two Dimensions

  Physical Review Letters **100**, 196402 (2008).

  Group: Margaritondo / Project: 3

K. Y. Choi, P. Lemmens, E. S. Choi, and H. Berger
Lattice anomalies and magnetic excitations of the spin web compound Cu_3TeO_6

Journal of Physics: Condensed Matter **20**, 505214 (2008).

Group: Margaritondo / Project: 3

- D. V. Evtushinsky, A. A. Kordyuk, V. B. Zabolotnyy, D. S. Inosov, B. Büchner, H. Berger, L. Patthey, R. Follath, and S. V. Borisenko
  Pseudogap-Driven Sign Reversal of the Hall Effect

  Physical Review Letters **100**, 236402 (2008).

  Group: Margaritondo / Project: 3

S. L. Gnatchenko, M. I. Kobets, E. N. Khatsko, M. Baran, R. Szymczak, P. Lemmens, and H. Berger
Magnetic and resonance properties of the two-dimensional $S = 1$ compound $Ni_5(TeO_3)_4Cl_2$ with frustrated geometry

Fizika Nizkikh Temperatur **34**, 798 (2008).

Group: Margaritondo / Project: 3

S. L. Gnatchenko, M. I. Kobets, E. N. Khatsko, M. Baran, R. Szymczak, P. Lemmens, and H. Berger
Magnetic and resonance properties of the two-dimensional $S = 1$ compound $Ni_5(TeO_3)_4Cl_2$ with frustrated geometry

Low Temperature Physics **34**, 630 (2008).

Group: Margaritondo / Project: 3

V. Gnezdilov, P. Lemmens, A. A. Zvyagin, V. O. Cheranovskii, K. Lamonova, Y. G. Pashkevich, R. K. Kremer, and H. Berger
Magnetic crossover and complex excitation spectrum of the ferromagnetic/antiferromagnetic spin-$\frac{1}{2}$ chain system $\alpha-TeVO_4$

Physical Review B **78**, 184407 (2008).

Group: Margaritondo / Project: 3

M. Herak, M. Miljak, A. Akrap, L. Forró, and H. Berger
Magnetic anisotropy of paramagnetic and ferromagnetically ordered state of single crystal $BaVSe_3$

Journal of the Physical Society of Japan **77**, 093701 (2008).

Groups: Forró, Margaritondo / Projects: 1, 3

D. S. Inosov, R. Schuster, A. A. Kordyuk, J. Fink, S. V. Borisenko, V. B. Zabolotnyy, D. V. Evtushinsky, M. Knupfer, B. Büchner, R. Follath, and H. Berger
Excitation energy map of high-energy dispersion anomalies in cuprates

Physical Review B **77**, 212504 (2008).

Group: Margaritondo / Project: 3

T. Ivek, T. Vuletić, S. Tomić, A. Akrap, H. Berger, and L. Forró
Collective charge excitations below the metal-to-insulator transition in $BaVS_3$

Physical Review B **78**, 035110 (2008).

Groups: Forró, Margaritondo / Projects: 1, 3

M. Miljak, M. Herak, O. Milat, N. Tomašić, and H. Berger
The magnetic state of the low dimensional $CuTe_2O_5$ compound below 20 K

Journal of Physics: Condensed Matter **20**, 505210 (2008).

Group: Margaritondo / Project: 3

L. Perfetti, P. A. Loukakos, M. Lisowski, U. Bovensiepen, M. Wolf, H. Berger, S. Biermann, and A. Georges
Femtosecond dynamics of electronic states in the Mott insulator 1T-TaS_2 by time resolved photoelectron spectroscopy

New Journal of Physics **10**, 053019 (2008).

Group: Margaritondo / Project: 3

M. Pregelj, D. Arčon, A. Zorko, O. Zaharko, L. C. Brunel, H. van Tool, A. Ozarowski, S. Nellutla, and H. Berger
Temperature dependence of antiferromagnetic resonance mode in two-dimensional system $Ni_5(TeO_3)_4Br_2$

Physica B **403**, 950 (2008).

Group: Margaritondo / Project: 3

M. Reibelt, A. Schilling, P. C. Canfield, G. Ravikumar, and H. Berger
Differential-thermal analysis around and below the critical temperature T_c of various low-T_c superconductors: A comparative study

Physica C **468**, 2254 (2008).

Groups: Margaritondo, Schilling / Projects: 3, 5

K. Schmalzl, D. Strauch, A. Hiess, and H. Berger
Temperature dependent phonon dispersion in 2H-$NbSe_2$ investigated using inelastic neutron scattering
Journal of Physics: Condensed Matter **20**, 104240 (2008).
Group: Margaritondo / Project: 3

▶ B. Sipos, A. F. Kusmartseva, A. Akrap, H. Berger, L. Forró, and E. Tutiš
From Mott state to superconductivity in 1T-TaS_2
Nature Materials **7**, 960 (2008).
Groups: Forró, Margaritondo / Projects: 1, 3

D. Stoltz, M. Bielmann, L. Schlapbach, M. Bovet, H. Berger, M. Göthelid, S. E. Stoltz, and H. I. Starnberg
Atomic origin of the scanning tunneling microscopy images of charge-density-waves on 1T-$TaSe_2$
Physica B **403**, 2207 (2008).
Groups: Margaritondo, Schlapbach / Project: 3

Group of J. Mesot

▶ B. Thielemann, C. Rüegg, K. Kiefer, H. M. Rønnow, B. Normand, P. Bouillot, C. Kollath, E. Orignac, R. Citro, T. Giamarchi, A. M. Läuchli, D. Biner, K. Krämer, F. Wolff-Fabris, V. S. Zapf, M. Jaime, J. Stahn, N. B. Christensen, B. Grenier, D. F. McMorrow, and J. Mesot
Field-controlled Magnetic Order in the Quantum Spin-Ladder System $(Hpip)_2CuBr_4$
Physical Review B **79**, 020408(R) (2009).
Groups: Giamarchi, Mesot / Project: 1

F. Anfuso, M. Garst, A. Rosch, O. Heyer, T. Lorenz, C. Rüegg, and K. Krämer
Spin-spin correlations of the spin-ladder compound $(C_5H_{12}N)_2CuBr_4$ measured by magnetostriction and comparison to quantum Monte Carlo results
Physical Review B **77**, 235113 (2008).
Group: Mesot / Project: 1

J. Chang, C. Niedermayer, R. Gilardi, N. B. Christensen, H. M. Rønnow, D. F. McMorrow, M. Ay, J. Stahn, O. Sobolev, A. Hiess, S. Pailhes, C. Baines, N. Momono, M. Oda, M. Ido, and J. Mesot
Tuning competing orders in $La_{2-x}Sr_xCuO_4$ cuprate superconductors by the application of an external magnetic field
Physical Review B **78**, 104525 (2008).
Group: Mesot / Project: 2

J. Chang, Y. Sassa, S. Guerrero, M. Månsson, M. Shi, S. Pailhés, A. Bendounan, R. Mottl, T. Claesson, O. Tjernberg, L. Patthey, M. Ido, M. Oda, N. Momono, C. Mudry, and J. Mesot
Electronic structure near the 1/8-anomaly in La-based cuprates
New Journal of Physics **10**, 103016 (2008).
Group: Mesot / Project: 2

J. Chang, M. Shi, S. Pailhés, M. Månsson, T. Claesson, O. Tjernberg, A. Bendounan, Y. Sassa, L. Patthey, N. Momono, M. Oda, M. Ido, S. Guerrero, C. Mudry, and J. Mesot
Anisotropic quasiparticle scattering rates in slightly underdoped to optimally doped high-temperature $La_{2-x}Sr_xCuO_4$ superconductors
Physical Review B **78**, 205103 (2008).
Group: Mesot / Project: 2

▶ D. Chernyshov, V. Dmitriev, E. Pomjakushina, K. Conder, M. Stingaciu, V. Pomjakushin, A. Podlesnyak, A. A. Taskin, and Y. Ando
Superstructure formation at the metal-insulator transition in $RBaCo_2O_{5.5}$ (R =Nd,Tb) as seen from reciprocal space mapping
Physical Review B **78**, 024105 (2008).
Group: Mesot / Project: 3

▶ M. Kenzelmann, T. Strässle, C. Niedermayer, M. Sigrist, B. Padmanabhan, M. Zolliker, A. D. Bianchi, R. Movshovich, E. D. Bauer, J. L. Sarrao, and J. D. Thompson
Coupled Superconducting and Magnetic Order in $CeCoIn_5$
Science **321**, 1652 (2008).
Groups: Mesot, Sigrist / Project: 2

▶ R. Khasanov, K. Conder, E. Pomjakushina, A. Amato, C. Baines, Z. Bukowski, J. Karpinski, S. Katrych, H.-H. Klauss, H. Luetkens, A. Shengelaya, and N. D. Zhigadlo
Evidence of nodeless superconductivity in $FeSe_{0.85}$ from a muon-spin-rotation study of the in-plane magnetic penetration depth
Physical Review B **78**, 220510(R) (2008).
Groups: Karpinski, Mesot / Projects: 3, 4

▶ R. Khasanov, A. Shengelaya, D. Di Castro, E. Morenzoni, A. Maisuradze, I. M. Savić, K. Conder, E. Pomjakushina,

A. Bussmann-Holder, and H. Keller
Oxygen isotope effects on the superconducting transition and magnetic states within the phase diagram of $Y_{1-x}Pr_xBa_2Cu_3O_{7-\delta}$
Physical Review Letters **101**, 077001 (2008).
Groups: Keller, Mesot / Project: 2

▶ R. Khasanov, S. Strässle, K. Conder, E. Pomjakushina, A. Bussmann-Holder, and H. Keller
Universal correlations of isotope effects in $Y_{1-x}Pr_xBa_2Cu_3O_{7-\delta}$
Physical Review B **77**, 104530 (2008).
Groups: Keller, Mesot / Project: 2

▶ T. Lorenz, O. Heyer, M. Garst, F. Anfuso, A. Rosch, C. Rüegg, and K. Krämer
Diverging Thermal Expansion of the Spin-Ladder System $(C_5H_{12}N)_2CuBr_4$
Physical Review Letters **100**, 067208 (2008).
Group: Mesot / Project: 1

▶ H. Luetkens, M. Stingaciu, Y. G. Pashkevich, K. Conder, E. Pomjakushina, A. A. Gusev, K. V. Lamonova, P. Lemmens, and H.-H. Klauss
Microscopic Evidence of Spin State Order and Spin State Phase Separation in Layered Cobaltites $RBaCo_2O_{5.5}$ with R =Y, Tb, Dy, and Ho
Physical Review Letters **101**, 017601 (2008).
Group: Mesot / Project: 3

A. D. Palczewski, T. Kondo, R. Khasanov, N. N. Kolesnikov, A. V. Timonina, E. Rotenberg, T. Ohta, A. Bendounan, Y. Sassa, A. Fedorov, S. Pailhés, A. F. Santander-Syro, J. Chang, M. Shi, J. Mesot, H. M. Fretwell, and A. Kaminski
Origins of large critical temperature variations in single-layer cuprates
Physical Review B **78**, 054523 (2008).
Group: Mesot / Project: 2

▶ A. Podlesnyak, M. Russina, A. Furrer, A. Alfonsov, E. Vavilova, V. Kataev, B. Büchner, T. Strässle, E. Pomjakushina, K. Conder, and D. I. Khomskii
Spin-State Polarons in Lightly-Hole-Doped $LaCoO_3$
Physical Review Letters **101**, 247603 (2008).
Group: Mesot / Project: 3

▶ C. Rüegg, K. Kiefer, B. Thielemann, D. F. McMorrow, V. Zapf, B. Normand, M. B. Zvonarev, P. Bouillot, C. Kollath, T. Giamarchi, S. Capponi, D. Poilblanc, D. Biner, and K. W. Krämer
Thermodynamics of the Spin Luttinger Liquid in a Model Ladder Material
Physical Review Letters **101**, 247202 (2008).
Groups: Giamarchi, Mesot / Project: 1

▶ M. Shi, J. Chang, S. Pailhés, M. R. Norman, J. C. Campuzano, M. Månsson, T. Claesson, O. Tjernberg, A. Bendounan, L. Patthey, N. Momono, M. Oda, M. Ido, C. Mudry, and J. Mesot
Coherent d-Wave Superconducting Gap in Underdoped $La_{2-x}Sr_xCuO_4$ by Angle-Resolved Photoemission Spectroscopy
Physical Review Letters **101**, 047002 (2008).
Group: Mesot / Project: 2

▶ M. Stingaciu, E. Pomjakushina, H. Grimmer, M. Trottmann, and K. Conder
Crystal Growth of $Tb_{0.9}Dy_{0.1}BaCo_2O_{5+\delta}$ using travelling solvent floating zone method
Journal of Crystal Growth **310**, 1239 (2008).
Group: Mesot / Project: 3

▶ B. Thielemann, C. Rüegg, H. M. Rønnow, A. M. Läuchli, J.-S. Caux, B. Normand, D. Biner, K. W. Krämer, H.-U. Güdel, J. Stahn, K. Habicht, K. Kiefer, M. Boehm, D. F. McMorrow, and J. Mesot
Direct Observation of Magnon Fractionalization in the Quantum Spin Ladder
Physical Review Letters **102**, 107204 (2008).
Group: Mesot / Project: 1

O. Zaharko, J. L. Gavilano, T. Strässle, C. F. Miclea, A. C. Mota, Y. Filinchuk, D. Chernyshov, P. P. Deen, B. Rahaman, T. Saha-Dasgupta, R. Valenti, Y. Matsushita, A. Dönni, and H. Kitazawa
Structural and magnetic aspects of the nanotube system $Na_{2-x}V_3O_7$
Physical Review B **78**, 214426 (2008).
Group: Mesot / Project: 1

Group of F. Mila

▶ N. Laflorencie and F. Mila
Theory of the field-induced BEC in the frustrated spin-$\frac{1}{2}$ dimer compound $BaCuSi_2O_6$
Physical Review Letters **102**, 060602 (2009).
Group: Mila / Project: 1

▶ S. R. Manmana and F. Mila
Torque anomalies at magnetization plateaux in quantum magnets with Dzyaloshinskii-Moriya interactions
Europhysics Letters **85**, 27010 (2009).
Group: Mila / Project: 1

- C. Weber, A. Läuchli, F. Mila, and T. Giamarchi
  Orbital Currents in Extended Hubbard Models of High-T_c Cuprate Superconductors
  Physical Review Letters **102**, 017005 (2009).
  Groups: Giamarchi, Mila / Projects: 1, 2

- J. Dorier, K. P. Schmidt, and F. Mila
  Theory of Magnetization Plateaux in the Shastry-Sutherland Model
  Physical Review Letters **101**, 250402 (2008).
  Group: Mila / Project: 1

V. V. Mazurenko, S. L. Skornyakov, V. I. Anisimov, and F. Mila
First-principles investigation of symmetric and antisymmetric exchange interactions of $SrCu_2(BO_3)_2$
Physical Review B **78**, 195110 (2008).
Group: Mila / Project: 1

F. Mila, J. Dorier, and K. P. Schmidt
Supersolid Phases of Hardcore Bosons on the Square Lattice: Correlated Hopping, Next-Nearest Neighbor Hopping and Frustration
Progress of Theoretical Physics Supplement **176**, 355 (2008).
Group: Mila / Project: 1

G. Misguich and F. Mila
Quantum dimer model on the triangular lattice: Semiclassical and variational approaches to vison dispersion and condensation
Physical Review B **77**, 134421 (2008).
Group: Mila / Project: 1

J.-D. Picon, A. F. Albuquerque, K. P. Schmidt, N. Laflorencie, M. Troyer, and F. Mila
Mechanisms for spinsupersolidity in $S = \frac{1}{2}$ spin-dimer antiferromagnets
Physical Review B **78**, 184418 (2008).
Groups: Troyer, Mila / Project: 1

I. Rousochatzakis, A. M. Läuchli, and F. Mila
Highly frustrated magnetic clusters: The kagomé on a sphere
Physical Review B **77**, 094420 (2008).
Group: Mila / Project: 1

- K. P. Schmidt, J. Dorier, A. M. Läuchli, and F. Mila
  Supersolid phase induced by correlated hopping in spin-1/2 frustrated quantum magnets
  Physical Review Letters **100**, 090401 (2008).
  Group: Mila / Project: 1

Group of A. Morpurgo

- R. Danneau, F. Wu, M. F. Craciun, S. Russo, M. Y. Tomi, J. Salmilehto, A. F. Morpurgo, and P. J. Hakonen
  Shot Noise in Ballistic Graphene
  Physical Review Letters **100**, 196802 (2008).
  Group: Morpurgo / Project: 5

S. Fratini, A. F. Morpurgo, and S. Ciuchi
Tuning electron-phonon and Coulomb interactions in organic field effect transistors
Physica Status Solidi (c) **5**, 718 (2008).
Group: Morpurgo / Project: 5

S. Fratini, A. F. Morpurgo, and S. Ciuchi
Electron-phonon and electron-electron interactions in organic field effect transistors
Journal of the Physics and Chemistry of Solids **69**, 2195 (2008).
Group: Morpurgo / Project: 5

- H. Alves, A. S. Molinari, H. Xie, and A. F. Morpurgo
  Metallic Conduction at Organic Charge-Transfer Interfaces
  Nature Materials **7**, 574 (2008).
  Group: Morpurgo / Project: 5

R. Danneau, F. Wu, M. F. Craciun, S. Russo, M. Y. Tomi, J. Salmilehto, A. F. Morpurgo, and P. J. Hakonen
Evanescent wave transport and shot noise in graphene: ballistic regime and effect of disorder
Journal of Low Temperature Physics **153**, 374 (2008).
Group: Morpurgo / Project: 5

- A. S. Molinari, I. Gutiérrez Lezama, P. Parisse, T. Takenobu, Y. Iwasa, and A. F. Morpurgo
  Quantitative analysis of electronic transport through weakly coupled metal/organic interfaces
  Applied Physics Letters **92**, 133303 (2008).
  Group: Morpurgo / Project: 5

S. Fratini, H. Xie, I. N. Hulea, S. Ciuchi, and A. F. Morpurgo
Current saturation and Coulomb interactions in organic single-crystal transistors
New Journal of Physics **10**, 033031 (2008).
Group: Morpurgo / Project: 5

- J. B. Oostinga, H. B. Heersche, X. Liu, A. F. Morpurgo, and L. M. K. Vandersypen
  Gate-induced insulating state in bilayer graphene devices

Nature Materials **7**, 151 (2008).
Group: Morpurgo / Project: 5

S. Russo, J. B. Oostinga, D. Wehenkel, H. B. Heersche, S. S. Sobhani, L. M. K. Vandersypen, and A. F. Morpurgo
Observation of Aharonov-Bohm conductance oscillations in a graphene ring
Physical Review B **77**, 085413 (2008).
Group: Morpurgo / Project: 5

▶ I. Martin, Y. M. Blanter, and A. F. Morpurgo
Topological confinement in bilayer graphene
Physical Review Letters **100**, 036804 (2008).
Group: Morpurgo / Project: 5

Group of R. Nesper

▶ U. Aydemir, A. Ormeci, H. Borrmann, B. Böhme, F. Zürcher, B. Uslu, T. Goebel, W. Schnelle, P. Simon, W. Carrillo-Cabrera, F. Haarmann, M. Baitinger, R. Nesper, H. G. von Schnering, and Y. Grin
The Metallic Zintl Phase Ba_3Si_4 – Synthesis, Crystal Structure, Chemical Bonding, and Physical Properties
Zeitschrift für Anorganische und Allgemeine Chemie **634**, 1651 (2008).
Group: Nesper / Project: 4

▶ I. Djerdj, D. Sheptyakov, F. Gozzo, D. Arčon, R. Nesper, and M. Niederberger
Oxygen Self-Doping in Hollandite-Type Vanadium Oxyhydroxide Nanorods
Journal of the American Chemical Society **130**, 11364 (2008).
Group: Nesper / Project: 4

T. Gao, M. Glerup, F. Krumeich, R. Nesper, H. Fjellvåg, and P. Norby
Microstructures and Spectroscopic Properties of Cryptomelane-type Manganese Dioxide Nanofibers
The Journal of Physical Chemistry C **112**, 13134 (2008).
Group: Nesper / Project: 4

W. Höland, C. Ritzberger, E. Apel, V. Rheinberger, R. Nesper, F. Krumeich, C. Mönster, and H. Eckert
Formation and crystal growth of needle-like fluoroapatite in functional glass-ceramics
Journal of Materials Chemistry **18**, 1318 (2008).
Group: Nesper / Project: 4

M. Wörle, F. Krumeich, T. Chatterji, S. Kek, and R. Nesper
On the structure and twinning of $PtAl_4$
Journal of Alloys and Compounds **455**, 130 (2008).
Group: Nesper / Project: 4

▶ Q. Xie, C. Kubata, M. Wörle, and R. Nesper
Tt-Tt (Tt = Si, Ge) Dumb-Bell Structures at Different Valence Electron Concentrations: Ln_2MgSi_2 (Ln = La, Ce), $Yb_2Li_{0.5}Ge_2$, and $Yb_{1.75}Mg_{0.75}Si_2$
Zeitschrift für Anorganische und Allgemeine Chemie **634**, 2469 (2008).
Group: Nesper / Project: 4

Group of H.-R. Ott

▶ M. Weller, A. Sacchetti, H.-R. Ott, K. Mattenberger, and B. Batlogg
Melting of the Na layers in solid $Na_{0.8}CoO_2$
Physical Review Letters **102**, 056401 (2009).
Group: Ott / Project: 1

A. Sacchetti, M. Weller, J. L. Gavilano, R. Mudliar, B. Pedrini, K. Magishi, H.-R. Ott, R. Monnier, B. Delley, and Y. Ōnuki
$^{63,65}Cu$ NMR and NQR evidence for an unusual spin dynamics in $PrCu_2$ below 100 K
Physical Review B **77**, 144404 (2008).
Group: Ott / Project: 1

A. Sacchetti, M. Weller, H.-R. Ott, and Y. Ōnuki
Magnetic Properties of $PrCu_2$ at high pressure
The European Physical Journal B **66**, 307 (2008).
Group: Ott / Project: 1

M. Weller, J. L. Gavilano, A. Sacchetti, and H.-R. Ott
Low temperature NMR study of $CeAl_3$ under hydrostatic pressure
Physica B **403**, 834 (2008).
Group: Ott / Project: 1

M. Weller, J. L. Gavilano, A. Sacchetti, and H.-R. Ott
Pressure-induced variation of the ground state of $CeAl_3$
Physical Review B **77**, 132402 (2008).
Group: Ott / Project: 1

Group of P. Paruch

- H. Béa and P. Paruch
  Multiferroics: A way forward along domain walls
  Nature Materials **8**, 168 (2009).
  Group: Paruch / Project: 5

- G. Catalan, H. Béa, S. Fusil, M. Bibes, P. Paruch, A. Barthélémy, and J. F. Scott
  Fractal Dimension and Size Scaling of Domains in Thin Films of Multiferroic $BiFeO_3$
  Physical Review Letters **100**, 027602 (2008).
  Group: Paruch / Project: 5

- P. Paruch, A.-B. Posadas, M. Dawber, C. H. Ahn, and P. L. McEuen
  Polarization switching using single-walled carbon nanotubes grown on epitaxial ferroelectric thin films
  Applied Physics Letters **93**, 132901 (2008).
  Group: Paruch / Project: 1

Group of Ch. Renner

- C. Renner
  Hands-on inspiration for science
  Nature Materials **8**, 245 (2009).
  Group: Renner / Project(s): Education

- A. C. H. Rowe, A. Donoso-Barrera, C. Renner, and S. Arscott
  Giant Room-Temperature Piezoresistance in a Metal-Silicon Hybrid Structure
  Physical Review Letters **100**, 145501 (2008).
  Group: Renner / Project: 6

Group of T. M. Rice

W.-Q. Chen, K.-Y. Yang, T. M. Rice, and F.-C. Zhang
Quantum oscillations in magnetic-field–induced antiferromagnetic phase of underdoped cuprates: Application to ortho-II $YBa_2Cu_3O_{6.5}$
Europhysics Letters **82**, 17004 (2008).
Group: Rice / Project: 2

- M. Ossadnik, C. Honerkamp, T. M. Rice, and M. Sigrist
  Breakdown of Landau Theory in Overdoped Cuprates near the Onset of Superconductivity
  Physical Review Letters **101**, 256405 (2008).
  Groups: Sigrist, Rice / Project: 2

Group of A. Schilling

E. F. C. Chimamkpam, F. Hussain, A. Engel, A. Schilling, and G. R. Patzke
Synthesis and Characterization of Hybrid Materials derived from Polyaniline and Lacunary Keggin-type Polyoxotungstates
Zeitschrift für Anorganische und Allgemeine Chemie **635** (2009), dOI:10.1002/zaac.200801394.
Group: Schilling / Project: 5

R. Dell'Amore, A. Schilling, and K. Krämer
$U(1)$ symmetry breaking and violated axial symmetry in $TlCuCl_3$ and other insulating spin systems
Physical Review B **79**, 014428 (2009).
Group: Schilling / Project: 5

A. Schilling, R. Dell'Amore, J. Karpinski, Z. Bukowski, M. Medarde, E. Pomjakushina, and K. A. Müller
$LaBaNiO_4$: A Fermi glass
Journal of Physics: Condensed Matter **21**, 015701 (2009).
Groups: Karpinski, Schilling / Projects: 3, 4, 5

- H. Bartolf, A. Engel, A. Schilling, K. Il'in, and M. Siegel
  Fabrication of metallic structures with lateral dimensions less than 15 nm and $j_c(T)$-measurements in NbN micro- and nanobridges
  Physica C **468**, 793 (2008).
  Group: Schilling / Project: 5

R. Dell'Amore, A. Schilling, and K. Krämer
Fraction of Bose-Einstein condensed triplons in $TlCuCl_3$ from magnetization data
Physical Review B **75**, 224403 (2008).
Group: Schilling / Project: 5

A. Engel, H. Bartolf, A. Schilling, K. Il'in, M. Siegel, A. Semenov, and H.-W. Hübers
Temperature- and field-dependence of critical currents in NbN microbridges
Journal of Physics: Conference Series **97**, 012152 (2008).
Group: Schilling / Project: 5

- A. Engel, H. Bartolf, A. Schilling, A. Semenov, H.-W. Hübers, K. Il'in, and M. Siegel
  Magnetic Vortices in Superconducting Photon Detectors
  Journal of Modern Optics **56**, 352 (2008).
  Group: Schilling / Project: 5

K. Il'in, R. Schneider, D. Gerthsen, A. Engel, H. Bartolf, A. Schilling, A. Semenov, H.-W. Hübers, B. Freitag, and M. Siegel
Ultra-thin NbN films on Si: crystalline and superconducting properties
Journal of Physics: Conference Series **97**, 012045 (2008).
Group: Schilling / Project: 5

K. Il'in, M. Siegel, A. Engel, H. Bartolf, A. Schilling, A. Semenov, and H.-W. Huebers
Current-Induced Critical State in NbN Thin-Film Structures
Journal of Low Temperature Physics **151**, 585 (2008).
Group: Schilling / Project: 5

M. Reibelt, A. Schilling, P. C. Canfield, G. Ravikumar, and H. Berger
Differential-thermal analysis around and below the critical temperature T_c of various low$-T_c$ superconductors: A comparative study
Physica C **468**, 2254 (2008).
Groups: Margaritondo, Schilling / Projects: 3, 5

A. D. Semenov, P. Haas, H.-W. Hübers, K. Ilin, M. Siegel, A. Kirste, T. Schurig, and A. Engel
Vortex-based single-photon response in nanostructured superconducting detectors
Physica C **468**, 627 (2008).
Group: Schilling / Project: 5

Group of L. Schlapbach

M. H. Aguirre, D. Logvinovich, L. Bocher, R. Robert, S. G. Ebbinghaus, and A. Weidenkaff
High-temperature thermoelectric properties of Sr_2RuYO_6 and Sr_2RuErO_6 double perovskites influenced by structure and microstructure
Acta Materialia **57**, 108 (2009).
Group: Schlapbach / Project: 4

D. Logvinovich, J. Hejtmánek, K. Knížek, M. Maryško, N. Homazava, P. Tomeš, R. Aguiar, S. G. Ebbinghaus, A. Reller, and A. Weidenkaff
On the magnetism, thermal- and electrical transport of $SrMoO_2N$
Journal of Applied Physics **105**, 023522 (2009).
Group: Schlapbach / Project: 4

I. Marozau, A. Shkabko, G. Dinescu, M. Döbeli, T. Lippert, D. Logvinovich, M. Mallepell, C. W. Schneider, A. Weidenkaff, and A. Wokaun
Pulsed laser deposition and characterization of nitrogen-substituted $SrTiO_3$ thin films
Applied Surface Science (2009).
Group: Schlapbach / Project: 4

A. Shkabko, M. H. Aguirre, I. Marozau, M. Doebeli, M. Mallepell, T. Lippert, and A. Weidenkaff
Characterization and properties of microwave plasma-treated $SrTiO_3$
Materials Chemistry and Physics (2009).
Group: Schlapbach / Project: 4

A. Tolvanen, G. Buchs, P. Ruffieux, P. Gröning, O. Gröning, and A. Krasheninnikov
Modifying the electronic structure of semiconducting single-walled carbon nanotubes by Ar^+ ion irradiation
to be published in Physical Review B (2009).
Group: Schlapbach / Project: 1

R. Aguiar, A. Kalytta, A. Reller, A. Weidenkaff, and S. G. Ebbinghaus
Photocatalytic decomposition of acetone using $LaTi(O,N)_3$ nanoparticles under visible light irradiation
Journal of Materials Chemistry **18**, 4260 (2008).
Group: Schlapbach / Project: 4

M. H. Aguirre, S. Canulescu, R. Robert, N. Homazava, D. Logvinovich, L. Bocher, T. Lippert, M. Döbeli, and A. Weidenkaff
Structure, microstructure, and high-temperature transport properties of $La_{1-x}Ca_xMnO_{3-\delta}$ thin films and polycrystalline bulk materials
Journal of Applied Physics **103**, 013703 (2008).
Group: Schlapbach / Project: 4

B. Balke, G. H. Fecher, A. Gloskovskii, J. Barth, K. Kroth, C. Felser, R. Robert, and A. Weidenkaff
Doped Semiconductors as half-metallic materials: $CoTi_{1-x}M_xSb$ (M = Sc, V, Cr, Mn, Fe)
Physical Review B **77**, 045209 (2008).
Group: Schlapbach / Project: 4

L. Bocher, M. H. Aguirre, D. Logvinovich, A. Shkabko, R. Robert, M. Trottmann, and A. Weidenkaff
$CaMn_{1-x}Nb_xO_3$ ($x \leq 0.08$) perovskite-type phases as promising new high-temperature $n-$type thermoelectric materials
Inorganic Chemistry **47**, 8077 (2008).
Group: Schlapbach / Project: 4

L. Bocher, R. Robert, M. H. Aguirre,

S. Malo, S. Hébert, A. Maignan, and A. Weidenkaff
Thermoelectric and magnetic properties of perovskite-type manganate phases synthesised by ultrasonic spray combustion (USC)
Solid State Sciences **10**, 496 (2008).
Group: Schlapbach / Project: 4

G. Buchs
Local Modification and Characterization of the Electronic Structure of Carbon Nanotubes
Ph.D. thesis, University of Basel (2008).
Group: Schlapbach / Project: 1

▶ G. Buchs, P. Ruffieux, P. Gröning, and O. Gröning
Defect-induced negative differential resistance in single-walled carbon nanotubes
Applied Physics Letters **93**, 073115 (2008).
Group: Schlapbach / Project: 1

D. Logvinovich, M. H. Aguirre, J. Hejtmanek, R. Aguiar, S. G. Ebbinghaus, A. Reller, and A. Weidenkaff
Phase formation, structural and microstructural characterization of novel oxynitride-perovskites synthesized by thermal ammonolysis of (Ca,Ba)MoO_4 and (Ca,Ba)MoO_3
Journal of Solid State Chemistry **181**, 2243 (2008).
Group: Schlapbach / Project: 4

I. Marozau, A. Shkabko, G. Dinescu, M. Döbeli, T. Lippert, D. Logvinovich, M. Mallepell, A. Weidenkaff, and A. Wokaun
RF-plasma assisted pulsed laser deposition of nitrogen-doped $SrTiO_3$ thin films
Applied Physics A **93**, 721 (2008).
Group: Schlapbach / Project: 4

R. Robert, M. H. Aguirre, L. Bocher, M. Trottmann, S. Heiroth, T. Lippert, M. Döbeli, and A. Weidenkaff
Thermoelectric properties of $LaCo_{1-x}Ni_xO_3$ polycrystalline samples and epitaxial thin films
Solid State Sciences **10**, 502 (2008).
Group: Schlapbach / Project: 4

D. Stoltz, M. Bielmann, L. Schlapbach, M. Bovet, H. Berger, M. Göthelid, S. E. Stoltz, and H. I. Starnberg
Atomic origin of the scanning tunneling microscopy images of charge-density-waves on 1T-$TaSe_2$
Physica B **403**, 2207 (2008).
Groups: Margaritondo, Schlapbach / Project: 3

A. Weidenkaff, R. Robert, M. Aguirre, L. Bocher, T. Lippert, and S. Canulescu
Development of thermoelectric oxides for renewable energy conversion technologies
Renewable Energy **33**, 342 (2008).
Group: Schlapbach / Project: 4

Group of M. Sigrist

M. H. Fischer and M. Sigrist
Dimensional crossover in Sr_2RuO_4 within a slave-boson mean-field theory
Europhysics Letters **85**, 27011 (2009).
Group: Sigrist / Projects: 1, 2

H. Adachi and M. Sigrist
Anomalous Thermal Conductivity of Semi-Metallic Superconductors with Electron-Hole Compensation
Journal of the Physical Society of Japan **77**, 053704 (2008).
Group: Sigrist / Project: 2

P. M. R. Brydon, D. Manske, and M. Sigrist
Origin and Control of Spin Currents in a Magnetic Triplet Josephson Junction
Journal of the Physical Society of Japan **77**, 103714 (2008).
Group: Sigrist / Project: 2

N. Hayashi, C. Iniotakis, M. Machida, and M. Sigrist
Josephson effect between conventional and non-centrosymmetric superconductors
Journal of the Physics and Chemistry of Solids **69**, 3225 (2008).
Group: Sigrist / Project: 2

N. Hayashi, C. Iniotakis, M. Machida, and M. Sigrist
Josephson effect between conventional and Rashba superconductors
Physica C **468**, 844 (2008).
Group: Sigrist / Project: 2

▶ C. Iniotakis, S. Fujimoto, and M. Sigrist
Fractional Flux Quanta at Intrinsic Metallic Interfaces of Noncentrosymmetric Superconductors
Journal of the Physical Society of Japan **77**, 083701 (2008).
Group: Sigrist / Project: 2

Y. Kasahara, T. Iwasawa, H. Shishido, T. Shibauchi, K. Behnia, Y. Haga, T. D. Matsuda, Y. Onuki, M. Sigrist, and Y. Matsuda
Exotic superconducting state embedded in the hidden order of URu_2Si_2
Journal of the Physics and Chemistry of Solids

69, 3187 (2008).

Group: Sigrist / Project: 2

- M. Kenzelmann, T. Strässle, C. Niedermayer, M. Sigrist, B. Padmanabhan, M. Zolliker, A. D. Bianchi, R. Movshovich, E. D. Bauer, J. L. Sarrao, and J. D. Thompson
  Coupled Superconducting and Magnetic Order in $CeCoIn_5$
  Science **321**, 1652 (2008).
  Groups: Mesot, Sigrist / Project: 2

- M. Ossadnik, C. Honerkamp, T. M. Rice, and M. Sigrist
  Breakdown of Landau Theory in Overdoped Cuprates near the Onset of Superconductivity
  Physical Review Letters **101**, 256405 (2008).
  Groups: Sigrist, Rice / Project: 2

- A. Rüegg, S. Pilgram, and M. Sigrist
  Aspects of metallic low-temperature transport in Mott-insulator/band-insulator superlattices: Optical conductivity and thermoelectricity
  Physical Review B **77**, 245118 (2008).
  Group: Sigrist / Project: 1

- R. Roldán, A. Rüegg, and M. Sigrist
  Interplay of metamagnetic and structural transitions in $Ca_{2-x}Sr_xRuO_4$
  The European Physical Journal B **64**, 185 (2008).
  Group: Sigrist / Project: 1

S. Schnez, K. Ensslin, M. Sigrist, and T. Ihn
Analytic model of the energy spectrum of a graphene quantum dot in a perpendicular magnetic field
Physical Review B **78**, 195427 (2008).
Group: Sigrist / Project: 1

K. Wakabayashi and M. Sigrist
Enhanced Conductance Fluctuation due to the Zero-Conductance Fano Resonances in the Quantum Point Contact on Graphene
Journal of the Physical Society of Japan **77**, 113708 (2008).
Group: Sigrist / Project: 1

K. Wakabayashi, Y. Takane, M. Yamamoto, and M. Sigrist
Edge effect on electronic transport properties of graphene nanoribbons and presence of perfectly conducting channel
Carbon **47**, 124 (2008).
Group: Sigrist / Project: 1

Y. Yanase and M. Sigrist
Superconductivity and Magnetism in Noncentrosymmetric System: Application to $CePt_3Si$
Journal of the Physical Society of Japan **77**, 124711 (2008).
Group: Sigrist / Project: 2

- T. Yokoyama, C. Iniotakis, Y. Tanaka, and M. Sigrist
  Chirality Sensitive Effect on Surface States in Chiral p-Wave Superconductors
  Physical Review Letters **100**, 177002 (2008).
  Group: Sigrist / Project: 2

Group of J.-M. Triscone

- S. Gariglio, N. Reyren, A. D. Caviglia, and J.-M. Triscone
  Superconductivity at the $LaAlO_3/SrTiO_3$ interface
  to be published in Journal of Physics: Condensed Matter (2009).
  Group: Triscone / Project: 2

- E. Bousquet, M. Dawber, N. Stucki, C. Lichtensteiger, P. Hermet, S. Gariglio, J.-M. Triscone, and P. Ghosez
  Improper ferroelectricity in perovskite oxide artificial superlattices
  Nature **452**, 732 (2008).
  Group: Triscone / Project: 5

- A. D. Caviglia, S. Gariglio, N. Reyren, D. Jaccard, T. Schneider, M. Gabay, S. Thiel, G. Hammerl, J. Mannhart, and J.-M. Triscone
  Electric field control of the $LaAlO_3/SrTiO_3$ interface ground state
  Nature **456**, 624 (2008).
  Group: Triscone / Project: 2

M. Dawber, C. Lichtensteiger, and J.-M. Triscone
Phase transitions in ultra-thin ferroelectric films and fine period multilayers
Journal of Phase Transitions **A81**, 623 (2008).
Group: Triscone / Project: 5

M. Dawber, N. Stucki, C. Lichtensteiger, S. Gariglio, and J.-M. Triscone
New phenomena at the interfaces of very thin ferroelectric oxides
Journal of Physics: Condensed Matter **20**, 264015 (2008).
Group: Triscone / Project: 5

J. Mannhart, D. H. A. Blank, H. Y. Hwang, A. J. Millis, and J.-M. Triscone

Two dimensional Electron Gas at Oxide Interfaces

MRS bulletin **33**, 1027 (2008).

Group: Triscone / Project: 2

R. Salut, S. Gariglio, W. Daniau, H. Majjad, G. Triscone, J.-M. Triscone, and S. Ballandras

Direct writing of high frequency surface acoustic wave devices on epitaxial $Pb(Zr_{0.2}Ti_{0.8})O_3$ thin layers using focus ion beam etching

Ferroelectrics **362**, 105 (2008).

Group: Triscone / Project: 6

Group of M. Troyer

V. W. Scarola, K. B. Whaley, and M. Troyer

Thermal Canting of Spin-Bond Order

Physical Review B **79** (2009).

Group: Troyer / Project: 1

A. F. Albuquerque, H. G. Katzgraber, M. Troyer, and J. Blatter

Engineering exotic phases for topologically-protected quantum computation by emulating quantum dimer models

Physical Review B **78**, 014503 (2008).

Groups: Troyer, Blatter / Project: 1

A. F. Albuquerque, M. Troyer, and J. Oitmaa

Quantum Phase Transition in a Heisenberg Antiferromagnet on a Square Lattice with Strong Plaquette Interactions

Physical Review B **78**, 132402 (2008).

Group: Troyer / Project: 1

▶ E. Burovski, E. Kozik, N. V. Prokof'ev, B. V. Svistunov, and M. Troyer

Critical Temperature Curve in the BEC-BCS Crossover

Physical Review Letters **101**, 090402 (2008).

Group: Troyer / Project: 1

P. Corboz, M. Boninsegni, L. Pollet, and M. Troyer

Phase diagram of ^{4}He adsorbed on graphite

Physical Review B **78**, 245414 (2008).

Group: Troyer / Project: 1

▶ P. Corboz, L. Pollet, N. Prokof'ev, and M. Troyer

Binding of a ^{3}He impurity to a screw dislocation in solid ^{4}He

Physical Review Letters **101**, 155302 (2008).

Group: Troyer / Project: 1

P. Corboz, M. Troyer, A. Kleine, I. P. McCulloch, U. Schollwöck, and F. F. Assaad

Systematic errors in Gaussian quantum Monte Carlo and a systematic study of the symmetry projection method

Physical Review B **77**, 085108 (2008).

Group: Troyer / Project: 1

S. Gürtler, M. Troyer, and F.-C. Zhang

Quantum Monte-Carlo study of a two-species bosonic Hubbard model

Physical Review B **77**, 184505 (2008).

Group: Troyer / Project: 1

▶ F. Gerbier, S. Trotzky, S. Fölling, U. Schnorrberger, J. D. Thompson, A. Widera, I. Bloch, L. Pollet, M. Troyer, B. Capogrosso-Sansone, N. Prokof'ev, and B. Svistunov

Expansion of a quantum gas released from an optical lattice

Physical Review Letters **101**, 155303 (2008).

Group: Troyer / Project: 1

▶ E. Gull, P. Werner, O. Parcollet, and M. Troyer

Continuous-time auxiliary field Monte Carlo for quantum impurity model

Europhysics Letters **82**, 57003 (2008).

Group: Troyer / Project: 1

▶ E. Gull, P. Werner, X. Wang, M. Troyer, and A. J. Millis

Local Order and the gapped phase of the Hubbard model: a plaquette dynamical mean field investigation

Europhysics Letters **84**, 37009 (2008).

Group: Troyer / Project: 1

▶ A. B. Kuklov, M. Matsumoto, N. V. Prokof'ev, B. V. Svistunov, and M. Troyer

Deconfined Criticality: Generic First-Order Transition in the SU(2) Symmetry Case

Physical Review Letters **101**, 050405 (2008).

Group: Troyer / Project: 1

P. N. Ma, L. Pollet, M. Troyer, and F.-C. Zhang

A classical picture of the role of vacancies and interstitials in Helium-4

Journal of Low Temperature Physics **152**, 156 (2008).

Group: Troyer / Project: 1

P. N. Ma, K. Y. Yang, L. Pollet, J. V. Porto, M. Troyer, and F.-C. Zhang

Influence of the trap shape on the detection of the superfluid-Mott-insulator transition

Physical Review A **78**, 023605 (2008).

Group: Troyer / Project: 1

J.-D. PICON, A. F. ALBUQUERQUE, K. P. SCHMIDT, N. LAFLORENCIE, M. TROYER, AND F. MILA

Mechanisms for spinsupersolidity in $S = \frac{1}{2}$ spin-dimer antiferromagnets

Physical Review B **78**, 184418 (2008).

Groups: Troyer, Mila / Project: 1

- L. POLLET, M. BONINSEGNI, A. KUKLOV, N. PROKOF'EV, B. SVISTUNOV, AND M. TROYER

  Local stress and superfluid properties of solid Helium-4

  Physical Review Letters **101**, 097202 (2008).

  Group: Troyer / Project: 1

L. POLLET, C. KOLLATH, U. SCHOLLWÖCK, AND M. TROYER

Mixture of bosonic and spin-polarized fermionic atoms in an optical lattice

Physical Review A **77**, 023608 (2008).

Group: Troyer / Project: 1

L. POLLET, C. KOLLATH, K. VAN HOUCKE, AND M. TROYER

Temperature changes when adiabatically ramping up an optical lattice

New Journal of Physics **10**, 065001 (2008).

Group: Troyer / Project: 1

D. N. SHENG, O. I. MOTRUNICH, S. TREBST, E. GULL, AND M. P. A. FISHER

Strong-Coupling Phases of Frustrated Bosons on a 2-leg Ladder with Ring Exchange

Physical Review B **78**, 54520 (2008).

Group: Troyer / Project: 1

- S. TREBST, E. ARDONNE, A. FEIGUIN, D. A. HUSE, A. W. W. LUDWIG, AND M. TROYER

  Collective states of interacting Fibonacci anyons

  Physical Review Letters **101**, 050401 (2008).

  Group: Troyer / Project: 1

S. TREBST, M. TROYER, Z. WANG, AND A. W. W. LUDWIG

A short introduction to Fibonacci anyon models

Progress of Theoretical Physics Supplement **176** (2008).

Group: Troyer / Project: 1

- M. TROYER, S. TREBST, K. SHTENGEL, AND C. NAYAK

  Local interactions and non-Abelian quantum loop gases

  Physical Review Letters **101**, 230401 (2008).

  Group: Troyer / Project: 1

- P. WERNER, E. GULL, M. TROYER, AND A. J. MILLIS

  Spin freezing transition and non-Fermi-liquid self energy in a 3-orbital model

  Physical Review Letters **101**, 166405 (2008).

  Group: Troyer / Project: 1

Group of K. Yvon

G. SCHÖLLHAMMER, W. WOLF, P. HERZIG, K. YVON, AND P. VAJDA

A first-principles study of the La-H system

Journal of Alloys and Compounds (2008), doi:10.1016/j.jallcom.2008.10.009.

Group: Yvon / Project: 6

8.5.2 Scientific articles in journals without peer review

Group of D. Baeriswyl

L. Tincani, R. M. Noack, and D. Baeriswyl
Critical properties of the band-insulator-to-Mott insulator transition in the strong-coupling limit of the ionic Hubbard model
arXiv:0902.1057 (2009).
Group: Baeriswyl / Project: 2

Group of G. Blatter

A. U. Thomann, V. B. Geshkenbein, and G. Blatter
Quantum instability in a dc-SQUID with strongly asymmetric dynamical parameters
arXiv:0812.4039 (2008).
Group: Blatter / Project: 2

Group of M. Büttiker

P. Samuelsson, I. Neder, and M. Büttiker
Entanglement at finite temperatures in mesoscopic conductors
arXiv:0808.4090 (2008).
Group: Büttiker / Project: 1

Group of L. Degiorgi

F. Pfuner, J. G. Analytis, J.-H. Chu, I. R. Fisher, and L. Degiorgi
Charge dynamics of the spin-density-wave state in $BaFe_2As_2$
arXiv:0811.2195 (2008).
Group: Degiorgi / Project: 1

M. Lavagnini, A. Sacchetti, C. Marini, M. Valentini, R. Sopracase, A. Perucchi, P. Postorino, S. Lupi, J.-H. Chu, I. R. Fisher, and L. Degiorgi
Pressure dependence of the single particle excitation in the charge-density-wave $CeTe_3$ system
arXiv:0811.0342 (2008).
Group: Degiorgi / Project: 1

A. Sacchetti, C. L. Condron, S. N. Gvasaliya, F. Pfuner, M. Lavagnini, M. Baldini, M. F. Toney, M. Merlini, M. Hanfland, J. Mesot, J.-H. Chu, I. R. Fisher, P. Postorino, and L. Degiorgi
Pressure-induced quenching of the charge-density-wave state observed by x-ray diffraction
arXiv:0811.0338 (2008).
Groups: Degiorgi, Mesot / Project: 1

Group of R. Flükiger

R. Flükiger, M. S. A. Hossain, and C. Senatore
Strong enhancement of J_c in binary and alloyed in-situ MgB_2 wires by a new approach: Cold high pressure densification
arXiv:0901.4546 (2009).
Group: Flükiger / Project: 6

R. Flükiger
Irradiation effects in low T_c superconductors
in *Proceedings of the 2008 Workshop on Accelerator Magnet, Superconductor, Design and Optimization (WAMSDO)* (2008).
Group: Flükiger / Project: 6

B. Seeber, C. Senatore, F. Buta, R. Flükiger, T. Boutboul, C. Scheuerlein, L. Oberli, and L. Rossi
Electromechanical behaviour of PIT Nb_3Sn wires for NED
in *Proceedings of the 2008 Workshop on Accelerator Magnet, Superconductor, Design and Optimization (WAMSDO)* (2008).
Group: Flükiger / Project: 6

Group of T. Giamarchi

T. Jarlborg
Spin-phonon coupling, q-dependence of spin excitations and high-T_c superconductivity from band models
arXiv:0804.2403 (2008).
Group: Giamarchi / Project: 2

Group of J. Karpinski

F. Giubileo, F. Bobba, A. Scarfato, A. M. Cucolo, A. Kohen, D. Roditchev, N. D. Zhigadlo, and J. Karpinski
Local study of the $Mg_{1-x}Al_xB_2$ single crystals by scanning tunneling spectroscopy in magnetic field up to 3 Tesla
Physica C **468**, 828 (2008).
Group: Karpinski / Projects: 3, 4

D. Daghero, M. Tortello, R. S. Gonnelli, V. A. Stepanov, N. D. Zhigadlo, and J. Karpinski
Evidence for two-gap nodeless superconductivity in $SmFeAsO_{0.8}F_{0.2}$ from point-contact Andreev-reflection spectroscopy
arXiv:0812.1141v1 (2008).
Group: Karpinski / Projects: 3, 4

L. Balicas, A. Gurevich, Y. J. Jo, J. Jaroszynski, D. C. Larbalestier, R. H. Liu, H. Chen, X. H. Chen, N. D. Zhigadlo, S. Katrych, Z. Bukowski, and J. Karpinski

Probing multi-band superconductivity and magnetism in $SmFeAsO_{0.8}F_{0.2}$ single crystals by high-field vortex torque magnetometry

arXiv:0809.4223v1 (2008).

Group: Karpinski / Projects: 3, 4

L. Malone, J. D. Fletcher, A. Serafin, A. Carrington, N. D. Zhigadlo, S. Katrych, Z. Bukowski, and J. Karpinski

Magnetic penetration depth of single crystal $SmFeAsO_{1-x}F_y$: a fully gapped superconducting state

arXiv:0806.3908v1 (2008).

Group: Karpinski / Projects: 3, 4

Group of H. Keller

▶ H. Keller, A. Bussmann-Holder, and K. A. Müller

Jahn-Teller physics and high-T_c superconductivity

Materials Today **11**, 38 (2008).

Group: Keller / Project: 2

Group of D. van de Marel

A. B. Kuzmenko, E. van Heumen, D. van der Marel, P. Lerch, P. Blake, K. S. Novoselov, and A. K. Geim

Infrared spectroscopy of electronic bands in bilayer graphene

arXiv:0810.2400 (2008).

Group: van der Marel / Project: 1

▶ E. van Heumen, E. Muhlethaler, A. B. Kuzmenko, D. van der Marel, H. Eisaki, M. Greven, W. Meevasana, and Z. X. Shen

Observation of a robust peak in the glue function of the high-T_c cuprates in the 50-60 meV range

arXiv:0807.1730 (2008).

Group: van der Marel / Project: 2

S. I. Mirzaei, V. Guritanu, A. B. Kuzmenko, C. Senatore, D. van der Marel, G. Wu, R. H. Liu, and X. H. Chen

Far-infrared probe of superconductivity in $SmO_{1-x}F_xFeAs$

arXiv:0806.2303 (2008).

Group: van der Marel / Project: 2

R. Lortz, R. Viennois, A. Petrovic, Y. Wang, P. Toulemonde, C. Meingast, M. M. Koza, H. Mutka, A. Bossak, and A. San Miguel

Phonon density of states, anharmonicity, electron-phonon coupling and possible multigap superconductivity in the clathrate superconductors Ba_8Si_{46} and $Ba_{24}Si_{100}$: Why is T_c different in these two compounds?

arXiv:0804.0535 (2008).

Group: van der Marel / Projects: 1, 2, 3

Group of J. Mesot

A. Sacchetti, C. L. Condron, S. N. Gvasaliya, F. Pfuner, M. Lavagnini, M. Baldini, M. F. Toney, M. Merlini, M. Hanfland, J. Mesot, J.-H. Chu, I. R. Fisher, P. Postorino, and L. Degiorgi

Pressure-induced quenching of the charge-density-wave state observed by x-ray diffraction

arXiv:0811.0338 (2008).

Groups: Degiorgi, Mesot / Project: 1

Group of F. Mila

V. Lante, I. Rousochatzakis, K. Penc, O. Waldmann, and F. Mila

Spin-Peierls instabilities of antiferromagnetic rings in a magnetic field

arXiv:0810.3837 (2008).

Group: Mila / Project: 1

K. P. Schmidt, J. Dorier, and F. Mila

Magnetization plateaux in an extended Shastry-Sutherland model

arXiv:0810.1596 (2008).

Group: Mila / Project: 1

Group of T. M. Rice

K.-Y. Yang, H. B. Yang, P. D. Johnson, T. M. Rice, and F.-C. Zhang

Quasiparticles in the Pseudogap Phase of Underdoped Cuprate

arXiv:0812.3045 (2008).

Group: Rice / Project: 2

K. Le Hur and T. M. Rice

Superconductivity close to the Mott state: From condensed-matter systems to superfluidity in optical lattices

arXiv:0812.1581 (2008).

Group: Rice / Project: 2

K.-Y. Yang, W.-Q. Chen, T. M. Rice, M. Sigrist, and F.-C. Zhang

Nature of Stripes in the Generalized t-J Model Applied to The Cuprate Superconductors

arXiv:0807.3789 (2008).

Groups: Sigrist, Rice / Project: 2

Group of A. Schilling

▶ H. Bartolf, A. Engel, L. Gómez, and A. Schilling
Multi-project wafer scale process for productive research and development
Raith application note, Physics Institute of the University of Zurich, Switzerland (2008).

Group: Schilling / Project: 5

Group of M. Sigrist

A. Rüegg and M. Sigrist
Role of multiple subband renormalization in the electronic transport of correlated oxide superlattices
arXiv:0812.0442 (2008).

Group: Sigrist / Project: 1

C. F. Miclea, A.-C. Mota, M. Sigrist, F. Steglich, T. A. Sayles, B. J. Taylor, C. McElroy, and M. B. Maple
Vortex avalanches in the non-centrosymmetric superconductor Li_2Pt_3B
arXiv:0808.2498 (2008).

Group: Sigrist / Project: 2

K.-Y. Yang, W.-Q. Chen, T. M. Rice, M. Sigrist, and F.-C. Zhang
Nature of Stripes in the Generalized t-J Model Applied to The Cuprate Superconductors
arXiv:0807.3789 (2008).

Groups: Sigrist, Rice / Project: 2

Group of J.-M. Triscone

▶ D. Isarakorn, D. Briand, S. Gariglio, A. Sambri, N. Stucki, J.-M. Triscone, F. Guy, S.-H. Baek, C.-B. Eom, J. W. Reiner, C. H. Ahn, and N. F. de Rooij
Establishement of a technology platform for epitaxial piezoelectric MEMS
in *Eurosensors XXII* (Dresden, Germany, 2008), p. 819.

Group: Triscone / Project: 6

▶ D. Isarakorn, D. Briand, S. Gariglio, A. Sambri, N. Stucki, J.-M. Triscone, F. Guy, J. W. Reiner, C. H. Ahn, and N. F. de Rooij
A study of epitaxial piezoelectric thin films grown on silicon for energy scavenging applications
in *Proceedings of PowerMEMS + microEMS 2008* (Sendai, Japan, 2008).

Group: Triscone / Project: 6

Group of M. Troyer

C. Gils
Ashkin-Teller universality in a quantum double model of Ising anyons
arXiv:0902.0168 (2009).

Group: Troyer / Project: 1

C. Gils, E. Ardonne, S. Trebst, A. W. W. Ludwig, M. Troyer, and Z. Wang
Topological stability of anyonic quantum spin chains and formation of new topological liquids
arXiv:0810.2277 (2008).

Group: Troyer / Project: 1

V. W. Scarola, L. Pollet, J. Oitmaa, and M. Troyer
Discerning Incompressible and Compressible Phases of Cold Atoms in Optical Lattices
arXiv:0809.3239 (2008).

Group: Troyer / Project: 1

A. F. Albuquerque, H. G. Katzgraber, and M. Troyer
ENCORE: An Extended Contractor Renormalization algorithm
arXiv:0805.2290 (2008).

Group: Troyer / Project: 1

8.5.3 Publications involving several groups

- C. Monney, H. Cercellier, F. Clerc, C. Battaglia, E. F. Schwier, C. Didiot, M. G. Garnier, H. Beck, P. Aebi, H. Berger, L. Forró, and L. Patthey
  Spontaneous exciton condensation in $1T-TiSe_2$: BCS-like approach
  Physical Review B **79**, 045116 (2009).
  Groups: Margaritondo, Aebi, Forró / Projects: 1, 3

J. Karpinski, N. D. Zhigadlo, S. Katrych, Z. Bukowski, P. Moll, S. Weyeneth, H. Keller, R. Puzniak, M. Tortello, D. Daghero, R. Gonnelli, I. Maggio-Aprile, Y. Fasano, Ø. Fischer, and B. Batlogg
Single crystals of $LnFeAsO_{1-x}F_x$ (Ln=La, Pr, Nd, Sm, Gd) and $Ba_{1-x}Rb_xFe_2As_2$: growth, structure and superconducting properties
Physica C (2009), doi: 10.1016/j.physc.2009.03.048.
Groups: Karpinski, Keller, Fischer / Projects: 2, 3, 4

- G. Ghiringhelli, A. Piazzalunga, C. Dallera, T. Schmitt, V. Strocov, J. Schlappa, L. Patthey, X. Wang, H. Berger, and M. Grioni
  Observation of Two Nondispersive Magnetic Excitations in NiO by Resonant Inelastic Soft-X-Ray Scattering
  Physical Review Letters **102**, 027401 (2009).
  Groups: Grioni, Margaritondo / Projects: 2, 3

F. Roy, M. Therasse, B. Dutoit, F. Sirois, L. Antognazza, and M. Decroux
Numerical studies of the quench propagation in coated conductors for fault current limiters
to be published in IEEE Transactions on Applied Superconductivity (2009).
Groups: Fischer, Hasler / Project: 6

B. M. Wojek, E. Morenzoni, D. G. Eshchenko, A. Suter, T. Prokscha, E. Koller, E. Treboux, Ø. Fischer, and H. Keller
Magnetism and superconductivity in cuprate heterostructures studied by low energy μSR
Physica B (2009), doi: 10.1016/j.physb.2008.11.189.
Groups: Fischer, Keller / Projects: 2, 5

S. Weyeneth, R. Puzniak, N. D. Zhigadlo, S. Katrych, Z. Bukowski, J. Karpinski, and H. Keller
Evidence for two distinct anisotropies in the oxypnictide superconductors $SmFeAsO_{0.8}F_{0.2}$ and $NdFeAsO_{0.8}F_{0.2}$
Journal of Superconductivity and Novel Magnetism **22**, 347 (2009).
Groups: Karpinski, Keller / Projects: 2, 3, 4

- A. J. Drew, J. Hoppler, L. Schulz, F. L. Pratt, P. Desai, P. Shakya, T. Kreouzis, W. P. Gillin, A. Suter, N. A. Morley, V. K. Malik, A. Dubroka, K. W. Kim, H. Bouyanfif, F. Bourqui, C. Bernhard, R. Scheuermann, G. J. Nieuwenhuys, T. Prokscha, and E. Morenzoni
  Direct measurement of the electronic spin diffusion length in a fully functional organic spin valve by low-energy muon spin rotation
  Nature Materials **8**, 109 (2009).
  Groups: Bernhard, Keller / Project: 2

- L. Antognazza, M. Therasse, M. Decroux, F. Roy, B. Dutoit, M. Abplanalp, and Ø. Fischer
  Comparison between the behavior of HTS thin film grown on sapphire and coated conductors for fault current limiter applications
  to be published in IEEE Transactions on Applied Superconductivity (2009).
  Groups: Fischer, Abplanalp, Hasler / Project: 6

S. Weyeneth, R. Puzniak, U. Mosele, N. D. Zhigadlo, S. Katrych, Z. Bukowski, J. Karpinski, S. Kohout, J. Roos, and H. Keller
Anisotropy of superconducting single crystal $SmFeAsO_{0.8}F_{0.2}$ studied by torque magnetometry
Journal of Superconductivity and Novel Magnetism **22**, 325 (2009).
Groups: Karpinski, Keller / Projects: 2, 3, 4

- R. Khasanov, S. Strässle, K. Conder, E. Pomjakushina, A. Bussmann-Holder, and H. Keller
  Universal correlations of isotope effects in $Y_{1-x}Pr_xBa_2Cu_3O_{7-\delta}$
  Physical Review B **77**, 104530 (2008).
  Groups: Keller, Mesot / Project: 2

- P. Legendre, Y. Fasano, I. Maggio-Aprile, Ø. Fischer, Z. Bukowski, S. Katrych, and J. Karpinski
  Unexpectedly wide reversible vortex region in β-pyrochlore $RbOs_2O_6$: Bulk magnetization measurements

Physical Review B **78**, 144513 (2008).
Groups: Fischer, Karpinski / Projects: 2, 3, 4

▶ N. D. Zhigadlo, J. Karpinski, S. Weyeneth, R. Khasanov, S. Katrych, P. Wägli, and H. Keller
Synthesis and bulk properties of oxychloride superconductor $Ca_{2-x}Na_xCuO_2Cl_2$
Journal of Physics: Conference Series **97**, 012121 (2008).
Groups: Karpinski, Keller / Projects: 2, 3, 4

▶ C. Dubois, G. Santi, I. Cuttat, C. Berthod, N. Jenkins, A. P. Petrović, A. A. Manuel, Ø. Fischer, S. M. Kazakov, Z. Bukowski, and J. Karpinski
Scanning Tunneling Spectroscopy in the Superconducting State and Vortex Cores of the β-pyrochlore KOs_2O_6
Physical Review Letters **101**, 057004 (2008).
Groups: Giamarchi, Fischer, Karpinski / Projects: 2, 3, 4

▶ G. Levy de Castro, C. Berthod, A. Piriou, E. Giannini, and Ø. Fischer
Preeminent Role of the Van Hove Singularity in the Strong-Coupling Analysis of Scanning Tunneling Spectroscopy for Two-Dimensional Cuprates Superconductors
Physical Review Letters **101**, 267004 (2008).
Groups: Giamarchi, Fischer, van der Marel / Project: 2

▶ R. Khasanov, A. Shengelaya, D. Di Castro, E. Morenzoni, A. Maisuradze, I. M. Savić, K. Conder, E. Pomjakushina, A. Bussmann-Holder, and H. Keller
Oxygen isotope effects on the superconducting transition and magnetic states within the phase diagram of $Y_{1-x}Pr_xBa_2Cu_3O_{7-\delta}$
Physical Review Letters **101**, 077001 (2008).
Groups: Keller, Mesot / Project: 2

K.-Y. Yang, W.-Q. Chen, T. M. Rice, M. Sigrist, and F.-C. Zhang
Nature of Stripes in the Generalized t-J Model Applied to The Cuprate Superconductors
arXiv:0807.3789 (2008).
Groups: Sigrist, Rice / Project: 2

J.-D. Picon, A. F. Albuquerque, K. P. Schmidt, N. Laflorencie, M. Troyer, and F. Mila
Mechanisms for spinsupersolidity in $S = \frac{1}{2}$ spin-dimer antiferromagnets
Physical Review B **78**, 184418 (2008).
Groups: Troyer, Mila / Project: 1

M. Herak, M. Miljak, A. Akrap, L. Forró, and H. Berger
Magnetic anisotropy of paramagnetic and ferromagnetically ordered state of single crystal $BaVSe_3$
Journal of the Physical Society of Japan **77**, 093701 (2008).
Groups: Forró, Margaritondo / Projects: 1, 3

▶ A. Akrap, A. Rudolf, F. Rullier-Albenque, H. Berger, and L. Forró
Influence of point defects on the metal-insulator transition in $BaVS_3$
Physical Review B **77**, 115142 (2008).
Groups: Forró, Margaritondo / Projects: 1, 3

▶ B. Sipos, A. F. Kusmartseva, A. Akrap, H. Berger, L. Forró, and E. Tutiš
From Mott state to superconductivity in 1T-TaS_2
Nature Materials **7**, 960 (2008).
Groups: Forró, Margaritondo / Projects: 1, 3

▶ R. Khasanov, K. Conder, E. Pomjakushina, A. Amato, C. Baines, Z. Bukowski, J. Karpinski, S. Katrych, H.-H. Klauss, H. Luetkens, A. Shengelaya, and N. D. Zhigadlo
Evidence of nodeless superconductivity in $FeSe_{0.85}$ from a muon-spin-rotation study of the in-plane magnetic penetration depth
Physical Review B **78**, 220510(R) (2008).
Groups: Karpinski, Mesot / Projects: 3, 4

A. F. Albuquerque, H. G. Katzgraber, M. Troyer, and J. Blatter
Engineering exotic phases for topologically-protected quantum computation by emulating quantum dimer models
Physical Review B **78**, 014503 (2008).
Groups: Troyer, Blatter / Project: 1

▶ M. Therasse, M. Decroux, L. Antognazza, M. Abplanalp, and Ø. Fischer
Electrical characteristics of DyBCO coated conductors at high current densities for fault current limiter application
Physica C **468**, 2191 (2008).
Groups: Fischer, Abplanalp / Project: 6

A. Piriou, Y. Fasano, E. Giannini, and Ø. Fischer
Effect of oxygen-doping on $Bi_2Sr_2Ca_2Cu_3O_{10+\delta}$ vortex matter: crossover from electromagnetic to Josephson interlayer coupling
Physical Review B **77**, 184508 (2008).
Groups: Fischer, van der Marel / Projects: 2, 3

M. Reibelt, A. Schilling, P. C. Canfield, G. Ravikumar, and H. Berger

Differential-thermal analysis around and below the critical temperature T_c of various low−T_c superconductors: A comparative study

Physica C **468**, 2254 (2008).

Groups: Margaritondo, Schilling / Projects: 3, 5

- M. KENZELMANN, T. STRÄSSLE, C. NIEDERMAYER, M. SIGRIST, B. PADMANABHAN, M. ZOLLIKER, A. D. BIANCHI, R. MOVSHOVICH, E. D. BAUER, J. L. SARRAO, AND J. D. THOMPSON

  Coupled Superconducting and Magnetic Order in $CeCoIn_5$

  Science **321**, 1652 (2008).

  Groups: Mesot, Sigrist / Project: 2

T. IVEK, T. VULETIĆ, S. TOMIĆ, A. AKRAP, H. BERGER, AND L. FORRÓ

Collective charge excitations below the metal-to-insulator transition in $BaVS_3$

Physical Review B **78**, 035110 (2008).

Groups: Forró, Margaritondo / Projects: 1, 3

- M. OSSADNIK, C. HONERKAMP, T. M. RICE, AND M. SIGRIST

  Breakdown of Landau Theory in Overdoped Cuprates near the Onset of Superconductivity

  Physical Review Letters **101**, 256405 (2008).

  Groups: Sigrist, Rice / Project: 2

D. STOLTZ, M. BIELMANN, L. SCHLAPBACH, M. BOVET, H. BERGER, M. GÖTHELID, S. E. STOLTZ, AND H. I. STARNBERG

Atomic origin of the scanning tunneling microscopy images of charge-density-waves on 1T-$TaSe_2$

Physica B **403**, 2207 (2008).

Groups: Margaritondo, Schlapbach / Project: 3

S. WEYENETH, T. SCHNEIDER, Z. BUKOWSKI, J. KARPINSKI, AND H. KELLER

3D-xy critical properties of $YBa_2Cu_4O_8$ and magnetic-field-induced 3D to 1D crossover

Journal of Physics: Condensed Matter **20**, 345210 (2008).

Groups: Karpinski, Keller / Projects: 2, 3, 4

8.6 Lectures, seminars and colloquia

8.6.1 Lectures at congresses

Group of P. Aebi, project 5

- C. BATTAGLIA, *A new structural model for the Si(331)-(12x1) reconstruction*, 29th International Conference on the Physics of Semiconductors ICPS 2008, Rio de Janeiro, Brazil, July 2008
- C. BATTAGLIA, *A new structural model for the Si(331)-(12x1) reconstruction*, 9th International Conference on the Structure of Surfaces ICSOS 2008, Salvador, Brazil, August 2008
- E. F. SCHWIER, *Probing nanoscale ferroelectricity with photoemission - the $PbTiO_3$ / Nb-$SrTiO_3$ system*, SPS meeting 2008, Geneve, Switzerland, 27. 3. 2008
- E. F. SCHWIER, *Probing nanoscale ferroelectricity with photoemission - the $PbTiO_3$ / Nb-$SrTiO_3$ system*, THIOX meeting 2008, Sistri Levante, Italy, 8. 4. 2008
- C. MONNEY, *Photoemission sheds light on the excitonic insulator phase in $TiSe_2$*, SPS meeting, Geneva, March 2008.
- C. MONNEY, *BCS-like phase transition in $TiSe_2$*, Workshop Statistical Physics and Low Dimension Systems, Nancy, May 2008.
- C. DIDIOT, *Nanopatternig the Electronic Properties of Gold surfaces with Self-Organized Superlattices of Metallic Nanostructures*, ICN+T 08, Keystone, Colorado – USA, July 20-25 – 2008

Group of D. Baeriswyl, projects 1 & 2

- Peter BARMETTLER, *Quantum spin systems far from equilibrium*, workshop on Correlations and coherence in quantum matter, Evora, Portugal, November 2008.

Group of C. Bernhard, project 2

- C. BERNHARD, *Competition between high T_c superconductivity and ferromagnetism in oxide multilayers,* SPS annual meeting 2008, Geneva, Switzerland, 26.3.-27.3.2008.
- C. BERNHARD, *Competition between high T_c superconductivity and ferromagnetism in oxide multilayers*, The International Conference on Low-Energy Electrodynamics in Solids 2008, Vancouver, Canada, 30.6.-4.7.2008.
- C. BERNHARD, *Study of spin transport and novel quantum states in thin film multilayers from organic and oxide materials*, International Conference on "Trends in Nanotechnology – TNT 2008", Oviedo, Spain, 01.09.-05.09.2008.
- C. BERNHARD, *Spin transport and novel quantum states in thin film multilayers from organic and oxide materials,* Swiss Workshop on Nanoscience, Davos, Switzerland, 04.06.-06.06.2008.
- C. BERNHARD, *Competition between superconductivity and ferromagnetism in oxide-based heterostructures*, 7th PSI Summer School on Condensed Matter Research, Zuoz, Switzerland, 16.8.-22.8.2008.
- C. BERNHARD, *Coexistence of magnetism and superconductivity in $SmFeAsO_{1-x}F_x$ studied by muon spin rotation and infrared spectroscopy*, International Workshop "Physics and Chemistry of FeAs-based Superconductors", Dresden, Germany, 27.10.-29.10.2008.
- C. BERNHARD, *Energy gaps in cuprate and pnictide high T_c superconductors*, International Workshop of the DFG Research Unit 538 on "Properties of Cuprate Superconductors III", Schloss Ringberg, Germany, 3.11.-7.11.2008.

Group of G. Blatter, projects 1 & 2

- BLATTER Gianni, *Higgs Mode in Strongly Correlated Bose Fluids*, Quantum Science and Technology, QSIT Start meeting, Arosa, Switzerland, January 24, 2008
- BLATTER Gianni, *Wave packet formulation of full counting statistics*, International workshop on Interaction and Interference in Nanoscopic Transport, Dresden, Germany, February 20, 2008
- BLATTER Gianni, *Excitations in strongly correlated superfluids*, Meeting of the Swiss Physical Society, Geneva, Switzerland, March 26, 2008
- BLATTER Gianni, *Wave packet formalism of full counting statistics*, Landau Memorial Conference on Advances in Theoretical Physics, Chernogolovka, Russia, June 22-26, 2008

- BLATTER Gianni, *Exact N-particle scattering matrix for electrons interacting on a quantum dot*, ESF Int. Conference on `Quantum Dynamics in Dots and Junctions', Riva del Garda, Italy, October 5--10, 2008
- HUBER Sebastian, *How to Characterize a Mott Insulator by Dynamically Generating Double Occupancy*, Workshop on Correlations and Coherence in Quantum Matter Evora, Portugal, November 13, 2008
- LEBEDEV Andrey, *Exact N-particle scattering matrix for electrons interacting on a quantum dot*, VIth Rencontres de Moriond in Mesoscopic Physics: Quantum Transport and Nanophysics (Moriond 2008), La Thuile, Italy, 8-15 March 2008
- HASSLER Fabian, *Full Counting Statistics of Mesoscopic Transport*, QSIT Start Meeting, Arosa, Switzerland, January 24, 2008
- GESHKENBEIN Vadim, *Munchhausen effect, tunneling in an asymetric SQUID*, VI International Conference Rencontres de Moriond "Quantum Transport and Nanophysics", La Thuile, Italy, March 8-15, 2008
- GESHKENBEIN Vadim, *Munchhausen effect, tunneling in an asymetric SQUID*, L. D. Landau Memorial Conference on "Advances in Theoretical Physics", Chernogolovka, Russia, June 2008
- GESHKENBEIN Vadim, *Munchhausen effect, tunneling in an asymetric SQUID*, International Conference "Quantum Dynamics in Dots and Junctions: Coherent Solid State Systems", Riva del Garda, Italy, October 5-10, 2008.

Group of M. Büttiker, projects 1 & 2

- M. BÜTTIKER, *Fluctuation relations*, RTN Nano Meeting 2008 - Fundamentals of Nanoelectronics, Jacobs University, Bremen, Germany, April 7 - 11, 2008
- M. BÜTTIKER, (invited), *The two-particle Aharonov-Bohm effect: Bell Inequality and Quantum Tomography at finite Temperature*, Conference on "Trends in Quantum Solid State Physics", Weizmann Institute, Rehovot, Israel, May 4-5, 2008
- M. BÜTTIKER, (invited), *The two-particle Aharonov-Bohmeffect and finite temperature entanglement,* Workshop on Quantum Phenomena and Information: From Atomic to Mesoscopic systems, ICTP, Trieste, Italy, May 5 – 16, 2008
- M. BÜTTIKER, *Fluctuation Relations*, *SUBTLE (Sub kT low energy transistors and switches)* 6-th project meeting, University of Lund, Sweden, may 26-27, 2008
- M. BÜTTIKER (three invited lectures), *Mesoscopic Electron Transport*, ESONN (European School on Nanosciences and Nanotechnologies) Grenoble, France, August 25 – September 12 (2008)
- M. BÜTTIKER (two invited lectures), *Scattering Theory of Conductance and Noise* and *A two-particle Aharonov-Bohm effect: Bell Inequality and Quantum Tomography at finite temperatures,* VI International Workshop on Disordered Systems, Cordoba, Argentina, September 8-12, 2008
- M. BÜTTIKER (invited), *Linear and nonlinear conductance in mesoscopic structures,* Physics School on Functional Nanostructures, Bad Honef, Germany, September 14-19, 2008
- M. BÜTTIKER, *Few electron coherent transport from single electron injectors and absorbers*, SUBTLE 7th Project Meeting, Reutlingen, Germany, September 24-25, 2008
- M. BÜTTIKER (five invited lectures), *Mesoscopic electron transport*, Ecole de Physique Mesoscopique, GDR, Cargese, Corsica, Oct. 6-11, 2008
- M. BÜTTIKER, (invited), *Fluctuation theorems and interactions, in Quantum coherence and many-body correlations*: *from mesoscopic to macroscopic scales*, Saclay, Paris, France, October 22-23, 2008.

Group of L. Degiorgi, project 1

- L. DEGIORGI (invited), *Infrared and Raman study of the charge-density-wave in the rare earth polychalcogenides RTen*, International Conference on Low Energy Electrodynamics in Solids 2008, Vancouver - Whistler, Canada, June 30 – July 4 2008
- L. DEGIORGI (invited), *Infrared and Raman study of the charge-density-wave in the rare earth polychalcogenides RTen*, International Workshop on Electronic Crystals, ECRYS 2008, Cargese, France, August 24 - 30 2008
- L. DEGIORGI (invited), *Infrared and Raman study of the charge-density-wave ground state,* Conference on Concepts in Electron Correlation, Hvar, Croatia, September 24 - 30, 2008.

Group of Ø. Fischer, projects 2, 5 & 6

- PETROVIC Alexander, *Phonon Mode Spectroscopy and Electron-Phonon Coupling in the Quasi-One-Dimensional $M_2Mo_6Se_6$ family: Competing Instabilities, Ultra-Strong Coupling and Phonon-Boosted Superconductivity*, Swiss Physical Society Annual Meeting, Geneva, Switzerland, 26th March 2008
- FASANO Yanina, *Scanning Tunneling Spectroscopy on $Sm(O_{1-x}F_x)FeAs$ pellets*,

MaNEP topical meeting, Fribourg, Switzerland May 16th 2008
- CURTZ Noé, *Nanopatterning of Superconducting Thin Films with FIB for photon detection,* MicroNanoFabrication Annual review meeting, May 20th 2008
- MAGGIO-APRILE Ivan, *Pseudogap and Vortex Cores : exotic signatures of non-conventional superconductors probed with Scanning Tunneling Spectroscopy*, NES Workshop Alicante, Spain June 6th, 2008
- FASANO Yanina, *Atomic-scale collective-mode-energy spectroscopy in high-T_c Bi-based cuprates*, NES Workshop Alicante, Spain June 6th, 2008
- MAGGIO-APRILE Ivan, *Unveiling the vortex cores of superconductors with Scanning Tunneling Spectroscopy*, ESF Workshop "Interplay between superconductivity and Magnetism at Nanometer Scale", Paestum, Italy June 21st 2008
- PETROVIC Alexander, *Superconductivity and dimensionality in molybdenum chalcogenides*, International Workshop on Transition Metal Clusters, Rennes, France, 3rd July 2008
- ANTOGNAZZA Louis, *Comparison between the behaviour of HTS thin film grown on sapphire and coated conductors for fault current limiter application*, Applied Superconductivity Conference, Boston (USA), August 21st 2008
- FASANO Yanina, *Superconducting gap and dip-hump-like feature in single-crystalline $SmFeAsO_{0.86-x}F_x$ probed by STM*, Physics and Chemistry of FeAs-based Superconductors, Dresden, Germany, Oct 28th 2008
- MAGGIO-APRILE Ivan, *STM measurements of the superconducting gap and the dip-hump-like feature in single-crystalline $SmFeAsO_{0.86-x}F_x$*, International Conferences on Stripes, Roma, Italy Dec 11th, 2008
- DECROUX Michel, ANTOGNAZZA Louis, *TIC et supraconductivité: Y a-t-il un futur commun ?,* Inforum 2009, Genève, Switzerland March 17th 2009
- Øystein FISCHER, *The physics of molybdenum cluster compounds*, International Workshop on Transition Metal Clusters, Rennes, France, 3rd – 5th July 2008
- Øystein FISCHER, *High temperature superconductors today: a key scientific and technological challenge*, Headways in materials science, Empa, Dübendorf, Switzerland, 6th March 2009.

Group of R. Flükiger, project 6

- C. SENATORE (invited), *Sn gradient, T_c distribution and flux pinning in industrial Nb_3Sn wires,* SATT 14 - Italian Conference of Superconductivity, IMEM-CNR Institute, Parma, Italy, 19-21.3.2008
- R. FLÜKIGER (invited), *Superconductivity in Switzerland,* IEA Workshop, Erlangen (D), 7-9.4.2008
- R. FLÜKIGER (invited), *Tasks of the Implementing Agreement on High Temperature Superconductivity (HTS),* IEA Ad-Hoc Group on Science & Energy Technology (AHGSET), Paris 2008
- R. FLÜKIGER (invited), *Irradiation Effects in Low T_c Superconductors,* WAMSDO '08, Workshop: Accelerator Magnet, Design and Optimization, CERN, 19-23.5.2008
- R. FLÜKIGER, C. SENATORE (invited), *Upper critical fields well above 100 T for $Sm(O_{0.85}F_{0.15})FeAs$: consequences,* ESF Workshop, Paestum (I), 19-22.6.2008
- C. SENATORE, B. SEEBER, F. BUTA, and R. FLÜKIGER, *Effect of the uniaxial strain on the calorimetric T_c distribution in Bronze Route Nb_3Sn wires,* ASC Conference, Chicago, USA, 16-21.8.2008
- C. SENATORE, R. LORTZ, and R. FLÜKIGER, *Distribution of T_c and magnetic relaxation analysis of Y-123 coated conductors,* ASC Conference, Chicago, USA, 16-21.8.2008
- C. SENATORE, R, FLÜKIGER, *Calorimetric study of various superconducting iron-based pnictides with and without Fluorine at fields up to 20 T,* ASC Conference, Chicago, USA, 16-21.8.2008
- R. FLÜKIGER, M.S.A. HOSSAIN, C. SENATORE, *Internal stresses and anisotropy in MgB_2 tapes,* ASC Conference, Chicago, USA, 16.-21.8.2008
- R. FLÜKIGER, *Developments of in-situ routes for A15 superconductors in the laboratory of Simon Foner,* ASC Conference, Chicago, USA, 16-21.8.2008
- B. SEEBER, *Electromechanical properties and synchrotron micro-tomography of Nb_3Sn wires with reduced void density obtained by hot isostatic pressing*, ASC Conference, Chicago, USA, 16-21.8.2008
- R. FLÜKIGER (invited), *Characterization of bulk and filamentary MgB_2 "in situ" tapes and anisotropy in tapes up to 20 K*, ICSM Conference, Antalya (Turkey), 25-29.8.2008
- R. FLÜKIGER (invited), *Energy: Implementing Agreement on High Temperature Superconductivity (HTS)*, FASI-IEA Workshop, Energy technologies: global challenges, Moscow, 30.9-01.10.2008
- R. FLÜKIGER (invited), *Supraconductivité: fascination et applications réelles*, Institut National Genevois, Genève, 07.10.2008
- R. FLÜKIGER (invited) , *State 2008 of HTS Applied Superconductivity*, Bundesamt für Energie, BFE, Bern (CH), 12.11.2008
- R. FLÜKIGER (invited), *Recent advances of superconductors for high field*

applications: the material aspect, IOP Workshop, London (GB), 30.01.2009.

Group of T. Giamarchi, projects 1 & 2

- T. GIAMARCHI (invited), *Low dimensional physics, cold atomic gases and quantum phase transitions,* International workshop, Theory of quantum gases and quantum coherence, Grenoble, June 3-7 2008
- T. GIAMARCHI (invited), *Spin ladders, BEC, Luttinger liquids and beyond*, Workshop on Correlated electrons in high magnetic field, Dresden, Oct 13-17 2008
- T. GIAMARCHI (invited), *Spin ladders, BEC, Luttinger liquids and beyond*, Conference Concepts in electron correlations, Hvar, Sept. 25-30 2008
- T. GIAMARCHI (invited), *Luttinger liquids: from spin chains to cold atoms*, School on "Physics in low dimensions", Lucca, Oct 11-18 2008
- T. GIAMARCHI (invited), *Orbital currents in one and two-dimensional strongly correlated systems,* March Meeting of the APS, New Orleans, March 10-14 2008
- T. GIAMARCHI (invited), *Cold atomic gases, low dimensions, Luttinger liquids and beyond*, Symposium on Quantum fluids and strongly correlated systems, Paris, Sept. 15-16 2008
- T. GIAMARCHI (invited), *Low dimensional systems and cold atomic gases*, Workshop Quantum coherence and controllability at the mesoscale, San Sebastian, May 12-16 2008
- T. GIAMARCHI (invited), *Dirty bosons and cold atomic gases,* Workshop on Non-equilibrium dynamics and correlations in strongly interacting atomic, optical and solid state systems, Harvard, Jan. 26-29 2009
- T. JARLBORG (invited), *Properties of high-T_c copper oxides from band models of spin-phonon coupling*, Workshop on Quantum Phenomena in Complex Matter "Stripes08", Erice (Sicily), 26 July - August 1st, 2008.

Group of M. Grioni, projects 1 & 2

- M. GRIONI (invited), *Tailoring spin-split states at surfaces*, 14th Int'l Conference on Solid Films and Surfaces, Dublin (Ireland), June 30 – July 4, 2008
- M. GRIONI (invited*), Spin-split states at surfaces*, SRC Users Meeting, Madison, WI (USA), 26-27 July, 2008
- M. GRIONI (invited), *High-resolution soft x-ray RIXS*, 3rd European X-FEL Users Meeting, Hamburg 28-29 January, 2009
- S. PONS (invited), *Hybridization induced spin gaps in a assymetric quantum well system*, Statistical Physics and Low Dimensional Systems 2008, Nancy, France, 21-23 May 2008
- E. FRANTZESKAKIS, *Silicon Compatible Tailored Interfacial Electronic States with Giant Spin-Splitting*, 5th International Workshop on Electronic Crystals, ECRYS 2008, 24-30 August 2008, Cargèse, France
- E. FRANTZESKAKIS, *Silicon Compatible Tailored Interfacial Electronic States with Giant Spin-Splitting,* SPS Annual Meeting 2008, Geneva, 26-27 March 2008.

Group of M. Hasler, project 6

- F. ROY, Applied Superconductivity Conference (ASC), Chicago-IL, USA, August 17-22, 2008
- F. ROY, 21st International Symposium of Superconductivity (ISS), Tsukuba, Japan, October 27-29, 2008.

Group of J. Karpinski, projects 3 & 4

- J. KARPINSKI (invited), *Hole and electron doping in MgB_2 single crystals: Influence of substitutions and vacancies on superconducting properties*, Workshop on the European Project: COMEPHS, University of Rome "La Sapienza" Roma, April 9-11, 2008
- J. KARPINSKI (invited), *Hole and electron doping in MgB_2 single crystals: Influence of substitutions and vacancies on superconducting properties*, International conference: From Solid State to BioPhysics IV, Cavtat, Kroatia June 6-13, 2008
- J. KARPINSKI (invited), *High pressure growth, structure refinement and superconducting properties of $SmAsFeO_{1-x}F_x$ single crystals and polycrystalline samples,* Exploratory Workshop on: Interplay between Superconductivity and Magnetism at nanometer scale Paestum (Salerno), Italy, 20-21 June 2008
- J. KARPINSKI, A. BELOUSOV, B. BATLOGG, *$Ga_{1-x}Al_xN$ crystals growth at high nitrogen pressure*, IUMRS-ICEM 2008, International Conference on Electronic Materials 2008, Sydney, Australia, 28th July to 1st August 2008
- J. KARPINSKI (invited), *High pressure growth, structure refinement and superconducting properties of $SmAsFeO_{1-x}F_y$ single crystals*, IUMRS-ICEM 2008, International Conference on Electronic Materials 2008, Sydney, Australia, 28th July to 1st August 2008
- J. KARPINSKI (invited), *$SmAsFeO_{1-x}F_y$ single crystals, high pressure growth, structure and superconducting properties*, International Conference on Superconductivity and Magnetism (ICSM

2008) 25-29 August 2008, Side-Antalya Turkey

- J. KARPINSKI (invited), *Single crystals of $RFeAsO_{1-x}F_y$ (R = Sm, Nd, Gd, La): high pressure growth, structure and superconducting properties*, International Workshop on iron-based superconductors, Beijing, Oct. 17-19, 2008
- J. KARPINSKI (invited), *High pressure growth, structure and superconducting properties of single crystals of $RFeAsO_{1-x}F_y$ (R = Sm, Nd, Gd, La)*, Intl. Workshop "Physics and Chemistry of FeAs-based Superconductors" October 27 - 29, 2008 IFW Dresden, Germany
- N.D. ZHIGADLO, *Single crystals of superconducting $SmFeAsO_{1-x}F_y$ grown at high pressure,* 25th International Conference on Low Temperature Physics (LT25), Amsterdam, Netherland, 6-13 August 2008.

Group of H. Keller, project 2

- H. KELLER (invited), *Universal correlations of unconventional isotope effects in cuprate superconductors*, CoMePhS Meeting Rome, University of Rome "La Sapienza", Rome, Italy, April 9-11, 2008
- H. KELLER (invited), *Unconventional isotope effects and multi-component superconductivity in cuprates*, 6th International Conference of the Stripes Series, Stripes08, Quantum Phenomena in Complex Matter, Erice (Sicily), Italy, July 26 - August 1, 2008
- H. KELLER (invited), *Unconventional Isotope effects in cuprate superconductors*, 22nd General Conference of the Condensed Matter Division of the European Physical Society, University of Rome "La Sapienza", Rome, Italy, August 25-29, 2008
- H. KELLER (invited), *Unconventional isotope effects and multi-component superconductivity in Cuprates*, Second CoMePhS Workshop in Controlling Phase Separation in Electronic Systems, Nafplion, Greece, September 30 - October 4, 2008
- S. WEYENETH (invited), *Temperature dependent anisotropy of $SmFeAsO_{1-x}F_y$ single crystals studied by torque magnetometry*, International Workshop on Iron-(Nickel)-Based Superconductors, Institute of Physics, Chinese Academy of Sciences, Beijing, China, 19 October 19, 2008
- E. MORENZONI (invited), *Depth dependent μSR on nanometer scale*, International Symposium on Pulsed Neutron and Muon Sciences (IPS 08) Mito, Japan, March 5-7, 2008
- E. MORENZONI (invited), *A closer look below surfaces and at heterostructures with muons (Yamazaki Prize Lecture)*, International Conference on Muon Spin Rotation, Relaxation and Resonance, Tsukuba, Japan, 21-25th July 2008
- E. MORENZONI (invited), *Superconductivity and Magnetism in Cuprate Heterostructures,* 6th International Conference on Low Temperature Physics, Amsterdam, 6-13.08.2008.

Group of G. Margaritondo, project 3

- D. PAVUNA (invited), *Direct ARPES on High-Tc Oxide Films : Doping, Strains and Superconductivity,* Stripes 2008 conference, Erice, Italy, July, 2008
- D. PAVUNA (invited), *Direct ARPES on High-Tc Oxide Films : Doping, Strains and Superconductivity,* CoPSES Insternational workshop, Nafplio, Greece, September, 2008
- D. PAVUNA (invited), *Physics and Nano Engineering of Complex Metallic Alloys: From Disordered Alloys to HeteroEpitaxy of Functional Multilayers*, Intl. Workshop on Complex Metallic Systems, Zagreb, Croatia, October, 2008
- D. PAVUNA (invited), *Physics and NanoEngineering of Functional and High-Tc Oxides,* Superstripestripes 2008 conference,Roma, Italy, December, 2008.

Group of J. Mesot, projects 1, 3 & 6

- J. CHANG (invited), *Electronic structure of La-based cuprates near the 1/8-anomaly*, UMD CNAM/ICAM Workshop on Cuprate Fermiology, University of Maryland, USA, Nov. 14-15, 2008
- N. B. CHRISTENSEN, *Diffuse scattering in Co_3O_4 and $Co(Al_{1.3}Co_{0.7})O_4$ studied by neutron diffraction and spectroscopy. An indication of a spiral spin liquid phase*, Materials for Frustrated Magnetism, Grenoble, France, 2008
- N. B. CHRISTENSEN, *Magnetic order and excitations in $La_{1.48}Nd_{0.4}Sr_{0.12}CuO_4$*, 29th Risø International Symposium on Materials Science, Roskilde, Denmark, 2008
- A. FURRER (invited), *Admixture of an s-wave component to the d-wave gap symmetry in high temperature superconductors*, 22nd General Conference of the Condensed Matter Division, EPS Rome, Itay, August 25-29, 2008
- A. FURRER (invited), *Towards establishing a Swiss partnership with the ILL*, Symposium 20 Years Partnership, Villigen PSI, Switzerland, Nov. 28, 2008
- A. FURRER (invited), *Bose-Einstein Condensation in Magnetic Materials,* 2008 Latsis Symposium, Lausanne Switzerland, January 28-30, 2008

- S. N. GVASALIYA (invited), G.M. Rotaru, B. Roessli, R.A. Cowley, S. Kojima, *Phase transitions and lattice dynamics in relaxors,* Frontiers in Ferroelectricity, St. Petersburg, Russia, June 12 - June 14, 2008
- S. N. GVASALIYA (invited), *Phase Transitions in Relaxors: Neutron Scattering Studies*, SNSF Scopes Workshop Tashkent, Uzbekistan, Sept. 11- Sept 14 2008
- Y. KAWASAKI, J.L. Gavilano, L. Keller, B. Roessli, N. Christensen, T. Ohno, Z. He, Y Ueda, *Neutron Scattering Studies of BaCo2V2O8,* 7th PSI Summer School on Condensed Matter Research, Lyceum Alpinum, Zuoz, Switzerland, 2008
- L. KELLER, *Magnetic Order In $CuCrS_2$ Investigated By Neutron Diffraction*, INTAS Workshop, New Layered 3d-Materials for Spintronics, Villigen PSI, Switzerland, 2008
- L. KELLER (invited), *Upgrade Of The Cold Neutron Powder Diffractometer DMC At SINQ JCNS*, Workshop 2008, Modern Trends in Neutron Scattering Instrumentation, Bernried, Germany, October 15-17, 2008
- M. KENZELMANN (invited), *Nanoscale Magnetization Dynamics*, XFEL, Bern, Switzerland, June 5, 2008
- M. KENZELMANN (invited), *Superconducting Vortices in $CeCoIn_5$: Toward the Pauli-Limiting Field*, MANEP Review, Geneva, Switzerland, Mai 20, 2008
- M. KENZELMANN (invited), *Coupled magnetic and superconducting order in $CeCoIn_5$*, Conference on Correlated Electron Systems in High Magnetic Fields, Dresden, Germany, Oct. 13-17, 2008
- M. KENZELMANN (invited), *Ferroelectricity from magnetic order*, International Conference on Highly Frustrated Magnetism, Braunschweig, Germany, Sept. 8-12, 2008
- M. KENZELMANN (invited), *Ferroelectricity from magnetic order*, International Union of Crystallography, Osaka Japan, Aug. 23-20, 2008
- M. KENZELMANN (invited), *Unconventional magnetism in an unconventional superconductor*, Stripes 2008, Erice, Italy, July 27-31, 2008
- M. KENZELMANN (invited), *Magnetically-induced ferroelectricity in frustrated quantum magnets*, American Crystallographic Association, Oak Ridge USA, May 31st - June 5, 2008
- M. KENZELMANN (invited), *Unconventional magnetism in an unconventional superconductor*, Annual Meeting of the Swiss Physical Society/MANEP Meeting, Geneva Switzerland, March 26-27, 2008
- M. KENZELMANN (invited), *Multiferroic Materials*, 7th PSI Summer School on Condensed Matter Research, Zuoz, Switzerland, Aug 20-22, 2008
- M. KENZELMANN (invited), *Magnetically-driven ferroelectric polarization in a molecule-based quantum magnet*, Materials for Frustrated Magnetism, Grenoble, France, March 3-5, 2008
- M. KENZELMANN*, Spin dynamics in $SrHo_2O_4$ and $SrDy_2O_4$*, μSR user meeting, PSI, Switzerland, January 23-24, 2008
- M. KENZELMANN, *Electric control and switching frequency of magnetism in thin films of $Ni_3V_2O_8$,* μSR user meeting, Villigen PSI, Switzerland, January 23-24, 2008
- M. KENZELMANN, *Superconducting Vortices in $CeCoIn_5$: Toward the Pauli-Limiting Field*, Fifth International Workshop on Sample Environment at Neutron Scattering Facilities, Villard de Lans, France, May 25-27, 2008
- M. KENZELMANN (invited), *Introduction to multiferroics & Ferroelectricity from magnetic order*, 2nd European School on Multiferroics, Girona, Spain, 1.9.2008-5.9.2008 (two presentations)
- M. KENZELMANN (invited), *Magnetic Structures in Crystalline Materials & Symmetry of Multiferroic Structures*, ICMR Summer School on Multiferroics, Santa Barbara, USA, 19.7.2008-26.7.2008 (two presentations)
- C. KRAEMER (invited), H. Ronnow, K. Kiefer, G. Aeppli, T. F.Rosenbaum, K. Habicht, K.Prokes, A. Podlesnyjak, Th. Straessle, O Zaharko, J. Gavilano, A. Schneidewind, P. Link, *Quantum Phasetransition of a Magnet in a Spin bath,* Departement of Physik, Neutron-Seminar TU München, Garching, Germany, January 19, 2008
- C. KRAEMER, H. Ronnow, K. Kiefer, G. Aeppli, T. F. Rosenbaum, K. Habicht, *Quantum Phase transition of a Magnet in a Spinbath*, DPG-Conference, TU Berlin, Germany
- J. MESOT (invited), *Neutron Scattering Investigation of High-Temperature Superconductors*, International Symposium on Neutron Scattering, Mumbai, India, Jan. 15-18, 2008
- J. MESOT (invited), *Doping Dependent Anisotropic Electronic Scattering Rate in $La_{2-x}Sr_xCuO_4$*, American Physical Society (APS) March meeting, New Orleans, USA, March 10-14, 2008
- J. MESOT (invited), *Multiple Energy Scales and FS pockets : Neutron and ARPES Studies*, CIFAR QM workshop, Toronto, Canada, April 7-11, 2008
- J. MESOT (invited), *Neutron and ARPES evidences for two energy scales in $La_{2-x}Sr_xCuO_4$*, The International Conference on Low-Energy Electrodynamics in Solids 2008, Vancouver June 30-July 4, 2008

- M. SHI, J. MESOT (invited*), Electronic and Magnetic Excitations of High-Temperature Cuprate Superconductors Probed by ARPES and Neutron Scattering*, 22nd General Conference of the Condensed Matter Division of the European Physical Society, Rome, Italy, August 25-29, 2008
- C. NIEDERMAYER (invited), *Tuning competing orders in $La_{2-x}Sr_xCuO_4$ cuprate superconductors by the application of an external magnetic field Stripes 08,* Quantum Phenomena in Complex Matter, Erice, Italy, July 26 - August 1, 2008
- C. NIEDERMAYER (invited), *Tuning competing orders in cuprate superconductors by the application of an external magnetic field*, Manep Internal Workshop, Neuchâtel, Switzerland, January 15, 2008
- J.C.E. RASCH, *Layered compounds for spintronics*, Metal Physics and Technology Winter Colloquium, Stoos, Switzerland
- J.C.E. RASCH, *Neutron and synchrotron X-ray diffraction on $Pb_3Mn_7O_{15}$*, INTAS Workshop, New Layered 3d-Materials for Spintronics, Villigen PSI, Switzerland
- J.C.E. RASCH, *Magnetism induced lattice distortion in $CuCrS_2$*, 16th SCTE Dresden, Germany
- J.C.E. RASCH, D.V. Sheptyakov, M. Boehm, J. Schefer, L. Keller, N.V. Volkov, K.A. Sablina and G.A. Petraskovskii, *Magnetism in $Pb_3Mn_7O_{15}$*, Annual Meeting of the Swiss Physical Society/MANEP Meeting, Geneva Switzerland
- J.C.E. RASCH, D.V. Sheptyakov, M. Boehm, J. Schefer, L. Keller, F. Gozzo, N.V. Volkov, K.A. Sablina, G.A. Petrakovskii*, Magnetic and Structural Properties of $Pb_3Mn_7O_{15}$*, INTAS Workshop: New layerd 3d-Materials for Spintronics, Villigen PSI, Switzerland
- J.C.E. RASCH*, Magnetism in $Pb_3Mn_7O_{15}$*, 72nd Annual Meeting of the DPG, Berlin, Germany
- J.C.E. RASCH, *Magnetism induced lattice distortion in $CuCrS_2$*, 16th ICTMC, Berlin, Germany
- B. ROESSLI (invited), *Neutron Polarimetry in Ferroic $NdFe_3(^{11}BO_3)_4$,* Intl. Seminar on Ferroelectricity, St-Petersburg, Russia, June 12 - June 14, 2008
- B. ROESSLI (invited), *Neutron Polarimetry in Ferroic $NdFe_3(^{11}BO_3)_4$,* PNCMI2008, Tokai Japan, Sept. 1-5, 2008
- B. ROESSLI (invited), *Three-dimensional polarimetry*, from ILL to PSI Symposium 20 Years Partnership, Villigen PSI, Switzerland, Nov. 28, 2008
- J. SCHEFER (invited), *Neutron Diffraction at the Swiss Neutron Spallation Source SINQ*, 1st Status Meeting of MaMaSELF, Rigi Kulm, Switzerland, May 6-10, 2008
- J. SCHEFER (invited), *Neutron Scattering at the Swiss Neutron Spallation Source SINQ*, INTAS Workshop: New layerd 3d-Materials for Spintronics, Villigen PSI, Switzerland, March 30-April 4, 2008
- J. STAHN (invited), *Laterally graded and complex multilayers for neutron optical elements,* NMI3 annual meeting 2008, Corse, France
- J. STAHN (invited*), Elliptic neutron guides from the idea to the implementation*, NMI3 annual meeting 2008, Corse, France
- Th. STRÄSSLE (invited), *Neutron spectroscopy under high pressure: a vibrational study on the amorphization process of ice,* 11ème Journée de la Matière Condensée, Strasbourg, France
- Ph. TREGENNA-PIGGOTT (invited), *Co-operative Jahn-Teller Phenomena in Titanium(III) and Manganese(III) Co-ordination Compounds,* Conference on the Jahn-Teller effect vibronic interactions in physics and chemistry, Heidelberg, Germany
- R. VAVRIN (invited), Probing *the phase diagram of a colloidal suspension under high pressure by neutron and light scattering*, Conference of the European Colloid and Interface Society (ECIS), Cracow Poland
- O. ZAHARKO (invited), *Magnetic structure determination combining nonpolarized and polarized neutron diffraction*, 21st Congress of International Union of Crystallography, Osaka, Japan
- M. ZAYED (invited), *Pressure induced phase transitions in the Shastry-Sutherland compound $SrCu_2(BO_3)_2$*, Journée de la matière condensée (JMC11), Strasbourg, France
- M. ZAYED, *Evidence of pressure induced phase transitions in the Shastry-Sutherland compound $SrCu_2(BO_3)_2$*, Materials for Frustrated Magnetism, Grenoble, France, March 3-5, 2008.

Group of F. Mila, project 1

- F. MILA, *The search for exotic phases of quantum magnets,* Satellite meeting of the De Gennes days on Superconductivity and magnetism, Paris, May 14-17, 2008
- F. MILA, *Non-magnetic degrees of freedom in frustrated magnetic clusters,* 57th Fujihara Seminar “New Prospects on Molecular magnetism”, Tomakomai, Japan, July 28-31, 2008
- F. MILA, *Vortex dispersion and condensation in the RVB phase of Quantum Dimer Models*, International conference “Highly Frustrated Magnetism 2008” Braunschweig, September 7-12, 2008
- F. MILA, *Magnetization plateaux: the intriguing case of $SrCu_2(BO_3)_2$,* International Workshop “Correlated Electron Systems in High Magnetic Fields” Dresden, October 13 - 17, 2008

- F. MILA, *Magnetization plateaux: the intriguing case of $SrCu_2(BO_3)_2$,* Mini-colloque Chaire Pierre de Fermat/Société Française de Physique "La physique en champ magnétique intense" Toulouse, October 24, 2008
- F. MILA, *Magnetization plateaux: the intriguing case of $SrCu_2(BO_3)_2$,* Groupement de Recherche du CNRS "MICO" Autrans, December 2-4, 2008.

Group of A. Morpurgo, project 5

- A. MORPURGO, *Transport at the charge neutrality point in graphene*, Low Temperatures 2008, Helsinky, March-April 2008
- A. MORPURGO, *Transport at the charge neutrality point in graphene*, 2008 Correlated Electron Systems Gordon Research Conference, New Biddeford, June 2008
- A. MORPURGO, *Quantum transport in graphene*, LEES08, Vancouver-Whistler, June-July 2008
- A. MORPURGO, *Transport at the charge neutrality point in single- and double-layer graphene,* European Conference of Surface Science, Liverpool, July 2008
- A. MORPURGO, *P-type, N-type, and PN-type transport at the surface of organic crystals*, Workshop on Organic Transistors and Functional Interfaces, Sendai, August 2008
- A. MORPURGO, *Electron-Phonon and Electron-electron interactions in organic field-effect transistors*, Ordering Phenomena in Transition Metal Oxides, Augsburg, October 2008
- A. MORPURGO, *Superconducting proximity effect and quantum interference in graphene,* Unconventional proximity effect in novel materials, Bad Honnef, October 2008
- A. MORPURGO, *P-type, N-type, and PN-type transport at the surface of organic crystals,* MRS Fall Meeting, Boston, November-December 2008.

Group of R. Nesper, projects 4 & 6

- F. KRUMEICH, *Novel ReO_3-related aluminium tungsten oxides*, 14th European Microscopy Congress, Aachen/D, 1.-5.09.2008
- F. KRUMEICH, *Zur Struktur ReO_3-verwandter Aluminium-Wolframoxide*, 14. Vortragstagung der GdCh-Fachgruppe Festkörperchemie und Materialforschung, Bayreuth/D, 24-26.09.2008
- R. NESPER, *New Materials for Energy Storage and transport*, Empa Dübendorf, 10.07.2008.

Group of H.-R. Ott, project 1

- H.R. OTT (invited), *Anomalous mobility of Na in $NaxCoO_2$,* Workshop on Low-Temperature Physics , Taiwan, Taipei, 5.-11.7.2008

Group of P. Paruch, projects 1 & 5

- H. BÉA, *Nanoscale study of ferroic domains in $BiFeO_3$ -based multiferroic thin films*, MACOMUFI meeting, Groningen (Pays-Bas), November 2008
- H. BÉA, *Nanoscale study of ferroelectric domain walls in $BiFeO_3$ multiferroic thin films*, WOE15, Estes Park (USA), September 2008
- H. BÉA (invited), *Multiferroics for Spintronics*, Moscow International Symposium on Magnetism, Moscow (Russia), June 2008
- H. BÉA, *Related exchange bias and ferroic domains with $BiFeO_3$ epitaxial thin films,* EMRS Spring Meeting, Strasbourg (France), May 2008
- H. BÉA, *Related exchange bias and ferroic domains with $BiFeO_3$ epitaxial thin films,* THIOX Meeting, Sestri Levante (Italy), April 2008
- P. PARUCH, *Polarization switching using single-walld carbon nanotubes grown on epitaxial $BaTiO_3$ thin films*, SPS Meeting, Geneva (Switzerland), March 2008
- P. PARUCH (invited), *Nanoscale ferroelectric domains: a model disordered elastic system with multifunctional device applications,* ECRYS Meeting, Cargèse (France), August 2008
- P. PARUCH, *Polarization switching using single-walled carbon nanotubes grown on epitaxial $BaTiO_3$ thin films*, WOE15, Estes Park (USA), September 2008.

Group of C. Renner, project 6

- C. RENNER (invited), *Ordered electronic phases in manganites,* 6th International conference on stripes, Erice, Italy, July 30, 2008.

Group of A. Schilling, project 5

- L. GÓMEZ (invited), *Josephson junction arrays for THz radiation detection*, Conference on Quantum Metrology 2008 (QM2008), Poznan University of Technology - Faculty of Electronics and Telecommunications, Poznañ, Poland, May 5, 2008
- H. BARTOLF, *Fabrication of superconducting single-photon detectors,* 9th International Conference on

Nanostructured Materials (NANO 2008), Rio de Janeiro, Brazil, 5th June 2008.

Group of L. Schlapbach, projects 1 & 4

- A. WEIDENKAFF (invited), *Development of Thermoelectric Oxides for High Temperature Converters*, Gordon Res. Conf. GRC, Colby College, ME., July 20-25, 2008
- A. WEIDENKAFF (invited), *Perovskite-type Functional Materials for Energy Technologies*, Workshop on Atomic Network Compounds, NIMS Tsukuba Sept 16, 2008
- A. WEIDENKAFF (invited), *Development of thermoelectric oxides for high temperature converters*, MS&T Pittsburgh, Oct. 6-10, 2008
- A. WEIDENKAFF (invited*), Oxidische Thermoelektrische Konverter*, 1. Tagung Thermoelektrik, Berlin, Oct. 23-24, 2008
- A. WEIDENKAFF (invited), *Thermoelektrische Oxide*, Hauptvortrag, Deutsche Thermoelektrische Gesellschaft, Freiburg, Nov 20, 2008
- A. WEIDENKAFF (invited), *Perovskitic p- and n-type materials*, IUMRS (International Union of Materials Research Societies - International Conference in Asia) Nagoya - Japan, Dec 9-13, 2008
- A. WEIDENKAFF, M.H. Aguirre, R. Robert, L. Bocher, P. Tomes, M. Trottmann, *High temperature thermoelectric properties of perovskite-type ceramics*, E-MRS, Strasbourg, May 26-30, 2008
- A. WEIDENKAFF, *Nanostructured perovskite-type thermoelectrics*, ECT Paris, July 1-4, 2008
- T. LIPPERT (invited), *Excimer laser for the deposition/transfer of thin films and structuring: Applications for fuel cells and OLEDs*, plenary talk at 2nd International Symposium on Laser-Micromachining, Chemnitz Germany, November 2008
- G. BUCHS, *Local Modification and Characterization of the electronic structure of carbon nanotubes*, TRNM08 conference, Levi, Finland, 04.12.2008.

Group of M. Sigrist, projects 1 & 2

- M. SIGRIST (invited), *Chiral p-wave superconductivity: Debates on the pairing symmetry of Sr_2RuO_4,* COFUS08, MPI-PKS, Dresden, Germany, July 2, 2008
- M. SIGRIST (School), *Symmetry aspects of superconductivity*, Le VIème Séminaire Transalpin de Physique, Lyon, France, Feb. 11, 2008
- M. SIGRIST (School), *Superconductivity with broken time reversal symmetry*, Le VIème Séminaire Transalpin de Physique, Lyon, France Feb. 13, 2008
- M. SIGRIST (School), *Introduction to Unconventional Superconductivity*, XIII Training Course in the Physics of Correlated Electron Systems and High-T_c Superconductors, Vietri, Italy, Oct. 5-8, 2008
- M. SIGRIST (invited), *Non-centrosymmetric Superconductors - Cooper pairs deprived of a key symmetry*, MECO 33, Wels, Austria, April 15, 2008
- M. SIGRIST (invited), *Unconventional Superconductivity in non-centrosymmetric materials,* International workshop on "Spin Helicity and Chirality in Superconductor and Semiconductor Nanostructures: Novel Phenomena and Emergent Functionality", Karlsruhe, Germany, July 14, 2008
- M. OSSADNIK, *Competing Instabilities in One Dimension - Functional Renormalization Group With Symmetry Breaking Terms*, DPG Spring Meeting 2008, Berlin, Germany, Feb. 27, 2008
- K.-Y. YANG (invited), *Quasiparticles in the Pseudogap Phase of Underdoped Cuprate*, Hong Kong Forum of Physics 2008 – Quantum Matters and Quantum Simulations, Hong Kong, Dec. 13, 2008
- A. RUEGG (invited), *Physical properties of artificially structured strongly correlated electron systems*, International Workshop on "Ordering Phenomena in Transition Metal Oxides", Augsburg, Germany, Oct. 8, 2008
- A. RUEGG (invited), *Role of multiple subband renormalization in the electronic transport of correlated oxide superlattices*, ARW Workshop on Correlated Thermoelectric Materials, Hvar, Croatia, Sept. 23, 2008
- A. RUEGG, *Studying correlation effects in metallic band-insulator/Mott-insulator heterostructures by means of slave bosons,* Conference on Concepts in Electron Correlation, Hvar, Croatia, Sept. 26, 2008
- T. M. RICE (invited), *Energetics of the stripe phase of the underdoped cuprates revisited,* International workshop on Unconventional Phases and Phase Transitions in Strongly Correlated Electron Systems, PPI-PKS Dresden, Germany, June 4, 2008
- T. M. RICE (invited), *Microscopic model for the cuprates,* International workshop on Unconventional Phases and Phase Transitions in Strongly Correlated Electron Systems, PPI-PKS Dresden, Germany, June 9, 2008
- T. M. RICE (invited), *Hi-T_c cuprates, still a challenge after 20 years*, Workshop in honor of Prof. Pascal Lederer, Université de Paris Sud Orsay, France, June 17, 2008
- T.M. RICE (invited), *Fermi arcs, superconducting stripes and other peculiarities of underdoped cuprates*, MPI

Conference on Physics of the Cuprates, Schloss Ringberg, Germany, Nov. 4, 2008
- T.M. RICE (invited), *The breakdown of the Landau Fermi liquid theory in overdoped cuprates,* Hong Kong Forum of Physics 2008 – Quantum Matters and Quantum Simulations, Hong Kong, Dec. 13, 2008.

Group of J.-M. Triscone, projects 5 & 6

- J.-M. TRISCONE (invited), *Tailored and improper ferroelectricity in $PbTiO_3/SrTiO_3$ superlattices I. Experimental results*, Fundamental physics of ferroelectrics, Williamsburg, USA, February 2-8 2008
- J.-M. TRISCONE (invited), *Field effect tuning of superconductivity at the $LaAlO_3/SrTiO_3$ interface*, APS March meeting, New Orleans, USA, March 10-15 2008
- J.-M. TRISCONE (invited), *Nanoscale ferroelectrics: artificial materials and novel devices*, Workshop sur les Oxydes fonctionnels pour l'intégration en micro et nano-électronique, Autrans, France, 16-19 mars 2008
- J.-M. TRISCONE (invited), *Superconducting interfaces between insulating oxides*, de Gennes days, Paris, May 14
- J.-M. TRISCONE (invited), *Nanoscale ferroelectrics, thin films and superlattices*, Ferroelectric meeting and applications FMA25, Kyoto, May 27-30 2008
- J.-M. TRISCONE (invited), *Superconductivity at the $LaAlO_3/SrTiO_3$ interface*, LT 25, Amsterdam, August 10-12 2008
- J.-M. TRISCONE (invited), *Superconducting interfaces between insulating oxides*, Summer school on condensed matter research, Zuoz, August 16-22 2008
- J.-M. TRISCONE (invited), *Electrostatic tuning of the $LaAlO_3/SrTiO_3$ interface groundstate*, International workshop on oxide electronics WOE15, Denver, September 13-18 2008
- J.-M. TRISCONE (invited), *Superconductivity at the $LaAlO_3/SrTiO_3$ interface*, Nanoxide meeting, Göteborg, September 28-30 2008
- J.-M. TRISCONE (invited), *Two dimensional superconductivity at the $LaAlO_3/SrTiO_3$ interface*, 3rd International workshop on Ordering phenomena in transition metal oxides, Augsburg, October 5-8 2008
- N. REYREN (Invited), *2D Superconductivity at the $LaAlO_3$ and $SrTiO_3$ Interface*, International Workshop on Superconductivity in Diamond and Related Materials 2008, Tsukuba, July 7 2008
- N. REYREN, *2D Superconductivity at the $LaAlO_3$ and $SrTiO_3$ Interface*, Thin Films for Novel Oxide Devices - Final Meeting, Sestri Levante, April 10 2008
- P. ZUBKO, *Strain-gradient-induced polarisation in $SrTiO_3$ single crystals*, THIOX, Sestri-Levante, April 9 2008
- A. CAVIGLIA , *Electrostatic modulation of 2D superconductivity and magnetoresistance at the $LaAlO_3/SrTiO_3$ interface*, Advances and new challenges in oxide electronics, THIOX meeting, Sestri Levante, Italy, April 9-11 2008
- A. CAVIGLIA (invited), *Electric field control of the $LaAlO_3/SrTiO_3$ interface ground state*, Non-centrosymmetric superconductors, Zurich, Switzerland, May 30-31 2008
- A. CAVIGLIA (invited), *Electric field control of the $LaAlO_3/SrTiO_3$ interface ground state*, International workshop on nanoferronics, Aachen, Germany, October 9-10 2008
- A. CAVIGLIA (invited), *Electric field control of the $LaAlO_3/SrTiO_3$ interface ground state*, Villa conference on complex oxide heterostructures, Clermont, Florida, USA, November 2-6 2008
- N. STUCKI, *Interfacial interactions in ferroelectric superlattices revealed through their phase transitions*, THIOX Final Meeting, Sestri Levante, Italy, April 9 2008
- N. STUCKI, *Interactions d'interface dans des superréseaux ferroélectriques révélées par leurs transitions de phase*, GDR MICO, Autrans, France, 2008
- S. GARIGLIO (invited), *Electric Field Control of the $LaAlO_3/SrTiO_3$ Interface Ground State*, Material Research Society, Boston, USA, December 1-5 2008
- S. GARIGLIO (invited), *MEMS Fabrication based on Epitaxial Piezoelectric Thin Films on Silicon*, 3rd International Conference "Smart Materials, Structures and Systems, Acireale, Italy, June 8-13 2008.
- S. GARIGLIO (invited), *Electric field effect in superconducting high temperature superconductors*, Italian National Conference on Superconductivity SATT-14, Parma, Italy, March 19-21 2008.

Group of M. Troyer, project 1

- TROYER Matthias, *The golden chain*, Leeds, 5-th Symposium on topological quantum computing, April 2008
- TROYER Matthias, *Quantum loop gases and topological order*, ICTP conference, Trieste, Italy, May 2008
- TROYER Matthias, *Introduction to Monte Carlo Methods*, Summer schoo, Sherbrooke, Canada, May 2008l
- TROYER Matthias, *Simulating exotic phases of matter*, Canadian Association of

Physisicists, Annual Meeting, Quebec, Canada, June 2008

- TROYER Matthias, *The ALPS project*, Workshop on Correlations, Manchester, England, July 2008
- TROYER Matthias, *The solid state of Helium-4: to flow or not to flow*, Conference on Computational Physics, Ouro Preto, Brazil, August 2008
- TROYER Matthias, *Quantum Monte Carlo Methods*, 5 lectures at XIII Training Course in the Physics of Strongly Correlated Systems, Salerno, Italy, October 2008
- TROYER Matthias, *Local interactions and non-Abelian phases*, Workshop on Tensor Network States, Madrid, October 2008
- TROYER Matthias, *The solid state of Helium-4: to flow or not to flow*, Conference "Quantum coherence and many-body correlation", Paris, October 2008
- TROYER Matthias, *Validating a quantum simulator*, Hong Kong Forum on Condensed Matter Physics, Hong Kong, December 2008
- POLLET Lode, *The binding of a He-3 impurity to the screw dislocation in He-4*, Royal Holloway, London, UK, August 2008
- POLLET Lode, *The binding of a He-3 impurity to the screw dislocation in He-4*, ICTP Trieste, Italy, August 2008, Supersolid Workshop
- POLLET Lode, *Blowing hot and cold on atomic gases in an optical lattice*, Aspen, CO, USA, August 2008
- ISAKOV Sergei, *Quantum Monte Carlo simulations of frustrated quantum magnets*, workshop on quantum magnetism, Minneapolis, USA, May 2008
- GILS Charlotte, *Non-abelian topological phases and unconventional criticality in a model of interacting anyons*, Quantum information and graph theory: emerging connections, Perimeter institute, Waterloo, Canada, 2008
- TROYER Matthias, *The negative sign problem,* IPAM tutorials, UC Los Angeles, USA, January 2009
- TROYER Matthias, *The ALPS project*, IPAM tutorials, UC Los Angeles, USA, January 2009
- TROYER Matthias, *Calculating entropy in Monte Carlo simulations*, IPAM workshop, UC Los Angeles, USA, January 2009
- TROYER Matthias, *Continuous time QMC solvers for fermions*, SciSSP2009 conference, Tokyo, Japan, February 2009
- TROYER Matthias, Pleanary talk at MECO 2009, Leipzig, March 2009
- SCAROLA Vito (invited), *Possibility of a Supersolid State of Cold Atoms in Optical Lattices*, APS March Meeting, Pittsburgh PA, USA, March 2009.

Group of van der Marel, projects 1, 2, 3 & 5

- Dook VAN MECHELEN, *Electron-phonon interaction and charge carrier mass enhancement in $SrTiO_3$*, APS March meeting 2008, New Orleans, USA, March 11, 2008
- Florence LEVY (invited), *Coexistence and interplay of superconductivity and ferromagnetism in URhGe*, Conference on Low Temperature Physics, LT25, Amsterdam, the Netherlands, August 5-13, 2008
- Alexey KUZMENKO, *Infrared conductance of graphene: universality vs. c-axis hopping*, International Workshop "Graphene weeks", Trieste, Italy, August 28, 2008
- Alexey KUZMENKO, *Infrared spectroscopy of bilayer graphene, Intl. Conf. on Low Energy Electrodynamics in Solids*, Vancouver-Whistler, Canada, July 1, 2008
- Alexey KUZMENKO, *Universal infrared conductance of graphite*, SPS 2008 Meeting,
  Geneva, Switzerland, March 27, 2008
- Alexey KUZMENKO (invited), *Infrared probe of superconductivity in Sm(O,F)FeAs*, Topical Workshop on Novel Iron Pnictide Superconductors, Fribourg, Switzerland, May 16, 2008
- Dirk VAN DER MAREL (invited), *Optical mass enhancement in strongly correlated metals*, Unconventional Phases and Phase Transitions in Strongly Correlated Electron Systems, MPIPKS Dresden, Germany, June 04 - 07, 2008
- Dirk VAN DER MAREL (invited), *Observation of robust 55 meV resonance in the glue function of high T_c cuprates*, The Fifth International Conference on Mathematical Modeling and Computer Simulation of Materials Technologies (MMT-2008), Ariel, Israel, September 08 - 12, 2008
- Dirk VAN DER MAREL (invited), *Polaron liquid in electron doped strontium titanate*, The International Conference on Low-Energy Electrodynamics in Solids 2008, Vancouver - Whistler, British Columbia, June 30 - July 4, 2008
- Erik VAN HEUMEN (invited), *Optics clues to pairing glues in the cuprates*, Conference on Concepts in Electron Correlation, Hvar, Croatia, September 24-30, 2008
- Erik VAN HEUMEN (invited), *Optics clues to pairing glues in the cuprates*, Conference on Low Temperature Physics, LT25, Amsterdam, the Netherlands, August 5-13, 2008.

8.6.2 Seminars and colloquia

Group of D. Baeriswyl, projects 1 & 2

- Peter BARMETTLER, *Quantum many-body dynamics of coupled double-well superlattices*, EPFL, April 2008
- D. EICHENBERGER, *Superconductivity and antiferromagnetism in the two-dimensional Hubbard model: A variational study*, University of Geneva, April 2008
- Dionys BAERISWYL, *Superconductivity in the Hubbard model*, University of Geneva, October 2008.

Group of C. Bernhard, project 2

- C. BERNHARD, *Energy gaps in high T_c superconductors studied with infrared ellipsometry,* Max Planck Institut für Festkörperforschung, Stuttgart, Germany, 9.1.2009
- C. BERNHARD, *Infrared ellipsometry studies on oxides with strongly correlated electrons,* Universität Konstanz, Konstanz, Germany, 27.1.2009
- J. HOPPLER, *Stress induced modulation of the magnetic profile in $Y_{0.6}Pr_{0.4}Ba_2Cu_3O_7/La_{2/3}Ca_{1/3}MnO_3$ superlattices,* Max Planck Institut für Festkörperforschung, Stuttgart, Germany, 14.3.2008.

Group of G. Blatter, projects 1 & 2

- HUBER, Sebastian, *Collective excitations in strongly correlated superfluids, Lorentz versus Galilei*, Max Planck Institut für Quantenoptik, Garching, Germany, April 21, 2008
- HUBER, Sebastian, *Collective excitations in strongly correlated superfluids, Lorentz versus Galilei*, AMO/Keck Seminar, Rice University, Houston, USA, July 14, 2008
- HUBER, Sebastian, *Characterizing a Mott Insulator by Dynamically Generating Double Occupancy,* University of Colorado, Boulder, USA, July 21, 2008
- HUBER, Sebastian, *Characterizing a Mott Insulator by Dynamically Generating Double Occupancy*, University of Pittsburgh, Pittsburgh, USA, July 24, 2008
- THOMANN, Alexander, *Munchhausen Effect: Quantum decay in a dynamically asymmetric SQUID*, QSIT Junior Meeting, Ausserferrera, June 10-13, 2008
- LEBEDEV, Andrey, *Statistics of photon radiation emitted form a quantum point contact*, ETH Zurich, April 3, 2008
- THEILER, Barbara, *Substrate-Induced Order in Two-Dimensional Dipolar Gases*, QSIT Junior Meeting, Ausserferrera, Switzerland, June 10 - 13, 2008
- HASSLER, Fabian, *Full Counting Statistics of Mesoscopic Transport*, QSIT Start Meeting, Arosa, Switzerland, January 24, 2008
- HASSLER, Fabian, *Full Counting Statistics: from Few to Many Particles*, Leiden University, Leiden, Netherlands, March 4, 2008
- HASSLER, Fabian, *Signature of exchange statistics in the measurement of the average current*, QSIT Junior Meeting, Ausserferrera, Switzerland, June 10, 2008
- HASSLER, Fabian, *A First-Quantized Way to Tackle Constant Voltage in Quantum Transport,* ETH Zürich, Switzerland, October 2, 2008
- GESHKENBEIN, Vadim, *Munchhausen effect, tunneling in an asymetric SQUID*, P. L. Kapitza Institute for Physical Problem, Moscow, Russia, January 10, 2008
- GESHKENBEIN, Vadim, *Munchhausen effect, tunneling in an asymetric SQUID*, Technion, Haifa, Israel, February 12, 2008.

Group of M. Büttiker, projects 1 & 2

- M. BUTTIKER, *The two-particle Aharonov-Bohm effect,* Arnold Sommerfeld Center - Theory colloquium, Ludwig Maximillian University, Munich, Germany, June 4, 2008
- M. BUTTIKER, *A two-particle Aharonov-Bohm effect: Bell Inequality and Quantum Tomography at finite temperatures*, Departamento de Fisica, FCEyN, UBA, Pabellon 1, Ciudad Universitaria, 1428 Buenos Aires, Argentina, September 5, 2008
- M. BUTTIKER, *Fluctuation relations*, VI International Workshop on Disordered Systems, in Cordoba, Argentina, September 8 -12, 2008.

Group of L. Degiorgi, project 1

- L. DEGIORGI, *Infrared and Raman study of the charge-density-wave ground state*, Walther Meissner Institut Münich Garching, Münich, Germany, June 19 2008
- L. DEGIORGI, *Infrared and Raman study of the charge-density-wave ground state*, Seminar Series of the Nebraska Center for Materials and Nanoscience, University of Nebraska, Lincoln, U.S.A., June 23 2008
- L. DEGIORGI, *Infrared and Raman study of the charge-density-wave ground state*,

University of California San Diego, San Diego, U.S.A., June 26 2008
- L. DEGIORGI, *Infrared and Raman study of the charge-density-wave ground state*, Stanford University, Stanford, U.S.A., July 7 2008.

Group of Ø. Fischer, project 2, 5 & 6

- PETROVIC Alexander, *Several puzzles in molybdenum cluster-based superconductors,* DPMC Forum, University of Geneva, Switzerland, 11th April 2008
- TREBOUX Emmanuel, *STM measurements on YBCO123*, ARPES-STM meeting, EPFL Lausanne , Switzerland May 8th, 2008
- MAGGIO-APRILE Ivan*, Etudes des vortex par microscopie à effet tunnel : BCS vs non BCS*, University of Paris Paris, France May 15th, 2008
- MAGGIO-APRILE Ivan, *Scanning Tunneling Spectroscopy studies of high T_c Superconductors,* Università di Napoli - Napoli, Italy June 24th, 2008
- PETROVIC Alexander, *Multi-gap Superconductivity and Vortex Core Spectroscopy in the Chevrel Phase $SnMo_6S_8$* , University of Fribourg, Fribourg, Switzerland, 15th August 2008
- FASANO Yanina, *Atomic-scale collective mode energy spectroscopy in Bi-based cuprates,* Leuven University, Leuven, Belgium Sept 12th, 2008
- PETROVIC Alexander, *Short Coherence Length Superconductivity and its Consequences in $SnMo_6S_8$* , Nanyang Technological University, Singapore, October 21st , 2008
- FASANO Yanina, *Imaging the essential role of spin-fluctuations in high-T_c superconductivity*, Paris University, Paris, France, Oct 14th, 2008
- Øystein FISCHER, *Exploring high temperature superconducting cuprates and pnictides with the scanning tunnelling microscope,* Chalmers University of Technology, Göteborg, Sweden, 8th November 2008.

Group of R. Flükiger, project 6

- C. SENATORE, *Upper critical fields above 100 Tesla in $SmFeAsO_{0.85}F_{0.15}$*, University of Fribourg, Fribourg, Switzerland, 16.05.2008
- R. FLÜKIGER, *High field investigations in MgB_2 wires and Y-123 Coated Conductors,* Technical University Beijing, Beijing (China), 02.6.2008
- R. FLÜKIGER, C. SENATORE, *High field investigations in Y-123 Coated Conductors and $SmFeAsO_{1-x}F_x$ bulk samples,* University of Hefei, Hefei (China), 03.6.2008
- R. FLÜKIGER, *Radiation effects in superconductors in view of LHC Upgrade,* CERN Seminars on Magnet and Materials, 11.11.2008
- R. FLÜKIGER, *Recent results on MgB_2 in Geneva,* University of Cambridge, Cambridge (GB), 29.1.2009
- C. SENATORE, *Physical Properties and Microstructure of Superconducting Materials for Applications,* University of Geneva, Geneva, Switzerland, 04.02.2009.

Group of L. Forró, projects 1, 4 & 6

- SIPOS Balázs, *Normal state transport properties of novel superconductors*, Oak Ridge National Laboratory, USA, 25.11.2008
- KUSMARTSEVA Ana, *From Mott state to superconductivity in 1T-TaS2*, University of Cambridge, UK, April 2008
- NAFRADI Balint, *High frequency ESR investigation of organic conductors*, University of Stuttgart, Deutschland, Sept. 2008.

Group of T. Giamarchi, projects 1 & 2

- T. GIAMARCHI, *Quantum physics in one dimension: Luttinger liquids and beyond*, Utrecht University, Dec. 10 2008.

Group of M. Hasler, project 6

- F. ROY, 1er colloque *Supraconductivité et calcul numérique* de Nancy, Modélisation multiphysique de rubans supraconducteurs, Nancy, France, June 9, 2008.

Group of J. Hulliger, project 4

- J. HULLIGER, *Magnetic Separation in Solid State Chemistry and its Application to Superconductivity*, Geological Institute of Berne, Switzerland, 19th Nov. 2008.

Group of J. Karpinski, projects 3 & 4

- J. KARPINSKI, *Influence of substitutions and vacancies in MgB_2 single crystals on superconducting properties and structure,* Physics Department University of Leipzig May 27th 2008
- J. KARPINSKI, *High pressure growth and properties of superconducting single crystals $SmFeAsO_{1-x}F_y$ and $NdFeAsO_{1-x}F_y$,* Institute of Physics PAN, September 3rd 2008, Warszawa

- J. KARPINSKI, *Single crystals of $RFeAsO_{1-x}F_y$ (R = Sm, Nd, Pr, Gd, La) : high pressure growth, structure and superconducting properties*, Physik-Institut der Universität Zürich, Nov. 19th, 2008.

Group of H. Keller, project 2

- H. KELLER, *Von Positronen zu Myonen*, Mini-Symposium (Dr. Dierk Herlach), Paul Scherrer Institute, Villigen, Switzerland, March 28, 2008
- H. KELLER, *Unconventional isotope effects and multi-component superconductivity in cuprate high-temperature superconductors*, University of Augsburg, Augsburg, Germany, December 16, 2008
- B.M. WOJEK, *Superconductivity and Magnetism in Cuprate Heterostructures Studied by Low Energy muSR*, University of Zurich, Zurich, Switzerland, May 14, 2008
- E. MORENZONI, *Introduction to polarized low energy muons as depth dependent probes of thin films and heterostructures,* 7th PSI Summer School on Condensed Matter Research, Zuoz 17.8.2008.

Group of G. Margaritondo, project 3

- D. PAVUNA, *Direct ARPES on High-T_c Oxide Films : Doping, Strains and Superconductivity,* Physics Dept., University of Miami, Coral Gables, April 16, 2008
- D. PAVUNA, *The Centenary of Liquifaction of Liquid Helium: How 'Esoteric' Low Temperature Physics Transforms Our Civilization*, University Santiago de Compostela, 11 October, 2008
- Co-chairs : L. FORRO and D. PAVUNA, International conference ''*From Solid State to BioPhysics IV*'', Dubrovnik, Croatia, June 6-13, 2008.

Group of J. Mesot, project 1, 3 & 6

- J. CHANG, *Magnetic and Electronic properties of the high-temperature superconductor $La_{2-x}Sr_xCuO_4$*, Université de Sherbrooke, Canada, Mar. 15th, 2008
- J. HOPPLER, *Stress induced modulation of the magnetic profile in $Y_{0.6}Pr_{0.4}Ba_2Cu_3O_7/La_{2/3}Ca_{1/3}MnO_3$ superlattices,* MPI fuer Festkörperfoerschung, Stuttgart Germany, March 14, 2008
- M. KENZELMANN, *Quantum magnetism, multiferroics and heavy-fermion superconductivity,* Dept. of Physics, University of Karlsruhe, Karlsruhe, Germany April 14, 2008
- M. KENZELMANN, *Multiferroic Materials*, Dept of Materials, ETH Zürich, Zürich, Switzerland, October 1, 2008
- J. MESOT, *Electronic and magnetic excitations of high-temperature cuprate superconductors probed by ARPES and neutron scattering*, Condensed Matter Colloquium, University of Fribourg, April 15, 2008
- J.C.E. RASCH, *Neutron scattering on magnetoelastic $CuCrS_2$*, ETH Zurich, Advanced Materials Science Seminar, Zürich, Switzerland
- J. SCHEFER, *SINQ and selected Applications: Metastable states, oxygen transport in periovsiktes and other applications using novel materials*, Institut für Experimentalphysik, Universität Wien, Austria, Oct. 20, 2008
- J. SCHEFER, *Neutron Scattering at the Swiss Neutron Spallation Source SINQ,* Department of Materials Engineering and Industrial Technologies, University of Trento, Italy, May 26, 2008
- Ph. TREGENNA-PIGGOTT, *High-Resolution Inelastic Neutron Scattering Studies of Transition Metal Compounds*, Copenhagen, 2008
- O. ZAHARKO, *Isolated tetrahedra system $Cu_4OCl_6L_4$. magnetic exchange against cluster plasticity,* Lab. of Crystallography, Lausanne, Switzerland.

Group of F. Mila, project 1

- F. MILA, *Exotic order in spin liquids,* University of Utrecht, Utrecht, The Netherlands, May 7, 2008
- F. MILA, *Spin liquids*, Theoretical Physics, ETH Zürich/Universität Zürich, Zürich, Switzerland, September 29, 2008
- F. MILA, *Exploring the physics of lattice bosons with quantum magnets*, Max-Planck Institute for Complex systems, Dresden, Germany, November 10, 2008
- F. MILA, *Antiferroaimants quantiques frustrés et bosons sur réseau*, Université Pierre et Marie Curie, Paris, France, January 22, 2009.

Group of A. Morpurgo, project 5

- A. MORPURGO, *Organic Single Crystal Transistors,* CEA, Saclay, France, September 2008
- A. MORPURGO, *Mesoscopic physics with organic transistors*, Université de Grenoble, Grenoble, France, November 2008
- A. MORPURGO, *Quantum transport through graphene*, Massachussets Institute of Technology, Boston, USA, December 2008

- A. MORPURGO, *Quantum Transport through graphene*, MaNEP Winter School, Saas Fee, Switzerland, January 2009.

Group of R. Nesper, projects 4 & 6

- R. NESPER, *Superconductors, Battery and Other Challenging Materials for Future Applications,* Institute of Chemistry, University of Stockholm, Sweden, 02.06.2008.

Group of H.-R. Ott, project 1

- H.R. OTT, *Energy transport in spin chains,* Kolloquium Low-Temperatures, Finland, Helsinki, 30.3.-3.4.2008
- H.R. OTT, *100 years of liquid Helium,* The Zurich Physics Colloquium, Switzerland, Zürich, 23.4.2008
- M. WELLER, *NMR/NQR studies in rare earth metallic systems*, HFML Grenoble, France, Grenoble, 10.6.2008.

Group of P. Paruch, projects 1 & 5

- P. PARUCH, *Ferroelectric domains: imaging static and dynamic behaviour using atomic force microscopy*, Mini-symposium on ferroelectrics, ICMAB, Barcelona, Spain, January 2008.

Group of A. Schilling , project 5

- L. GÓMEZ, *New approach for fabricating HTS Josephson weak links suitable for large scale integration*, The Jagiellonian University, Krakow, Poland, March 10, 2008
- A. ENGEL, *Physics and Statistics of Football*, Physics Institute, University of Zürich, Switzerland, 29 May 2008
- H. BARTOLF, *Fabrication process for superconducting single-photon detectors*, Physics Institute, University of Zürich, Switzerland, 25 June 2008
- L. GÓMEZ, *Josephson weak links as THz radiation detectors*, University of Zurich, Physics Institute, Dec. 10th, 2008.

Group of L. Schlapbach, projects 1 & 4

- A. WEIDENKAFF, *Synthesis and characterisation of tailor-made functional materials for future energy conversion technologies,* BASF, Ludwigshafen, April 17, 2008
- A. WEIDENKAFF, *Perovskite-type Oxynitrides as potential Photocatalysts*, EPFL, May 7, 2008
- A. WEIDENKAFF, *Perovskite-type materials for energy conversion technologies,* TU Berlin, June 30, 2008
- A. WEIDENKAFF, *Development of functional materials for future energy conversion technologies*, Siemens München, September 19, 2008
- A. WEIDENKAFF, *Ceramic Thermoelectric Converters,* Schott, Mainz, December 18, 2008
- A. WEIDENKAFF, *Perovskite-type ceramics for future energy technologies*, Chemie, Uni Bochum, January 9, 2009
- T. LIPPERT, *Thin Films Prepared by Pulsed Laser Deposition for Renewable Energy Applications*, FZ Karlsruhe, Germany, November 2008
- T. LIPPERT, *Laser Interaction with Materials: From Structuring to Thin Film Deposition,* RIKEN, Wako, Japan, August 2008
- T. LIPPERT, *From laser ablation to laser transfer techniques – experiences and current developments*, IMM Mainz, Germany, June 2008
- T. LIPPERT, *Thin film deposition by laser based methods*, University of Vienna, Physical Chemistry Dept, Austria, April 2008
- G. BUCHS, *Local Modification and Characterization of the electronic structure of carbon nanotubes*, ETH Zürich Micro- and Nanosystems Group, Zurich, Switzerland, 04.04.2008
- O. GRÖNING, *Carbon Nanotubes: A Prototype Nanomaterial from basic Research to Applications*, Leave-Taking Colloquium for Prof. Louis Schlapbach, Empa Dübendorf, Switzerland, 06.03.2009.

Group of M. Sigrist, projects 1 & 2

- M. SIGRIST, *How to form Cooper pairs without inversion symmetry?,* COFUS-Colloquium, MPI-PKS, Dresden, Germany, July 7, 2008
- M. SIGRIST, *Key symmetries for superconductivity: Cooper pairs without inversion symmetry,* Augsburg University, Augsburg, Germany, Dec. 11, 2008
- A. RUEGG, *Studying correlation effects in the metallic transport of band-insulator Mott-insulator by means of slave bosons*, Université Paris-Sud, Orsay, France, Nov. 6, 2008
- T.M. RICE, *Hi-T_c cuprates, still a challenge after 20 years*, Condensed Matter Physics, Brookhaven Natl. Lab. Upton NY, USA, July 30, 2008
- T.M. RICE, *A phenomenological theory for the transition from full Fermi surface to Fermi arcs as the hole density is reduced in overdoped cuprates*, MPI-FKF Stuttgart, Germany, Sept. 10, 2008.

Group of M. Troyer, project 1

- TROYER Matthias, *Simulations of quantum phase transitions*, Universität Wien, April 2008
- TROYER Matthias, *Continuous time solvers for quantum impurity problems*, Los Alamos National Laboratories, September 2008
- TROYER Matthias, *Recent progress in Monte Carlo simulations*, Hong Kong University, December 2008
- SCAROLA Vito, *Thermal Canting in Quantum Magnets,* USA, Washington DC, November 2008
- SCAROLA Vito, *Discerning Compressible and Incompressible Phases of Cold Atoms in Optical Lattices*, University of Pittsburgh, USA, September 2008
- SCAROLA Vito, *Quantum Hall Quantum Dots,* Laboratory for Physical Sciences at the University of Maryland, USA College Park, MD, November 2008
- SCAROLA Vito, *Quantum Hall Quantum Dots,* Naval Research Laboratory Washington DC, USA, August 2008
- KOZIK Evgeny, *Strongly correlated systems: is an exact solution possible?,* Moscow institute of Physics and Technology, Russia, December 2008
- BAUER Bela, *Tensor-product state simulations of quantum spin systems on infinite lattices,* Aachen, Germany, December 2008
- BAUER Bela, *Tensor-product state simulations of quantum spin systems on infinite lattices*, Wien, Austria, December 2008
- TROYER Matthias, *Validating a quantum simulator*, UCLA, USA, January 2009
- TROYER Matthias, *Recent progress in QMC simulations,* Rome, February 2009
- TROYER Matthias, *The solid state of Helium-4: to flow or not to flow*, Rome, February 2009
- GILS Charlotte, *Models of internacting non-abelian anyons*, University of Waterloo Canada, January 2009
- GILS Charlotte, *Models of internacting non-abelian anyons*, University of British Columbia, Canada, January 2009
- GILS Charlotte, *Models of internacting non-abelian anyons*, Sherbrooke University, Canada, January 2009
- GILS Charlotte, *Models of internacting non-abelian anyons,* Perimeter institute, Waterloo, Canada, January 2009
- GILS Charlotte, *Models of internacting non-abelian anyons*, University of Illinois, Urbana-Champaign, IL, USA, January 2009
- SCAROLA Vito, *Quantum Hall Rotons*, Tech, Blacksburg VA, USA, February 2009
- BAUER Bela, *Tensor-product state simulations of quantum spin systems on infinite lattices,* UC Santa Barbara, California, USA, February 2009.

Group of van der Marel, projects 1, 2 ,3 & 5

- Dirk VAN DER MAREL, *Optics clues to pairing glues in the cuprates*, University of Groningen, The Netherlands, October 26, 2008
- Dirk VAN DER MAREL, *Optics clues to pairing glues in the cuprates*, Weizmann Institute, Israel, September 10, 2008
- Dook VAN MECHELEN, *Electron-phonon interaction and charge carrier mass enhancement in $SrTiO_3$*, Johns Hopkins University, Baltimore (MD), USA, March 6, 2008
- Dook VAN MECHELEN, *Electron-phonon interaction and charge carrier mass enhancement in $SrTiO_3$*, Prague Institute of Physics, Prague, Czech Republic, July 18, 2008
- Florence LEVY, *Optical study of the metal-insulator transition in $Bi_{1-x}Sb_x$*, Grenoble High Magnetic Field Laboratory, Grenoble, France, December 12, 2008.
- Florence LEVY, *Coexistence and interplay of superconductivity and ferromagnetism in URhGe*, Stuttgart Physics Institute, Stuttgart, Germany, June 24, 2008
- Alexey KUZMENKO, *Optics of Graphene*, University of Alberta , Edmonton, Canada, July 7, 2008
- Alexey KUZMENKO, *Infrared conductance of graphite: implications for graphene physics*, Manchester University, Manchester, UK, January 23, 2008.

Appendix Milestones of the MaNEP projects

The tables of milestones (with colors) allow one to follow the time evolution of MaNEP scientific activities. The tables below are drawn from the situation at the end of the previous reporting period (Year 7) and display the changes for Year 8.

Color codes:

Milestones unchanged since last year:	
Milestones added this year:	
Milestones suppressed this year:	

A-1 Project 1: Strongly interacting electrons, low-dimensional and quantum fluctuation dominated systems

	Milestones	Year 5	Year 6	Year 7	Year 8
1.	**Systems with localized electronic degrees of freedom**				
	Magneto optical spectroscopy TiOCl, TiOBr *[Degiorgi]*				
	Magneto optical spectroscopy $Cu_2Te_2O_5Cl_2$ *[Degiorgi]*				
	Magneto optical spectroscopy $Cu_2Te_2O_5Br_2$ *[Degiorgi]*				
	Optical investigation of the CDW polychalcogenides as a function of temperature and pressure *[Degiorgi]*				
	Magneto optical investigation of $Eu_{1-x}Ca_xB_6$ and $EuIn_2P_2$ *[Degiorgi]*				
	SDW state $BaFe_2As_3$ *[Degiorgi]*				

	Raman spectroscopy of TiOCl, TiOBr *[Lemmens (outside MaNEP)]*				
	NMR and thermal properties of $Na_{1-x}CoO_2$ *[Ott]*				
	NMR and magnetic properties of MVT_2O_2 (M = Li, Na; T = Si,Ge) *[Ott]*				
	Dimer systems				
	structure determination *[Mesot]*				
	pressure dependence of magnetic structure *[Degiorgi]*				
	inelastic neutron scattering: magnetic spectra *[Mesot]*				
	theoretical discussion of phase diagram and excitation spectra *[Sigrist, Mila, Giamarchi]*				
	$A_3Cu_2Ni(PO_4)_4$ (A = Ca, Sr, Pb)				
	synthesis, determination structure and intratrimer coupling *[Mesot]*				
	single crystal growth, INS: magnetic spectra *[Mesot]*				
	test of field-induced order *[Mesot]*				
	$Cu_2Te_2O_5X_2$ (X = Cl, Br)				
	Magnetic structure determination *[Mesot]*				
	INS: spectra, development of theoretical models *[Mesot, Mila]*				
	Alloy $Cu_2Te_2O_5Cl_{2-x}Br_s$: structure determination *[Mesot]*				
	INS: spin spectra *[Mesot]*				
	High-pressure/-field studies *[Degiorgi]*				
	Theoretical investigation of microscopic models *[Mila]*				
	$LiCu_2O_2$: on-campus ARPES *[Grioni]*				

	Optical investigation of $LiCu_2O_2$ combined with ARPES data *[Degiorgi]* Ab-initio calculations on $LiCu_2O$: *[Mila]* $BaVS_3$: temperature-dependent ARPES *[Grioni]* Sr-Ba- / S-Se-substitutions *[Grioni]* 1st high-resolution resonant X-ray emission spectroscopy at SLS *[Grioni]* Combined high-resolution X-ray ARPES-RIXS at SLS *[Grioni]* RIXS on heavy fermions *[Grioni]*				
	Investigation of microscopic models for quantum phases with topological properties *[Blatter, Mila, Troyer, Sigrist]* Determination of phase diagrams of various dimer models *[Blatter, Mila, Troyer, Sigrist]* Investigation of effective models for quantum liquids with defects *[Blatter, Mila, Troyer, Sigrist]*				
	Formulation of reduced versus projected entanglement *[Büttiker]* Analysis of cross-relation measurements and quantum limits *[Büttiker]*				
2.	**Itinerant electrons**				
	Synthesis of doped fullerene (DWNT) *[Forró]* Synthesis of organic conductors *[Forró]* Low-field ESR studies *[Forró]* High-field ESR studies *[Forró]* High pressure study of superconducting intercalated graphite *[Forró]*				
	STM characterization of H-adsorption and vacancy defects on SWNT, modeling *[Schlapbach]*				

	Characterization of “quantum dot” states between two defects, barrier transparency dependence on topology of SWNT *[Schlapbach]* Transport and optical properties *[Schlapbach]*				
	$BaVS_3$: crystal growth *[Forró]* Crystal growth: $BaVSe_3$ *[Forró]* High-pressure NMR- and transport study of $CePd_2In$, CeTe *[Ott]* NMR- and transport study of $BaVS_3$ *[Ott]* NMR-studies on $BaVSe_3$ *[Ott]* NMR- and transport study of $PrCu_2$ *[Ott]* High pressure NMR on $CeAl_3$ *[Ott]*				
	Optical study of MnSi near QPT *[van der Marel]* Optical study of UGe_2, $CeRhIn_5$ near QPT *[van der Marel]* Optical study of $Lu_5Ir_4Si_{10}$ near CDW transition *[van der Marel]*				
	Investigation of spectral properties of Mott insulators and superfluid/Fermi liquid phases including behavior across phase transitions *[Blatter, Giamarchi, Troyer, Mila]* Microscopic modeling of Bose-Hubbard systems with truncated Hilbert space, properties of superfluid-insulator interface *[Blatter, Giamarchi, Troyer]* Construction and investigation of low-energy effective field theories *[Blatter, Giamarchi, Troyer, Mila]* Thermometry of fermionic cold gases in optical lattices *[Blatter, Giamarchi, Troyer]* Development of new impurity solvers for dynamical mean field theory and related methods for fermionic materials *[Troyer]*				

	Competing structural orders in polar-molecule systems *[Blatter]* Transport across correlated boundaries *[Troyer, Blatter]* Effects of disorder in cold atom gas *[Giamarchi, Blatter, Troyer]*				
3.	**Magnetism and the interface to spintronics**				
	$Fe_{1-x}Co_xSi$: Synthesis *[van der Marel]* Magneto-optical, X-ray absorption / dichroism measurement *[Degiorgi, van der Marel]*				
	Magnetic nanoparticles: Synthesis and characterization *[Forró, Seo, Nesper]* ESR measurements *[Forró, Seo, Nesper]* **Magnetic semiconductor: Mn-doped GaAs, InAs:** Synthesis and characterization *[Forró, Seo]* ESR measurements *[Forró, Seo]*				
	Spin polarized STM: Commission and demonstrate novel dual tip STM *[Renner]* Demonstrate atomic scale imaging and spectroscopy using novel dual tip STM on test systems *[Renner]*				

A-2 Project 2: Superconductivity, unconventional mechanisms and novel materials

	Milestones	Year 5	Year 6	Year 7	Year 8
1.	**Superconducting and magnetic properties of novel and/or unconventional superconductors**				
1.1	**Cuprate superconductors** Transport properties of $Na_xCa_{2-x}CuO_2Cl_2$ *[Karpinski, Forro]* Transport properties of $SrCaCu_2O_4Cl_2$ *[Karpinski]* Spectroscopic properties of $YBa_2Cu_4O_8$ *[Fischer, van der Marel]* Spectroscopic properties of $Na_xCa_{2-x}CuO_2Cl_2$ *[Grioni, van der Marel]* Spectroscopic properties of $SrCaCu_2O_4Cl_2$ *[Grioni, van der Marel]*				
1.2	**Other unconventional superconductivity** Transport properties of $T_xMg_{1-x}B_{2-y}C_y$ (T = Mn, Fe, Co, Ni) *[Karpinski]* Spectroscopic properties of $T_xMg_{1-x}B_{2-y}C_y$ *[van der Marel]* Transport properties of $K_xRb_{1-x}Os_2O_6$ *[Karpinski, Forró]* Spectroscopic properties of $K_xRb_{1-x}Os_2O_6$ *[Fischer]* Spectroscopic properties of pnictide superconductors *[Fischer, Bernhard, van der Marel, Grioni]* Spectroscopic properties of Chervrel phases *[Fischer]*				

2.	**Topological defects in superconductors, vortex matter**				
2.1	**Experimental study of the vortex liquid** STM of vortex liquids *[Fischer]* SANS of vortex lattice *[Mesot]* STM of trapped vortices *[Fischer]* STM of a vortex in double potential well *[Fischer]*				
2.2	**Theoretical study of the effects of the strong disorder on the vortex lattice** Transition in layered superconductors and films *[Giamarchi]* Density functional theory of (surface-) melting of the vortex lattice in layered superconductors *[Blatter]* Properties of disordered elastic manifolds, including pinning and creep of vortices in disordered superconductors *[Blatter, Giamarchi]*				
2.3	**Theoretical study of unusual topological structures due to multi-component order parameters** Phenomenological description and properties *[Sigrist]* Spectral features from microscopic modeling *[Giamarchi, Sigrist]*				
2.4	**Local magnetic field profiles in multilayered superconductors** Bulk μSR of SC multilayers *[Keller, Morenzoni]* Local magnetic field profiles near surfaces *[Keller, Morenzoni]*				

	μSr experiments on Y123/Pr123 superlattices-study of the anomalous proximity effect coupling *[Keller, Morenzoni, Bernhard, Fischer]* Study of the competition between superconductivity and magnetism in oxide superlattices *[Bernhard, Morenzoni]*	
2.5	**Superconducting devices** Phase diagram of dynamically asymmetric SQUID *[Blatter]*	
3.	**Microscopic properties of high temperature superconductors**	
3.1	**Experimental and investigation of the pseudogap state** STM of local order in pseudogap-state *[Fischer]* Inelastic neutron scattering of LSCO in B-field *[Mesot]*	
3.2	**Microscopic theory of high temperature superconductors** Theory of electronic structure of cuprates *[Sigrist, Baeriswyl, Giamarchi]* Comparison of latter with STM and ARPES in Bi2223 *[Fischer, Grioni, Mesot]*	
3.3	**Search for the mechanisms which give rise to high-Tc superconductivity** Optics of spectral weight transfer Bi2223 *[van der Marel]* Optics of spectral weight transfer in Y124 *[van der Marel]* Optics of spectral weight transfer in Bi2201 *[van der Marel]* ARPES and STM of Bi-cuprates *[Fischer, Grioni, Mesot]* Preparation of high T_c thin films *[Fischer]*	

A-3 Project 3: Crystal growth

	Milestones	Year 5	Year 6	Year 7	Year 8
1	**Two-dimensional superconductors**				
	Exploring the miscibility limits of Pr in the preparation of $Bi_{2-x}Pr_xSr_2CaCu_2O_{8-\delta}$ by the self-flux method. Optimizing the crystal homogeneity. *[Margaritondo, Berger]*				
	Synthesizing the above family with the traveling solvent floating zone method and compare the quality of the crystals *[van der Marel]*				
	Optimize the high pressure synthesis of $YBa_2Cu_4O_8$ single crystals of large size. *[Karpinski]*				
	Growing $Ca_{2-x}Na_xCuO_2Cl_2$ and $(Sr,Ca)_3Cu_2O_{4+\delta}Cl_{2-y}$ single crystals of oxochlorates which mimic the underdoped cuprates. *[Karpinski]*				
	Crystal growth of hole-doped and Co-doped MgB2 *[Karpinski]*				
2	**Geometrically frustrated systems**				
	Optimizing the growh conditions of $BaVS_3$ for NMR measurements *[Margaritondo, Berger]*				
	Synthesis of doped single crystals of $BaVS_3$ with Cr and Ti. *[Margaritondo, Berger]*				
	Exploring growth and synthesis of pyrochlores. *[Karpinski]*				
	Single crystals of $RFeAsO_{1-x}F_x$ (R = La, Pr, Nd, Sm, Gd) *[Karpinski]*				

3	**Magnetic materials**	
	Exploring the synthesis of the magnetic chain system $Cu_2Te_2O_5Cl_{2-x}Br_x$ *[Margaritondo, Berger]*	
	Preparation a wide range of metal oxide crystals *[Mesot]*	
	Processing and crystal growth of half-metallic magnetic alloys, like some Transition Metal Silicides *[van der Marel]*	
	Improved quality of single crystals of perovskite-type $REMnO_3$ manganites *[Mesot]*	

A-4 Project 4: Novel materials

	Milestones	Year 5	Year 6	Year 7	Year 8
1	**Synthesis of new bulk materials at ambient and high pressure**				
1.1	**Synthesis at high pressure and of iron based pnictides** Crystal growth of borides, superconducting pyrochlor oxides, oxychloride cuprates, reaction of multicomponent oxide systems *[Karpinski]* Single crystals of $Ba_{1-x}Rb_xFe_2As_2$				
1.2	**Synthesis of potentially superconducting Ni-oxides** (i) $LnANiO_4$ solid state chemistry (variation of Ln, A and incorporation of F) *[Schilling, Karpinski]* (ii) $LnANiO_2$ solid state chemistry (doping experiments) *[Schilling, Karpinski]* (iii) characterization of physical properties *[Schilling]*				
1.3	**A new method of combinatorial chemistry for finding ferromagnetic and superconducting oxides** (i) Theoretical studies on the exploration of phase systems by the SSC. Modeling of magnetic separation columns for superconductors. *[Hulliger]* (ii) SSC syntheses by using Cu, Ni and Co for a lead element. Study of reaction performance in SSC samples. *[Hulliger]* (iii) Characterization of SSC probes by various physical techniques. *[Hulliger]* (i) Modeling magnetic separation and construction of final set up [Hulliger]				

	(ii) Search for grains with higher Tc than known in Bi, Tl, Hg cuprates. [Hulliger] (iii) Physical, structural characterization of isolated special grains. Exploring new phase systems involving Cu, Co, Ru, Re and elements not appearing in typical cuprate superconductors. [Hulliger]				
2	**Preparation of thin films (2D)**				
2.1	**Perovskite Oxynitrides by Pulsed Laser Deposition** (i) Pulsed reactive crossed beam experiments using ammonia to obtain films of oxynitride titanates and molybdates. *[Schlapbach]* (ii) rf-plasma pulsed laser deposition of oxynitride titanates and molybdates *[Schlapbach]* (iii) microwave induced plasma ammonolysis of surfaces of large perovskite-type titanate single crystals. *[Schlapbach]* (iv) Conductivity measurements and general physical and chemical characterization *[Schlapbach]*				
2.2	**Ferromagnetic oxides prepared by thin film techniques** (i) Doped oxide semiconductors, thin film growth using titanates doped by transition metal ions *[Seo, Forro]* (ii) Study on the origin of ferromagnetism in low doped oxide systems *[Seo, Forro]* (iii) Structural, chemical and physical characterization of films *[Seo, Forro]*				
3	**Preparation and modification of 1D fiber-type materials**				
	(i) Optimized preparation of boride and oxide fibers [Nesper] (ii) Superconducting Ca_xB_xC compounds and K(Al,Si) compounds with MgB_2 structure *[Nesper]*				

	(iii) Novel conducting carbon based solids *[Nesper]* (iv) Novel rare earth metal nitrides *[Nesper]*				

A-5 Project 5: Thin films, artificial materials, and novel devices

	Milestones	Year 5	Year 6	Year 7	Year 8
1	**Epitaxial ferroelectric films and artificial insulating superlattices for basic studies and future applications**				
	Explore size effects in ferroelectric $PbTiO_3$ thin films using strained films and X-rays, AFM and XPD *[Triscone, Aebi]*				
	Explore size effects in ferroelectrics using superlattices *[Triscone]*				
	Study the role of screening on the properties of ultrathin films, modifying the electrostatic boundary conditions *[Triscone, Aebi]*				
	Use superlattices to realize new materials with tailored properties-induction of ferroelectricity in dielectric materials such as $SrTiO_3$ *[Triscone]*				
	Use superlattices to realize new materials with tailored properties *[Triscone]*				
	Writing of nanoscale domains in ferroelectric films using carbon nanotubes AFM tips *[Triscone, Paruch]*				
	Writing of nanoscale domains in strained ferroelectric films and in artificial superlattices *[Triscone, Paruch]*				
	Exploration of dimensional crossovers in ferroelectric domain wall static - dynamics in superlattices containing ultrathin films and in multiferroic films *[Triscone, Paruch]*				
2	**Oxide thin films and heterostructures as model systems for spectroscopic, field effect and transport studies**				
	Realize infrared optical spectroscopy on Nb-STO thin films (determination of carrier density, cyclotron mass, carrier life-time) *[van der Marel]*				

	Realize infrared optical spectroscopy on Nb-STO thin films whose carrier density is modulated by field effect (determination of the induced carrier density, cyclotron mass changes, carrier life-time) *[van der Marel, Triscone]* Probe the polaronic nature of the carriers in Nb-STO *[van der Marel]* Probe the polaronic nature of the carriers in manganites (and in manganites whose carrier density is modified by field effect-coupling with project SNSF-divisionII) *[van der Marel, Triscone]*	
	Realization of large area Y123/Pr123 superlattices suitable for muons spin resonance studies *[Fischer]* Realization of high quality 214 films with transfer under vacuum for ARPES-STM/STS studies *[Fischer, Aebi]* Development of surface cleaning procedures *[Aebi]* Fabrication of $La_{1-x}Ca_xMnO_3$ films under different strain conditions *[Fischer]* Spectroscopy on 124 films and on $(BaCuO_x)(CaCuO_2)$ multilayers *[Fischer]*	
	Realize field effect devices using 214 superconducting channels and amorphous gate oxides *[Martinoli]* Determine the Cooper pair effective mass using the Bernouilli effect *[Martinoli]*	
3	**Novel single photon detectors using low and high Tc superconducting nanostructures**	
	Realization of superconducting films of NbN, TiN, TaN and others *[Schilling]* Film nanostructuring and realization of superconducting meander photon detectors based on NbN, TiN, or TaN *[Schilling]*	

	Study and improvement of detector performance (detection efficiency, sensitivity, energy dispersion) *[Schilling]* Study of thermal and quantum fluctuations in nanometer size superconductors *[Schilling]* Film/superlattice nanostructuring and realization of superconducting meander photon detector *[Fischer]* Study of the detector response to voltage and current pulses *[Fischer]*				
4	**Giant electroresistive effect in correlated oxide thin films**				
	Theoretical investigations of the process *[Blatter, Rice]*				

A-6 Project 6: Industrial applications and pre-application development

	Milestones	Year 5	Year 6	Year 7	Year 8
1	***Applied superconductivity***				
	New specific heat device for rapid determination of the Sn distribution in Nb_3Sn multifilamentary wires up to 21 T *[Flükiger]*				
	New device for studying the effect of transverse compressive stress on J_c of multifilamentary Nb_3Sn and MgB_2 wires up to 21 T *[Flükiger]*				
	Improvement of Nb_3Sn Internal Sn at very high fields for NMR. Goal: J_c(overall) ≥ 150 A/mm^2 at 4.2Kand 21T (30% enhancement) *[Flükiger]*				
	Improvement of Nb_3Sn Internal Sn at intermediate fields (for high field dipoles): J_c(overall) ≥ 500 A/mm^2 at 4.2K, 15 T *[Flükiger]*				
	Improvement of MgB_2 wires and tapes. New goal: J_c(4.2K) ≥ 10^2 A/mm^2 at 12 T *[Flükiger]*				
	Improvement of Nb_3Sn Internal Sn at very high fields for NMR. New goal: J_c(overall) ≥ 180 A/mm^2 at 4.2Kand 21T *[Flükiger]*				
	Preparation of MgB_2 wires with full thermal stabilization. Optimization of the current carrying properties at 20 K for MRI applications: J_c(20K) ≥ 10^2 A/mm^2 at 5 T *[Flükiger]*				
	Doped MgB_2 coated metal wires and free-standing MgB_2 forms *[Nesper]*				
	Synthesis of nanoscopic boron for enhancing critical currents in MgB_2 ceramics *[Nesper, Flükiger]*				

	Improving single wafer for homogeneous switching at low voltage *[Fischer]* Test of a 10 kVA FCL in a series and or parallel configuration *[Fischer]* Test of coated conductors on various substrates for FCL applications *[Fischer]* Validation of electro-thermal FEM simulations with measurements *[Hasler]* FEM testing of new coated conductors geometries *[Hasler, Fischer]* Dynamic Hall probe field mapping development *[Hasler]* Dynamic Hall probe field mapping of current limiter *[Hasler, Fischer]*	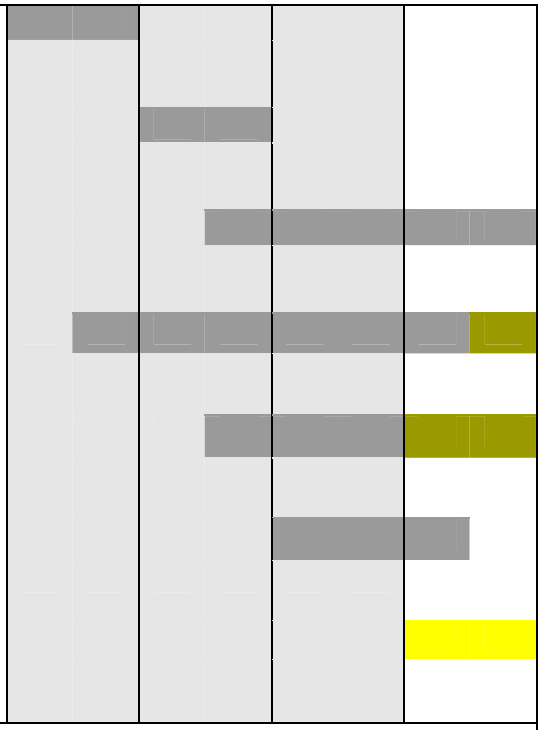
2	***MaNEP sensors***	
	Synthesis and test of ESR materials for weak field measurements *[Forró]* Set-up of experimental tools for gas sensors. Identification of loss of sensitivity causes using local probe techniques. Fabrication of electrodes with selected thin film coatings *[Fischer]* Set-up of experimental tools and electronics (IDT structure and SAW resonators at 40MHz). Measure electrical conductivity of various sensing nano-materials in NH_3, H_2 and O_3. Stability versus temperature *[Fischer]* First frequency-shift measurements at 40MHz with reference gas samples *[Fischer]* Best choice of thin film electrodes and surface morphology upon resistance to passivation, speed of response, sensitivity and selectivity *[Fischer]*	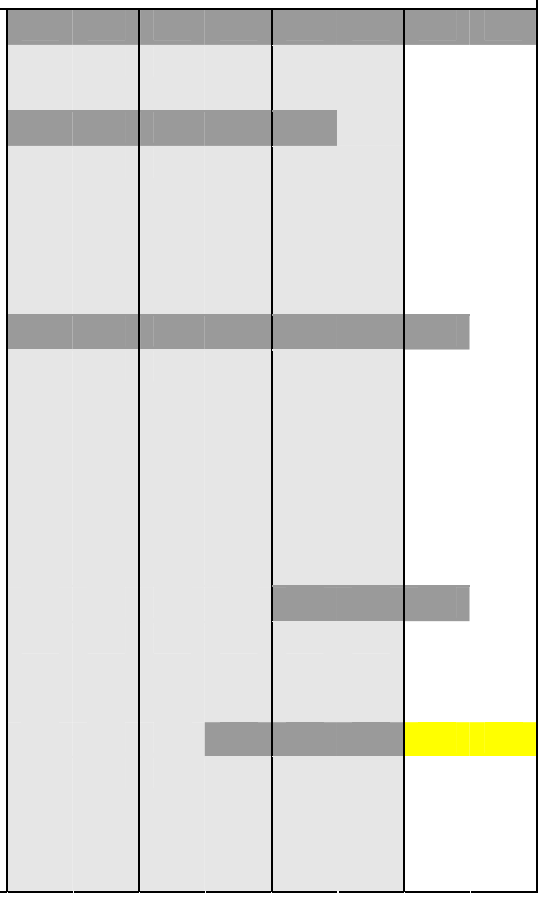

	Resistance and frequency-shift measurements of the response of sensing layers to NH_3, H_2 and O_3 *[Fischer]*				
	Integration of the new cathodes in working sensors *[Fischer]*				
	Identification of the best sensitive layer for each environment. Selectivity, speed of response and stability assessments. Measurement of the kinetics of adsorption/desorption *[Fischer]*				
	Field test of new cathodes at end-user site *[Fischer]*				
	Optimization, fine-tuning of the morphology / chemistry of the sensing layers *[Fischer]*				
	Implementation of SAW/resistive sensor on a commercial device for field testing *[Fischer]*				
3	***Thin film preparation and Applications***				
	Ni/Ti multilayers: Improved design of magnetic field and sputter targets *[Mesot]*				
	Neutron and X-ray diffraction and reflection investigation of substrates and coatings *[Mesot]*				
	Investigation of substrates and coatings by X-rays and local probes *[Mesot, Triscone]*				
	Investigation of multilayers prepared by simultaneous running of sputtering targets in pure Ar and Ar/N_2 gas *[Mesot]*				
	Determination of reflectivity by neutrons and X-rays *[Mesot]*				

	Scanning probe investigation of films prepared by reactive sputtering *[Triscone]*				
	Fabrication of polarizing multilayers of type FeCo/Ti *[Mesot]*				
	Explore controlled interdiffusion on magnetization *[Mesot]*				
	Realization of epitaxial $SrTiO_3$ buffer layers on silicon *[Triscone]*				
	Realization of epitaxial piezoelectric layers on buffered silicon *[Triscone]*				
	Realization of a pyroelectric sensor using epitaxial PZT films on silicon *[Triscone]*				
	Realization of MEMS structures using epitaxial oxide films *[Triscone]*				
	Realization of PIT-SAW devices on $SrTiO_3$-doped $SrTiO_3$ / PZT structures *[Triscone]*				
	Characterization of the structures (high frequency / elastic constants) *[Triscone]*				
	Demonstration of the “frequency doubling” capability of the PIT-SAW technology *[Triscone]*				
	Realization of a PIT-SAW device on silicon *[Triscone]*				
	Realization of SAW devices on $SrTiO_3$ / PZT structures *[Triscone]*				
	High frequency characterization of epitaxial $SrTiO_3$ / PZT devices *[Triscone]*				